Durham University

Durham E-Theses

Geochemical and geochronological investigations of the vumba granite-greenstone terrain of NE Botswana

Bagai, Zibisani

How to cite:

Bagai, Zibisani (2000) *Geochemical and geochronological investigations of the vumba granite-greenstone terrain of NE Botswana*, Durham theses, Durham University. Available at Durham E-Theses Online: http://etheses.dur.ac.uk/4282/

Use policy

The full-text may be used and/or reproduced, and given to third parties in any format or medium, without prior permission or charge, for personal research or study, educational, or not-for-profit purposes provided that:

- a full bibliographic reference is made to the original source
- a link is made to the metadata record in Durham E-Theses
- the full-text is not changed in any way

The full-text must not be sold in any format or medium without the formal permission of the copyright holders.

Please consult the full Durham E-Theses policy for further details.

Academic Support Office, Durham University, University Office, Old Elvet, Durham DH1 3HP
e-mail: e-theses.admin@dur.ac.uk Tel: +44 0191 334 6107
http://etheses.dur.ac.uk

Geochemical and Geochronological investigations of the Vumba granite-greenstone terrain of NE Botswana.

Zibisani Bagai

A thesis submitted to the University of Durham for the degree of Master of Science

The copyright of this thesis rests with the author. No quotation from it should be published in any form, including Electronic and the Internet, without the author's prior written consent. All information derived from this thesis must be acknowledged appropriately.

Department of Geological Sciences September, 2000

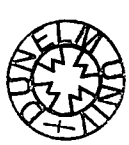

17 JAN 2001

Declaration

The content of this thesis is the original work of the author and has not previously been submitted for a degree at this or any other university. The work of other people is acknowledged by reference.

Zibisani Bagai

Department of Geological Sciences

University of Durham

September 2000

Copyright © 2000 by Zibisani Bagai

The copyright of this thesis rests with the author. No quotation or data from it should be published without Zibisani Bagai's prior written consent and any information derived from it should be acknowledged.

ACKNOWLEDGEMENTS

- I gratefully acknowledge the considerable constructive discussions and comments provided by Prof. Julian A. Pearce who supervised this study during the last two years. Zillion thanks!
- I also gratefully acknowledge the financial support provided by the University of Botswana through **Staff Development Training Office**. Furthermore, I greatly acknowledge the financial support given by the **Kaapvaal Craton Research Project** during the fieldwork. The Kaapvaal Craton Research Project has been financed by the University of Botswana through Research Grant# **R442**.
- Prof. Henri Kampunzu is thanked for his helpful advice and discussion during the fieldwork. He is also thanked for helping with the shipment of the samples from Africa to England and Australia. Thanks Henri!
- Dr. Richard Armstrong is thanked for carrying out U-Pb zircon dates for this study. Cheers Rich!
- Many thanks to Dr. Chris Ottley and Mr. Ron Hardy for their assistance in ICP-MS and XRF analyses respectively.
- I wish to thank Mrs Julie Harrison and Mr David Sales for the preparation of the thin-sections.
- I would like to thank Mr A.Carr for assisting in photographing thin-sections.
- I wish to thank my family at large for the moral support and encouragement they provided through out this study.
- I also wish to thank my friend Ishmael Baperi La-ka-Masesane for the time we spent together in Durham. Nda boka ntombo!
- Lastly, I must thank all other staff and students of the Department of Geology in Durham, who have made my time in Durham an enjoyable one.

Thanks!

Kelebogile! (setswana)

ABSTRACT

Geochemical and Geochronological investigations of the Vumba granite-greenstone terrain of NE Botswana

By Zibisani Bagai

U-Pb SHRIMP ages were determined for five samples representative of various granitoid groups from the Vumba granite-greenstone terrain, southwestern margin of the Zimbabwe craton in NE Botswana. These age data range from 2733 ± 5 Ma or 2696 ± 3.5 Ma (if the age for the protolith of an orthogneiss xenolith is excluded) to 2647 ± 4 Ma; they are in the range of published U-Pb zircon ages of 2710 ± 19 to 2639 ± 2 Ma for the Matsitama granite-greenstone terrain in NE Botswana. Precise crystallisation ages for granitoids from these two granite-greenstone terrains are compared with published U-Pb zircon ages of Archaean rocks exposed in the Zimbabwe craton. This comparison suggests that the Neoarchaean granitoids from NE Botswana are correlatives of the Sesombi granitoids/upper Bulawayan volcanic sequence of the Zimbabwe craton. Data from this study support diachronous growth of the craton.

The granitoids and spatially associated felsic metavolcanics, amphibolites and ultramafic intrusives all possess volcanic arc geochemical signatures. There are three granitoid types recognised based on petrographic and geochemical analyses: (i) granodiorite-tonalite (gneissic), (ii) biotite-hornblende quartz monzonite (gneissic) and (iii) monzogranite (post-kinematic). All the granitoids are medium- to high-K calc-alkaline and they possess I-type characteristics.

The felsic metavolcanics are rhyodacite/dacite in composition with variable contents of biotite, muscovite and hornblende. They are calc-alkaline and metaluminous to weakly peraluminous. They are interpreted as a volcanic arc sequence that formed from and melting of hydrated oceanic crust during subduction probably along a volcanic arc which represented the nucleus of felsic continental crust. Some of the associated granitoids are plutonic equivalents of these felsic rocks. There are two types of amphibolite, namely metabasaltic and metagabbroic. They are characterised by flat REE pattern, high Th/Nb ratio and calc-alkaline affinity. The amphibolites are interpreted as volcanic arc basalts formed from mantle wedge as a result of subducting oceanic slab.

The ultramafic intrusives of the Vumba granite-greenstone terrain are characterised by Nb depletion and high Th/Nb ratios. A subduction-related genesis is preferred for these rocks.

This work is dedicated to my late dad who passed away during the course of this study and my mum for their love and support.

CONTENTS

CHAPTER 1: INTRODUCTION

PAGE

CHAPTER 2: GEOCHRONOLOGY

CHAPTER 3: GRANITOIDS

CHAPTER 4: AMPHIBOLITES

CHAPTER 5: INTRUSIVE ULTRAMAFICS

CHAPTER 6: FELSIC METAVOLCANICS

CHAPTER 7: PETROGENESIS OF THE METAVOLCANICS

CHAPTER 8: DISCUSSION AND CONCLUSIONS

Chapter 1

INTRODUCTION

1.1. Background of study

Granite-greenstone terrains occur in many cratonic provinces of the world. They have attracted much attention largely because they provide a "window" to the composition, structure, and physical conditions of the Archaean mantle. They are the key to understanding the generation of continental crust at the early stage in Earth history. Additionally, many mineral deposits occur in Archaean greenstone belts among the most important of which are Cu, Ni, Fe, Au and Cr. Despite numerous studies, the geodynamic environment of formation of granite-greenstone terrains is still a matter of controversy. Most granite-greenstone terrains appear to have formed between 2600 and 2700 Ma, although the oldest known terrains formed between 3500 and 3800 Ma. Classical examples of the oldest known are the Isua, Barberton and Sabakwian granite-greenstone terrains in Greenland, South Africa and Zimbabwe respectively. Granite-greenstone terrains have been envisaged to have formed in a variety of tectonomagmatic environments such as accreted oceanic plateaux formed by mantle plumes, accreted oceanic island chains, volcanic arcs, back arc basins, microcontinents, or intracontinental rifts (Ben-Avraham et al., 1981; Kusky, 1989, 1998; Card, 1990; Hoffman, 1991; de Wet et al., 1992; Arndt et al., 1993; Bickle et al., 1994; Dostal and Mueller, 1997; Hunter et al., 1998; Jelsma and Dirks, 2000).

1.2. Regional geology of granite-greenstone terrains of NE Botswana

The granite-greenstone terrains of NE Botswana are all located in the southwestern part of the Zimbabwe Craton (Fig.1.1). The Zimbabwe Archaean craton of southern Africa consists of numerous classic granite-greenstone terrains. It is largely exposed in Zimbabwe and extends to the southwest into Botswana where it occupies an area of about 60000 km^2 (Carney et al., 1994). That represents about 15% of the Zimbabwe craton which covers an area of 800 by 500 km (Jelsma and Dirk, 2000). In northeast Botswana, the Zimbabwe Archaean craton includes the Vumba, Tati, Maitengwe and Matsitama granite-greenstone terrains (Bennet, 1968; Litherland, 1975; Key, 1976; Lintern, 1982; Aldiss, 1989; Majaule et al., 1997; Majaule and Davis, 1998). The Vumba, Tati and Maitengwe granite-greenstone terrains constitute the Francistown Granite-Greenstone Complex (Carney et al., 1994). They are considered typical Archaean granite-greenstone terrains comparable with granite-greenstone terrains in Zimbabwe. The Matsitama granite-greenstone terrain, which is part of the Mosetse Complex, is regarded as atypical in the sense that it lacks acid volcanics and has a greater abundance of clastic metasediments compared to the other granite-greenstone terrains. The Matsitama terrain is situated west of the Vumba granite-greenstone terrain (see Fig.1.1).

The NE Botswana greenstone successions are engulfed in a sea of gneisses and various granitoid suites. The gneisses and granitoids have been largely regarded as contemporaneous to the greenstone successions. The nature of the basement upon which the greenstone successions were erupted is still a geological problem that needs to be resolved. Because contacts between greenstone successions and surrounding terrains are poorly exposed, it is hard to determine their relative age relationship.

The proposed geotectonic evolutionary models for the granite-greenstone terrains of NE Botswana have been controversial mainly because there has been no

comprehensive geochemical investigation on the greenstones and related granitoids in this area. The controversy is made worse by the lack of precise and reliable geochronological studies in the area. The ages of the granitoids and gneisses have largely been assumed from regional correlations with some granitoid suites in Zimbabwe. A few geochronological studies conducted in the Francistown Granite-Greenstone Complex yielded late Archaean ages. For instance, the Tati Volcanic Group yielded a Rb-Sr isotope age of 2523 ± 33 Ma and a granite from the same area gave K-Ar ages of 2500 ± 100 Ma and 2285 ± 70 Ma (Carney et al., 1994). It is worth noting that resetting and open-system behaviour of the Rb-Sr and K-Ar isotope systems as well as the large uncertainties associated with these ages, preclude any reliable correlation between the various units of the Granite-Greenstone Complex. However, most previous authors have used these relatively young ages to correlate the greenstone successions of the Francistown Granite-Greenstone Complex with the Upper Bulawayan Group which is constrained between 2700 Ma and 2650 Ma (Wilson et al., 1979, 1995).

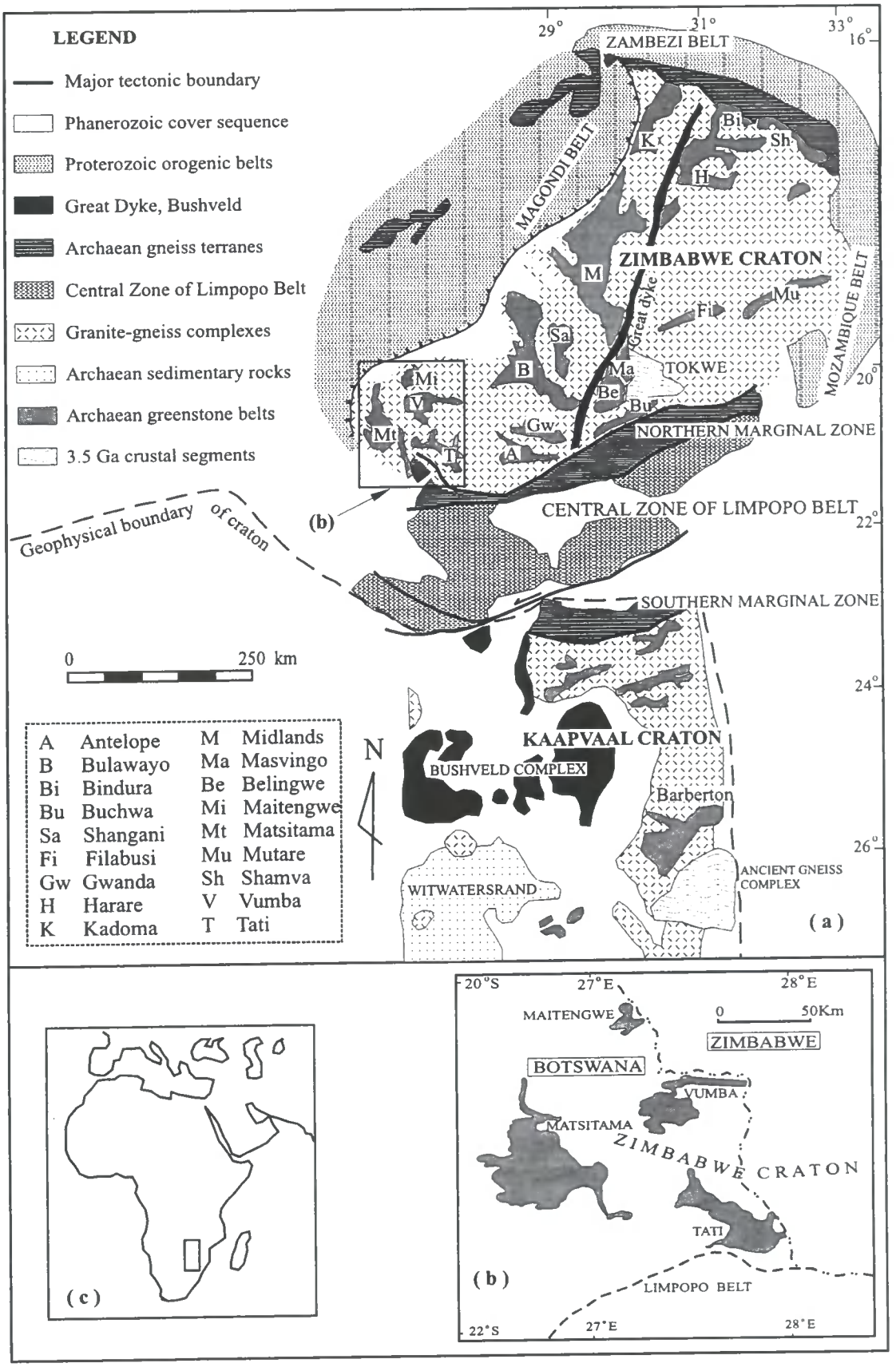

Figure. 1.1: (a) Map showing the main geological units of Southern African cratons and adjacent Proterozoic belts (Modified from Treloar and Blenkinsop, 1995, and Jelsma and Dirks, 2000). The rectangle locates the map of Fig. 1.1b. (b) Distribution of the four granite-greenstone terrains of the Zimbabwe craton in NE Botswana. (c) Location of the Southern Africa cratons.

1.3. Objectives of the study

The objectives of this study are as follows:

(i) to constrain the emplacement ages of granitoid rocks of the Vumba granite-greenstone terrain and compare the ages with those of felsic rocks in Zimbabwe craton. This will enable one to compare the evolution of the Archaean rocks of NE Botswana with the existing tectono-magmatic framework of the Zimbabwe craton. The absolute ages are an integral part of information necessary to characterise relationships within the group of plutons.

(ii) to characterise geochemically the granitoids, amphibolites, intrusive ultramafics and felsic metavolcanics of the Vumba granite-greenstone terrain.

(iii) to discuss the evolution of the Vumba granite-greenstone terrain.

(iv) to propose an appropriate geodynamic model of the Vumba granite-greenstone terrain. Special emphasis is placed on establishing geochemical signatures and geodynamic setting from the granitoids, amphibolites, intrusive ultramafics and felsic metavolcanics in this terrain.

1.4. Analytical techniques used in this thesis

The techniques used in this study in order to achieve the above-stated objectives are summarised below (Table 1.1). Methods of sample preparation, analytical procedures and estimates of precision and accuracy are presented in Appendices A and C.

ANALYTICAL TECHNIQUES	NUMBER OF SAMPLES	ELEMENTS	LABORATORY	EQUIPMENT
XRF (wr)	Granitoids = 51 Amphibolite = 29 Felsic metav = 28 Ultramafics = 12 **TOTAL = 120**	Major elements Trace elements (Sc, V, Cr, Co, Ni, Cu, Zn, Ga, Rb, Sr, Y, Zr, Nb, Ba, La, Ce, Nd, Pb, Th, U)	Durham University	Philips PW 1400
ICP-MS (wr)	Granitoids = 30 Amphibolite = 15 Felsic metav = 9 Ultramafics = 6 **TOTAL = 56**	Sc, Cr, V, Ni, Co, Zn, Ga, Rb, Sr, Y, Zr, Nb, Cs, Ba, La, Ce, Pr, Nd, Sm, Eu, Gd, Tb, Dy, Ho, Er, Tm, Yb, Lu, Hf, Ta, Pb, Th, U	Durham University	PE SCIEX ELAN 6000
U-Pb SHRIMP	Granitoids = **5**	^{206}Pb, ^{238}U, ^{204}Pb, ^{207}Pb, ^{235}U, Th	Australian National University	
MICROSCOPY	Granitoids = 27 Amphibolite=14 Felsic metav = 9 Ultramafics = 6		Durham University	MICROSCOPE SWIFT MODEL F POINT COUNTER

Table 1.1. Summary of analytical techniques used in this study. Abbreviation: metav – metavolcanics; wr – whole-rock.

1.5. Geological setting and sampling

As is typical for the Archaean terrains, the Vumba granite-greenstone terrain has a very complex tectonic history. Most of the lithological units have experienced intensive multiple deformation, medium to high-grade metamorphism, partial melting and magmatic injection (Litherland, 1975; Ludtke et al., 1989 and Carney et al., 1994). These tectonic events have obliterated much of the original geological and tectonic relationships, and possibly overprinted original crystallisation ages.

The geology of the Vumba granite-greenstone terrain is characterised by intrusive ultramafics, metavolcanics, metasediments and granitoid rocks (Fig.1.2). Intrusive ultramafics mainly comprise serpentinites and metapyroxenites. The metavolcanic rocks include mafic and felsic volcanic rocks. The mafic metavolcanic

rocks, in the form of amphibolites, dominate the stratigraphy of the area. Felsic metavolcanic rocks, which range from rhyolite to dacite (Ludtke et al., 1989), are ubiquitous. Metasediments are subordinate to metavolcanic rocks and include marbles, calc-silicates, aluminous schists and quartzite (Litherland, 1975). There are various generations of granitoids and these dominate the geology of the Vumba granite-greenstone terrain.

The complexity of the tectonic history coupled with poor grade of exposure in the Vumba granite-greenstone terrain prohibits any direct determination of the stratigraphy. Nevertheless, Litherland (1975) deduced the stratigraphy of the Vumba supracrustal rocks principally by means of regional correlation with the local greenstone successions and other greenstone sequences in Zimbabwe. He divided the supracrustal rocks into two lithological Groups that he termed the Tutume and the Vumba Volcanic Groups. Furthermore, he subdivided the later into six stratigraphic formations, namely in chronological order the Vukwi Meta-arkose, the Sebina Ultramafic, the Vumba Mixed Volcanic (VMV), the Vumba Lower Felsic (VLF), the Vumba Lower Mafic (VLM), the Vumba Upper Felsic (VUF) and the Vumba Upper Mafic (VUM) Formations (Fig. 1.2). For the purpose of the present investigation, only the Vumba Volcanic Group and the associated granitoids are considered. The Vukwi Meta-arkose and the Sebina Ultramafic Formations were omitted during sampling due to their worse exposure.

According to this stratigraphic succession, the mafic and felsic metavolcanics show cyclic deposition. However, the manner as to how these volcanic cycles formed is still unclear. One possibility is that crystal fractionation in the magma chamber may have been accompanied by episodic expulsion of successive magma batches. Another view is the possibility of imbricate thrust stacking of the rocks to produce repetitive cycles. This possibility is supported by the preponderance of mylonitic rocks and shear

zones observed in the area. Nonetheless, this needs verification by isotopic dating. Recently, Jelsma and Dirks (2000) have revealed that imbricate stacking is a common tectonic feature in the Zimbabwe craton, following a detailed structural-metamorphic and dating work on the Harare-Shamva granite-greenstone terrain. They discovered that some units that were interpreted as the stratigraphic base were significantly younger than their overlying units.

The stratigraphic division by Litherland as a whole is controversial (e.g. Ludtke et al., 1989). Key et al. (1976), on the basis of structural analysis, suggested that the Tati and Vumba greenstone terrains were overturned prior to penetrative deformation. The poor level of exposure in the area means that the nature of the boundaries between most of the lithological units is not fully understood. It also means that the geological boundaries are generally positioned on the geological map with uncertainty.

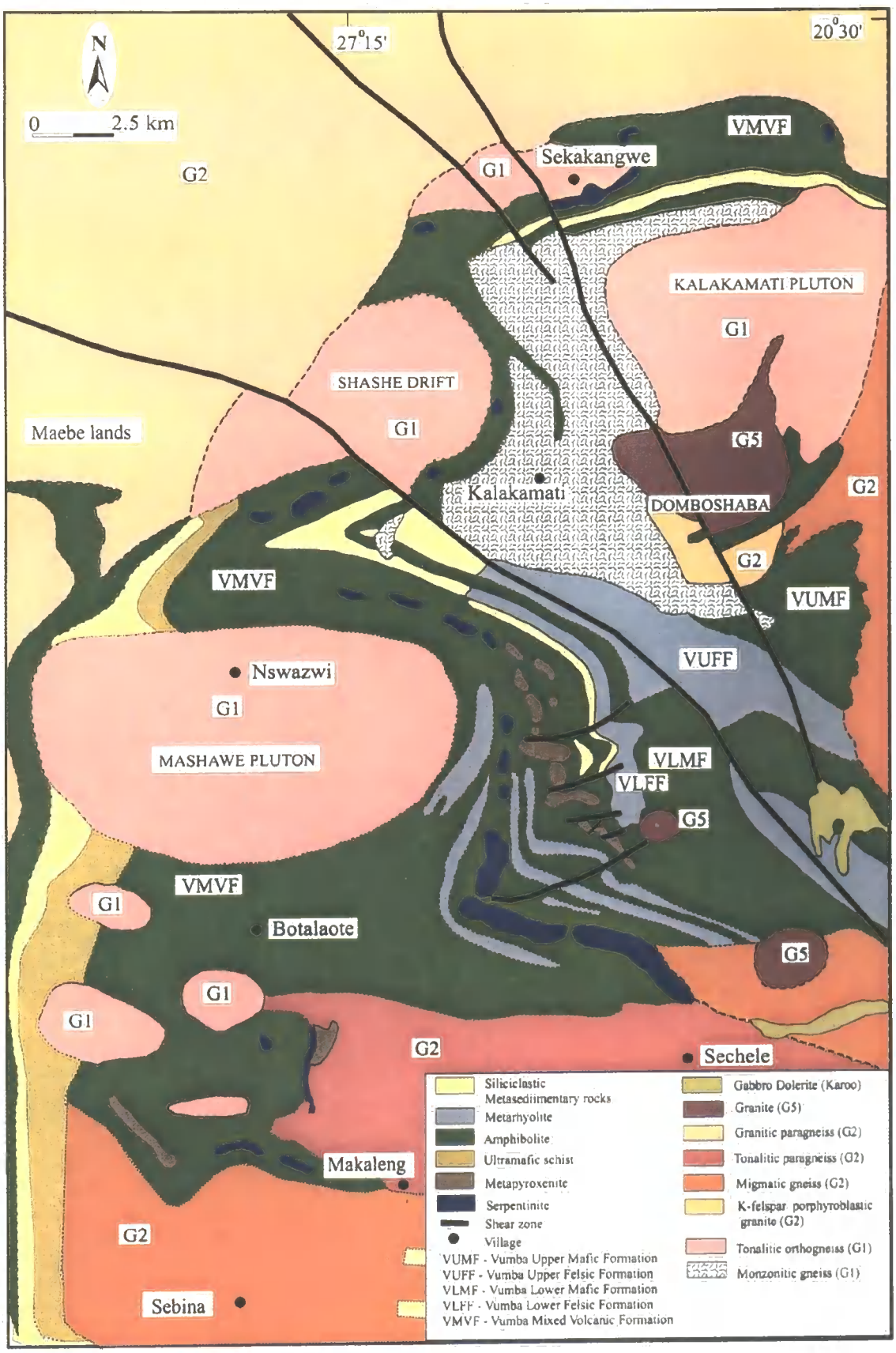

Figure. 1.2: Simplified map outlining the main geological units of the Vumba granite-greenstone terrain (slightly modified Litherland, 1975).

A total of one hundred and twenty (120) rock samples were collected for geochemical investigations over an area of about 750 km^2 in the Vumba granite-greenstone terrain. Five representative samples from different generations of granitoid units were selected for isotopic dating. Geochemical sampling was restricted to serpentinites, metapyroxenites, amphibolites, felsic metavolcanics and granitoids. It is important to realise that the total number of samples collected from each rock unit was dictated to a large extent by its areal size and exposure as well as deformation state. Weathered and sheared samples were avoided during sampling. Within these limits, sampling was conducted in a random manner.

Six representative samples were collected from the intrusive serpentinised ultramafics. This is intrusive into the Vumba Mixed Volcanic Formation and forms the most prominent kopje-rows in the Vumba granite-greenstone terrain. It forms a chain of boudin-shaped kopjes that can be traced from Sekakangwe village in the north throughout the Vumba Mixed Volcanic Formation to Sechele village in the south (Fig.1.2). The serpentinites are associated with metapyroxenites, which form similar kopje-row outcrops. The two bodies run parallel and locally contiguous to each other in the west, and they diverge in the southeast. Litherland (1975) interpreted these bodies of serpentinised ultramafic and metapyroxenite as syntectonic sills. Ludtke et al (1989) compared these bodies with the Mashaba and Shabani complexes in Zimbabwe and considered them to be the feeders to komatiitic flows. They reported remnants of komatiites in the Vumba granite-greenstone terrain, which the present study failed to observe despite considerable effort. Six metapyroxenite samples were collected for geochemical studies. Metagabbro is locally observed at the base of the serpentinised ultramafics. Loose blocks that fall from the hilltop obscure the contact. However, four representative samples of the metagabbro were collected for geochemical and petrographic investigations.

A total of twenty-nine samples of amphibolite were collected from the different formations as follows. Nineteen samples were collected from the Vumba Mixed Volcanic Formation, which is the most complex and widely distributed unit of the Vumba Volcanic Group. Six and four samples were collected from the Vumba Lower Mafic and Vumba Upper Mafic Formations respectively. The amphibolites in the Vumba granite-greenstone belt have been classified into six types: schistose, speckled, gabbroic, mesh, basaltic and porphyroblastic (Litherland, 1975). This classification was based on field description of grain size, texture, colour and fissility. The majority of the amphibolite types are confined to particular areas (Litherland, 1975). The basaltic and schistose amphibolites are the most common types, with the latter dominating the Vumba Mixed Volcanic Formation.

Felsic metavolcanics crop out in the Vumba Mixed Volcanic, Vumba Lower Felsic and Vumba Upper Felsic Formations. Eleven (11), eight (8) and nine (9) samples were collected respectively from each of these formations. In the Vumba Mixed Volcanic Formation, felsic metavolcanics form discontinuous lenses intercalated with amphibolites. Metarhyolites in the Lower Vumba Felsic and Upper Vumba Felsic Formations are associated with aluminous schists, quartzite, various types of amphibolite, marble and calc-silicate rocks.

The granitoids exhibit a wide range of composition and deformational states. Litherland (1975) first classified the granitoids in the Vumba granite-greenstone terrain on the basis of deformation state, mode of origin and mineral composition. On the basis of the above-mentioned criteria, Key et al. (1976) divided the granitoids in the NE-Botswana, including the Vumba granite-greenstone terrain, into five chronological groups which they denoted as G1, G2, G3, G4 and G5. According to these authors, the main characteristics of these five groups of granitoids are as follows: (i) G1 granitoids are tonalite and monzonite intrusive bodies and orthogneisses developed at their

margins; (ii) G2 granitoids are gneisses and migmatites formed from melting of a predominantly sedimentary protolith and containing various orthogneissic xenoliths from greenstone successions; (iii) G3 granitoids are anatectic adamellites originating from the melting of a gneissic protolith; (iv) unfoliated granitoids were grouped into G4 (tonalites) and G5 (granites). These two groups of granitoids were taken to be post-kinematic. In the current study, mineral fabrics and kinematic indicators were observed in some G5 stocks, which shows they have been subjected to tectonic deformation. Locally, the mineral fabric is more pronounced than in most G1 plutons.

G1 orthogneisses are the preponderant granitoids in the study area. They include the Mashawe, Shashe Drift, Kalakamati Monzonite, Kalakamati and Sekakangwe Plutons (Fig.1.2). All these plutons are tonalitic orthogneisses except the Kalakamati Monzonite Pluton, which is a monzonitic orthogneiss (Litherland, 1975; Key, 1976). However, the Kalakamati Monzonite was mapped as a tonalitic orthogneiss by Ludtke et al. (1989). The G1 plutons exhibit heterogeneous mineral fabrics.

The oval-shaped Mashawe Pluton, which is the largest G1 body in the study area, is mainly composed of poorly exposed "whale-back" outcrops. In hand specimen, it appears light grey, medium to coarse grained with conspicuous foliation. The contact of the Mashawe Pluton with the neighbouring units is poorly exposed. Five rock samples were collected from this pluton for geochemical investigation.

The Shashe Drift Pluton lies north of the Mashawe Pluton and is contiguous to the G2 unit. Its existence is speculative (Litherland, 1975). It forms kopje outcrops with relatively strong mineral fabrics. In hand specimen, it appears grey in colour with a medium to coarse grain size. It also appears richer in mafic minerals than the Mashawe Pluton. Moreover, the Shashe Drift Pluton contains mafic enclaves. The contact between this unit and the country rock is not exposed. Four rock samples were taken from this unit for geochemical investigation.

The Kalakamati Monzonite Pluton forms a cluster of kopjes with very strong mineral fabrics. It is coarse to medium-grained, grey and richer in mafic minerals than all the other G1 plutons in the study area. The Kalakamati Monzonite forms an extensive irregular body, which becomes thinner towards the north. In this project eight rock samples were obtained from this unit for investigations.

Contiguous to the Kalakamati Monzonite is the circular Kalakamati Pluton made of isolated kopjes. Its contact with adjacent units is poorly exposed. It is light grey, fine to medium grained and very weakly foliated. Three samples were collected from this pluton for geochemical investigation.

The Sekakangwe Pluton forms the smallest of the G1 bodies that are described above. It is a small, elongated body made of isolated "whale-back" outcrops. In hand specimen it is leucocratic, medium to coarse grained and weakly foliated.

The origin of G2 as a whole is contentious. It has previously been interpreted in terms of progressive granitisation largely of supracrustal lithologies. G2 granitoids in the Vumba granite-greenstone terrain comprise granitic and tonalitic gneisses (Key et al., 1976). The former is confined to the north and west, and the latter lies in the east and south of the area. The granitic gneisses on the western side form a cluster of kopje outcrops, which look similar to the tonalitic gneiss outcrops of the Shashe Drift Pluton. This study could not define the boundary between the two units using field criteria. Unlike the granitic gneisses, the tonalitic gneisses form poorly exposed isolated "whale-back" outcrops. For the present study eighteen rock samples were collected from the G2 granitic gneiss.

The G3 granitoids are subdivided into adamellite and tonalite anatectites. They form extensive bodies with very irregular contacts (Litherland, 1975; Key et al., 1976). Adamellite granitoids are well exposed in the form of isolated kopjes, whereas the tonalitic anatectites hardly form kopjes. No rock samples were collected for

geochemical investigation from this unit because they all crop out outside the study area.

The G5 granites are late-stage granites which form stock-like bodies with sharp contacts and little or no local metamorphism (Litherland, 1975). A typical example in the project area is the Domboshaba Granite, which invades the G1 Kalakamati Pluton and the G1 Kalakamati Monzonite. The Domboshaba Granite displays two phases, which Litherland (1975) defined as inner granite and outer granite. However, the latter does not completely encompass the former. The inner granite is pink, coarse to medium grained and granular while the outer granite is light pink, medium to fine grained and granular.

Other small G5 stocks, which invaded the Vumba greenstone terrain, include the Sechele and Vumba Central Stocks. The two stocks appear distinct from the Domboshaba granite in hand specimen. The Vumba Central Stock forms a small, circular, coarse grained body with a greenish tint to the plagioclase that is probably due to epidotisation. The Sechele Stock is composed of a medium to coarse-grained, light grey and granular biotite adamellite (Litherland, 1975). The intrusion is circular in plan. The present investigation identified a porphyritic texture in the central portion of the Sechele stock. Nine, three and one rock samples were collected from Domboshaba Granite, Sechele Stock and Vumba Central Stock respectively.

The Vumba granite-greenstone terrain is dissected by numerous mafic and felsic dyke swarms with a wide range of orientations. The mafic dykes are mainly dolerites of late Karoo provenance (Key et al., 1976). Litherland (1975) regarded felsic dykes, which are aplogranitic (Ludtke et al., 1989), as contemporaneous to G2 activity.

Geochronological information is necessary to complement and test geological inferences based on the geochemical and structural data. Samples were collected throughout the Vumba granite-greenstone terrain for U-Pb zircon geochronological

investigations. Representative samples were collected from all the granitoids including G1, G2, G4 and G5. In addition, a xenolith sample from the G2 granitoid near Sebina village was sampled for geochronological consideration.

1.6. Description of the thesis

This thesis consists of eight chapters. **Chapter 1** is the introduction. It covers the background of study, the regional geology and location of the study area as well as the geological setting and sampling. It also covers the objectives of the study as well as the analytical techniques used in this study.

Chapter 2 presents the geochronological results on the granitoids from the Vumba granite-greenstone terrain. In this chapter, the results from this study are compared with published data from other areas of the Zimbabwe craton. Regional implications and the validity of previous chronology of the granitoids are evaluated.

Chapter 3 documents the petrographic and geochemical characteristics of granitoids from the Vumba granite-greenstone terrain. The geochemistry component is divided into three sections. In the first section the granitoids are characterised on the basis of their major element contents. The second section presents the interpretation of their trace element characteristics as indicated by trace element variation diagrams, REE patterns, multi-element patterns and LILE modelling. In the third section the granitoids are interpreted in terms of geotectonic settings as shown by ORG-normalised diagrams and tectonic discrimination diagrams.

Chapter 4 documents the petrographic and geochemical characteristics of the amphibolite rocks. The geochemical component comprises the evaluation of element mobility, the identification of the amphibolite protoliths, the geotectonic settings of amphibolite protoliths and the geochemical and REE patterns.

Chapters 5 and **6** present petrographic and geochemical characteristics for the ultramafic intrusives and the felsic metavolcanics respectively. **Chapter 7** presents the petrogenetic modelling for the amphibolites and the felsic metavolcanics using Ti, Nb, Y and Zr. This is a brief chapter aimed at unravelling any petrogenetic relationship between the amphibolites and the felsic metavolcanics by magmatic evolution.

Chapter 8 discusses the evolution and geotectonic settings of the Vumba granite-greenstone terrain in view of new geochronological and geochemical data from this study. An attempt has been made to interpret the evolution of this terrain within the tectonomagmatic framework of the Zimbabwe craton (host craton for the Vumba granite-greenstone terrain). This chapter also summarises all the conclusions presented in previous chapters.

Chapter 2

GEOCHRONOLOGY OF THE GRANITOIDS

2.1. Introduction

The granite-greenstone terrains of Zimbabwe have been largely used in the ongoing debate on: (1) the geotectonic evolution and crust stabilization processes during the Archaean; and (2) the origin of Archaean granite-greenstone terrains around the world (Nisbet et al., 1981; Ridley and Kramers, 1990; de Wit et al., 1992; Kusky and Kidds, 1992; McCourt and Wilson, 1992; Treloar et al., 1992; Bickle et al., 1993, 1994; Chauvel et al., 1993; Blenkinsop et al., 1993, 1997; Fedo et al., 1995; Rollinson and Blenkinsop, 1995; Treloar and Blenkinsop, 1995; Jelsma et al., 1996; Ridley et al., 1997; Dirks and Jelsma, 1998a,b). One major problem in this debate has always been the limited amount of reliable geochronological constraints on which several models were based (see review in Taylor et al., 1991). However, during the last five years a number of precise zircon ages have been obtained on the felsic rocks from Archaean granite-greenstone terrains in Zimbabwe (e.g. Mkweli et al., 1995; Wilson et al., 1995; Vinyu et al., 1996; Jelsma et al., 1996). Most investigations on the Zimbabwe Archaean craton neglected the portion of the craton exposed in Botswana.

Two distinct geochronological projects have been undertaken to date the granite-greenstone terrains of NE-Botswana by the Geological Survey of Botswana (Matsitama area: Majaule and Davis, 1998) and the University of Botswana (Vumba area: this study).

2.2. Geological setting of granitoids in NE Botswana

The main lithological units in the Vumba granite-greenstone terrain are shown in Figure 2.1 on which the dated samples are also located. Based on the presence or not of a strong foliation and using petrographic features, Key et al. (1976) divided the granitoids from NE Botswana into five chronological groups named G1 (oldest), G2, G3, G4 and G5 (youngest). The G4 and G5 granitoids were taken to be post-kinematic and emplaced at 2560 ± 40 Ma (Key et al., 1976). Granite and pegmatite veins/dykes were assumed to be syn-or pre-G3. U-Pb zircon SHRIMP age obtained on these granite and pegmatite veins/dykes in the Tati granite-greenstone terrain yielded a Mesoproterozoic age of 1022 ± 6 Ma (van de Wel et al., 1998). This young age casts some doubts on the ages of granitoids in NE Botswana and on the tectono-magmatic evolution of the southwestern margin of the Zimbabwe craton. These enigmas have been addressed by: (1) dating granitoids in the Matsitama granite-greenstone terrain using the U-Pb conventional single zircon technique. All the samples of granitoids from the Matsitama area yielded U-Pb zircon ages which range from 2639 ± 2 to 2710 ± 19 Ma (Majaule and Davis, 1998); (2) dating granitoids in the Vumba granite-greenstone terrain using U-Pb SHRIMP zircon technique (this study). The results allow the author to constrain accurately the timing of emplacement of granitoids in this area. The new ages are compared to the ages of felsic igneous rocks in the Matsitama granite-greenstone terrain and allow the author to better constrain the felsic igneous events at the southwestern margin of the Zimbabwe craton in Botswana. Further comparison with the U-Pb zircon age data set for Archaean felsic rocks in Zimbabwe enables the author to integrate Archaean granite-greenstone terrains of NE Botswana into the wider picture of the Archaean evolution of the Zimbabwe craton.

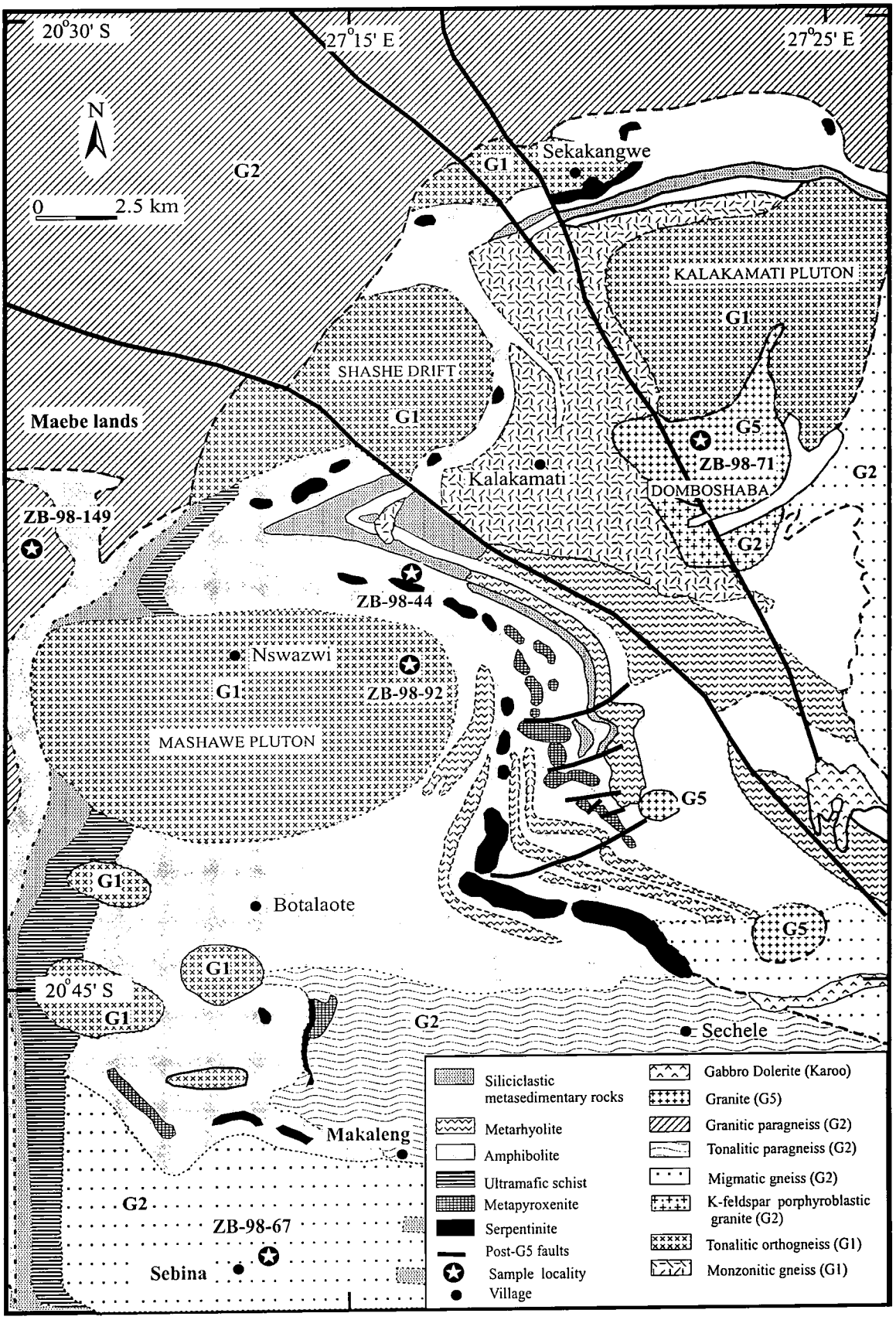

Figure 2.1: Simplified map outlining the main geological units of the Vumba granite-greenstone terrain with locations of dated samples (slightly modified Litherland, 1975).

2.3. Geochronological Results

U-Pb SHRIMP single zircon crystallisation ages were determined on five representative samples of various granitoids exposed in the Vumba granite-greenstone terrain in NE Botswana. The analytical procedure is documented in Appendix A while the zircon analytical data is listed in Appendix B (I). The results of zircon dating are presented in the previously assumed chronological order, i.e. from G1 to G5.

2.3.1. G1 Mashawe Tonalitic orthogneiss: sample ZB-98-92

Sample ZB-98-92 was collected from the Mashawe Pluton, which forms the largest body of the so-called G1 tonalitic orthogneiss in the Vumba granite-greenstone terrain. The Mashawe pluton forms an oval-shaped body (ca. 14.3 x 7.5 km) unequivocally intruding the lower volcanic sequence of the Vumba Group. It exhibits variable foliation trends with generally a sub-vertical dip. The dated sample is from a homogeneous kopje located east of the Nswazwi village (Fig. 2.1). The foliation attitude in the outcrop is 180 °/60°. In hand-specimen, the rock is homogeneous, leucocratic, light grey and medium-grained. Biotite and quartz define the conspicuous foliation. In thin section, the rock is granodioritic and consists of quartz, plagioclase (slightly sericitised), microcline and sporadic anhedral biotite. Zircon, Fe-Ti oxide, apatite and muscovite are accessory minerals.

Unlike the zircons separated from other samples, this rock yielded a crop of zircons, which are generally of poor quality. Subhedral to anhedral grains are zoned with some broad zones of intense alteration and radiation damage induced by high radioactive element contents. Some totally altered zircons are milky white. The least altered zircon grains or areas within grains were targeted for analysis. Sixteen analyses were performed on fifteen different zircons with the data plotted on a conventional concordia diagram (Figure 2.2) and

presented in Appendix D (ii). Although a number of the analyses show severe disturbance (Pb-loss) and are discordant, there are sufficient data which are concordant or near-concordant (>90%) to give confidence in a $^{207}Pb/^{206}Pb$ age calculated from these selected data. A weighted mean $^{207}Pb/^{206}Pb$ age gives 2686 ± 6 Ma for these data, with the exception of analysis 14.1 which is younger.

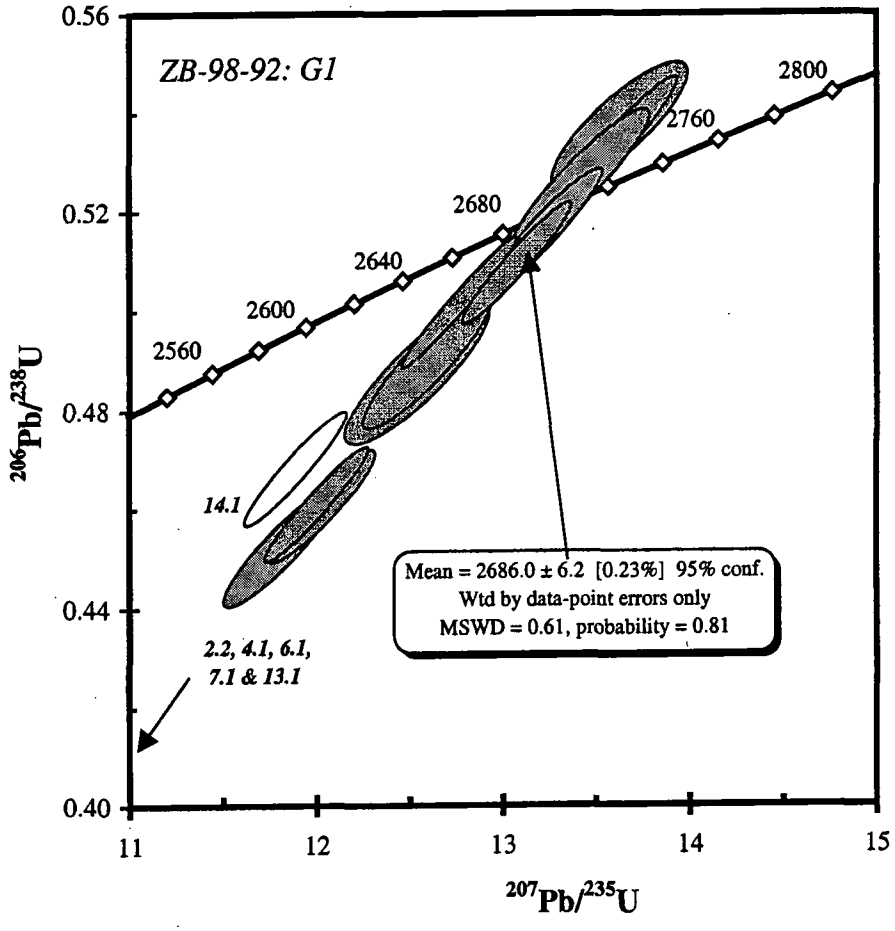

Figure 2.2: U-Pb concordia plot of SHRIMP data for sample ZB-98-92. The age shown is calculated from the filled ellipses. The discordant analyses 2.2, 4.1, 6.1, 7.1 and 13.1 plot out of the field of view and were not included in the $^{207}Pb/^{206}Pb$ age calculation shown

2.3.2. G2 Sebina paragneiss: Xenolith sample ZB98-67

Sample ZB-98-67 is a xenolith collected from the G2 granitoid, which was mapped as tonalitic paragneiss or xenolithic paragneiss by Litherland (1975) and Key et al. (1976), respectively. The sample was collected near Sebina village, where the unit is well exposed. This unit essentially forms discontinuous whaleback outcrops with an east-west-trending and sub-vertical foliation. In hand-specimen, the rock is grey, medium-grained and displays conspicuous preferred orientation of light and dark minerals. The sample is amphibolitic gneiss in thin section with hornblende, slightly sericitised plagioclase and sporadic quartz as essential phases.

The zircons from this sample show well-developed sector and concentric zoning and vary in shape from some distinctly oblate forms to euhedral grains up to 400 μm in length. All zircons are light brown in colour. Sixteen U-Th-Pb analyses were done on fifteen different zircons with the data reported in Appendix B (I) and plotted on a conventional Wetherill U-Pb concordia plot in Figure 2.3. Apart from two highly discordant analyses (8.1 and 14.1) all data plot in a group which straddles the concordia curve and gives a weighted mean $^{207}Pb/^{206}Pb$ age of 2733 ± 5 Ma (n = 14; MSWD = 0.33; probability = 0.99). The zircons from this rock generally have low U concentrations (from 49 ppm) with a few more enriched grains with up to 229 ppm. The $^{207}Pb/^{206}Pb$ age of 2733 ± 5 Ma is considered to be the magmatic age of these zircons and the emplacement age of the protolith to this orthogneiss xenolith.

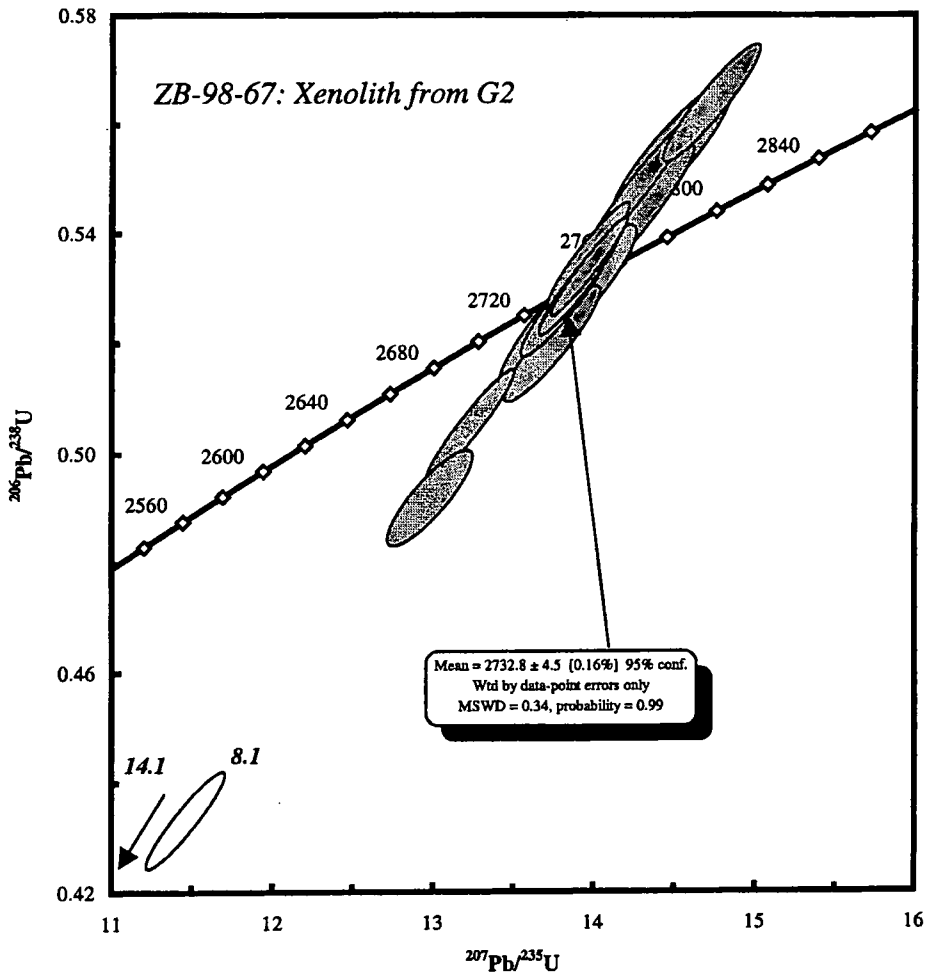

Figure 2.3: U-Pb concordia plot of SHRIMP data for sample ZB-98-67. The discordant analyses 8.1 and 14.1 were excluded from the calculated 207Pb/206Pb age.

2.3.3. Maebe G2 Granitic gneiss: sample ZB-98-149

Sample ZB-98-149 was collected from the so-called G2 granitic paragneiss. This group forms scattered kopjes of a gneiss showing an east-west-trending and sub-vertical foliation. The rock is homogeneous, greyish and medium-grained. It is tonalitic and consists of microcline, plagioclase (sericitised), quartz, hornblende and biotite. Zircon, Fe-Ti oxide, epidote and apatite are the accessory minerals. In thin section, the rock exhibits a solid-state deformation fabric marked by a mosaic of ductilely-deformed quartz, aligned mafic minerals and bent biotite.

The zircons from this sample are 90-80 μm in length, subhedral and euhedral, with magmatic compositional zoning preserved. Many zircon grains have fractures and occasional highly metamict zones. The SHRIMP U-Pb analyses of zircons from this rock show more complexity and disturbance (Appendix B (I); Figure 2.4) than for the other samples from this study. Most analyses are highly discordant. The lack of a single discordia also shows that there is more than one episode of Pb-loss to take into account when assessing the data for geochronology. Regression of all the data predictably shows that there is excess scatter (upper intercept = 2754 ± 71 Ma; MSWD = 12), attributable to some geological disturbance. The $^{207}Pb/^{206}Pb$ age of 2690 ± 4 Ma for the most concordant analysis (#1.1; 4% discordant) is the best minimum estimate of the age of this granitoid. Regression of the two points sited within this single grain gives 2714 + 46/-26 Ma (lower intercept = 775 ± 520 Ma).

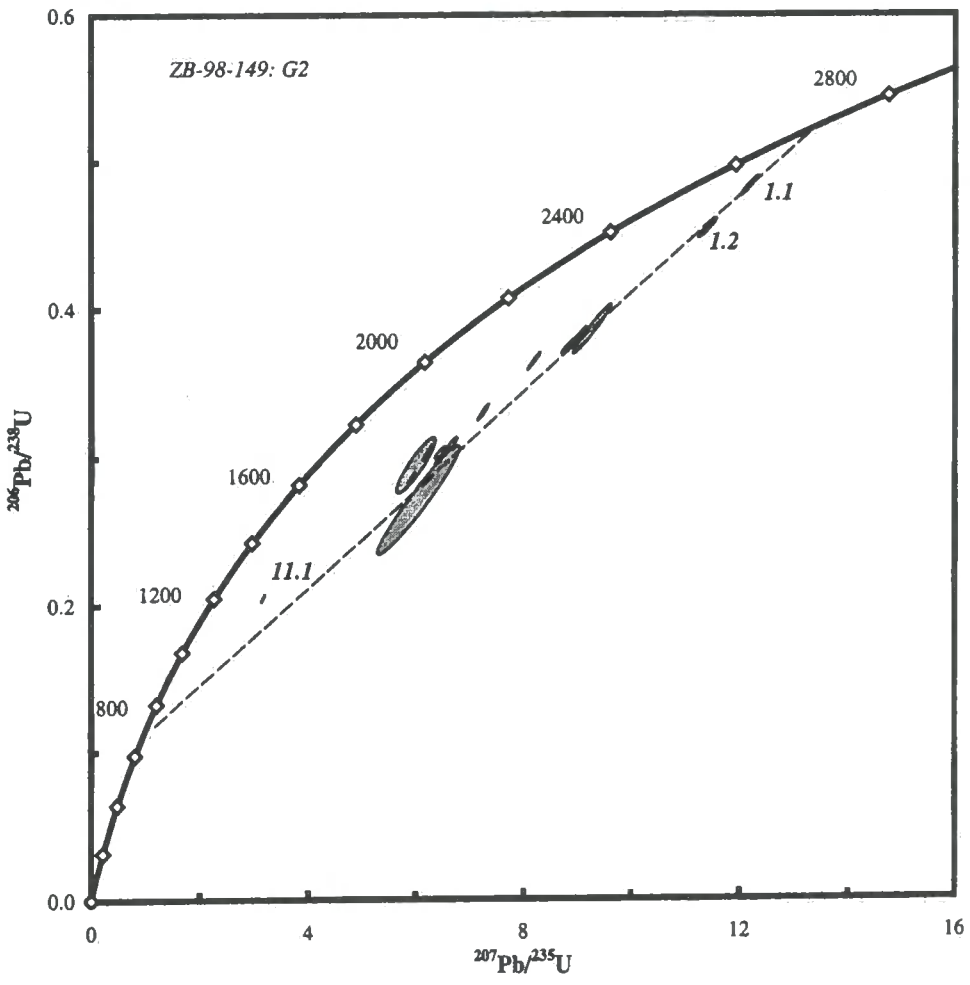

Figure 2.4: U-Pb concordia plot of SHRIMP data for sample ZB-98-149. The dashed line represents the regressed discordia chord for the two analyses from grain #1, and which yielded an upper intercept age of 2714 + 46/-26 Ma.

2.3.4. G4 Vumba Tonalitic granitoid: sample ZB-98-44

Sample ZB-98-44 was collected from a small intrusion (15 x 25 m) intersecting the west-east-trending serpentinite and metapyroxenite units in the Vumba Mixed Volcanic Formation. The rock is grey, massive, porphyritic and medium-grained. It is quartz dioritic and comprises anhedral to subhedral plagioclase phenocrysts in a groundmass of quartz, K-feldspar and hornblende. Zircon, apatite and opaques are accessory minerals.

The zircons from this rock are light purple, subhedral, and show a pronounced oblate form. All are strongly zoned with concentric compositional zoning from centres to rims.

The single magmatic population observed above yielded a tightly-constrained, concordant group of data (Appendix B(I); Figure 2.5). All but one of the fourteen analyses combine to define a single weighted mean $^{207}Pb/^{206}Pb$ age of 2696 ± 3.5 Ma (MSWD = 0.60). The one exception is analysis 2.1 which was very discordant and was excluded from the age calculation. The data for these zircons appear to give a straightforward age of crystallisation for this rock.

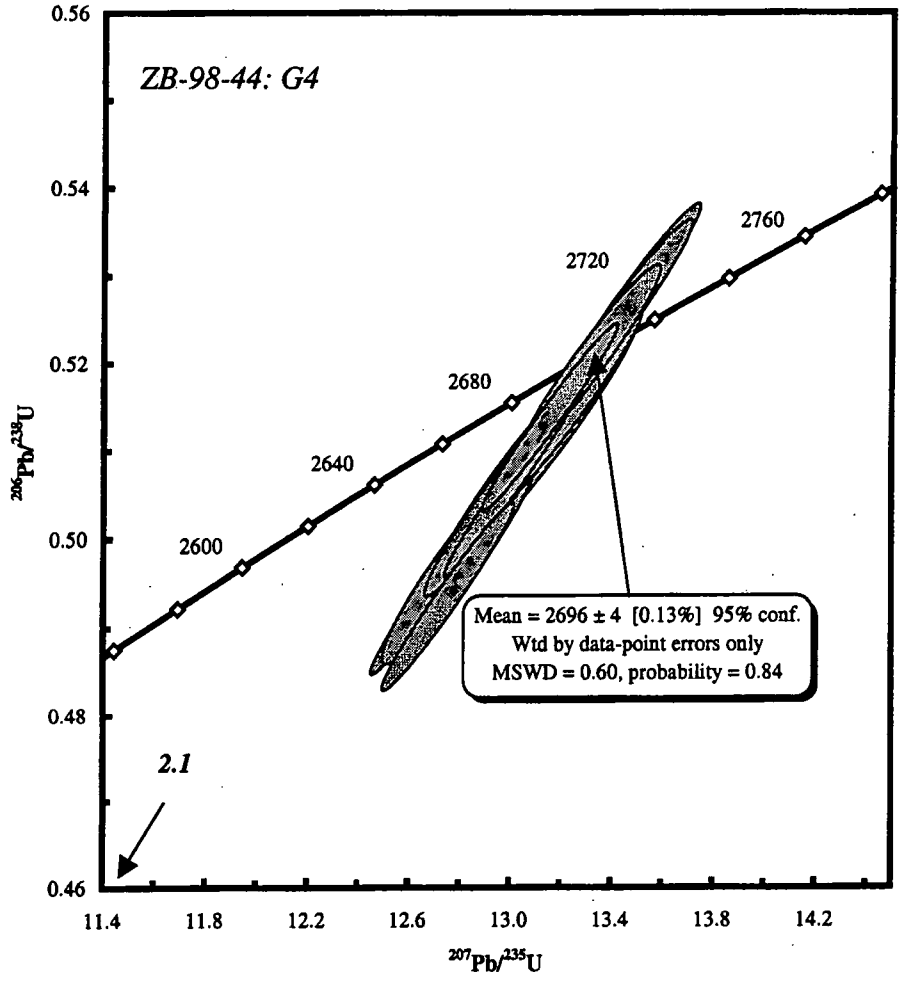

Figure 2.5: U-Pb concordia plot of SHRIMP data for sample ZB-98-44. The single discordant analysis 2.1 plots off-scale and was not included in any age calculation.

2.3.5. G5 Domboshaba Granite: sample ZB-98-71

Sample ZB-98-71 was collected from the Domboshaba Granite, which constitutes the biggest and most irregularly shaped body of the G5 granitoid group in theVumba granite-greenstone terrain. The Domboshaba Granite is exposed over c. 12 km^2 and does not show any deformation fabric. It is a massive, homogeneous, medium- to coarse-grained pink granite. The rock is monzogranitic and consists of microcline, perthite, plagioclase, quartz, biotite and sporadic calcic amphibole. Both biotite and amphibole are slightly chloritised. The granophyric texture is common in this granite. The accessory phases comprise zircon, apatite, and Fe-Ti oxide. Rare secondary muscovite occurs locally.

The zircons from this rock are subhedral, dark brown and appear to be somewhat altered. Nevertheless, they are clearly magmatic with well-developed compositional zoning and the high-U or metamict zones could be avoided when choosing a spot to analyze. The SHRIMP U-Pb analyses (Appendix B(I); Figure 2.6) show variable discordance, with two analyses (8.1 and 12.1) showing about 25% discordance. The remainder of the analyses plot in an array near concordia and a weighted mean calculated from the radiogenic $^{207}Pb/^{206}Pb$ ratios gives an age of 2647 ± 4 Ma (n = 10; MSWD = 0.41; probability = 0.92). Although, by definition, this must be a minimum estimate of the age, it is within error of an upper intercept age calculated by regression analysis of all the data. The upper intercept age is 2659 ± 20 Ma (lower intercept = 576 ± 220 Ma) but the high MSWD of 5.7 shows there is excess scatter in these data. The weighted mean $^{207}Pb/^{206}Pb$ age of 2647 ± 4 Ma is considered to be the most reliable age estimate for the crystallisation of this granitoid.

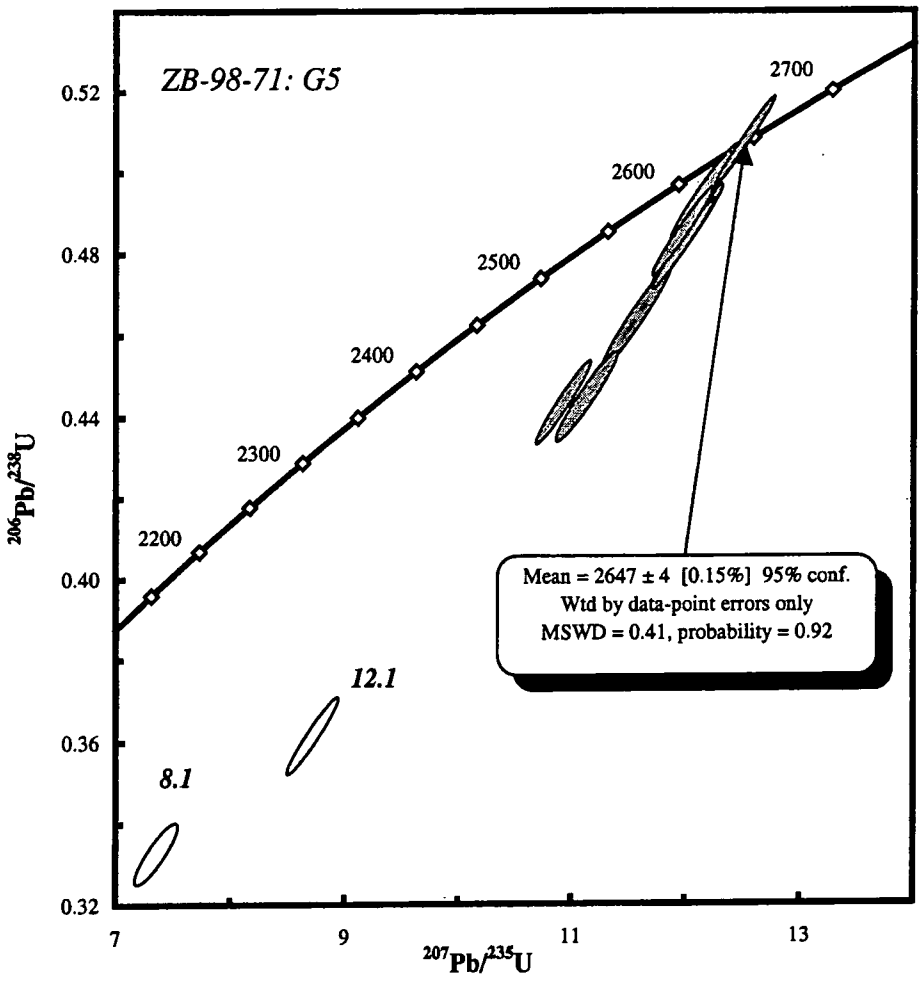

Figure 2.6: U-Pb concordia plot of all SHRIMP data for sample ZB-98-71. The discordant analyses 8.1 and 12.1 (represented here by unfilled error ellipses) are not included in the calculated $^{207}Pb/^{206}Pb$ age

2.4. Validity of the previous chronological succession

The age of the G5 Domboshaba Granite (2647 ± 4 Ma) is the youngest within this study's data set and supports the previous interpretation of Key et al. (1976) which assumed that this group of granitoids represents the youngest igneous event at the southwestern margin of the Zimbabwe craton. However, the age of the Domboshaba G5 Granite is more than 50 Ma older than previously assumed by Key et al. (1976). Neither Majaule and Davis (1998) nor myself found any Mesoproterozoic age data in our results. All the U-Pb zircon

ages obtained by Majaule and Davis (1998) are Archaean and define an age range (2639 ± 2 to 2710 ± 19 Ma) similar to that reported here for the Vumba granitoids.

Except for G5 (which is the youngest pluton), all the age data indicate that the previous relative chronology from G1 (oldest) up to G4 (youngest) is not valid. It is important to note that the geometric relationships on Figure 2.1 suggest that the G1 granitoids intrude the G2 granitoids of Key et al. (1976). The main criterion used by previous workers to establish the (G1 to G5) chronology of granitoids in NE Botswana was the presence or absence of foliation. This is not, however a valid chronological criterion because the deformation is not homogeneously distributed in the region and, within a single intrusive body, strongly foliated rocks are restricted to discrete shear zones. The G5 pink granites represent the only group of granitoids not affected by the discrete shear zones, so their age of 2647 ± 4 Ma is the minimum for the shear-fabric-forming event. The maximum age of this fabric is set by the age of the youngest deformed granitoid; i.e. 2686 ± 6 Ma. This age from the G1 tonalitic orthogneiss resembles, within the margin of errors, the ages of both G4 tonalite and G2 granitic gneiss.

The oldest emplacement age is recorded in the G4 tonalitic granitoid (2696 ± 3.5 Ma), whereas the oldest zircon age (2733 ± 5 Ma) is recorded in a xenolith from the G2 gneiss/migmatite. The xenolith age indicates that the protolith to the migmatite was not much older than the Archaean granitoids in the area. It is important to note that the zircons from the granitoids, including the xenolith from the G2 gneiss/migmatite, do not record any evidence of a Paleoproterozoic thermo-tectonic event. It is therefore inferred that the widespread 2 Ga Paleoproterozoic event documented in the Limpopo belt (Van Breemen, 1970; Van Breemen and Dodson, 1972: Barton et al., 1994; Kamber et al., 1995; Jaeckel et al., 1997; Holzer et al., 1998; McCourt and Armstrong, 1998; Kroner et al., 1999) did not

affect the Vumba granite-greenstone terrain or was a minor event in this area, unable to affect the zircon isotopic system.

2.5. Regional implications

Table 2.1 and Figure 2.7 summarize available U-Pb zircon ages for Neoarchaean felsic rocks from the Zimbabwe craton. The oldest major felsic event corresponds to the pre-Neoarchaean (ca. 3.2 Ga) accretion of the early Archaean Tokwe crustal segment which is exposed in a roughly triangular zone in the south-central zone of the craton (Dodson et al., 1988; Wilson et al., 1995).

The second major felsic igneous event (2.9-2.8 Ga) developed west of the Tokwe crustal block and the resulting rocks have been named the Chingezi suite (e.g. Wilson et al., 1995). The third major felsic igneous event, formed the Sesombi suite, developed west of the Chingezi suite between ca. 2.70-2.65 Ga. This polarity of age has been taken as evidence for a westward temporal crustal growth of the craton.

Table 2.1 U-Pb zircon ages for felsic igneous rocks from granite-greenstone belts in the Zimbabwe Craton, southern Africa. ZMC = Zimbabwe Craton; NMZ = Limpopo North Marginal Zone. Source of data: [1.] Wilson et al. (1995); [2.] Mkweli et al. (1995); [3.] Jelsma et al. (1996); [4.] This study; [5.] Majaule and Davies (1998); [6.] Vinyu et al. (1996).

Location	Occurrence/Ref.	Rock type	Age (Ma)
S.&C. Zimbabwe	Belingwe[1]	Felsic volcanic breccia	2904 ± 9
	Belingwe[1]	Dacitic volcanic breccia	2831 ± 6
	Filabusi[1]	Felsic gneiss	2799 ± 9
	Masvingo[1]	Banded felsite	2661 ± 17
	ZMC-NMZ[2] contact	Granite porphyry	2627 ± 7
W.&S. Zimbabwe	Bulawayo[1]	Rhyodacite	2696 ± 7
	Bulawayo[1]	Felsic volcanic rock	2788 ± 10
	Midlands[1]	Felsic volcanic breccia	2683 ± 8
	Midlands[1]	Banded Andesite	2702 ± 6
	Midlands[1]	Banded Rhyodacite	2805 ± 6
	Midlands[3]	Sesombi-granodiorite	2673 ± 5
NE-Botswana	Vumba[4]	Granodioritic gneiss (Mashawe)	2686 ± 6
	Vumba[4]	Amphibolitic gneiss xenolith	2733 ± 5
	Vumba[4]	Tonalitic gneiss (Maebe)	2690 ± 4
	Vumba[4]	Porphyritic quartz diorite	2696 ± 3.5
	Vumba[4]	Granite (Domboshaba)	2647 ± 4
	Matsitama[5]	Granodiorite gneiss	2648 ± 2
	Matsitama[5]	Monzodiorite	2639 ± 2
	Matsitama[5]	Monzodiorite	2646 ± 2.5
	Matsitama[5]	Tonalitic gneiss	2710 ± 19
	Matsitama[5]	Tonalitic gneiss	2648 ± 2.5
NE-Zimbabwe	Harare[1]	Felsic tuff	2643 ± 8
	Harare[1]	Banded rhyolite	2645 ± 4
	Harare[6]	Jumbo Granodiorite	2664 ± 15
	Harare[3]	Rhyodacite	2715 ± 15
	Shamva[1]	Water lain tuff	2679 ± 9
	Shamva[6]	Glendale Tonalite	2618 ± 6
	Shamva[3]	Porphyritic andesite	2672 ± 12
	Shamva[3]	Granitic gneiss (Wedza)	2667 ± 4
	Shamva[3]	Granite (Chilimanzi)	2601 ± 14
	Bindura[6]	Bindura Granodiorite	2649 ± 6

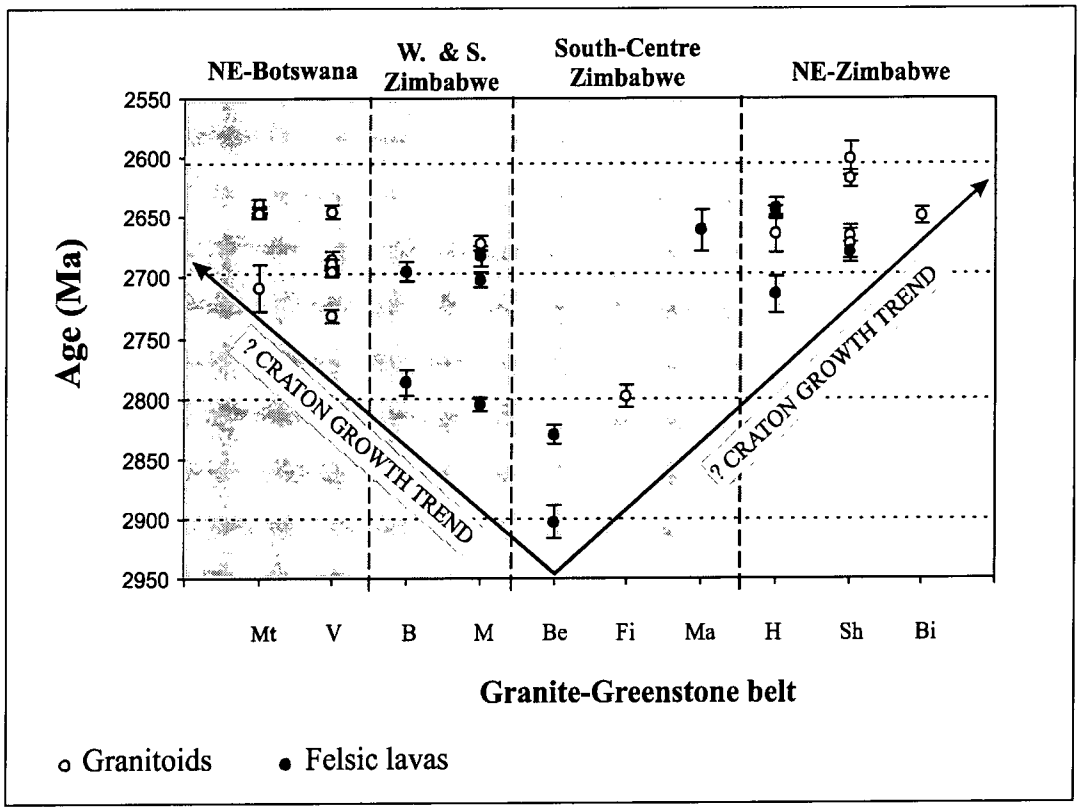

Figure 2.7: Schematic diagram showing the spatial variation of U-Pb zircon crystallisation ages of felsic igneous rocks in the Zimbabwe Craton. Abbreviations: B=Bulawayo; Be=Belingwe; Bi=Bindura; Fi=Filabusi; H=Harare; Ma=Masvingo; M=Midlands; Mt=Matsitama; Sh=Shamva; V=Vumba.

The Archaean granites from Botswana have an emplacement age of c. 2.73-2.65 Ga which makes them correlatives of the Sesombi igneous suite in Zimbabwe. Their location at the southwesternmost margin of the Zimbabwe craton supports the age polarity documented by Wilson et al. (1990). Wilson et al. (1995) discriminate two age sub-groups in the age range 2.7-2.65 Ga, i.e. the Sesombi suite at ca. 2.7 Ga and the Wedza suite at ca. 2.65 Ga. However, when all available geochronological data in that range in Zimbabwe are put together with our results (Fig. 2.7) they suggest a single major and continuous plutonic and volcanic event between ca. 2.73-2.65 Ga. The age of the Archaean granitoids in NE Botswana and the age of the Zimbabwean Sesombi suite support their emplacement

during the outpouring of the Upper Bulawayan felsic lavas (Wilson et al., 1981). On this basis, the author infers that the intermediate to felsic lavas associated with granitoids in the Vumba and Tati granite-greenstone terrains are correlatives of the Upper Bulawayan volcanism of Wilson et al. (1995).

The data from this study constrain the age of the shear fabric in the Vumba granite-greenstone terrain to be younger than 2686 ± 4 Ma and older than 2647 ± 4 Ma. Within the Zimbabwe craton, the greenstone terrains were affected by two deformation events dated at c. 2.68-2.64 Ga for D1 and 2.62-2.57 Ga for D2 (Dirks and Jelsma, 1998; Jelsma and Dirks, 2000). Assuming that there is no major spatial diachrony of the deformation events at the scale of the craton, the foliation in the Archaean granitoids in the Vumba terrain should correlate with the regional D1 Neoarchaean accretionary deformation event in Zimbabwe. It remains that, both in Zimbabwe and in Botswana, the mechanisms and the characteristics of blocks accreted during this Neoarchaean deformation event are still poorly constrained and a matter of controversy. The tectonic setting interpretations include accretion of oceanic crust formed along ridges/oceanic plateaus (e.g. Kusky and Kidd; 1992; Kusky and Winsky, 1995; Brake, 1996) or continental crust produced in arc/back-arc settings (Tomschi, 1987; Scholey, 1992; Jelsma et al., 1996) or even continental crust in extensional settings (Bickle et al., 1994; Blenkinsop et al., 1993).

2.6. Conclusions

This study of the age of the granitoid rocks in the Vumba granite-greenstone terrain, and of the age comparison with granitoid rocks in the Matsitama granite-

greenstone terrain (NE Botswana) and other parts of the Zimbabwe craton has led to the following conclusions:

(1) The oldest rocks (2733 ± 5 Ma) in the Vumba granite-greenstone terrain are preserved as xenoliths in the migmatitic complex.

(2) Ages of all granitoids indicate that the felsic magmatism in this terrain took place between ca. 2733 ± 5 or 2696 ± 3.5 Ma (if the xenolith protolith age is excluded) and 2647 ± 4 Ma. This age range is similar to that of 2710 ± 9 to 2639 ± 2 Ma recorded by Majaule and Davis (1998) in the Matsitama granite-greenstone terrain. In both terrains there are no Mesoproterozoic granite and pegmatite veins/dykes correlative to those documented in the Tati belt by van de Wel et al. (1998). Therefore, the Mesoproterozoic felsic igneous event recorded in the Tati granite-greenstone terrain by the above authors is a minor event in NE Botswana.

(3) The chronology (G1 to G5) of Archaean granitoids in NE Botswana proposed by Key et al. (1976) is not confirmed by isotopic data in this study. It is suggested that the structural fabric used to define the five-granitoid sub-groups post-dates most (G1 to G4) granitoids and developed only within discrete shear zones. The so-called G5 granitoids represent the only group of granitoids emplaced after the development of these shear zones.

(4) The age of the shear zones is constrained to be younger than 2686 ± 6 Ma and older than 2647 ± 5 Ma. Therefore, this fabric correlates with the D1 Neoarchaean fabric dated between ca. 2.68 and 2.64 Ga in Zimbabwe (Jelsma and Dirks, 2000 and references therein).

(5) The U-Pb zircon ages of the granitoids in the Vumba and Matsitama granite-greenstone terrains are similar to the age of the felsic igneous rocks of the

Sesombi/Upper Bulawayan suites in the Zimbabwe craton (Wilson et al., 1995). Geochronological data suggest that this major igneous event at the west and southwest of the craton was continuous for almost 80 Ma, between ca.2.73-2.65 Ga.

Chapter 3

GRANITOIDS

This chapter presents the petrographic and geochemical characteristics of the granitoid rocks from the Vumba granite-greenstone terrain.

3.1 Petrography

Detailed textural and mineralogical characteristics of the three granitoid units designated G5, G2 and G1 from the Vumba granite-greenstone terrain are given below, and a summary of all petrographical characteristics is presented in Table 3.1, which appears at the end of this section. The nomenclature through out follows the modal IUGS (International Union of Geological Sciences) classification scheme of Streckeisen (1976) given in Figure 3.1. The erroneous chronological classification of the granitoids (G1-G5) established by Key et al. (1976) is maintained in order to avoid confusion.

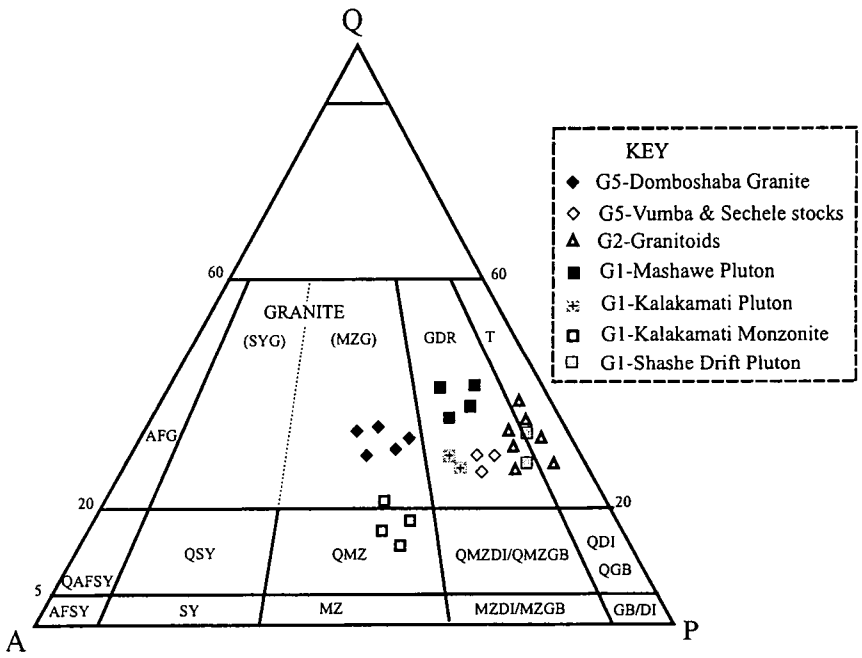

Figure 3.1. The G1, G2 and G5 granitiod rocks from the Vumba granite-greenstone terrain plotted in the Streckeisen diagram (1976). Abbreviations: AFG-alkali feldspar granite, AFSY-alkali feldspar syenite, DI/GB-diorite/gabbro, GDR-granodiorite, MZ-monzonite, MZG-monzogranite, MZDI/MZGB-monzodiorite/monzogabbro, QAFSY-quartz alkali feldspar syenite, QDI-quartz diorite, QGB-quartz gabbro, QMZDI/QMZGB-quartz monzodiorite/quartz monzogabbro, QMZ-quartz monzonite, QSY-quartz syenite, SY-syenite and T-tonalite.

Despite fresh-looking hand specimens, some thin sections exhibit mild to extensive sericitisation of feldspars. This type of alteration renders the distinction between alkali feldspars and plagioclase very difficult. Therefore, only the unaltered and slightly sericitised samples were considered for modal content determination. A Swift model F automatic point counter fitted with an automatic stage was utilised to obtain the modal contents of the rock forming minerals. The procedure is documented in Appendix A and the results are presented in Appendix B.

3.1.1 G5 granitoids

The G5 samples came from three different outcrops namely the Domboshaba Granite, Vumba Central Stock and Sechele Stock. The Domboshaba Granite is a heterogeneous outcrop consisting of two different sections. Samples from one section are mostly medium to coarse grained, massive, granular and pink in colour. They are monzogranitic in composition and consist of microcline, albitic plagioclase, quartz and low modal content of chloritised biotite. Microcline commonly occurs as microperthite in these samples. The samples from the other section are medium to fine grained, massive, granular and light pink. They are compositionally monzogranitic and composed of sericitised plagioclase, undulose quartz, alkali-feldspar, biotite and sporadic hornblende. Both samples exhibit granophyric texture. Zircon, apatite, muscovite and magnetite are the accessory phases in all the samples from both sections.

The Vumba Central Stock is a medium-grained, slightly deformed, homogeneous and granular rock with medium grey colour. It is granodioritic mainly composed of sericitised plagioclase, aggregates of quartz, alkali-feldspar, biotite and hornblende. Biotite and hornblende are more abundant than in the Domboshaba samples. Zircon, apatite and magnetite are accessory minerals.

The Sechele Stock is medium- to coarse-grained, slightly deformed and porphyritic with medium grey colour. It is a porphyritic granodiorite containing alkali-feldspar phenocrysts which poikilitically enclose fine crystals of plagioclase, biotite and quartz as well as microcline (Photo 3.1). Subhedral plagioclase commonly shows sericitisation. Biotite and hornblende exhibit anhedral habits. Hornblende is rare (<2%). The accessory minerals include zircon, apatite, magnetite and muscovite.

3.1.2 G2 granitoids

Samples from the G2 granitoid group are compositionally tonalite to granodiorite. As can be seen from Figure 3.1, they straddle the border between the granodiorite and tonalite fields. They are mostly medium-grained with medium-grey colour. Both in handspecimen and thin section, they display conspicuous preferred orientation of mafic minerals. The samples consist of sericitised plagioclase, fine microcline, quartz, biotite and hornblende as essential minerals. Zircon, apatite, magnetite and epidote are the accessory phases. Hornblende, biotite and magnetite are more abundant than in the G5 granitoids. Moreover, hornblende and biotite commonly form aggregates of fine subhedral crystals. In most instances, anhedral coarse quartz grains with undulatory extinction are set in a mosaic of fine equant quartz which is completely recrystallised (Photo 3.2).

3.1.3. G1 granitoids

Samples from this group were collected from four different plutons, namely the Mashawe, the Shashe Drift and the Kalakamati Plutons as well as the Kalakamati Monzonite Pluton. The samples from the Mashawe Pluton are medium-grained, light-grey coloured and well-foliated (Photo 3.3). The foliation is defined by the alignment of quartz and biotite. The samples consist mainly of plagioclase, perthitic alkali-feldspar

and abundant quartz. Plagioclase exhibits ubiquitous sericitisation. Anhedral quartz shows undulatory extinction and serrated grain boundaries. Biotite is very scarce with modal content of about 5%. No amphiboles were identified in these samples. The accessory phases include zircon, magnetite, muscovite and apatite.

Samples from the Shashe Drift Pluton are medium-grained, medium-grey and well-foliated. They are tonalitic to granodioritic in composition. In the Streckeisen diagram (1976), they straddle the border between the granodiorite and tonalite fields like the G2 samples. They are mainly composed of slightly sericitised plagioclase, microcline, recrystallised quartz, subhedral hornblende and biotite. Biotite and hornblende are locally chloritised. Foliation is conspicuous and defined by parallelism of the mafic phases and quartz. The mafic phases are more abundant than in the Mashawe Pluton (comparable to the G2). Muscovite, zircon, apatite and magnetite form accessory phases. Carbonitisation is locally observed in some samples.

The Kalakamati Pluton is medium-grey, mostly medium-grained, and moderately-deformed granodiorite. The samples locally exhibit porphyritic texture with phenocrysts of alkali-feldspars poikilitically enclosing quartz, biotite and plagioclase. The phenocrysts constitute 4 to 6% in volume. Myrmekite is observed in many of these samples. Plagioclase exhibits sericitisation. Biotite and hornblende comprise the mafic phases, with the latter being the prevalent phase. They are mildly chloritised. Muscovite, magnetite, apatite and zircon are the accessory phases.

Samples from the Kalakamati Monzonite Pluton are distinct from those of the other G1 plutons described above. They are medium- to coarse-grained, melanocratic, grey and conspicuously foliated. They are quartz monzonitic to monzogranitic and mainly composed of low abundance of quartz, perthitic microcline, slightly sericitised plagioclase, hornblende and biotite. Hornblende and biotite show average modal contents of 15% and 5% respectively. Hornblende forms coarse subhedral to anhedral

skeletal crystals with a conspicuous preferred orientation. In most instances, it poikilitically encloses tiny grains of quartz and feldspars (Photo 3.4). Biotite displays fine- to medium-sized grains with anhedral habits. It shows an obvious preferred orientation. Ubiquitous accessory phases in the Kalakamati Monzonite include apatite, zircon and magnetite. In general, the pluton has a granoblastic texture. Myrmekite and microperthite textures are commonly observed in these samples.

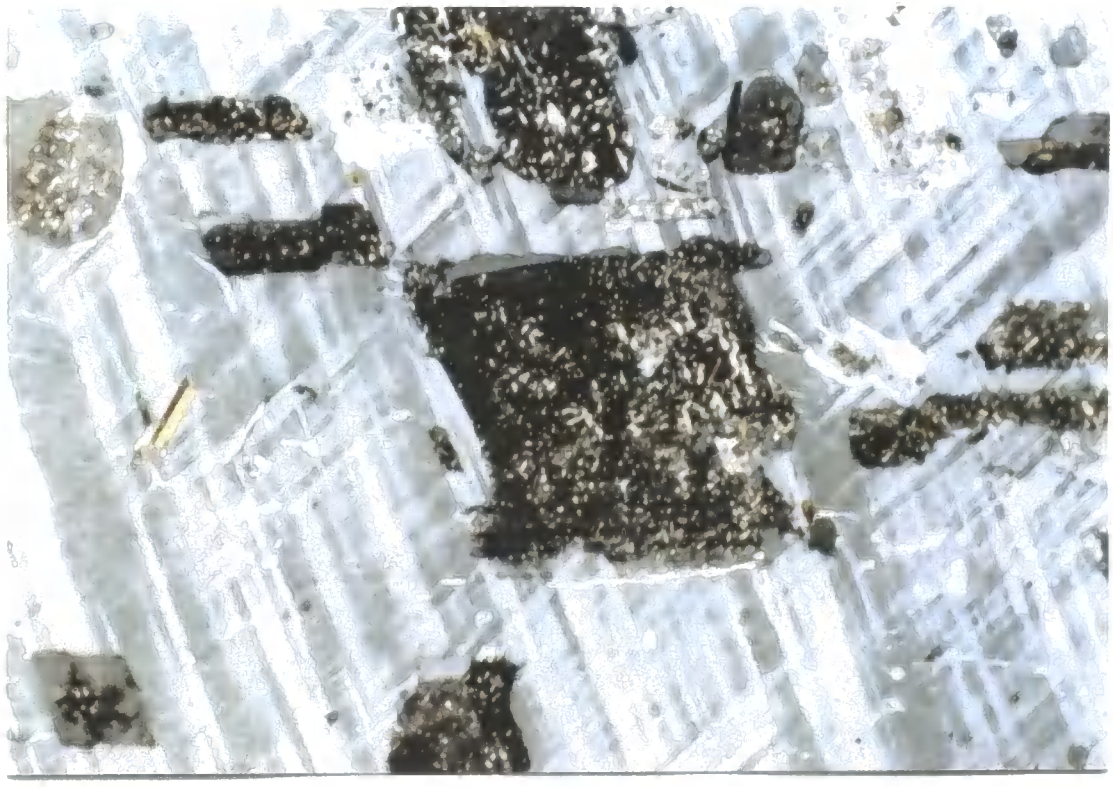

Photo 3.1. Microcline phenocryst from the Sechele stock exhibiting a poikilitic texture. Fine sericitised plagioclase crystals are enclosed in a microcline crystal. This is a common feature of the Sechele stock. Magnification: 3 x 1.9 mm. Sample ZB-98-81

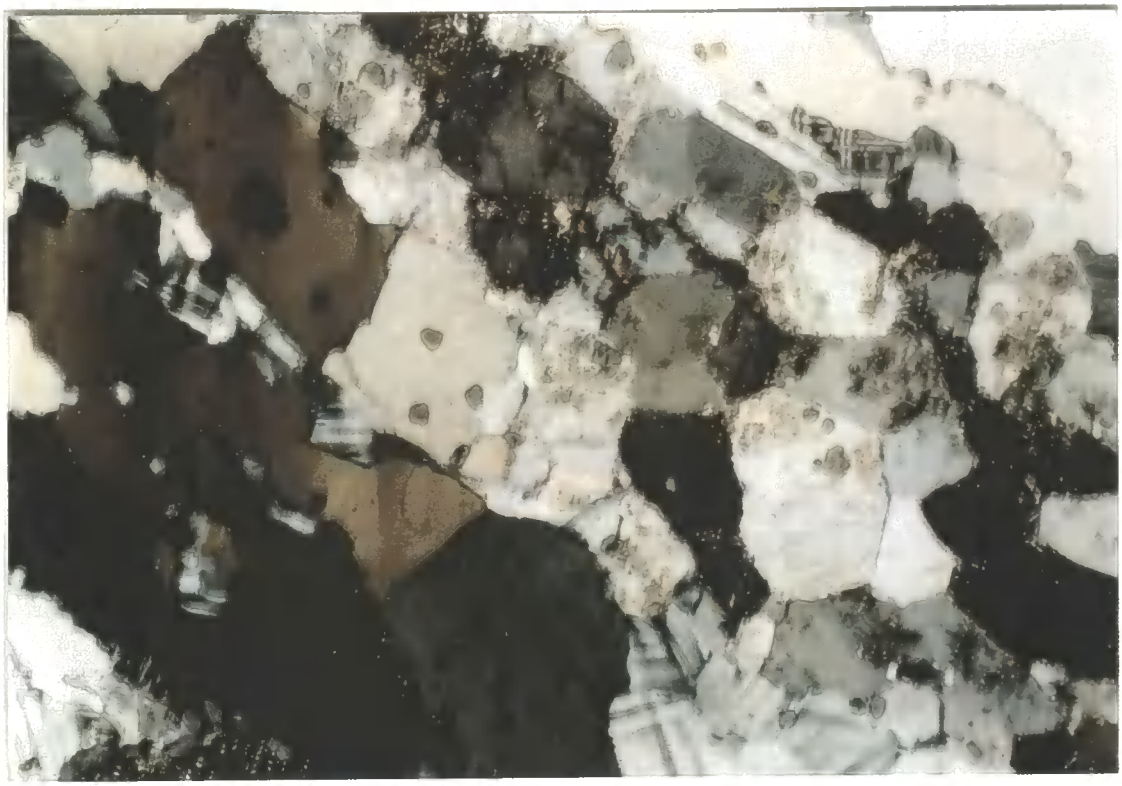

Photo 3.2. Recrystallisation texture where quartz and feldspar crystals meet at 120° triple point junction. This is a characteristic feature of the G2 granitoids. Magnification: 1.3 x 0.77 mm. Sample ZB-98-132.

Photo 3.3. Deformed quartz crystals defining foliation in the Mashawe Pluton (G1). Magnification: 3 x 1.9 mm. Sample ZB-98-89.

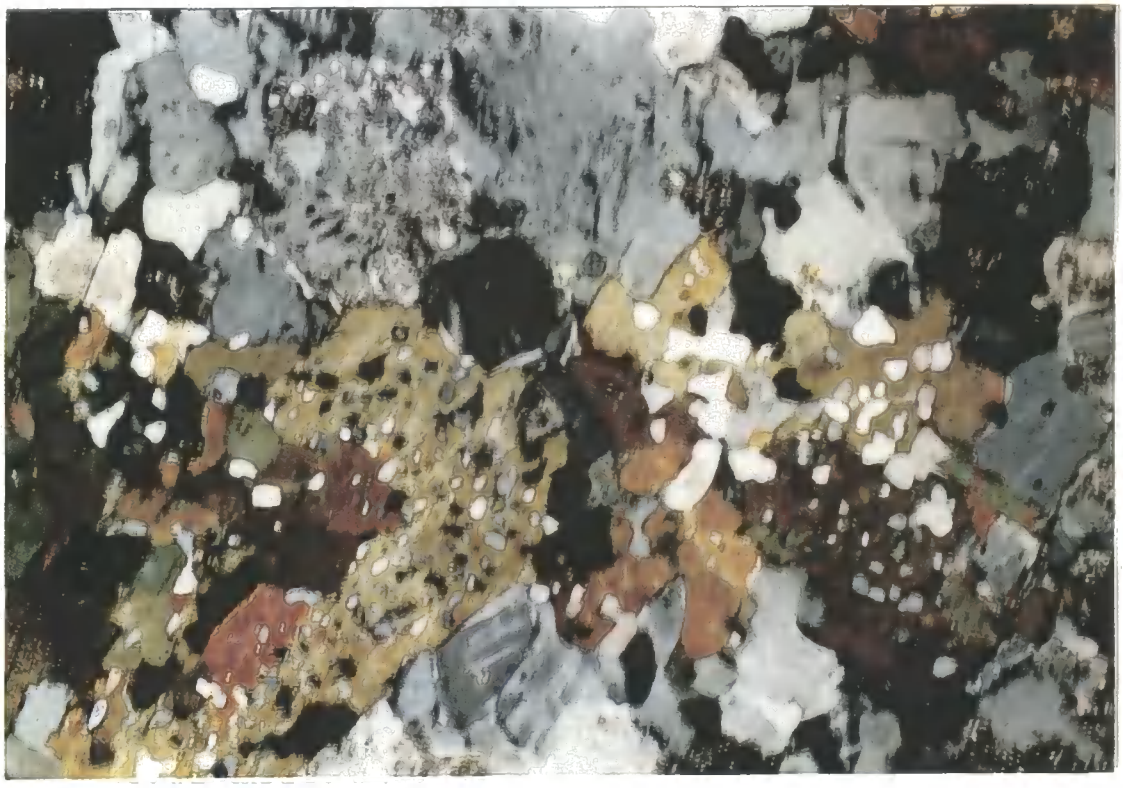

Photo 3.4. Skeletal clinoamphibole crystals poikilitically enclosing fine quartz grains. This is a characteristic feature of Kalakamati Monzonite (G1). Magnification: 1.3 x 0.77 mm. Sample ZB-98-85.

Group	G5			G2	G1			
Pluton	Domboshaba Granite	Vumba Central Stock	Sechele Stock	Granitoids	Mashawe Pluton	Shashe Drift Pluton	Kalakamati Pluton	Kalakamati Monzonite
Composition	Monzogranite	Granodiorite	Granodiorite	Tonalite-granodiorite	Granodiorite	Tonalite-granodiorite	Granodiorite	Quartz monzonite to monzogranite
Texture	Granular Massive	Granular Gneissic	Porphyritic Granular	Gneissic Granoblastic	Gneissic Granoblastic	Gneissic Granoblastic	Granoblastic Porphyritic	Gneissic Porphyroblastic Granoblastic
Grain Size	medium to coarse & fine to medium	medium	medium to coarse	medium	medium	medium	medium	medium to coarse
Mafic Phase	biotite (hornblende)	biotite hornblende	biotite (hornblende)	biotite hornblende	biotite	biotite hornblende	biotite hornblende	biotite hornblende
Accessory minerals	magnetite zircon apatite muscovite	magnetite zircon apatite	magnetite zircon apatite muscovite	magnetite zircon apatite epidote	magnetite zircon (apatite) muscovite	magnetite zircon apatite muscovite	magnetite zircon apatite muscovite	magnetite zircon apatite
Quartz & Feldspar texture	granophyric microperthite	myrmekite microperthite	myrmekite microperthite	microperthite myrmekite	microperthite myrmekite	microperthite myrmekite	myrmekite microperthite	myrmekite microperthite
Type of alteration	sericitisation chloritisation	sericitisation chloritisation carbonitisation	sericitisation	sericitisation chloritisation	sericitisation	sericitisation chloritisation carbonitisation	sericitisation chloritisation	sericitisation

Table 3.1: Summary of petrographic characteristics of the G5, G2 and G1 granitoid groups from the Vumba granite-greenstone terrain.

3.2. Geochemistry

Whole-rock major and trace element concentrations of 51 rock samples from the G1, G2 and G5 granitoid units from the Vumba granite-greenstone terrain were determined by X-Ray Fluorescence (XRF) spectrometry on fused glass discs and pressed powdered pellets respectively. The trace elements determined were Sc, V, Cr, Co, Ni, Cu, Zn, Ga, Rb, Sr, Y, Zr, Nb, Ba, La, Ce, Nd, Pb, Th and U. Additionally, a subset of 30 representative samples were analysed for Sc, V, Cr, Co, Cu, Zn, Ga, Rb, Sr, Y, Zr, Nb, Cs, Ba, Rare Earth Elements (REE), Hf, Ta, Pb, Th and U using the inductively coupled plasma mass spectrometry (ICP-MS) technique. Appendix A document the analytical procedure while Appendix B(III) presents the set of XRF and ICP-MS data. The accuracy and precision of the analytical data is given in Appendix C.

Three sections constitute the geochemistry component:

(1) The first section focuses on evaluation of the major element variation diagrams and major element characteristics.

(2) The second section concentrates on the trace element characteristics, as indicated by trace element variation diagrams, REE patterns and spidergrams as well as LILE modelling.

(3) The third section is restricted to the aspects of tectonic setting as demonstrated by ORG-patterns, Th/Yb vs Nb/Yb plot and tectonic discrimination diagrams.

3.2.1. Major elements characterisation of the granitoids

3.2.1.1. Harker diagrams of major elements

The average chemical compositions of the individual plutons or granitoid units from the Vumba granite-greenstone terrain are presented in Table 3.2. It is evident from this Table that all the investigated samples have high silica content except for the samples from the Kalakamati Monzonite Pluton which contain < 66% SiO_2. Moreover, there is a great overlap between the granitoid units or plutons in terms of their silica contents. It is worth noting that the Mashawe Pluton has the highest silica contents. The individual major elements are plotted in Figure 3.2 with SiO_2 as the index of differentiation.

The granitoids from the Vumba granite-greenstone terrain yield some well-defined geochemical trends as can be seen from Figure 3.2. TiO_2, Al_2O_3, Fe_2O_3*(total), MnO, MgO, CaO and P_2O_5 exhibit good negative correlation when plotted versus silica in most of the granitoids. Nevertheless, CaO and P_2O_5 in the G5 samples are virtually constant with increasing silica. Na_2O displays some scatter when plotted versus silica in all the plutons, except in the Kalakamati Monzonite Pluton where it remains constant with increasing silica. In practice, many intrusive rock suites yield poorly-defined geochemical trends, and these tend primarily to reflect shallow-level fractional crystallisation (Luas and Hawkesworth, 1991).

Notably, most of the granitoids from the Vumba granite-greenstone terrain are sodic with Na_2O/K_2O ratios above unity. However, the Domboshaba Granite and the Kalakamati Monzonite Plutons are potassic.

(wt %)	G5 *Domboshaba*	G5 *Stocks*	G2 *Granitoids*	G1 *Shashe Drift*	G1 *Mashawe*	G1 *Kalakamati*	G1 *K-Monzonite*
SiO_2	70.46	70.08	68.99	67.81	75.00	69.55	62.79
TiO_2	0.34	0.33	0.43	0.51	0.14	0.36	0.77
Al_2O_3	15.45	15.48	15.59	15.82	14.00	15.54	15.67
FeO*(total)	1.70	2.22	3.15	3.33	1.37	2.32	4.73
MnO	0.03	0.04	0.01	0.05	0.03	0.03	0.07
MgO	0.35	0.85	1.01	1.27	0.19	0.71	2.64
CaO	1.44	2.92	3.66	3.55	1.90	2.35	4.11
Na_2O	3.81	4.26	4.39	4.34	4.29	3.97	3.41
K_2O	5.56	2.90	1.58	1.90	2.51	3.84	4.44
P_2O_5	0.05	0.12	0.12	0.14	0.03	0.10	0.29
Total	99.17	99.20	98.92	98.71	99.45	98.77	98.93
LOI	0.66	0.86	0.75	1.02	0.58	0.93	0.68
Mg#	26.66	39.53	36.10	40.49	19.77	35.41	49.59
(In ppm)							
Sc	2.9	2.5	3.6	1.8	2.0	2.0	9.1
V	9	25	42	50	5	24	92
Cr	6	14	15	19	5	17	58
Co	2.2	3.8	5.2	7	1.2	3.3	16.1
Ni	5	12	10	11	4	10	30
Cu	7	3	8	7	3	2	66
Zn	41	56	53	56	35	55	89
Ga	21.6	20.5	21.1	19.3	19.2	20.3	22.3
Rb	146.2	84.5	53.5	60.3	84.0	107.7	199.9
Sr	226	500	304	397	153	300	459
Y	13.3	9.3	9.2	7.3	8.8	8.3	23.4
Zr	273.9	133.3	147.2	135.8	83.4	198.7	300.0
Nb	6.42	7.73	4.43	3.78	5.56	6.30	11.51
Cs	1.31	2.09	1.10	1.28	2.08	0.89	5.81
Ba	1345	1033	431	447	615	1235	940
La	32.32	14.52	8.72	12.7	6.72	16.76	27.73
Ce	65.86	81.22	46.18	67.18	37.47	80.84	153.15
Pr	18.63	9.52	4.89	7.25	4.06	8.37	18.88
Nd	64.58	34.77	17.1	24.65	14.04	27.89	71.64
Sm	9.25	5.34	2.7	3.21	2.52	4.19	12.15
Eu	2.13	1.48	0.9	0.9	0.67	0.91	2.29
Gd	6.5	3.84	2.23	2.39	2.18	3.09	9.00
Tb	0.67	0.43	0.28	0.28	0.29	0.34	1.07
Dy	3.02	1.96	1.48	1.39	1.49	1.57	4.99
Ho	0.47	0.32	0.27	0.25	0.28	0.24	0.85
Er	1.19	0.8	0.7	0.71	0.77	0.60	2.13
Tm	0.16	0.11	0.11	0.11	0.13	0.08	0.30
Yb	1.11	0.71	0.69	0.7	0.84	0.50	1.93
Lu	0.19	0.11	0.11	0.12	0.15	0.08	0.30
Hf	7.63	4.12	4.2	4.15	2.87	5.58	9.58
Ta	0.51	0.5	0.44	0.37	1.03	0.74	1.21
Pb	41.11	29.5	16.26	17.25	29.00	29.67	41.43
Th	68.02	21.35	15.72	20.83	23.34	46.40	65.59
U	6.00	4.55	2.17	3.73	3.80	5.00	7.29

Table 3.2: Average chemical compositions of the G5, G2 and G1 granitoids from the Vumba-granite-greenstone terrain.

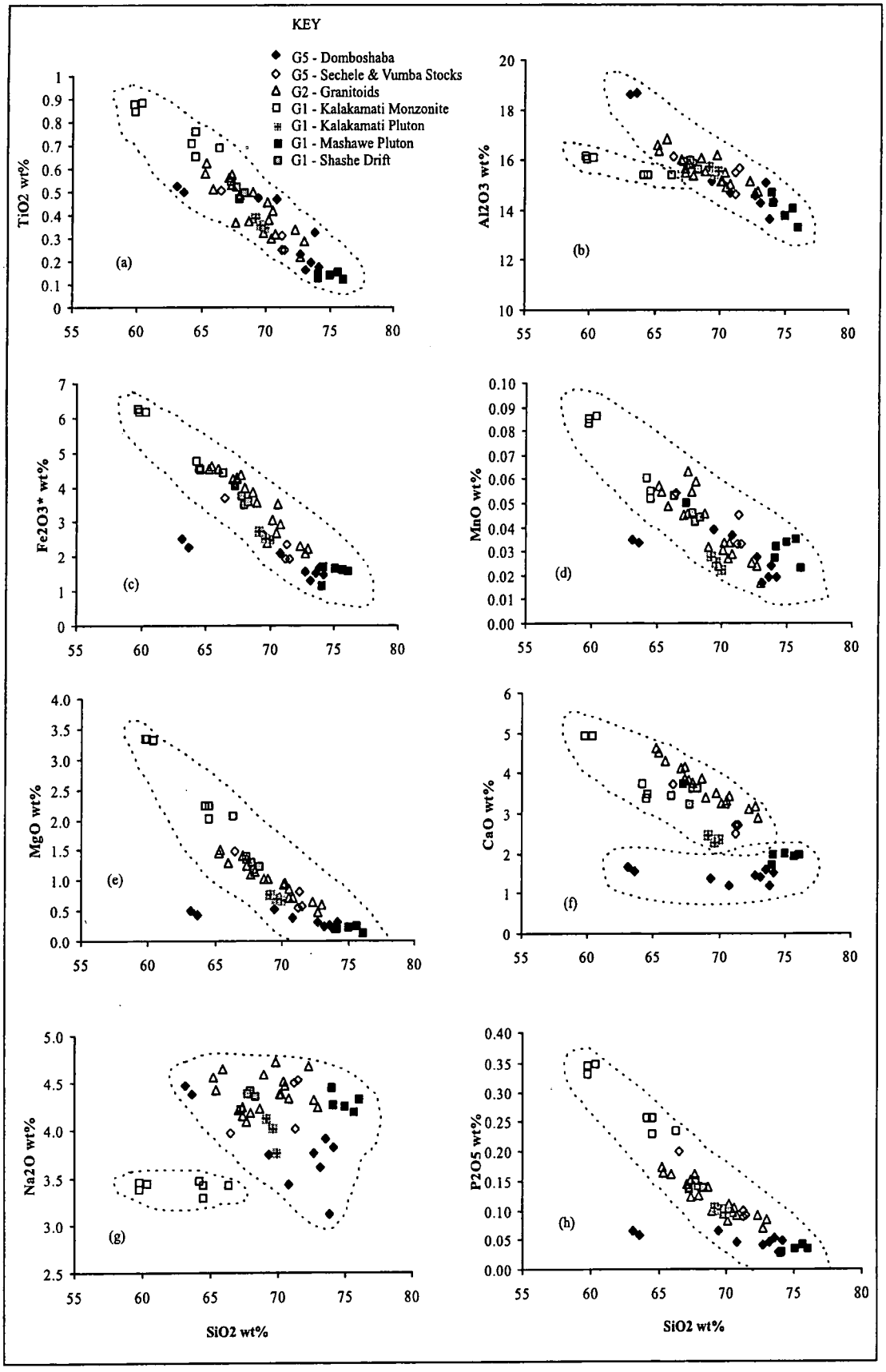

Figure 3.2: Harker variation diagrams of the granitoids from the Vumba granite-greenstone terrain.

3.2.1.2. *Classification of the granitoids using major element geochemistry*

The granitoid rocks from the Vumba granite-greenstone terrain have been classified using a cation-based [Si/3- (K + Na + 2Ca/3) versus K – (Na + Ca)] classification diagram of Debon & Le Fort (1983) presented in Figure 3.3. According to the classification diagram, samples from the Domboshaba Granite range from adamellites to granites, except for two samples that correspond to the syenite field. Other G5 samples from the Vumba Central and Sechele Stocks correspond to the granodiorite field. Samples from the G2 granitoid group plot in the tonalite-trondhjemite field. Among the G1 granitoids, the Mashawe Pluton classifies as granodiorite, whereas the Shashe Drift Pluton falls in the tonalite-trondhjemite field (as G2 rocks). The Kalakamati Pluton classifies as granodiorite to adamellite. Samples from the Kalakamati Monzonite Pluton essentially plot as quartz monzonite, with a few samples straddling the border between the quartz monzonite and adamellite fields.

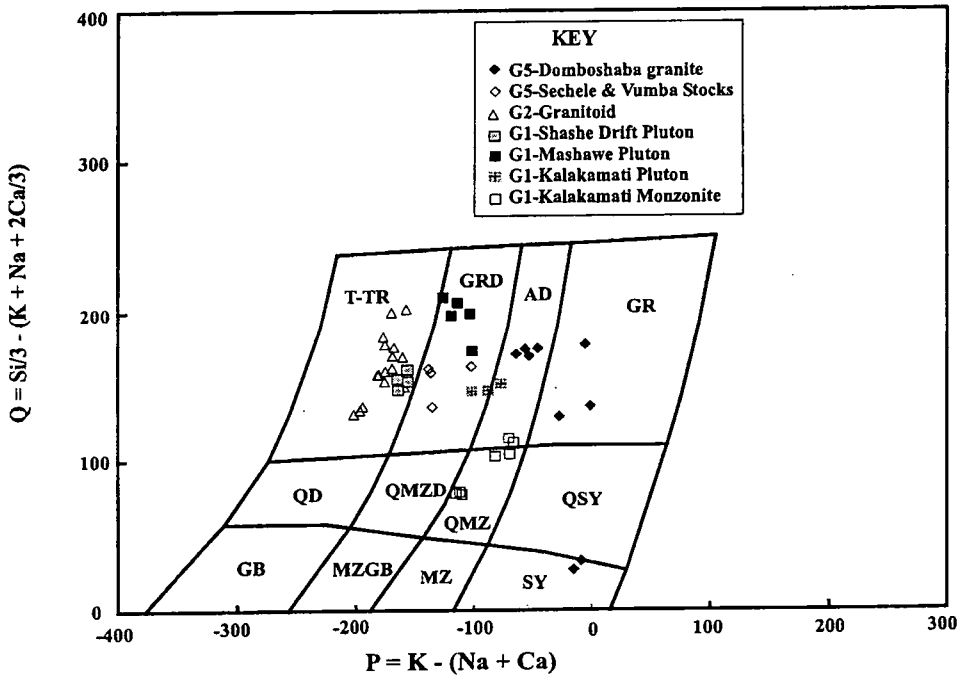

Figure 3.3: Classification of the granitoid rocks from the Vumba granite-greenstone terrain according to Debon & Le Fort (1983) diagram. Abbreviations: AD = Adamellite; GB = Gabbro; GR = Granite; GRD = Granodiorite; MZ = Monzonite; MZGB = Monzogabbro; QD = Quartz diorite; QMZD = Quartz monzodiorite; QMZ = Quartz monzonite; QSY = Quartz syenite; SY = Syenite; T-TR = Tonalite-Trondhjemite.

The results of the classification diagram of Debon & Le Fort (1983) may be compared with the results of the Streckeisen (1976) classification scheme which was adopted in the petrography section of this chapter (see Table 3.3 for the comparison). The Streckeisen (1976) diagram is based on modal analyses whereas the Debon & Le Fort (1983) diagram is based on normative analyses. Nevertheless, the results of the two independent classification diagrams are highly comparable. On the basis of the results in Table 3.3, the Vumba Central and the Sechele Stocks are granodioritic in composition, not granitic as the previous workers indicated (e.g. Litherland, 1975; Key et al., 1976). Furthermore, the results reveal that the so-called G2 granitic paragneiss is in reality tonalitic-trondhjemitic gneiss. Additionally, the G1 tonalitic and monzonitic gneisses (Litherland, 1975; Key et al., 1976) turn out to be primarily granodioritic and quartz monzonitic gneisses respectively.

GRANITOID UNITS (pluton)	**STRECKEISEN (1976)**	**DEBON & LE FORT (1983)**
G5 "granite"		
(Domboshaba granite)	Monzogranite	Adamellite, Granite, syenite
(Sechele & Vumba stocks)	Granodiorite	Granodiorite
G2 "granitic paragneiss"	Tonalite-Granodiorite	Tonalite-Trondhjemite
G1 "tonalitic orthogneiss"		
(Shashe Drift)	Tonalite-Granodiorite	Tonalite-Trondhjemite
(Kalakamati)	Granodiorite	Granodiorite-Adamellite
(Mashawe)	Granodiorite	Granodiorite
G1 "Monzonitic gneiss"	Quartz monzonite,	Quartz monzonite,
(Kalakamati Monzonite)	monzogranite	Adamellite

Table 3.3. Comparison of the Debon & Le Fort (1983) classification diagram which is based on normative analyses with the Streckeisen (1976) classification scheme based on modal analyses.

The granitoid units from the Vumba granite-greenstone terrain are also classified according to the Peacock classification diagram (1931) (Fig. 3.4). In this diagram four

magmatic rock series are defined namely alkalic, alkali-calcic, calc-alkalic and calcic. This classification diagram is made up of two Harker plots on the same diagram: SiO_2 versus (Na_2O + K_2O) and then versus CaO. The crucial value on this diagram is the SiO_2 value at the point where best fit-lines through the two trends intersect which is called "alkali-lime index". On the basis of the Peacock diagram (1931) in Figure 3.4, all the granitoids from the Vumba granite-greenstone terrain have calc-alkalic character with an alkali-lime index of about 60, except the Kalakamati Monzonite Pluton which exhibits the alkali-calcic affinity with an alkali-lime index of 54.

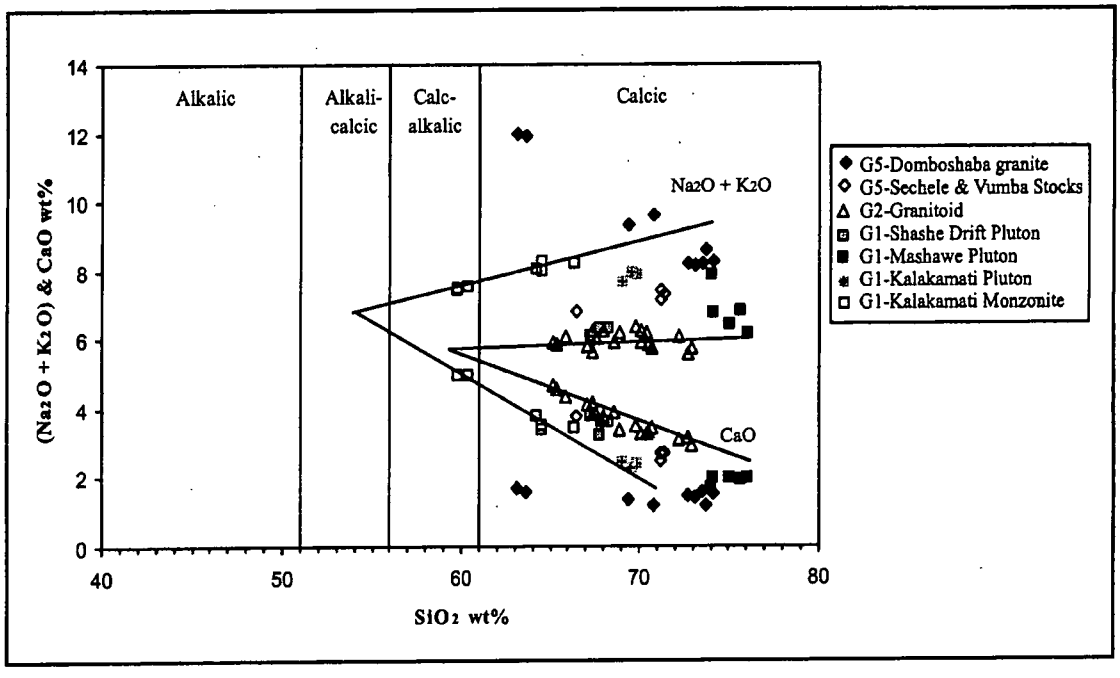

Figure 3.4: Plot of the granitoids from the Vumba granite-greenstone terrain on Peacock's (1931) alkali-lime diagram.

In addition, the granitoid rocks from the Vumba granite-greenstone terrain have been classified as medium-K to high-K granitoid types according to their K_2O and silica abundances (Le Maitre et al., 1989) (Fig. 3.5). The samples from the Domboshaba Granite, the Kalakamati Monzonite Pluton and the Kalakamati Pluton classify as high-K types. These high-K type granitoids are located in the same area and are contiguous to each other. The remainder of the granitoids classifies as medium-K types.

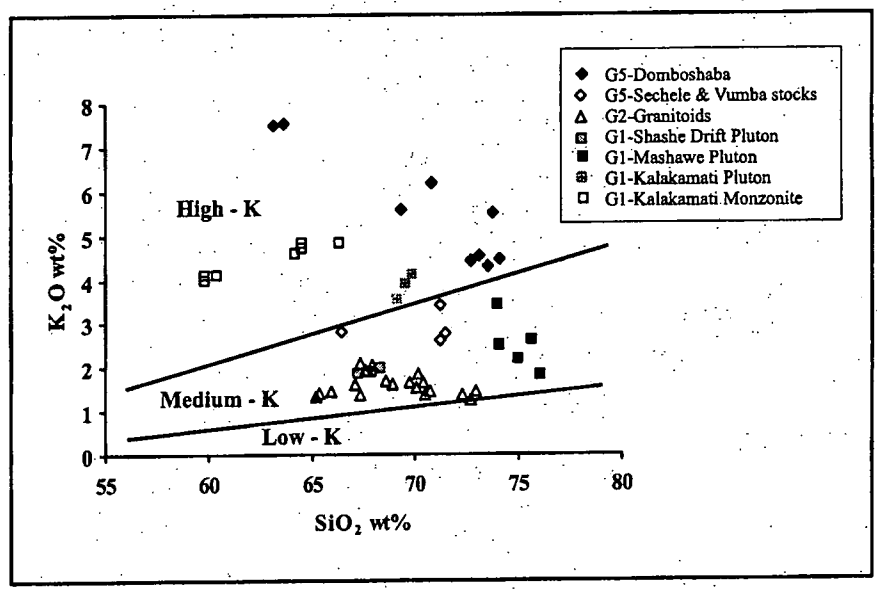

Figure 3.5: K_2O versus SiO_2 diagram of Le Maitre et al. (1989) for the Vumba granite-greenstone terrain granitoids.

Figure 3.6 illustrates the variations in the aluminium saturation index [A/NKC = mol% $Al_2O_3/(Na_2O + K_2O + CaO)$] which is often used to classify granitoids with special reference to inferred igneous or sedimentary origins. In the A/CNK versus SiO_2 diagram (Fig. 3.6), there is a progressive evolution from a metaluminous signature in the G1 Monzonitic gneiss (A/NKC < 1) to intermediate metaluminous-peraluminous characteristics in the G2 granitoids (1< A/NKC < 1.1). The G5 and G1 (granodioritic/tonalitic) samples have slightly peraluminous characteristics, with A/NKC ~ 1. The overall low A/NKC values suggest that these granitoids are I-type derived by fractional crystallisation of basic magmas, or by partial melting of igneous source rocks.

Chappell and White (1974) suggested that metaluminous (A/NKC < 1.1) I-type granitoids are derived from igneous (or meta-igneous) sources, whereas the peraluminous (A/NKC > 1.1), S-type granitoids are derived from metasedimentary sources. Even though this classification has been extensively applied in the

interpretation of the source of granitoids, it has some disadvantages. For instance, there are no well-defined boundaries between the two granite types. Furthermore, a granitoid can be derived from a combination of igneous and sedimentary sources.

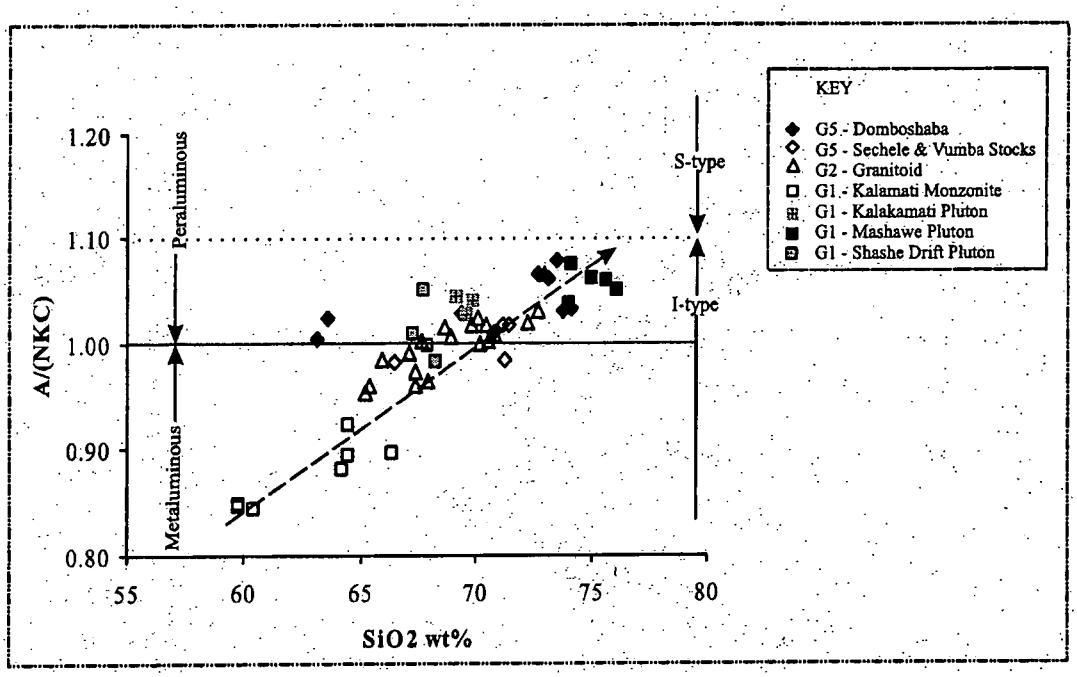

Figure 3.6: Alumina saturation (Shand, 1951) and I-&-S type (Chappell and White, 1974) diagram of the granitoids from the Vumba granite-greenstone terrain. Abbreviations: A/NKC = Mol% $Al_2O_3/(Na_2O + K_2O + CaO)$.

Table 3.5 below illustrates the comparison of the granitoids of the Vumba granite-greenstone terrain with the I- and S-type characteristics. It is evident from Table 3.5 that the granitoids from the Vumba granite-greenstone terrain possess geochemical characteristics of I-type granitoids.

I – type	S - type	G1	G2	G5
Metaluminous to weakly peraluminous	Strongly peraluminous	Metaluminous to weakly peraluminous	Metaluminous to weakly peraluminous	Metaluminous to weakly peraluminous
Amphibole common and cordierite absent; accessory titanite common	Biotite and muscovite predominate, cordierite present; monazite may be accessory	Amphibole common and cordierite absent: accessory titanite absent. Biotite predominate in Mashawe pluton	Amphibole common and cordierite absent: accessory titanite absent	Amphibole and biotite common, cordierite absent: accessory titanite absent
Normative diopside or <1% normative corundum	> 1% normative corundum	0-1.07% normative corundum in tonalitic gneiss 1.75-5.16% normative diopside in Monzonitic gneiss	0-1.05% normative corundum, 0-1.07% normative diopside	0-1.15% normative corundum
Magnetite common	Ilmenite common	Magnetite	Magnetite	Magnetite
High Na_2O > 3.2% for felsic varieties; > 2.2% for mafic varieties.	Low Na_2O < 3.2% when K_2O = 5%; 2.2% when K_2O = 2%	High Na_2O > 3.2%	High Na_2O > 4.0%	High Na_2O > 3.2%
Relatively high Ca and Sr	Relatively low Ca and Sr	Relatively low to high Ca and Sr	Relatively high Ca and Sr	Relatively low to high Ca and Sr
Regular inter-element variation within plutons and near linear variation diagrams	Variation diagrams more irregular	Near linear variation to irregular (see sections 3.2.	Near linear variation to irregular	Near linear variation to irregular
Mafic to felsic	Mainly felsic	Felsic and intermediate	Felsic	Felsic
Amphibole-bearing enclaves common	Metasedimentary enclaves common	Amphibole bearing enclave common in the Monzonitic gneiss	Amphibole bearing enclave common	No enclave observed

Table 3.5. Comparison of I- and S-type granitoids (Chappell and White, 1974) with the G1, G2 and G5 granitoids from the Vumba granite-greenstone terrain.

The general characteristics of the granitoid rocks from the Vumba granite-greenstone terrain are summarised in Table 3.6, which is based on the major element geochemistry and mineralogy. It is evident from this Table that the G5, G2 and G1 granitoids share a number of major element geochemical characteristics. Even the major element variation diagrams do not display distinctive differentiation trends. It is important to note that the G2 unit does not reflect any S-type granitoid affinities as would be anticipated from a paragneiss.

Granitoid	G5	G2	G1(other plutons)	G1(Kalakamati Monzonite Pluton)
Mineral composition	ksp + plg + qz + bi ± amp	plg + ksp + qz + amp + bi	plg + ksp + qz + bi ± amp	plg + ksp + qz + bi + amp
$Na_2O + K_2O$ wt%	6.51 – 11.09 wt%	5.47 – 6.35 wt%	6.09 – 8.27 wt%	7.42 – 8.28 wt%
Rock type	Granodiorite, monzogranite	Granodiorite, Tonalite-Trondhjemite	Granodiorite, Tonalite-trondhjemite	Quartz monzonite, Monzogranite
Alkali-lime index (Peacock, 1931)	Calc-alkalic	Calc-alkalic	Calc-alkalic	Alkali-calcic
K-series (Le Maitre et al.,1989)	Medium to high-K	Medium – K	Medium to high-K	High – K
Shand's index (1951)	Metaluminous to weakly peraluminous	Metaluminous to weakly peraluminous	Metaluminous to weakly peraluminous	Metaluminous
Granite type	I-type	I-type	I-type	I-type

Table 3.6. Summary of the mineralogy and major element-based geochemical characteristics of the granitoid rocks from the Vumba granite-greenstone terrain. Abbreviations: amp-amphibole; ksp-alkali-feldspar; plg-plagioclase; bi-biotite; qz-quartz

3.2.2. Trace element characteristics of the granitoids.

3.2.2.1. Trace element variation diagrams

The trace element variation diagrams plotted against SiO_2 as a differentiation index are presented as log-normal diagrams in Figure 3.7. Unlike the major elements, the trace elements rarely exhibit systematic trends against SiO_2. Only the transition metal elements (Sc, V, Cr, Co, Ni, Cu and Zn), Ga, Zr, Y and Sr exhibit a significant negative correlation with silica in the majority of the granitoids, except the Domboshaba Granite which mostly displays irregular patterns. It is argued in this case that this is not due to secondary alteration of the more mobile elements because only relatively undeformed and fresh samples were selected.

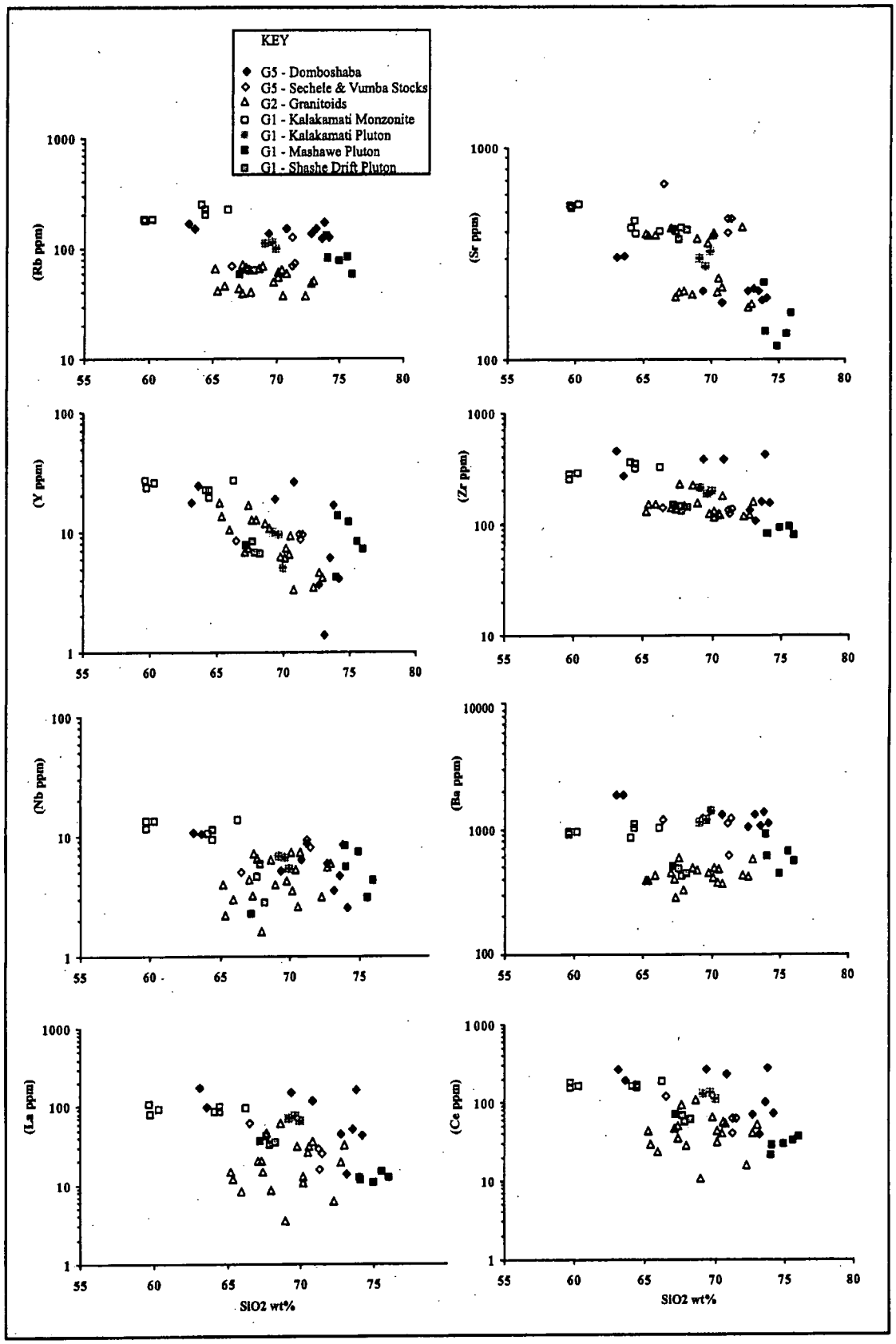

Figure 3.7: Trace element variation diagrams of the granitoids from the Vumba granite-greenstone terrain.

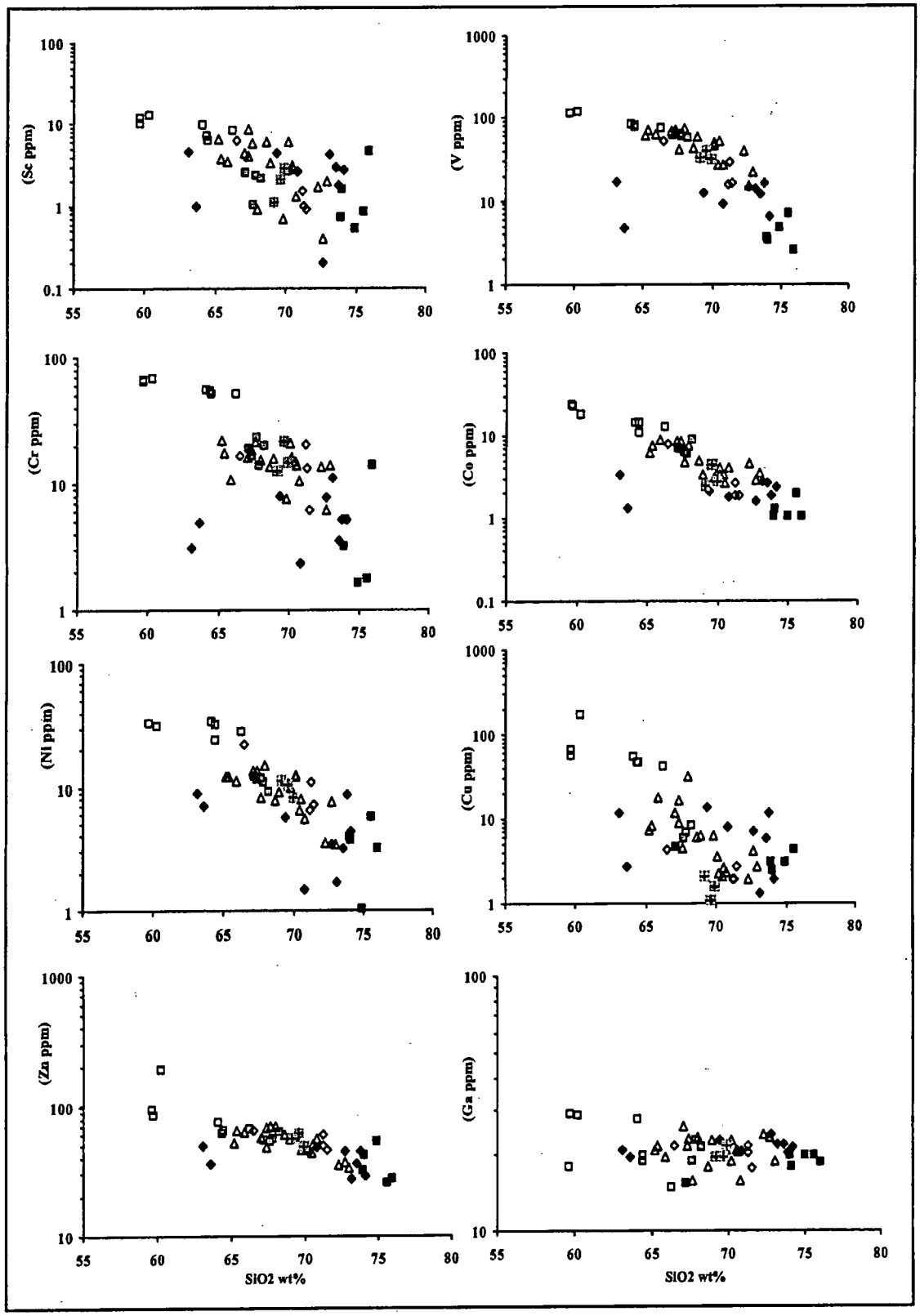

Figure 3.7 (continues)

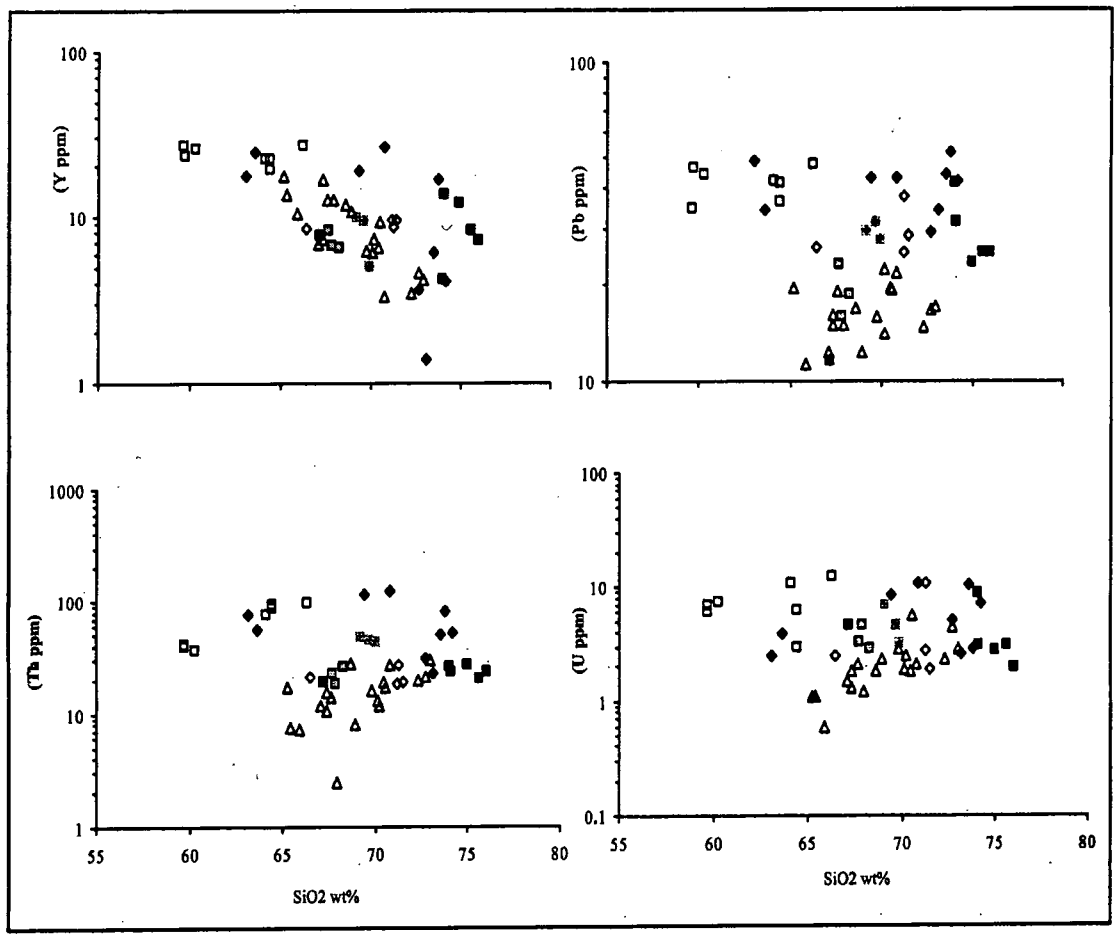

Figure 3.7 (continued).

3.2.2.2. Rare earth element (REE) geochemistry

The chondrite-normalised REE patterns for the granitoids from the Vumba granite-greenstone terrain are presented in Figure 3.8. As can be seen from this Figure, the granitoids are depleted in HREE relative to LREE. Additionally, Ce_N/Yb_N values in these granitoids vary from 10 to 55 with the Domboshaba Granite and the Kalakamati Pluton showing the highest Ce_N/Yb_N values. The lowest values were recorded from the Mashawe Pluton. The granitoid's REE patterns are variably characterised by negligible positive to negative Eu anomalies. However, some of the plutons virtually have no Eu anomalies

Furthermore, the granitoid rocks are characterised with low Yb_N values (< 5) except the Kalakamati Monzonite Pluton and few samples of the Domboshaba Granite that have Yb_N values between 8 and 10. Jahn et al (1981) and Martin (1986) have shown that the low Yb_N values ($Yb_N<9$) for Archaean granitoids are the result of partial melting of subducted metamorphosed basalt with amphibole and/ or garnet in the residue.

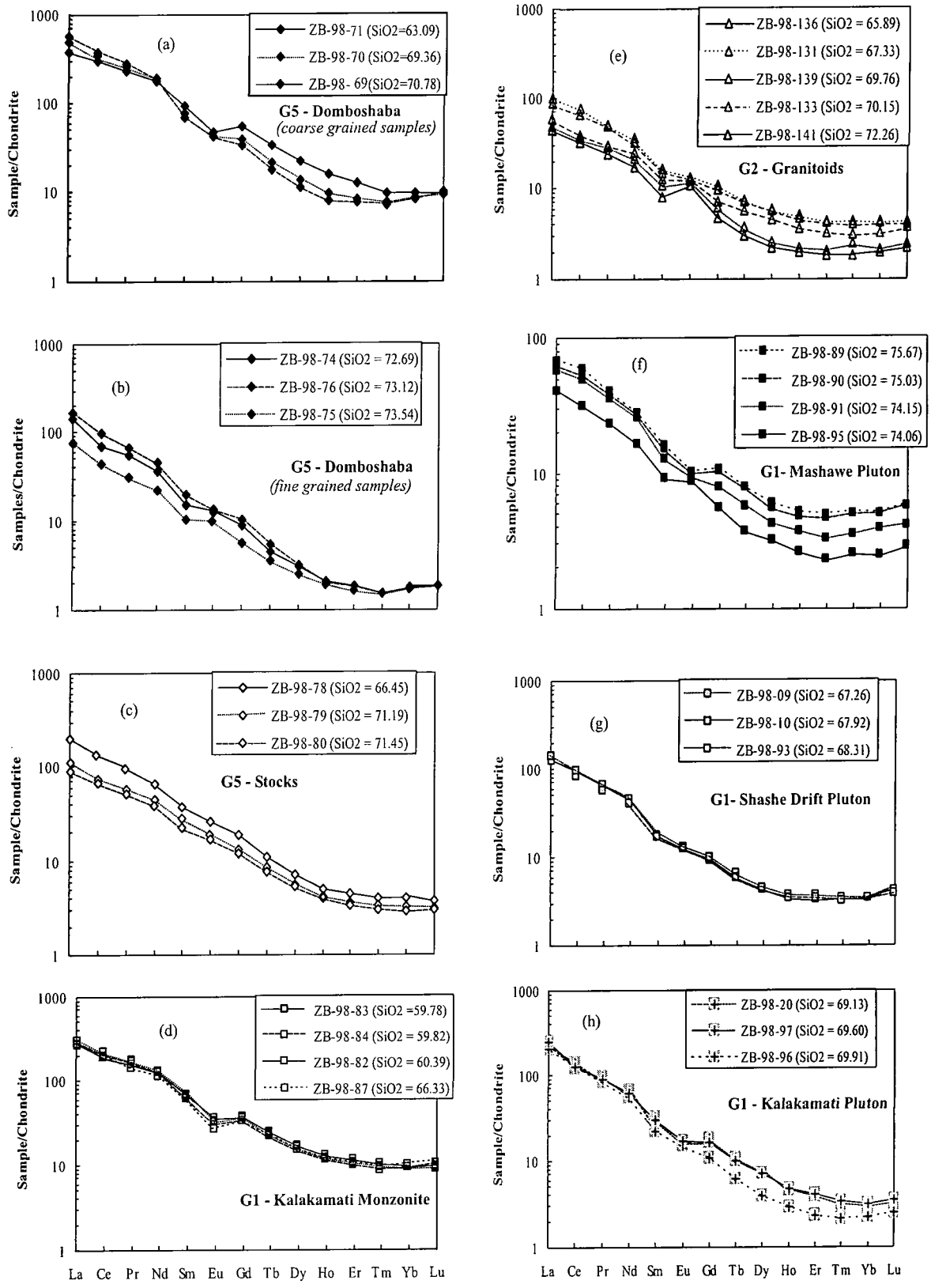

Figure 3.8: Representative chondrite-normalised REE patterns for the granitoids from the Vumba granite-greenstone terrain. Chondrite-normalising values from Boynton (1984)

3.2.2.3. Multi-element patterns

Chondrite-normalised multi-element patterns for the granitoid rocks from the Vumba granite-greenstone terrain are presented in Figure 3.9. Multi-element diagrams contain a heterogeneous mix of trace elements arranged in order of increasing compatibility in a small fraction of the mantle melt. The patterns of the so-called G5, G2 and G1 granitoids are broadly similar in shape.

The granitoids slightly differ in the absolute abundances of the elements. Overall, the patterns for all the granitoid rocks from the Vumba granite-greenstone terrain are characterised by high large ion lithophile element (LILE) contents (Ba, Rb, Th and K) relative to high field strength elements (Nb, Ti, Zr and Y). The enrichment of LILE and the Nb depletion are indicative of a crustal component introduced to the mantle by subduction or to the magma by assimilation and fractional crystallisation (AFC) (Pearce and Peate, 1995) or both. Most 'spidergrams' exhibit a pronounced positive Th anomaly with respect to Rb and K with the exception of some samples from the G2 granitoid rocks that show a negative Th anomaly. The shapes of 'spidergrams' of the granitoids from the Vumba granite-greenstone terrain do not resemble those for the upper and lower continental crust (see Fig.3.9h), except the coarse section of the Domboshaba Granite which resembles the upper continental crust.

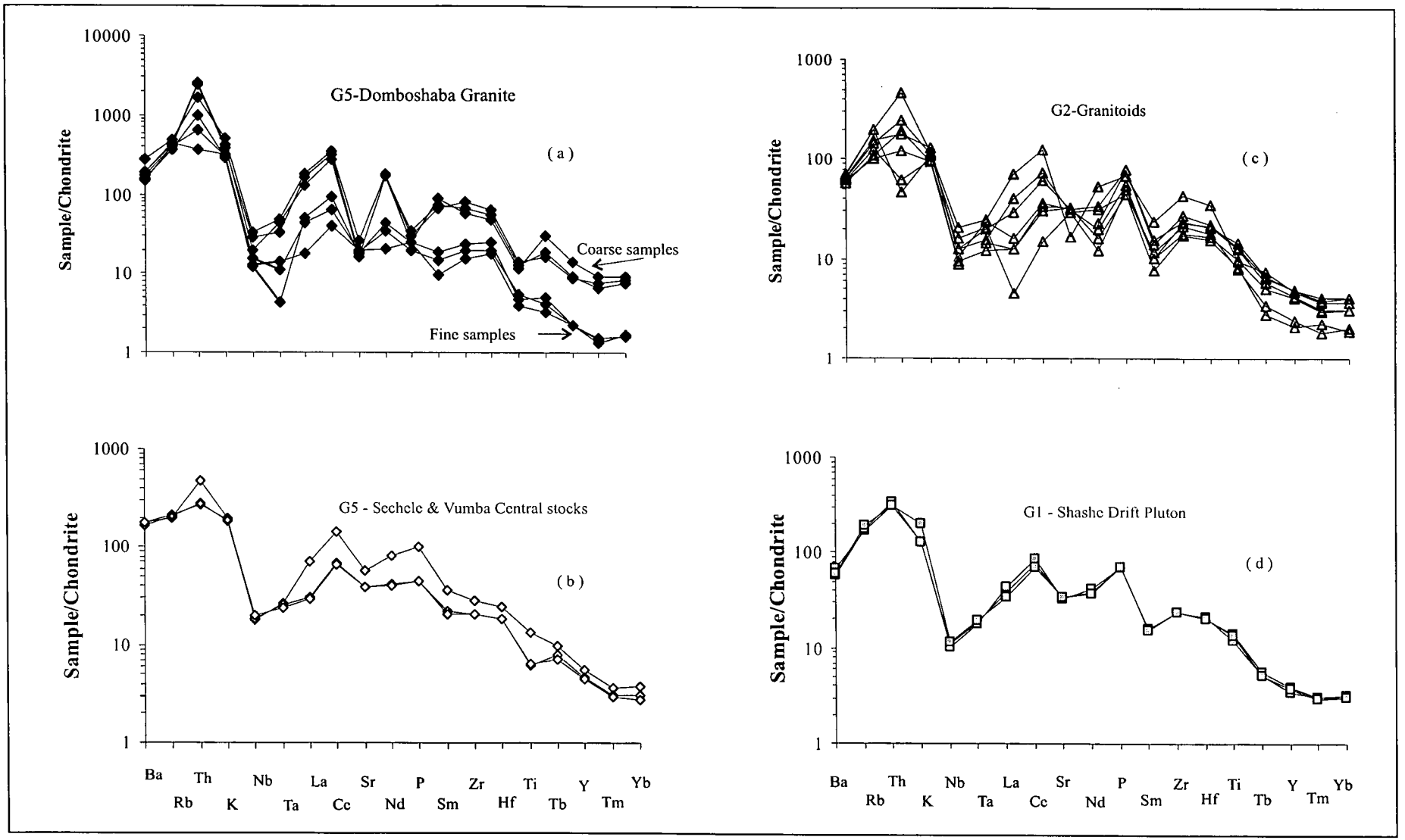

Figure 3.9: Representative chondrite-normalised spider diagrams for the granitoids from the Vumba grainite-greenstone terrain. Chondrite-normalising values from Thompson (1982). (h) is inserted for comparison purpose. Upper continental crust values are from Taylor and McLennan (1981); Lower continental crust values from Weaver and Tarney (1984). Chondrite-normalising values from Thompson (1982).

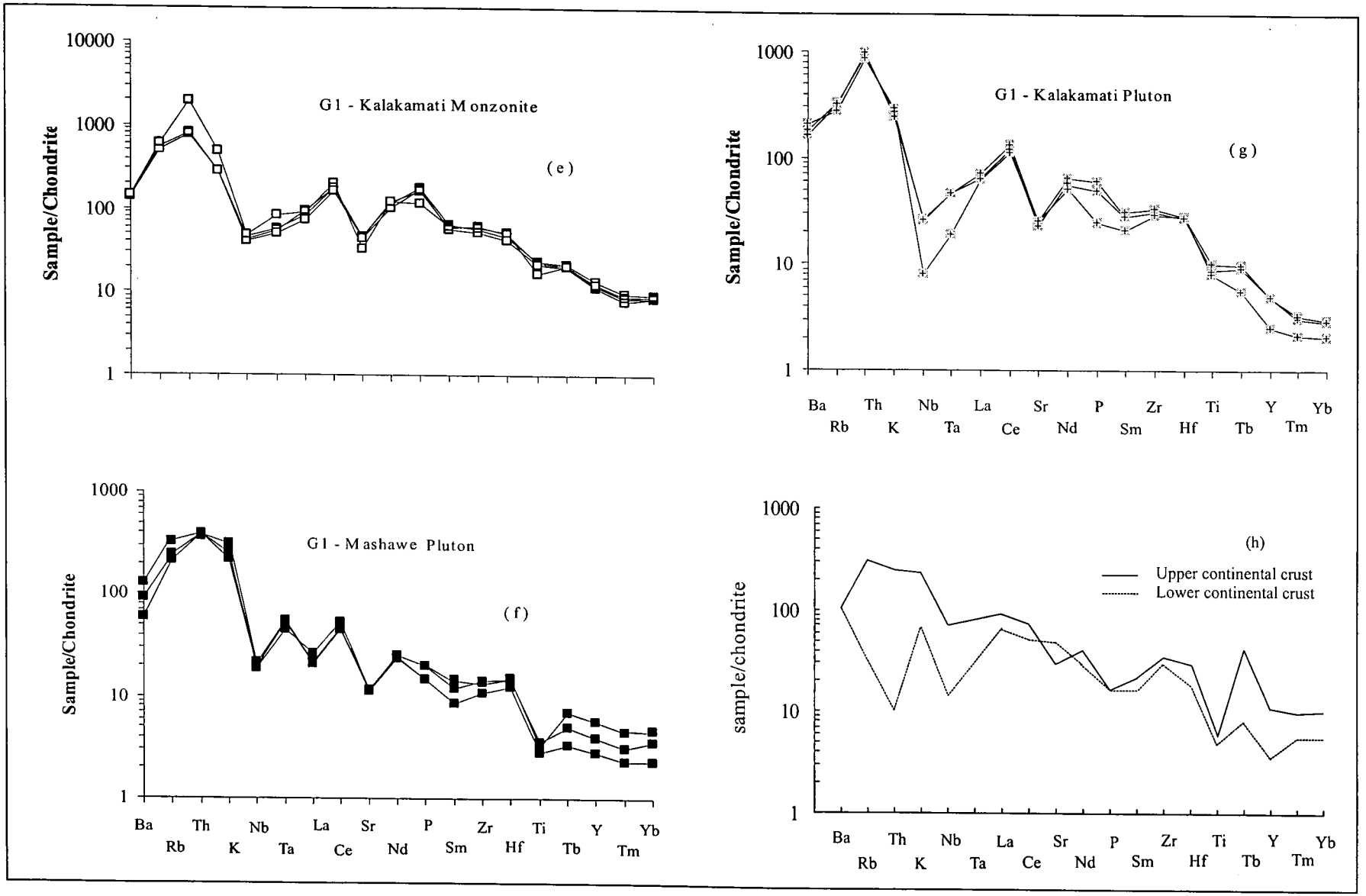

Figure 3.9: Continued.

3.2.2.4. Large Ion Lithophile Element Modelling

Several attempts at petrogenetic modelling of granite systems have been based on the large ion lithophile (LIL) elements, Ba, Rb and Sr (e.g. McCarthy and Hasty 1976; McCarthy and Groves 1979; Tindle and Pearce 1979). These elements are useful because they occur predominantly in the major silicate minerals, thus avoiding the need to know the abundances and behaviour of the accessory minerals. Here, the objective is to define the main fractionation trends followed by these elements in the discrete plutons of the Vumba granite-greenstone terrain and to compute the combinations of minerals that best simulate the observed trends.

Changes in LIL element concentrations during fractionation can be examined and modelled more quantitatively by comparing observed and theoretical fractionation vectors on log-log bivariate plots. Therefore, the LIL data are presented as logarithmic plots of Ba against Rb and Ba against Sr in Figure 3.10A. Three unambiguous trends show up on these diagrams: *trend a* followed by samples from the Domboshaba Granite in which Ba and Sr decrease while Rb increases slightly with fractionation; *trend b* followed by samples from the Kalakamati Pluton in which Ba and Sr decrease while Rb increases slightly with fractionation; *trend c* followed by samples from the Mashawe Pluton in which Ba, Sr and Rb increase with fractionation. The G2 granitoids, the Kalakamati Monzonite Pluton and the G5 stocks show ambiguous trends.

In theory, there are two basic equations that describe the extremes of behaviour of trace elements during crystallisation:

$$C_l/C_o = F^{(Da-1)} \qquad \text{(Eq. 1)}$$

For perfect (or Rayleigh) fractional crystallisation (where the surface of the crystals is in equilibrium with the melt)

$$C_l/C_0 = 1/[F + D(1 - F)] \qquad \text{(Eq. 2)}$$

For equilibrium crystallisation (where the whole of each solid phase remains at all times in equilibrium with the melt).

Where C_0 : *concentration of element a in the original melt.*

C_l : *concentration of element a in the residual melt.*

F : *weight fraction of melt remaining.*

D : *bulk distribution coefficient for element a*

($D_a = \Sigma_i K^i_a X_i$ *where* K^i_a = *distribution coefficient for element a in phase i and* X_i = *weight fraction of phase i)*

However, in carrying out the modelling only the Rayleigh fractionation equation (Eq. 1) was employed because crystals are commonly removed from the site of formation after crystallisation and the distribution of trace elements is not an equilibrium process (Tindle and Pearce, 1979). Theoretical vectors drawn for 50% crystallisation of single clinopyroxene, plagioclase, hornblende, biotite and alkali feldspar indicated in the variation diagrams (Fig.3.10B) show how melt composition should change during crystallisation of the single minerals. Thus alkali feldspar and some plagioclase could control *trends a* and *b,* and hornblende and clinopyroxene would enable *trend c* to be modelled. The likely proportions of the crystallising minerals were iteratively varied until the deviation of predicted vectors from observed was a minimum on both diagrams (Fig.3.10C). The vectors can be moved to any presumed parental compositions, so the starting composition is not crucial. The mineral/liquid partition coefficients used in the modelling are given in Table 3.7.

Element	Mineral				
	Cpx	Plg	Hbl	Bi	Ksp
Rb	0.032	0.048	0.014	4.200	0.487
Sr	0.516	2.840	0.022	0.120	3.870
Ba	0.131	0.360	0.044	6.360	6.120

Table 3.7. Mineral/liquid partition coefficients obtained from Arth (1976), Mahood and Hildreth (1983) and Nash & Crecroft (1985).

It is important to note that, in the LIL diagrams (Fig. 3.10) is not possible to move from one trend to another by a change in the crystallising assemblage. In other words, is not possible to genetically link the three discrete plutons. Furthermore, the field evidence favours a multiple intrusion of magmas rather than a continuous process.

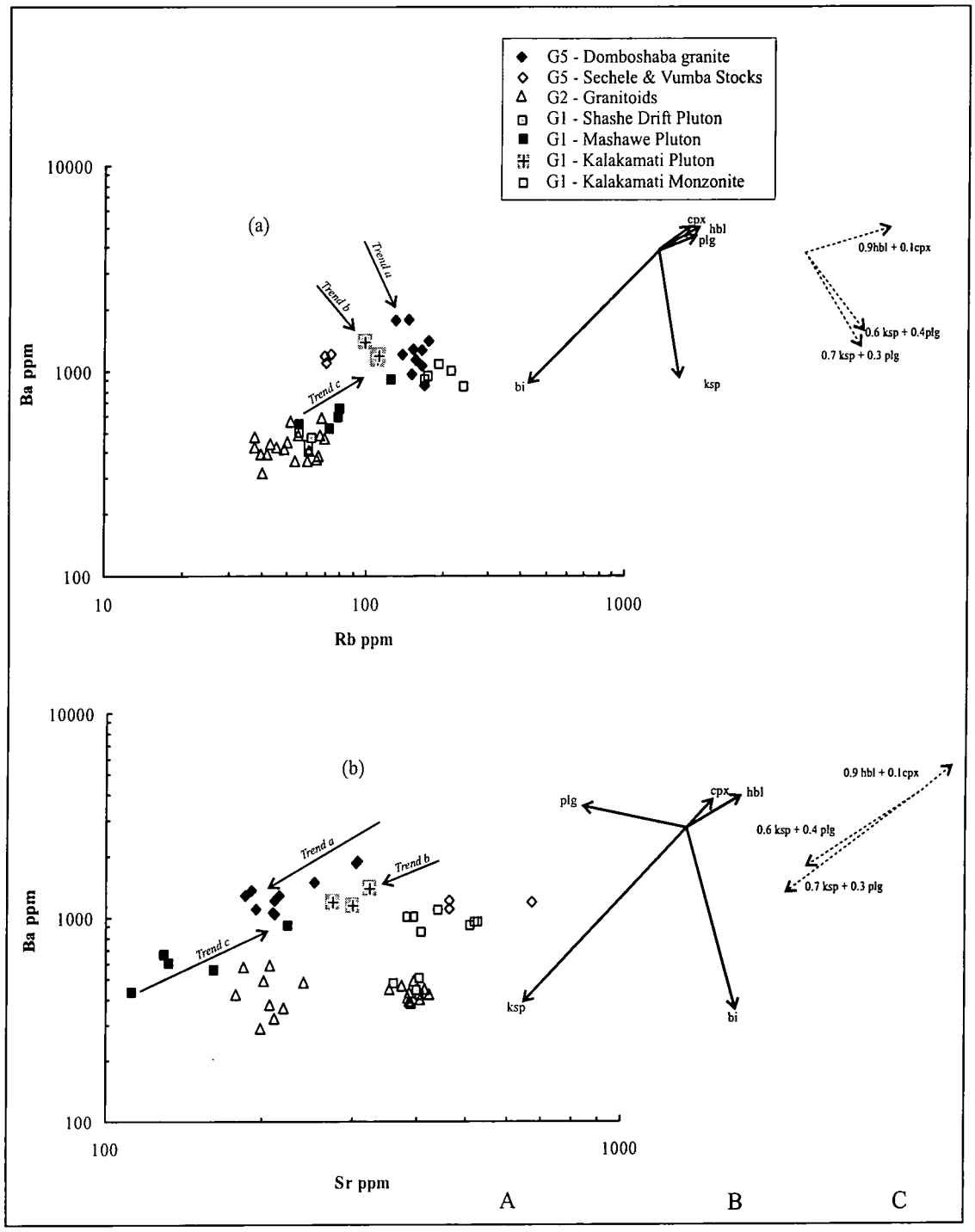

Figure 3.10A – C. Ba – Rb and Ba-Sr variation diagrams for the granitoids from the Vumba granite-greenstone terrain.The diagrams on the left (**A**) show the distribution of data points and direction of the three observed fractionation trends. The vectors in the middle (**B**) show theoretical effects on melt composition of crystallising single mineral phases (assuming Rayleigh fractionation). The diagrams on the right (**C**) present the modelled variations which combine the effects of certain minerals as discussed in the text. For distribution coefficients used in (**B**) and (**C**), see Table 3.6.

3.2.3 Tectonic setting

3.2.3.1. ORG-normalised Diagrams

Pearce et al (1984) proposed a normalised trace element pattern for granites to classify them on the basis of their tectonic settings. Trace element abundance are normalised to a hypothetical ocean ridge granite (ORG) produced by assuming 75% fractional crystallisation of average N-type mid ocean ridge basaltic magma (MORB) (Pearce et al., 1984). Pearce et al. (1984) arranged the chosen elements on the basis of their relative incompatibility during MORB genesis (which increases from Yb to Rb) and K_2O was added to the left-hand side of the pattern. Ce, Sm and Yb were used to represent REE. The normalising conditions, therefore, represent the composition of a granite would have had were it: (1) ultimately derived from convecting upper mantle unaffected by any mantle enrichment event; (2) derived from a basalt by fractional crystallisation of a plagioclase-olivine-clinopyroxene-magnetite assemblage; and (3) unaffected by crustal melting or assimilation or by volatile-dominated processes (Pearce et al., 1984). Deviations from a flat pattern should reflect deviations from this simple genetic history and should thus vary systematically from setting to setting.

The hypothetical ocean ridge granite normalised patterns for the granitoid samples from the Vumba granite-greenstone terrain are presented in Figure 3.11. Figure 3.11(e) shows the pattern of the well-known granites from the volcanic arc settings and is presented here for comparison purposes. As can be observed from Figure 3.11, the ORG normalised patterns of the granitoid rocks from the Vumba granite-greenstone terrain are typical of volcanic arc and post-collision granites. They resemble the Chilean arc granitoids, which are identical to the post-collision granitoids. All the samples exhibit the enrichments in large ion lithophile elements (K, Rb, Ba and Th) and LREEs (Ce and Sm) relative to high field strength elements (Ta, Nb, Hf, Zr, Y and Yb).

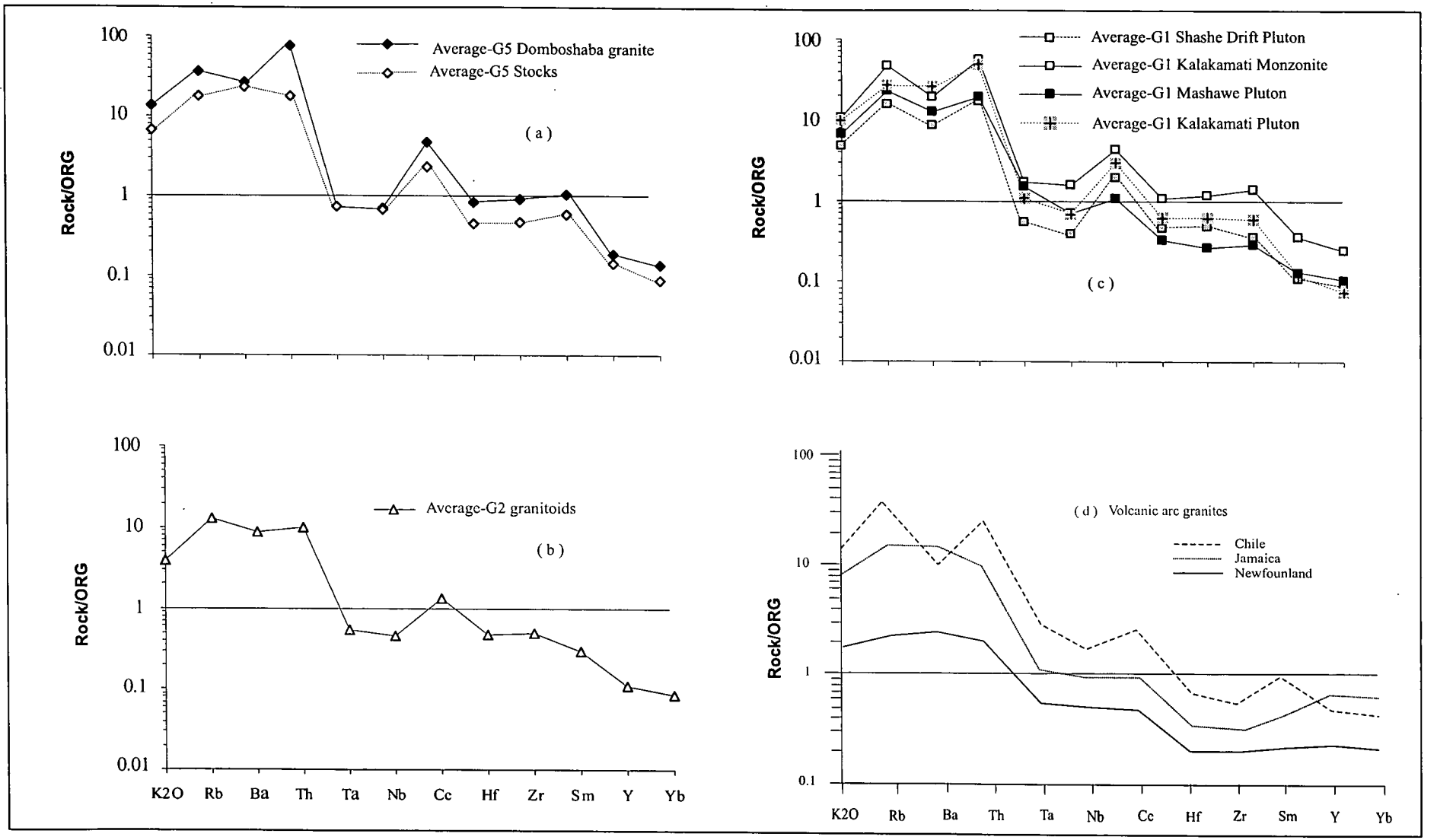

Figure 3.11:ORG-normalised patterns for the granitoids from the Vumba granite-greenstone terrain. Normalising values from Pearce et al. (1984). Figure3.11 (d) compares the granitoids from the Vumba granite-greenstone terrain to well-known granites from the volcanic arc setting.

The Th/Yb ratios of the Vumba granite-greenstone terrain granitoids out plotted against their Nb/Yb ratios in Fig. 3.12. As can be seen from Figure 3.12, all the granitoids are displaced from the mantle metasomatism array towards higher Th/Yb ratios, suggesting either derivation from an enriched mantle source to which a subduction component had been added, or coupled crustal contamination with fractional crystallisation or both. They plot above the average crust composition. In addition, Th/Yb ratio increases from the G2 granitoids through the Mashawe and the Kalakamati Monzonite Plutons to the Domboshaba Granite and Kalakamati Pluton. This probably indicates a variability in the magnitude of the subduction component.

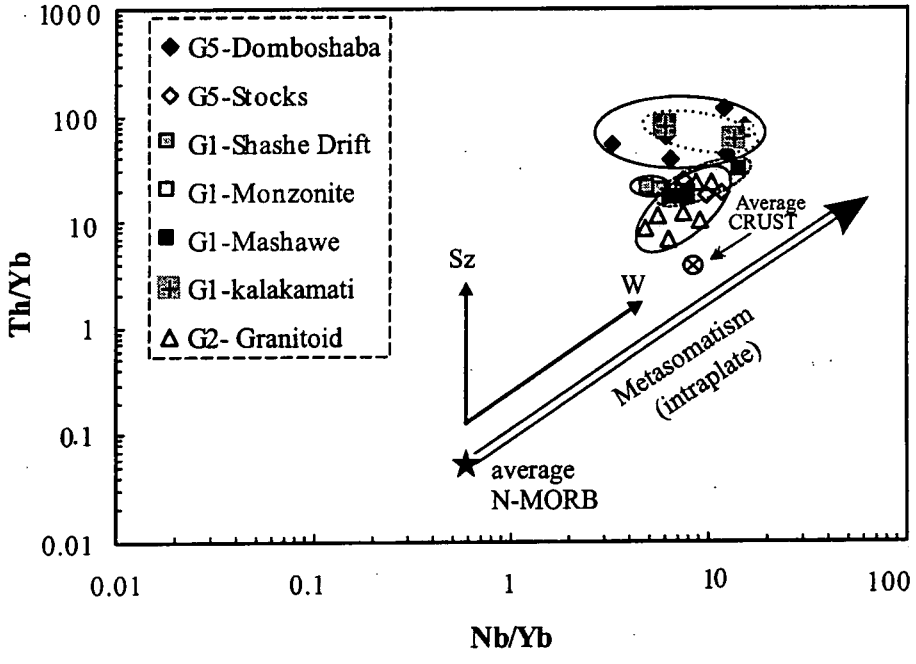

Figure 3.12: Th/Yb versus Nb/Yb diagram (after Pearce, 1983) for the granitoids. N-type MORB values from Sun and McDough (1989); Average continental crust values from Weaver and Tarney (1984). Abbreviations: Sz-Subduction zone enrichment; W-Within enrichment.

3.2.3.2. Tectonic discrimination diagrams

The most commonly used tectonic discrimination diagrams for granites were introduced by Pearce et al (1984). They classified granites into ocean-ridge, volcanic-arc, within-plate and collision types. Pearce et al. (1984) conducted a preliminary survey of trace element concentrations plotted against silica content from a suite of 600 selected granites. The survey revealed that amongst the list of trace elements Rb, Nb (or Ta) and Y (or Yb) were the most efficient discriminants between most types of ocean-ridge granites (ORG), within-plate granites (WPG), volcanic-arc granites (VAG) and syn-collision granites (syn-COLG). Pearce et al. (1984) noted that the granite composition is basically controlled by source rock composition and not by tectonic setting, but they also demonstrated that granites from different tectonic settings have distinct trace element characteristics.

On tectonic discrimination diagrams that employ the concentration of Nb and Y (Pearce et al., 1984) the granitoids from the Vumba granite-greenstone terrain fall entirely into the volcanic-arc and syn-collision granitoids field (Fig. 3.13a). In the Rb - (Nb + Y) discrimination diagram of Pearce et al. (1984) all the samples of the Vumba granitoids plot in the compositional field of volcanic arc granitoids except the samples from the Kalakamati Monzonite Pluton and the Domboshaba Granite which straddle the boundary between VAG and syn-COLG (Fig. 3.13b). It is worth noting the distinctive distribution of the granitoids groups in these tectonic discrimination diagrams, particularly in the Figure 3.13b.

Post-orogenic granites cannot be distinguished from volcanic-arc and syn-collision granites on the diagrams of Pearce et al. (1984), hence more geological input is required. This is deferred until the discussion chapter.

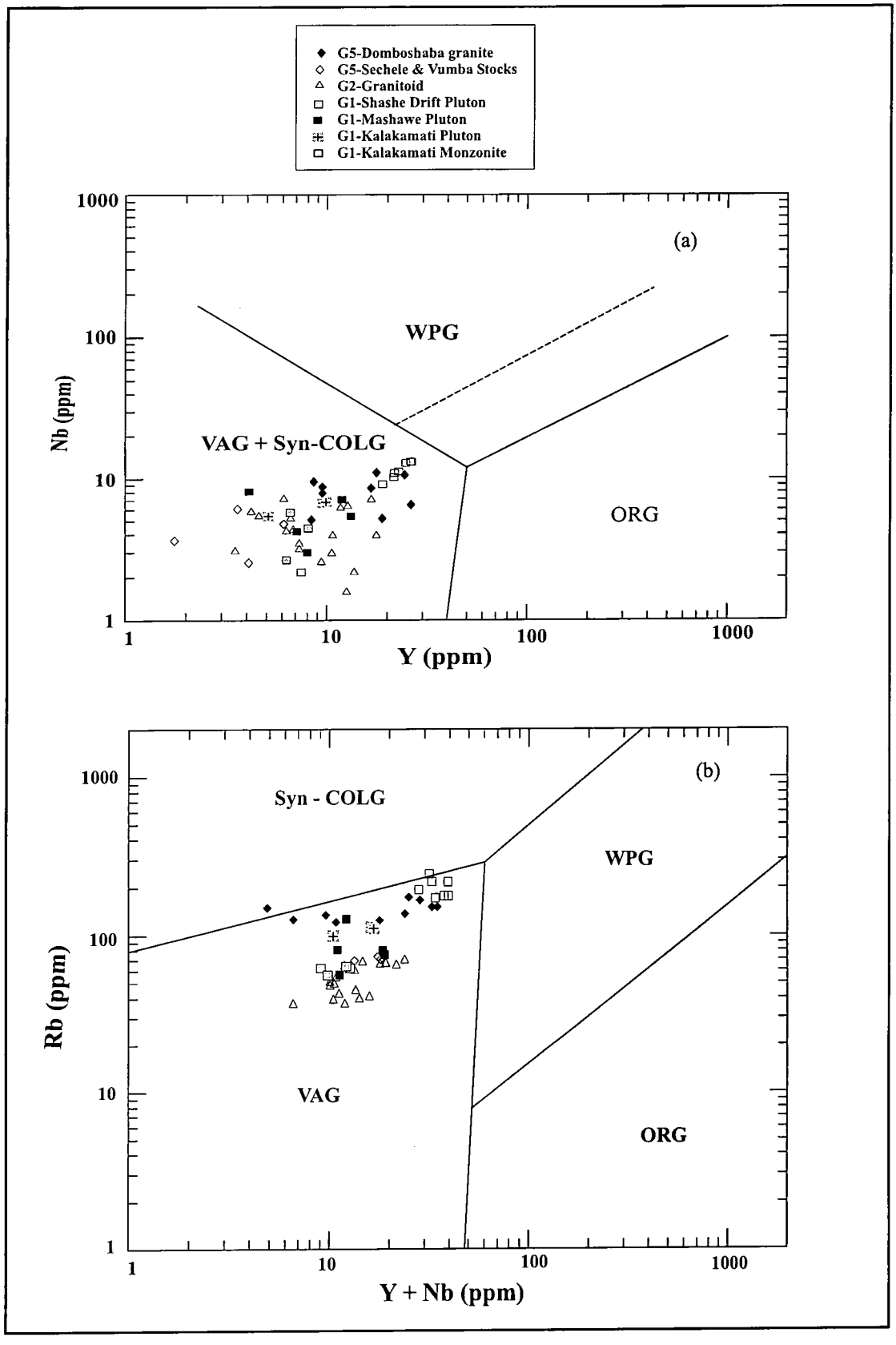

Figure 3.13: Plot of the granitoids from the Vumba granite-greenstone terrain on tectonic discrimination diagrams of Pearce et al. (1984). Abbreviations: ORG-oceanic ridge granite; COLG-collision granites; VAG-volcanic arc granites and WPG-within plate granites.

3.3. Summary

This section presents a summary of the general characteristics of the granitoids from the Vumba granite-greenstone terrain.

The Domboshaba Granite (youngest granitoid unit) is a monzogranite with biotite ± hornblende as ferromagnesian minerals. It is calc-alkalic according to Peacock's alkali-lime index, metaluminous to weakly peraluminous according to Shand's index and fits the description of I-type granites. It also high-K type granitoid.

The Vumba Central and Sechele Stocks which were previously identified as granites (Litherland, 1975; Key et al., 1976) are in reality granodiorites with hornblende and biotite as ferromagnesian minerals. Additionally, they are calc-alkalic and medium-K type granitoids. They vary from metaluminous to slightly peraluminous, and exhibit most of the characteristics of I-type granites.

The Mashawe and Kalakamati Plutons are in reality granodiorites not tonalites as previously indicated by Key et al (1976) and Litherland (1975). The Mashawe Pluton has biotite as the ferromagnesian mineral whereas the Kalakamati Pluton possesses both biotite and hornblende. They are both calc-alkalic according to Peacock's classification. The Mashawe and the Kalakamati Plutons are medium-K and high-K type respectively. Furthermore, they are metaluminous to weakly peraluminous and exhibit most of the features associated with I-type granites.

The Kalakamati Monzonite Pluton is primarily a quartz monzonite with hornblende and biotite as the ferromagnesian minerals. It is alkali-calic according to Peacock's alkali-lime index, and metaluminous according to Shand's index. It is also a high-K type granitoid. The Kalakamati Monzonite Pluton fits the description of I-type granites.

The so-called G2 granitic paragneisses and the Shashe Drift Pluton are in reality tonalitic-granodioritic gneisses characterised by hornblende and biotite as

ferromagnesian minerals. They vary from metaluminous to slightly peraluminous, and exhibit most of the characteristics of I-type granites. In addition, the G2 granitoids and the Shashe Drift Pluton are medium-K type granitoids belonging to calc-alkalic series.

According to geochemical patterns and tectonic discrimination diagrams, all the plutons of Vumba granite-greenstone terrain are either volcanic arc granites or post-collision granites. Additionally, trace element ratio plots reveal that the granitoids are subduction- and/or collision-related.

Chapter 4

AMPHIBOLITE

This chapter is subdivided into the petrography and geochemistry of the amphibolitic rocks from the Vumba granite-greenstone terrain in NE-Botswana. The amphibolites in this terrain occur in three Formations, which are called the Vumba Mixed Volcanic Formation (VMVF), Vumba Lower Mafic Formation (VLMF) and Vumba Upper Mafic Formation (VUMF), in chronological order (see Fig.1.2).

4.1. Petrography

Two types of amphibolite were distinguished in the study area namely the metabasalt and metagabbro. The metabasalt is the most common type of the two and it occurs in all the formations. The metagabbro was only encountered in the VMVF. The distinction between the two types was based on mineralogy and grain size. The metabasaltic type exhibits a variety of recrystallisation textures, essentially consisting of fine quartz, plagioclase and hornblende meeting at triple point junctions with interfacial angles of around 120°. The prevalent textures include porphyroblastic, schistose and equigranoblastic textures. Most plagioclase crystals with albite twinning are An_{48} to An_{60} in composition (andesine to labradorite). The proportions of quartz, plagioclase and hornblende are about 5%, 20% and 75% respectively. Iron oxide and sphene are the common accessory phases in this type of amphibolite.

The metagabbroic type is medium grained and grey in colour. This type is foliated in some places and massive in others. Five representative thin sections examined in this study exhibit ubiquitous skeletal augite poikilitically enclosing plagioclase crystals associated with hornblende and sporadic quartz. This appears to

represent an inherited sub-ophitic and ophitic texture. Locally, augite alters to hornblende. Plagioclase proportion ranges between 30 and 35% while the mafic phases (hornblende and augite) vary from 60 to 65%. Quartz forms relatively fine crystals, which constitute about 5% of the rock. Some thin sections contain calcite. Sphene, epidote and iron oxide are accessory phases.

4.2. Geochemistry

4.2.1. Introduction

29 amphibolitic rock samples from the Vumba granite-greenstone terrain were analysed for major and trace elements. Whole-rock major and trace element concentrations were determined by XRF on fused discs and pressed powdered pellets respectively. In addition, a subset of 15 representative samples was analysed for Sc, V, Cr, Co, Ni, Cu, Zn, Ga, Rb, Sr, Y, Zr, Nb, Cs, Ba, REE, Hf, Ta, Pb, Th and U using the ICP-MS technique. For the set of XRF and ICP-MS data, refer to Appendix B (IV). The accuracy and precision of the analytical data is listed in Appendix C.

4.2.2. Evaluation of element mobility

A major problem with the geochemical study of ancient volcanic sequences is to account for the effects of post-magmatic alteration and to identify the preserved primary geochemical signature, which is able to unravel the origin of the protolith and its geotectonic setting. For the amphibolites from the Vumba granite-greenstone terrain, the relative and absolute mobilities of elements were tested prior to interpretation. The test adopted in this study is the one first used by Cann (1970) where the correlation matrix for all the elements that should behave incompatibly during basalt fractionation was examined. Appendix D lists correlation matrices for all the

elements calculated by the Pearson product-moment coefficient of correlation. If the correlation coefficient for a pair of elements is high (e.g. >0.7 or < -0.7), the ratio of these elements is unlikely to have changed by post-magmatic alteration (Rollinson, 1993; Pearce, 1996).

According to observational and theoretical criteria, Ti, V, Zr, Hf, Nb, Ta, P, REE (except La), Cr, Th, Al and Ga are usually immobile up to upper amphibolite and granulite facies (Pearce, 1996). However, immobile elements can become mobile under high grades if the fluid composition changes from H_2O-rich to CO_2-rich (Janardhan et al., 1982; Pearce, 1996). Elements which are often used for discrimination are the incompatible high field strength elements (e.g. Zr, Ti, Nb, Y) and compatible elements like P and V. In this study, the correlation coefficients between pairs of these elements show high values, and hence immobile behaviour during post-magmatic alteration processes can be assumed (see Appendix D). It is important to realise that even immobile elements can increase in absolute abundance due to concentration by leaching of mobile elements (Pearce, 1976; Rollinson, 1993; Pearce, 1996). Nevertheless, most discrimination diagrams employed are based on immobile element ratios and these will not be affected.

4.2.3. Identification of the amphibolite

The content of SiO_2 in the amphibolites ranges from 47 to 54 wt.% (on LOI-free basis) manifesting basic to slightly intermediate composition. However, a vast number of the samples have basic composition (45 – 52 wt.% SiO_2). The Mg# [=100xMg/(Mg + Fe_{total})] ranges between 64 and 31. The normative compositions contain quartz or olivine + hypersthene and thus these amphibolites can be classified quartz or olivine tholeiites.

On the classification diagram of Pearce (1996) which is based on ratios of immobile elements (Zr/Ti and Nb/Y) (Fig.4.1), the amphibolitic samples from the Vumba granite-greenstone terrain plot in the subalkaline basalt field and correspond to the basic composition, except one sample from the Vumba Upper Mafic Formation, which corresponds to the intermediate composition. It is worth mentioning that the diagram of Pearce (1996) is equivalent to the diagram of Winchester and Floyd (1977). Nevertheless, the two diagrams exhibit different field boundaries despite equivalent axes. One advantage of the diagram of Pearce (1996), is that it enables basic, intermediate and evolved rocks to be distinguished and thus provides useful filter for the basalt discrimination diagrams.

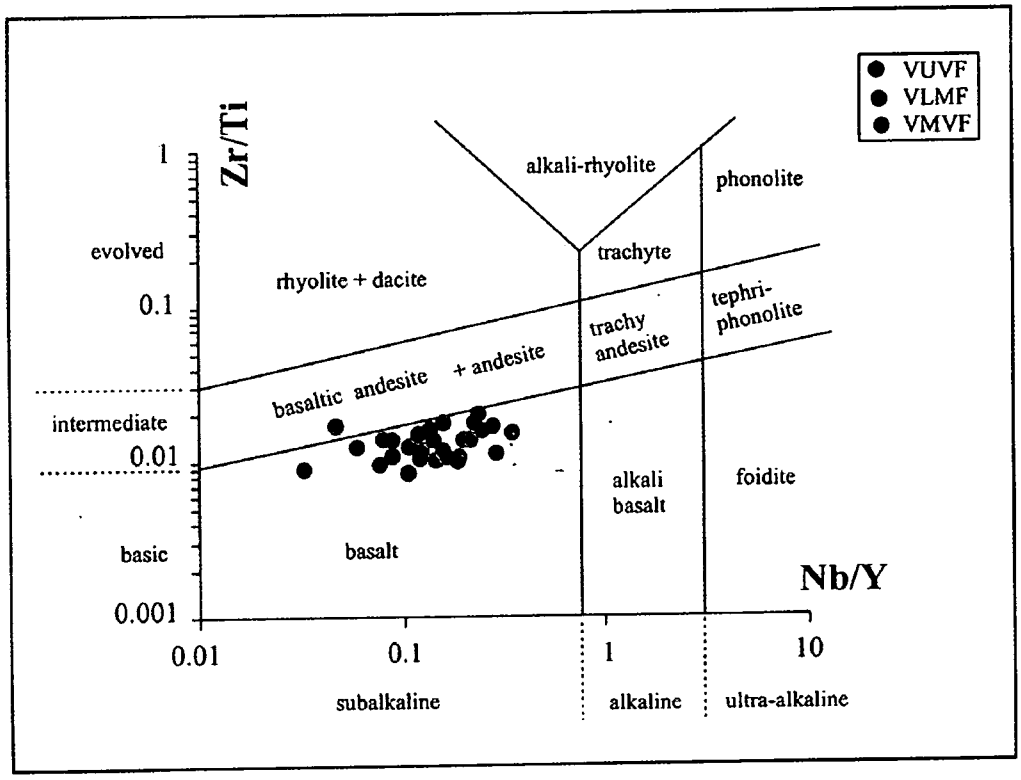

Figure 4.1 Classification of the amphibolitic rocks from the Vumba granite-greenstone terrain using log Zr/Ti vs log Nb/Y diagram. Fields are after Pearce (1996).

4.2.4. Geotectonic settings

A number of diagrams have been published for determining the tectonic environment of eruption of ancient mafic lavas. One commonly used discriminant plot is the Ti-Zr-Y diagram of Pearce and Cann (1973) which most effectively discriminates between within-plate basalts (i.e ocean-island or continental flood basalts) and other basalt types. As can be observed from Fig.4.2 the amphibolites from the Vumba granite-greenstone terrain plot in an ambiguous field B on the Ti-Zr-Y diagram. This is the field where basalts from volcanic arc (VAB) and mid ocean ridge (MORB) settings would plot (Pearce and Cann, 1973). Thus VAB versus MORB settings for the amphibolites from the three mafic formations of the Vumba granite-greenstone terrain.

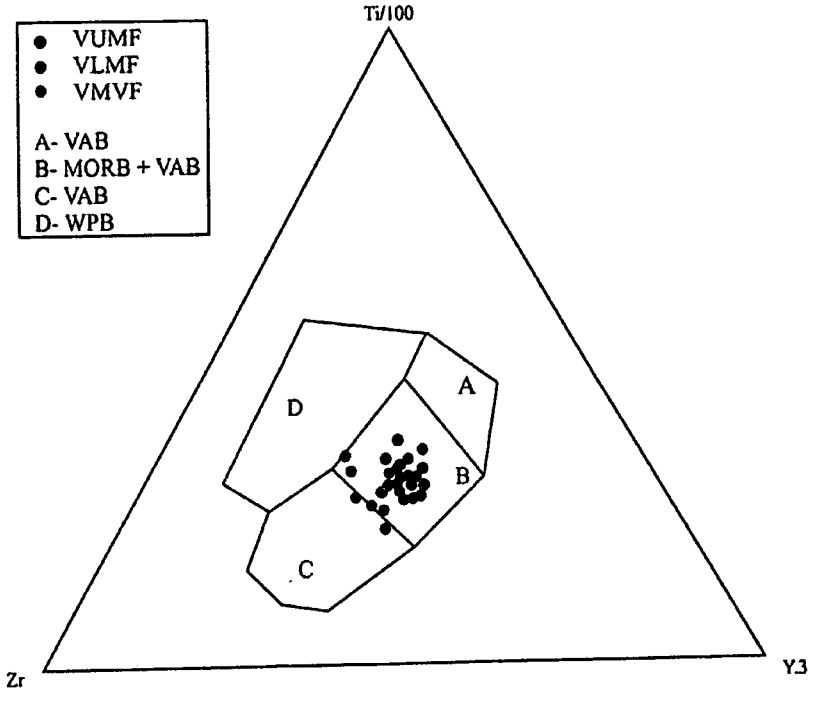

Figure 4.2. Plot of the amphibolites from the Vumba granite-greenstone terrain on Ti-Zr-Y tectonic discrimination diagram of Pearce and Cann (1973). Abbreviations: MORB-mid ocean ridge basalt; VAB-volcanic arc basalt; WPB-within plate basalts.

In order to determine whether the amphibolites belong to a VAB or MORB setting, the Th-Hf-Ta diagram of Wood (1980) was employed (Fig.4.3). The Th-Hf-Ta diagram unequivocally identifies the amphibolites from the Vumba granite-greenstone belt as VAB. Moreover, VABs in the Th-Hf-Ta diagram are subdivided into island-arc tholeiites (Hf/Th >3) and calc-alkaline basalts (Hf/Th <3) on the basis of their Hf/Th ratios. It is evident from Figure 4.3 that most of the amphibolites classify as calc-alkaline basalts, except one sample from the VUMF and VMVF each and all the samples from the VLMF which classify as tholeiitic basalts. It is important to mention that the Th, Hf and Ta concentrations used in Figure 4.3 are accurate ICP-MS determinations.

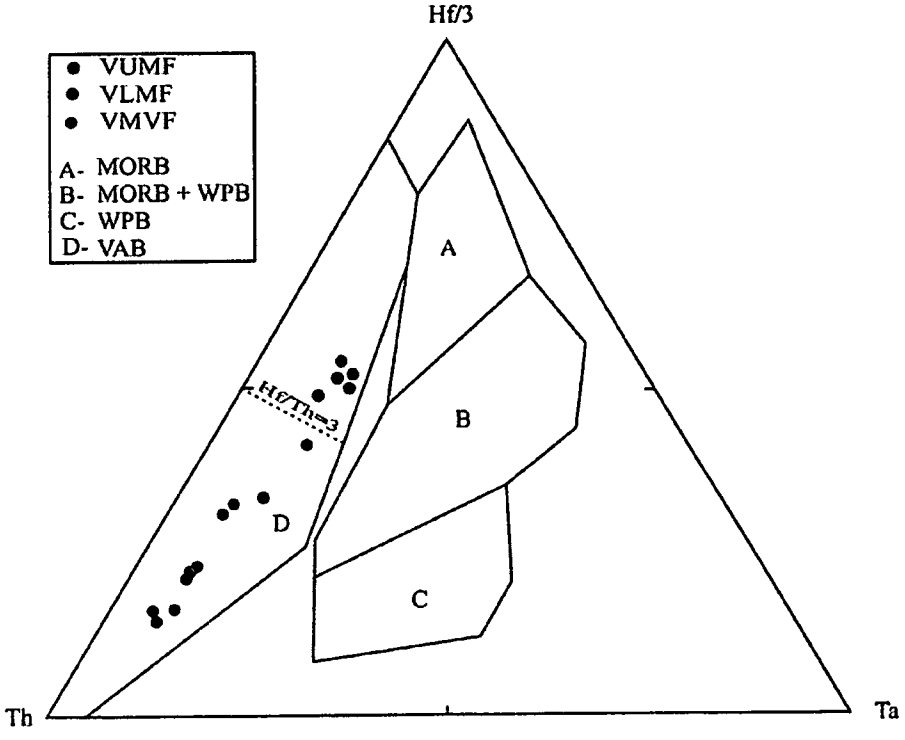

Figure 4.3: Plot of the amphibolites from the Vumba granite-greenstone terrain in the Th-Hf-Ta tectonic setting discrimination diagram of Wood (1980).

Unfortunately, there are other settings which would resemble VAB in the Ti-Zr-Y and Th-Hf-Ta discriminant plots and these include (a) some attenuated

continental lithosphere settings particularly those that involved extensive crustal assimilation, (b) some marginal basin spreading axes, those which lay directly above a subduction zone, and (c) some syn-collision settings or post-collision settings with extensive crustal assimilation (Pearce, 1996).

In the case of volcanic arc versus attenuated continental lithosphere, the Ti-V diagram of Shervais (1982) is commonly applied to resolve this ambiguity. This diagram distinguishes IAT (island arc tholeiites), MORB, CFB (continental flood basalts) and OIT (ocean-island tholeiites) on the basis of immobile elements, V and Ti. Amphibolitic samples from the Vumba granite-greenstone terrain show affinities to IAT in the Ti-V diagram (Fig.4.3). Additionally, the Ti/V ratios of the amphibolites from the Vumba granite-greenstone terrain are similar to the values in island arc tholeiitic basalts (Ti/V=10-18) (Shervais, 1982). Contaminated basalts from attenuated continental lithosphere, which commonly plot in the VAB field in the above-mentioned discrimination diagrams, would commonly plot in the CFB + MORB field on the Ti-V diagram (Shervais, 1982; Rollinson, 1993; Pearce, 1996). Therefore, the possibility of an attenuated lithosphere setting for the amphibolites has been eliminated.

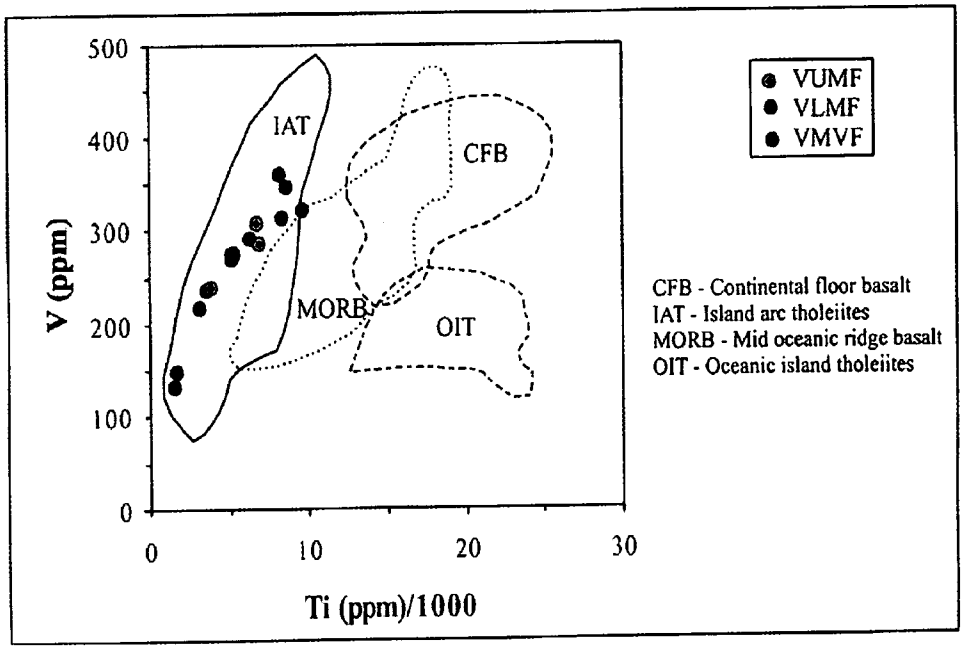

Figure 4.4: Plot of the amphibolites from the Vumba granite-greenstone terrain in the Ti versus V diagram of Shervais (1982).

It is important to note the dispersion of the mafic metavolcanic data on the Th-Hf-Ta diagram which is generally linear and displaced towards the Th corner of the triangle. According to Pearce (1996), sometimes volcanic arc basalts can be distinguished from post-collision basalts by their more linear distribution. Thus the conspicuous linear distribution in Figure 4.4 nullifies the possibility of post-collision setting for the amphibolites. The distinction between a true volcanic arc and a marginal basin setting requires geological input to augment the geochemical criteria. This will be covered later in the discussion chapter.

The Th/Yb versus Ta/Yb diagram of Pearce (1982) presented as Figure 4.5 was employed for further verification of the geotectonic setting for the amphibolites from the Vumba granite-greenstone terrain. This diagram uses Th/Yb and Ta/Yb ratios to separate subduction from mantle components. Yb is used as a normalising factor to largely eliminate variations due to partial melting and fractional crystallisation. It is an effective normalising factor because it does not participate in the enrichment processes

of Th and Ta. On the diagram (Fig. 4.5), vectors have been drawn to highlight the main components of variation. Pearce (1982, 1983) has demonstrated empirically that within-plate enrichment events enrich Ta and Th equally hence its vector has a slope of unity. He also demonstrated that the subduction component affects Th but not Ta hence its vector is sub-vertical and crustal contamination affects Th more than Ta hence its vector is also sub-vertical. As a result, MORB and within plate basalts plot within a well-defined band, while volcanic arc basalts and within plate basalts that have suffered contamination by continental crust, are displaced to higher Th values. The amphibolites from the Vumba granite-greenstone terrain are unequivocally displaced to higher Th values which manifests that they are subduction related or within plate basalts that suffered extensive contamination by continental crust (Fig.4.5). Nevertheless, previous discriminant diagrams have ruled out within plate settings for these amphibolites. It is worth mentioning that the amphibolitic samples are displaced above the average MORB and primordial mantle compositions along a steep vector and far from the average continental crust composition, which probably indicates subduction rather than crustal contamination (Fig.4.5). In this diagram volcanic arc basalts are subdivided into tholeiitic, calc-alkaline and shoshonitic varieties. Most of the amphibolitic samples plot as calc-alkaline basalts with a few showing tholeiitic affinity on the Th/Yb vs Ta/Yb diagram. This is consistent with the results from the Th-Hf-Ta diagram in Figure 4.3.

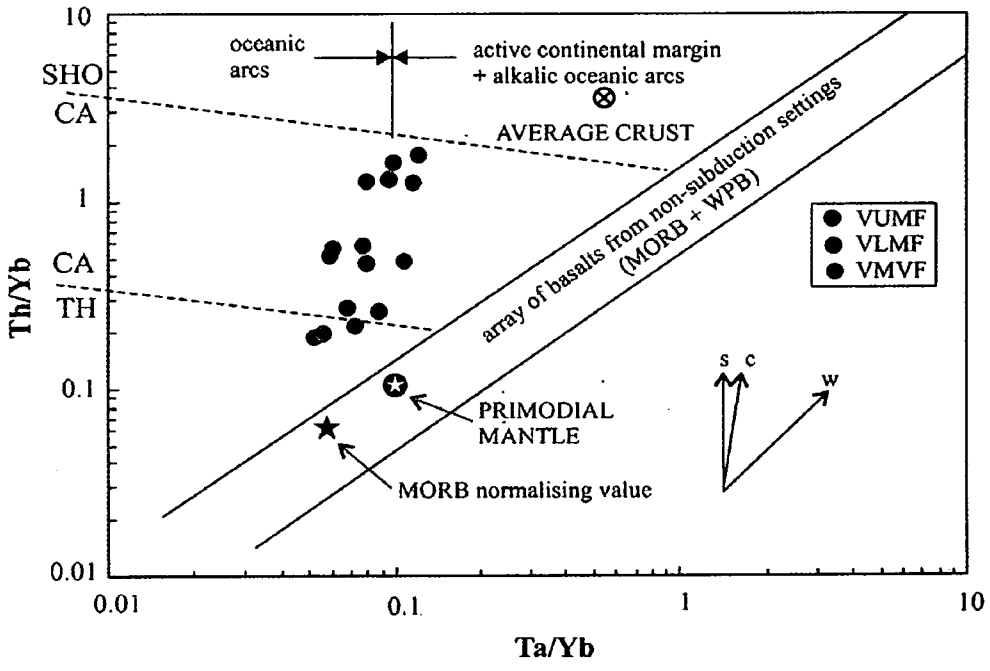

Figure 4.5: Th/Yb versus Ta/Yb diagram (after Pearce, 1983) for the mafic metavolcanics from the Vumba granite-greenstone terrain. Abbreviations: c-crustal contamination; CA-calc-alkaline; s-subduction zone enrichment; SHO-shoshonites; TH-tholeiites and w-within plate enrichment. Average continental crust values from Weaver and Tarney (1984).

Furthermore, volcanic arc basalts can be subdivided into oceanic and continental types. Pearce (1983) pointed out that most basalts from active continental margins have Ta/Yb values greater than 0.1 whereas basalts from oceanic arcs have values less than 0.1. However, the amphibolites from the Vumba granite-greenstone terrain have Ta/Yb values ranging from 0.04 to 0.15, which suggests both continental and oceanic type arcs. A more effective discriminant diagram for this purpose is the Zr/Y versus Zr diagram of Pearce (1983) presented as Figure 4.6. The amphibolites mainly plot in the continental margin field and only a few straddles the overlapping area, which essentially favours the predominant continental arc origin for the amphibolites of the Vumba granite-greenstone terrain.

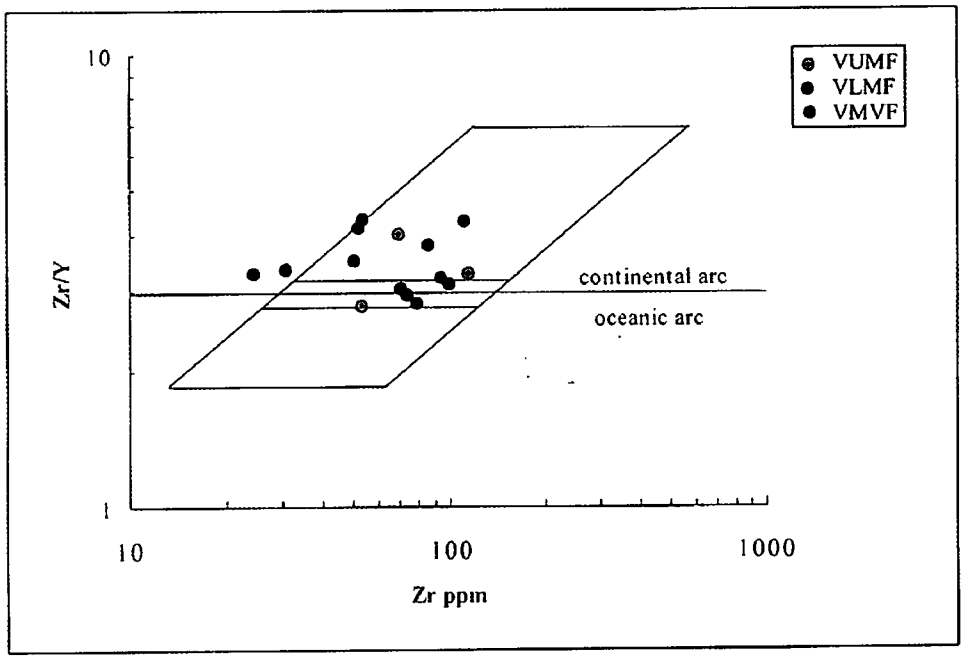

Figure 4.6: Plot of the amphibolites from the Vumba granite-greenstone terrain in the Zr/Y versus Zr diagram of Pearce (1983)

4.2.5. Geochemical patterns

Geochemical patterns are convenient representations of the complete trace element of individual rocks normalised by division by an appropriate composition, and the element are arranged in order of incompatibility during partial melting with increasing incompatibility toward the left. These patterns become useful in discriminating basalts of different eruptive settings when normalised by an average tholeiitic MORB (Pearce, 1996). However, Pearce (1983, 1996) discovered that few trace elements carry most of the discriminating power, and then devised geochemical patterns based on five highly incompatible elements (Th, Nb, Ce, Zr and Y). He chose the N-MORB as the normalising value because he believes it represents the composition that a magma would attain without mantle source enrichment, without complex residual assemblages during melting, and without interaction with continental crust.

Figure 4.7(a-c) shows the geochemical patterns that result when the amphibolites from the Vumba granite-greenstone terrain are plotted this way. The geochemical patterns for various averaged basalts from known eruptive settings are included here for comparison purpose [Fig.4.7 (d-g)]. Indeed, the geochemical patterns of the amphibolitic samples from the Vumba Mixed Volcanic Formation (VMVF) resemble those of the Phanerozoic volcanic arc basalts (Fig.4.7a). They are characterised by a pronounced negative Nb anomaly with respect to Th and Ce. The geochemical patterns for amphibolite samples picked from the Vumba Lower Mafic (VLM) and Vumba Upper Mafic (VUM) Formations resemble those of volcanic arc basalts in terms of high Th/Nb ratio. The Nb anomaly which is characteristic of volcanic arc basalts is virtually absent in the two formations which are believed to lie above the VMVF.

It is evident from Figure 4.7a that most samples from the VMVF are depleted in Zr, Ti and Y relative to N-MORB composition. VUMF is characterised by Nb, Ce, Zr, Ti and Y abundances that are virtually equivalent to the N-MORB. It is interesting to note that the VLMF, which is believed to lie between VMVF and VUMF, yielded geochemical patterns that partly resembles those of VMVF and VUMF. This seems to illustrate a systematic change in geochemical patterns with the succession, which could be possibly reflecting the maturity trend of the arc.

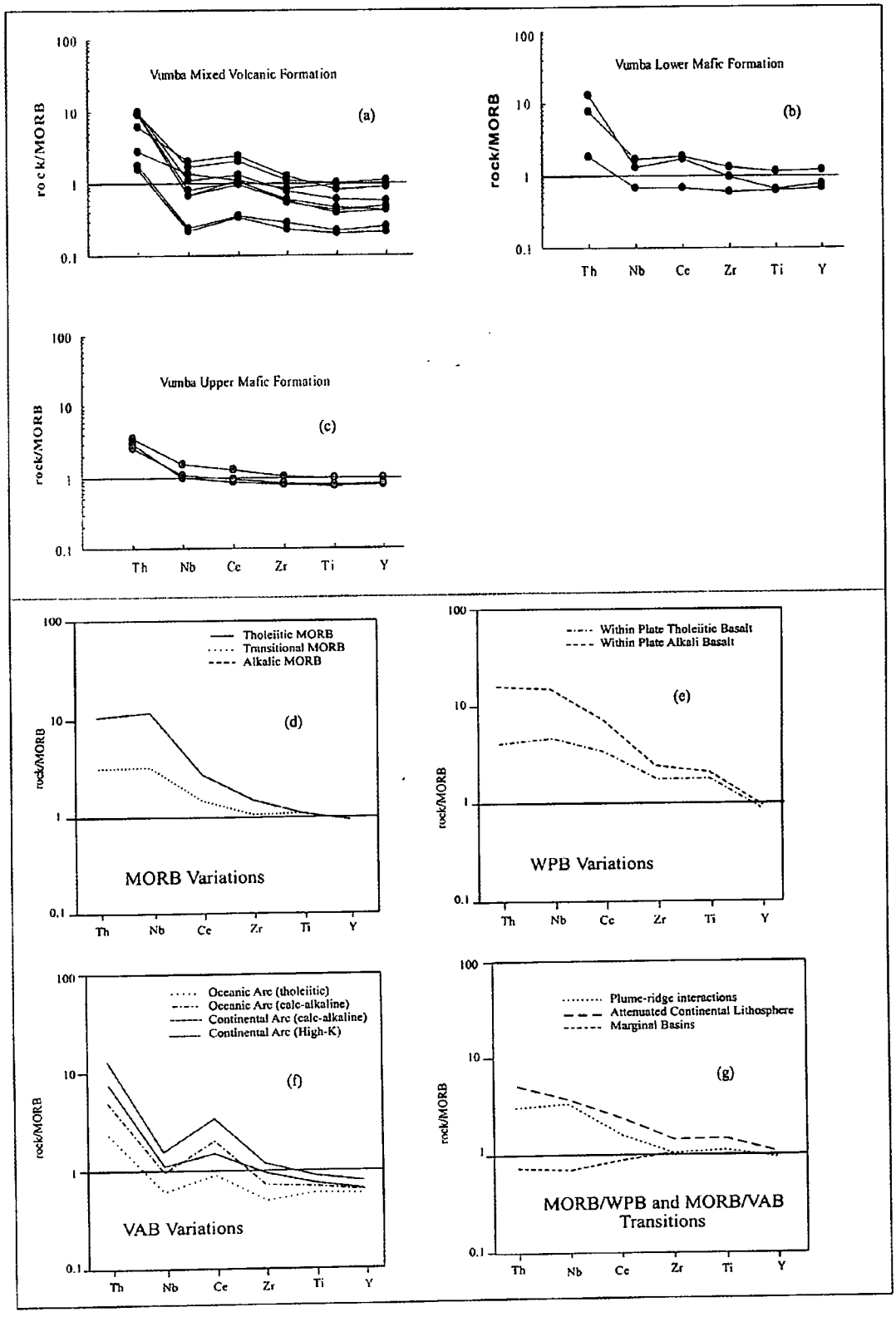

Figure 4.7 (a-c) Representative N-MORB normalised geochemical patterns for the amphibolites from the Vumba granite-greenstone terrain. Normalising values are from Pearce (1996). **(d-g)** Geochemical patterns of basalts from known tectonic settings inserted for comparison purpose (from Pearce, 1996).

4.2.6. REE Patterns

Chondrite-normalised REE patterns of eleven representative amphibolites from the Vumba Mixed Volcanic Formation (VMVF), Vumba Lower Mafic Formation (VLMF) and Vumba Upper Mafic Formation (VUMF) are presented separately in Figure 4.8. The average chondrite composition of Boynton (1984) was used for normalisation. The amphibolite samples are 3 to 30 times enriched in REE relative to chondrite and generally, exhibit flat REE patterns with negligible negative to positive Eu anomalies (Fig.4.8).

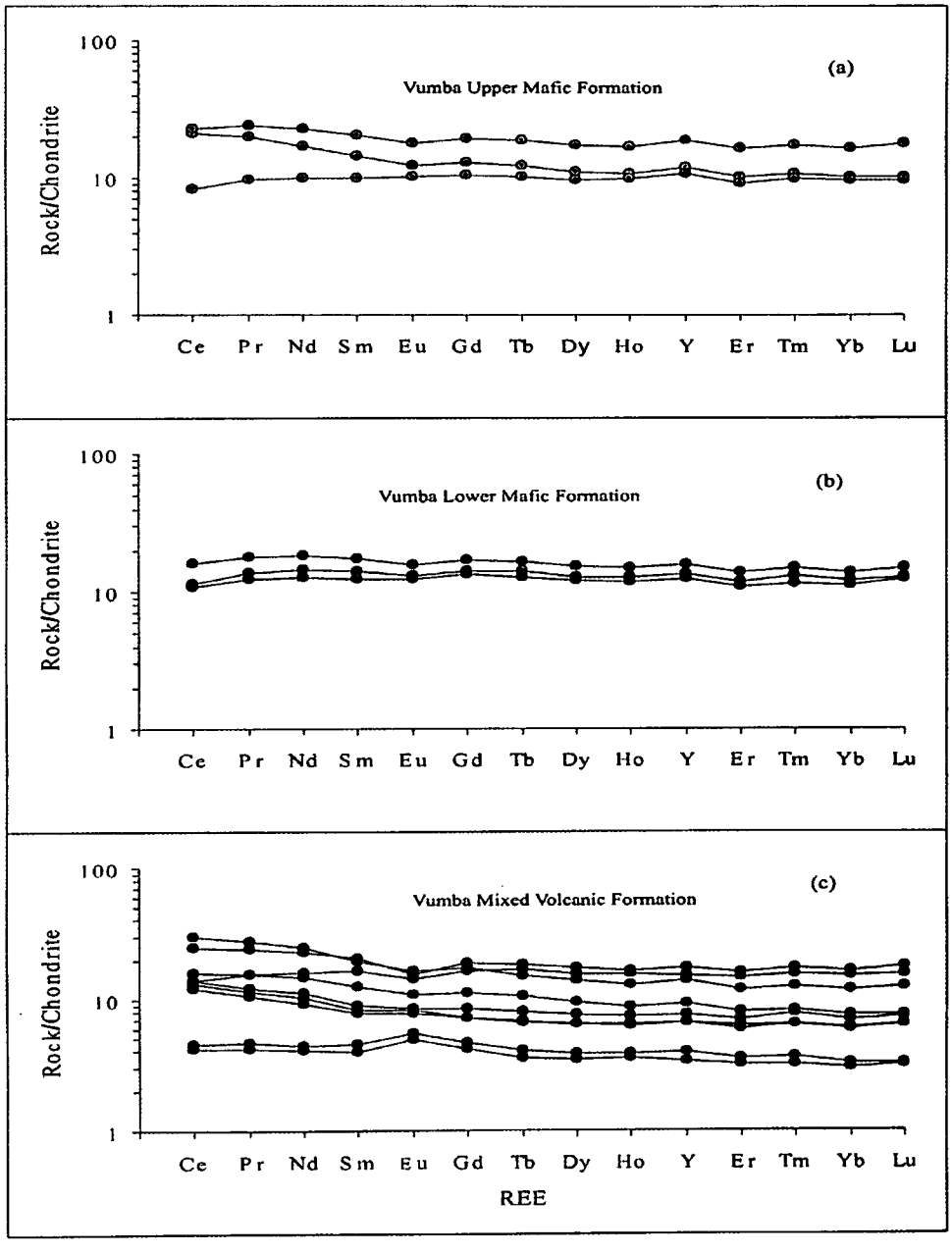

Figure 4.8: Representative chondrite-normalised REE patterns for the amphibolites from the Vumba granite-greenstone terrain. Chondrite-normalising values are from Boynton (1984).

4.3. Summary

The petrographic study has revealed that two types of amphibolite exist in the Vumba granite-greenstone terrain. These are the metabasaltic and metagabbroic amphibolites. The metabasaltic amphibolite, which is the predominant type, is composed of hornblende, andesine to labradorite plagioclase and sporadic quartz. It exhibits varieties of texture such as schistose, porphyroblastic and equigranoblastic. The metagabbro essentially consists of plagioclase, hornblende and augite as well as rare quartz. It is less common and its occurrence is restricted to the Vumba Mixed Volcanic Formation.

Generally, the distinction between the geochemistry of the amphibolites from the VMVF, VLMF and VUMF is not obvious in the discrimination diagrams applied in this study. The discrimination diagrams indicate that the magmatic nature of the amphibolites is mainly calc-alkaline. The REE geochemistry of the amphibolites yield flat REE patterns when normalised to chondrite composition. Geotectonic discrimination diagrams suggest volcanic arc and/or marginal basin settings as the tectonic environment in which the protoliths of the amphibolites from the Vumba granite-greenstone terrain were formed.

Chapter 5

ULTRAMAFIC INTRUSIVES

5.1 Petrography

The ultramafic intrusives (serpentinite and metapyroxenite) are variably metamorphosed in greenschist and amphibolite facies and hence any primary textures and mineralogy have been obliterated. Nevertheless, some thin sections of serpentinite samples exhibit preserved large euhedral to subhedral and small rounded olivine crystals pseudomorphed by serpentine. This texture advocates dunite as the protolith for the serpentinite. The remainder of the thin sections shows complete serpentinisation with no relict minerals. This poor state of preservation precludes any further petrographic analysis.

The samples from the metapyroxenite appear greenish grey and massive in hand specimen. In thin section, they contain anhedral diopside and augite crystals intermingled with anhedral plagioclase and rare quartz. Grain sizes are variable. Large clinopyroxene crystals are skeletal and locally altered to actinolite. A striking feature in the metapyroxenite thin sections is the chaotic distribution of fine crystals of clinopyroxene. In contrast, large crystals show a preferred orientation. Plagioclase crystals are poikilitically enclosed within the large clinopyroxenes or may be interstitial together with very fine rare quartz. Carbonate is ubiquitous.

5.2 Geochemistry

A total of twelve representative samples from the serpentinite and metapyroxenite units were analysed for major and some trace elements (Sc, V, Cr, Co, Ni, Cu, Zn, Rb, Sr, Y, Zr, Nb, Ba, La, Ce, Nd, Pb, Th and U) by XRF spectrometer on fused discs and powdered pellets respectively. Three representative samples from each unit were chosen

for determination of Sc, V, Cr, Co, Ni, Cu, Zn, Ga, Rb, Sr, Y, Zr, Nb, Cs, Ba, REE, Hf, Ta, Pb, Th and U using the ICP-MS technique. The results are given in Appendix B(V), and precisions and accuracies presented in Appendix C.

5.2.1 Geochemical characterisation

The serpentinite samples have SiO_2 (on LOI free basis) ranging from 41.33 to 44.71 wt.% and MgO contents ranging from 33.15 to 40.30 wt.% indicating ultrabasic compositions. They are characterised by high FeO_{total} (13.25-14.76 wt.%), Cr (2300-4100 ppm), Ni (1900-3050 ppm) and low CaO, Al_2O_3. High Cr contents indicate that olivine crystallisation was accompanied by chrome-spinel crystallisation probably as inclusions within the olivine.

The metapyroxenite samples have an intermediate composition in terms of silica content, which is within the range of 52-54 wt.%. The MgO and FeO_{total} contents vary from 12.92 to 14.72 wt.% and from 9.33 to 9.81 wt.% respectively. In addition it is characterised by distinctly high CaO content (13.50-15.20 wt.%).

Both the serpentinites and the metapyroxenites display flat REE patterns which are 1 – 3 and ~ 9 x chondrite enriched respectively (Fig.5.1). Mantle-normalised incompatible trace element patterns for the serpentinite and metapyroxenite are characterised by negative Nb and positive Ti anomalies (Fig.5.2).

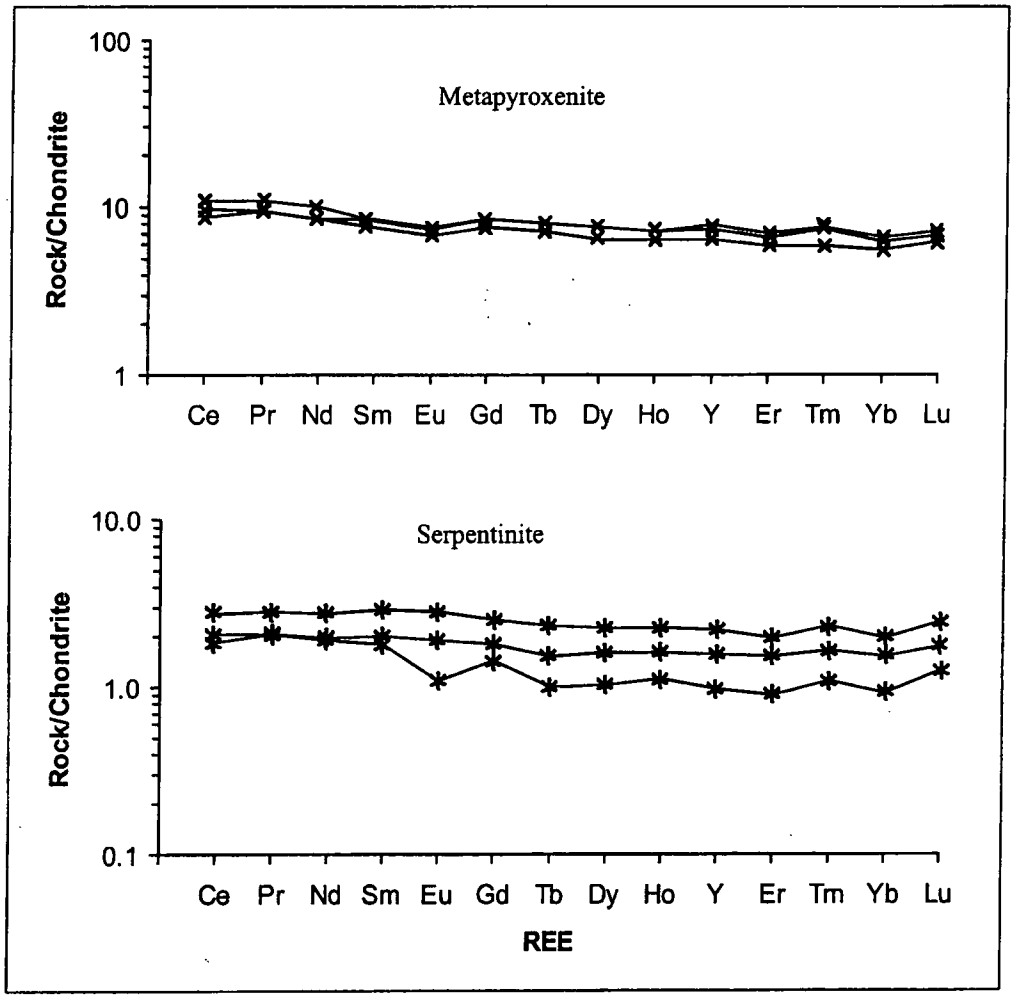

Figure 5.1: Rare-earth element abundances normalised to chondrite (after Boynton 1984) for the ultramafic intrusives from the Vumba granite-greenstone terrain.

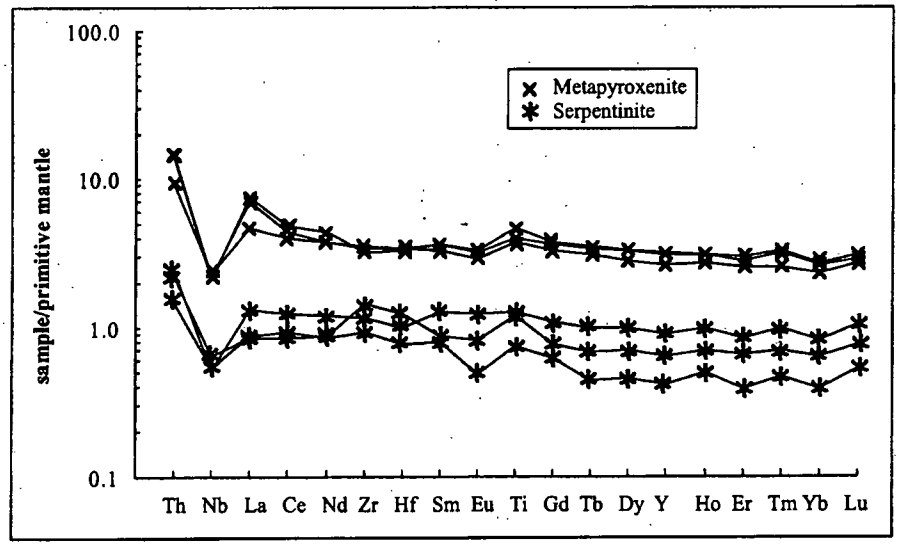

Figure 5.2 Mantle-normalised incompatible trace element patterns for the ultramafic intrusives from the Vumba granite-greenstone terrain. Normalising values are after Sun and McDonough (1989).

5.2.2 Geotectonic setting

Two models have frequently been advocated to explain the origin of high magnesium rocks namely subduction-related genesis (Allegre, 1982) and mantle plume induced melting (Dostal and Mueller, 1997). Subduction of an oceanic plate could lead to hydration of the overlying mantle wedge, which in turn would lower the mantle solidus temperature (Gallagher and Hawkesworth, 1992). Thus ultramafic intrusives could be residue from a large degree of melting at relatively shallow depth or cumulates from the magma. This mechanism can account for the association of ultramafic intrusive rocks with subduction-related rocks observed in Archaean greenstone belts. This model is favoured for the origin of the ultramafic intrusives of the Vumba granite-greenstone terrain. The presence of Nb depletion (Fig. 5.2) in the ultramafics is consistent with this subduction-related model.

High magnesium magmas are thought to be prone to crustal contamination, in part, because of their high temperature and inferred turbulent flow (Huppert and Sparks, 1985). Jochum et al (1990) demonstrated that element ratios such as Th/Nb, Th/La and La/Nb are very sensitive measures of crustal contamination. The values of the Th/Nb ratio in the ultramafics from the Vumba area are significantly high (Th/Nb = 0.34-0.78) like those affected significantly by crustal contamination (bulk continental crust 0.32; Hofmann, 1988). The implication of this is that the ultramafic intrusives experienced substantial crustal contamination.

5.3 Summary

Petrographical characteristics and major element geochemistry have revealed that the serpentinite unit of the Vumba granite-greenstone terrain originated as dunite. Both the serpentinites and metapyroxenites are alumina-undepleted. Moreover, they both have flat REE patterns, which differ mainly in absolute abundances of the elements.

Multi-element patterns of the serpentinite and metapyroxenite rocks are characterised by large Nb anomalies which indicate that the rocks were generated from a mantle source that carries a subduction component or interacted with the crust. Additionally, high Th/Nb ratios associated with these rocks indicate crustal contamination. The mantle plume origin is unlikely for ultramafic intrusives of the Vumba granite-greenstone terrain.

Chapter 6

FELSIC METAVOLCANICS

6.1 Petrography

The felsic metavolcanics involved in this study occur in three geological formations of the Vumba granite-greenstone terrain. These are Vumba Mixed Volcanic Formation (VMVF), Vumba Lower Felsic Formation (VLFF) and Vumba Upper Felsic Formation (VUFF). Two types are distinguishable at hand specimen scale namely, homogeneous and banded felsic metavolcanics. The former is the most prevalent and it occurs in all the formations, while the later is only encountered in the Vumba Lower Felsic Formation where it forms few kopje outcrops. A total of nine thin sections were examined.

The homogeneous felsic metavolcanics exhibit two types of textures, which are mainly characterised by fine quartz and feldspar crystals associated variably with biotite and muscovite. However, in some instances, fragmented or skeletal hornblende predominates over the micas. These textures are fine equigranoblastic and porphyroblastic. For the porphyroblastic texture, relatively coarse grains of quartz form aggregates within the groundmass of quartz and feldspars. Chloritisation of biotite was noted in some thin sections. The micas and amphiboles constitute 5 to 10% of the rock. Calcite is ubiquitous in most thin sections and iron oxide is a common accessory phase.

Banded felsic metavolcanics contain about 2 cm thick anatomising light and dark lenticular bands which all appear massive in a hand specimen. Under the microscope the dark bands turned out to be zones dominated by medium to coarse grains of hornblende with sporadic fine quartz and feldspar crystals. The hornblende crystals are mostly skeletal and bladed with a semi-preferred orientation. Light bands

mainly comprise fine quartz and feldspar crystals with sporadic euhedral to subhedral hornblende and bladed biotite. The mafic phases in the light bands exhibit a random orientation. On average the mafic phases constitute about 20% of the rock. Calcite interlocked with quartz and feldspar crystals is ubiquitous.

In general, the felsic metavolcanics from the Vumba granite-greenstone terrain are compositionally consistent regardless of the formation. Most thin sections have revealed that there is a pronounced calcite content in the felsic metavolcanics of the Vumba granite-greenstone terrain.

6.2 Geochemistry

Twenty-eight representative samples from the felsic metavolcanic units of the Vumba granite-greenstone terrain were analysed for whole-rock major and trace (Sc., V, Cr, Co, Ni, Cu, Zn, Rb, Sr, Y, Zr, Nb, Ba, La, Ce, Nd and Pb) elements concentrations using XRF spectrometry. A subset of twelve samples was selected for determination of Cs, Sc, V, Cr, Co, Ni, Cu, Zn, Rb, Sr, Y, Zr, Nb, Ba, REE, Hf, Ta, Pb, Th and U using inductively plasma mass spectrometry technique. The results are presented in Appendix B (VI) while the precisions and accuracies are given in Appendix C.

6.2.1 Major element geochemistry

The silica content of the felsic metavolcanics (on LOI free basis) varies broadly between 61 and 76 wt.% indicating intermediate to felsic composition. Nevertheless, most of the samples have silica composition within the 65 – 70 wt.% range. In Figure 6.1 K_2O versus SiO_2 is presented and compared with the compositional fields of Peccerillo and Taylor (1976). It is evident from the Figure that the felsic metavolcanics

are essentially medium-K calc-alkaline dacites. Rhyolites (SiO_2 > 70 wt.%) and andesites (SiO_2 < 63 wt.%) are rare according to Figure 6.1. However, the results of Figure 6.1 must be treated with caution because K and Si are mobile elements. Therefore, a classification diagram based on immobile elements is essential to complement the diagram of Peccerillo and Taylor (1976). The classification diagram of Winchester & Floyd (1977), presented as Figure 6.2, shows that these metavolcanics are dacites/rhyodacites.

The aluminium saturation index (ASI) widely varies from 0.4 to 1.3, which is indicative of metaluminous to peraluminous character. However, the majority of the samples yielded ASI < 1.1 showing that they are I-type melts (Chappell and White, 1992).

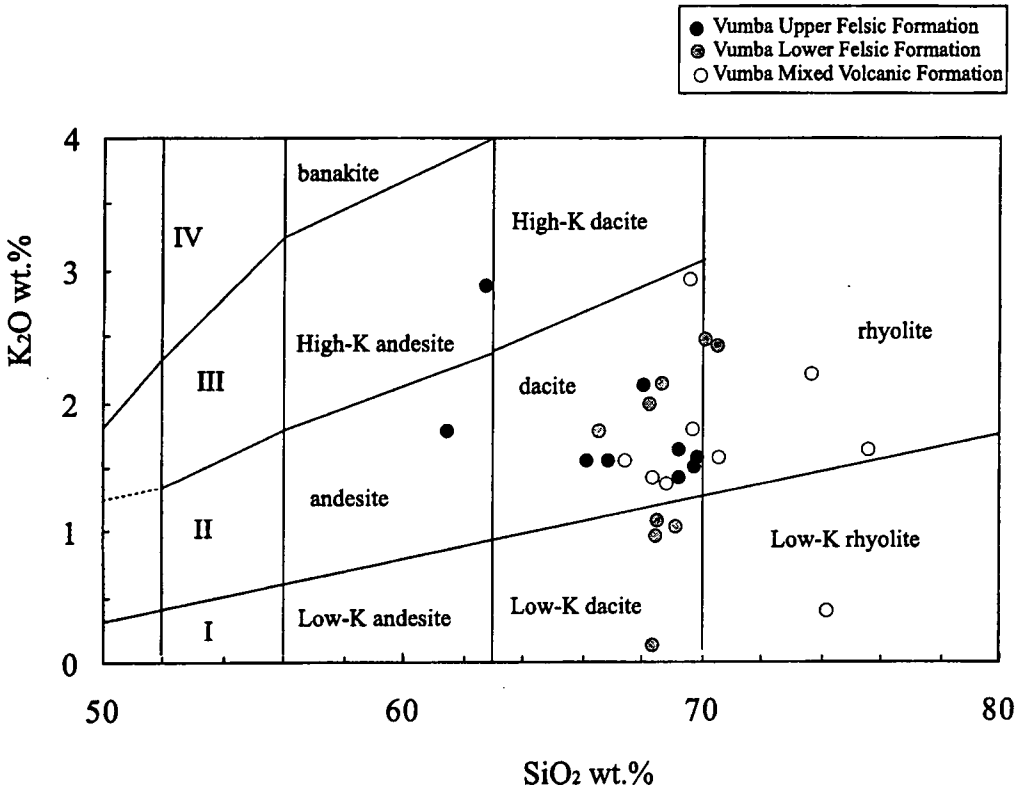

Figure 6.1: Felsic metavolcanic rocks from the Vumba granite-greenstone terrain plotted on the K_2O versus silica classification diagram of Peccerillo and Taylor (1976). Abbreviation: I = low-K calc-alkaline; II = medium-K calc-alkaline; III = high-K calc-alkaline and IV = shoshonite.

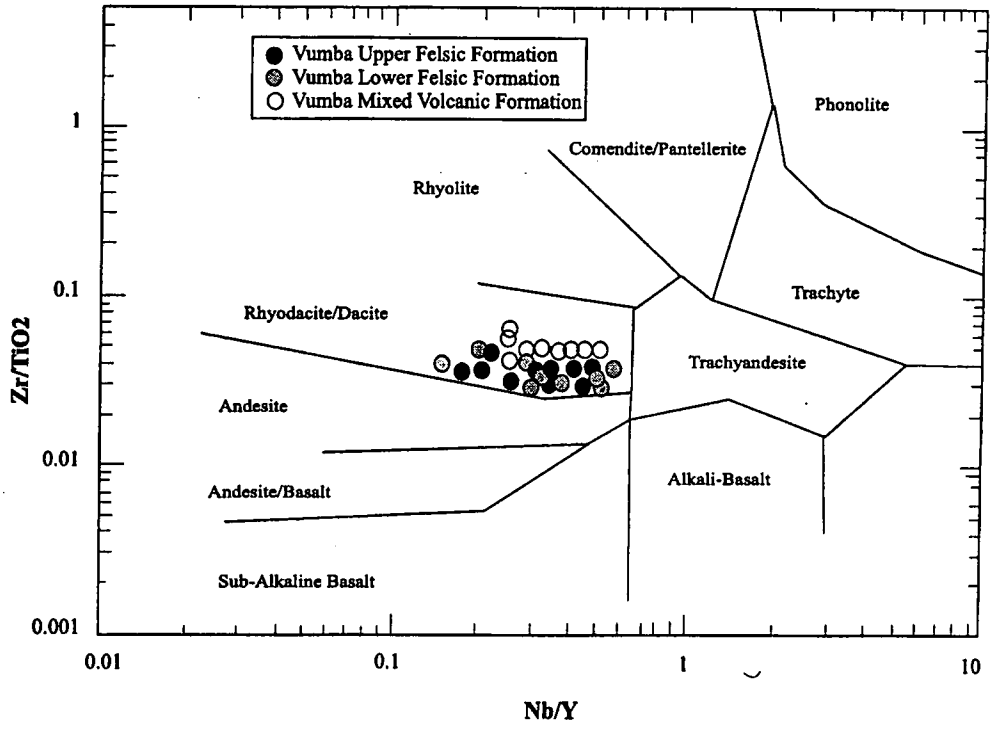

Figure 6.2: Classification of the felsic metavolcanics from the Vumba granite-greenstone terrain using the classification diagram of Winchester & Floyd (1977).

6.2.2. Trace element geochemistry

This section has been subdivided into three components namely; REE patterns, multi-element patterns and geotectonic setting.

6.2.2.1. REE patterns

The chondrite-normalised REE patterns for representative samples of felsic metavolcanics from the Vumba granite-greenstone terrain are presented in Figure 6.3 (a-c). The samples have been presented in three diagrams according to their formation as described previously. Only the data obtained from ICP analyses were used and the REE concentrations of the samples have been normalised to the chondritic abundances proposed by Boynton (1984). As can be seen from Figure 6.3 the felsic metavolcanics from the Vumba Upper Felsic, Vumba Lower Felsic and Vumba Mixed Volcanic Formations have similar REE patterns. The patterns are all characterised by enrichment

of LREE and relative depletion of HREE as evidenced by high Ce_N/Yb_N ratios (7 to 22). Furthermore, the patterns exhibit negligible positive Eu anomalies. It is important to realise that the felsic metavolcanic REE patterns are comparable to those of the granitoids described in chapter 3.

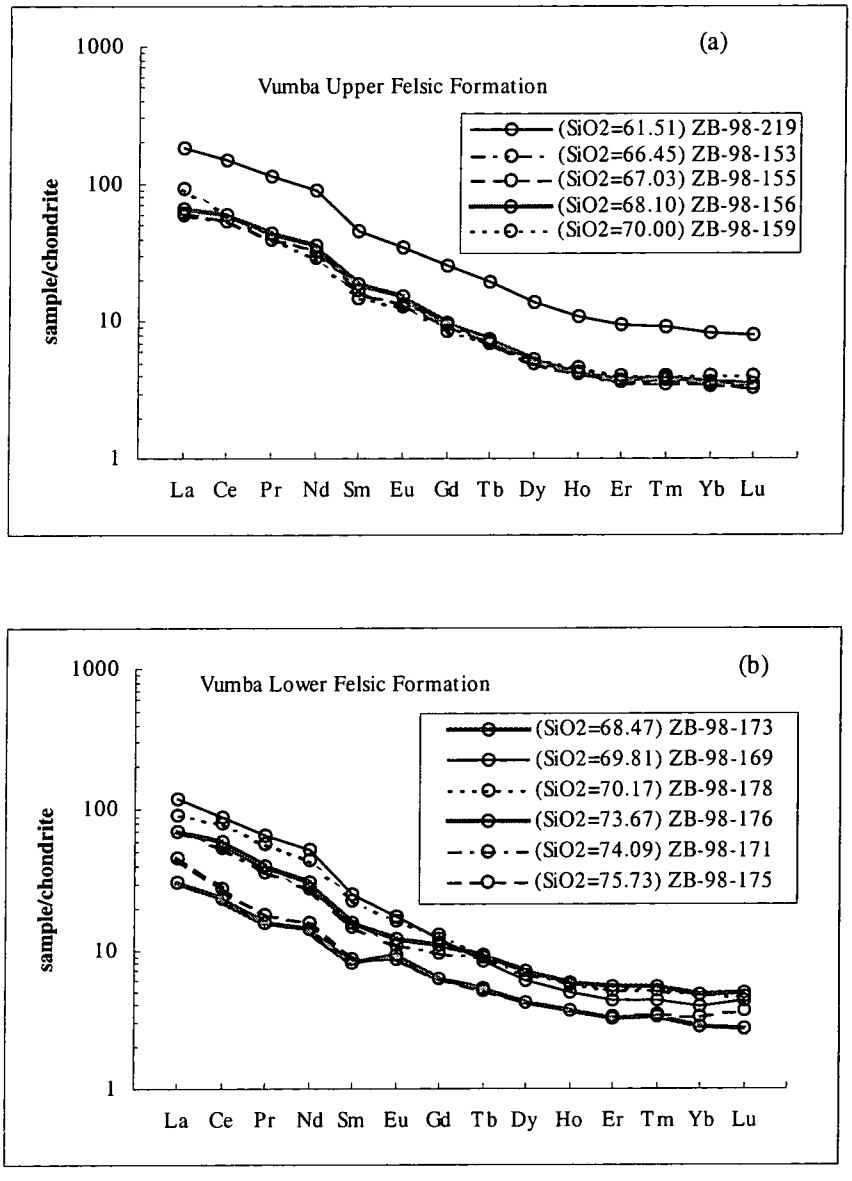

Figure 6.3: Chondrite-normalised REE plots for the felsic metavolcanics from the Vumba granite-greenstone terrain. Chondrite normalising values are taken from Boynton (1984).

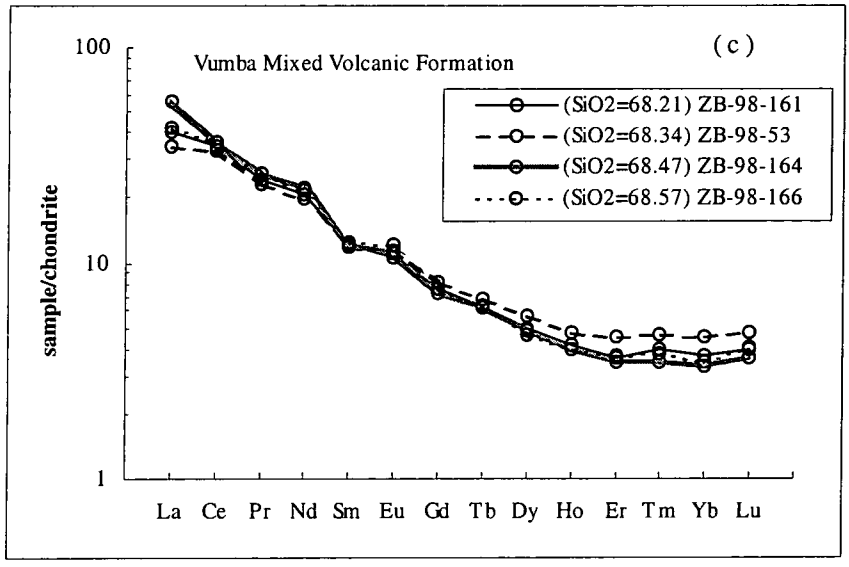

Figure 6.3: Continued.

6.2.2.2. Multi-element pattern

N-type MORB normalised trace element concentrations of representative felsic metavolcanics from the Vumba granite-greenstone terrain have been plotted on multi-element diagrams in Figure 6.4 (a-c). These metavolcanics have been plotted as three different Formations to detect some possible petrogenetic variation in space and time. Normalisation values (N-MORB) used for the diagrams are from Pearce (1983).

It is evident from Figure 6.4 that the rocks from the three formations have similar multi-element profiles though sporadic variations are observable in the large ion lithophile elements. This could be due to mobility of the LILE during metamorphism. These patterns are all characterised by significant enrichment of Rb, Ba, Th, K (LILE) and Ce relative to Ta, Nb, Zr, Hf, Ti, Y, P, Sm and Yb. Additionally, the patterns show depletion of Ti, Y and Yb relative to the MORB.

Moreover, the felsic metavolcanic patterns are characterised by Nb, Ta, P and Ti negative anomalies. These are similar to those from the subduction-related continental margins where the preferred explanation is the metasomatism of the mantle wedge by a

subduction component selectively enriched in LILE (Luhr, 1992). Experimental petrological studies have shown that calc-alkaline dacitic melts can be derived from partial melting of subducting basalts during the amphibolite-eclogite transition (Defant & Drummond, 1990). Such melts are marked by Al_2O_3 >15% and Y ≤ 18 ppm in rocks with c. 70% SiO_2. The Vumba felsic metavolcanics with c.70 wt.% have Al_2O_3 abundances between 15.45 and 16.81 wt.%, and Y absolute abundances below 15, which are consistent with the experimental findings. This suggests that the felsic metavolcanics from the Vumba granite-greenstone terrain could have been derived directly from partial melting of the subducted basaltic lithosphere. However, an origin by fractional crystallisation of mafic magma and crystallisation of phases that accommodate Y (e.g. amphibole) is also possible.

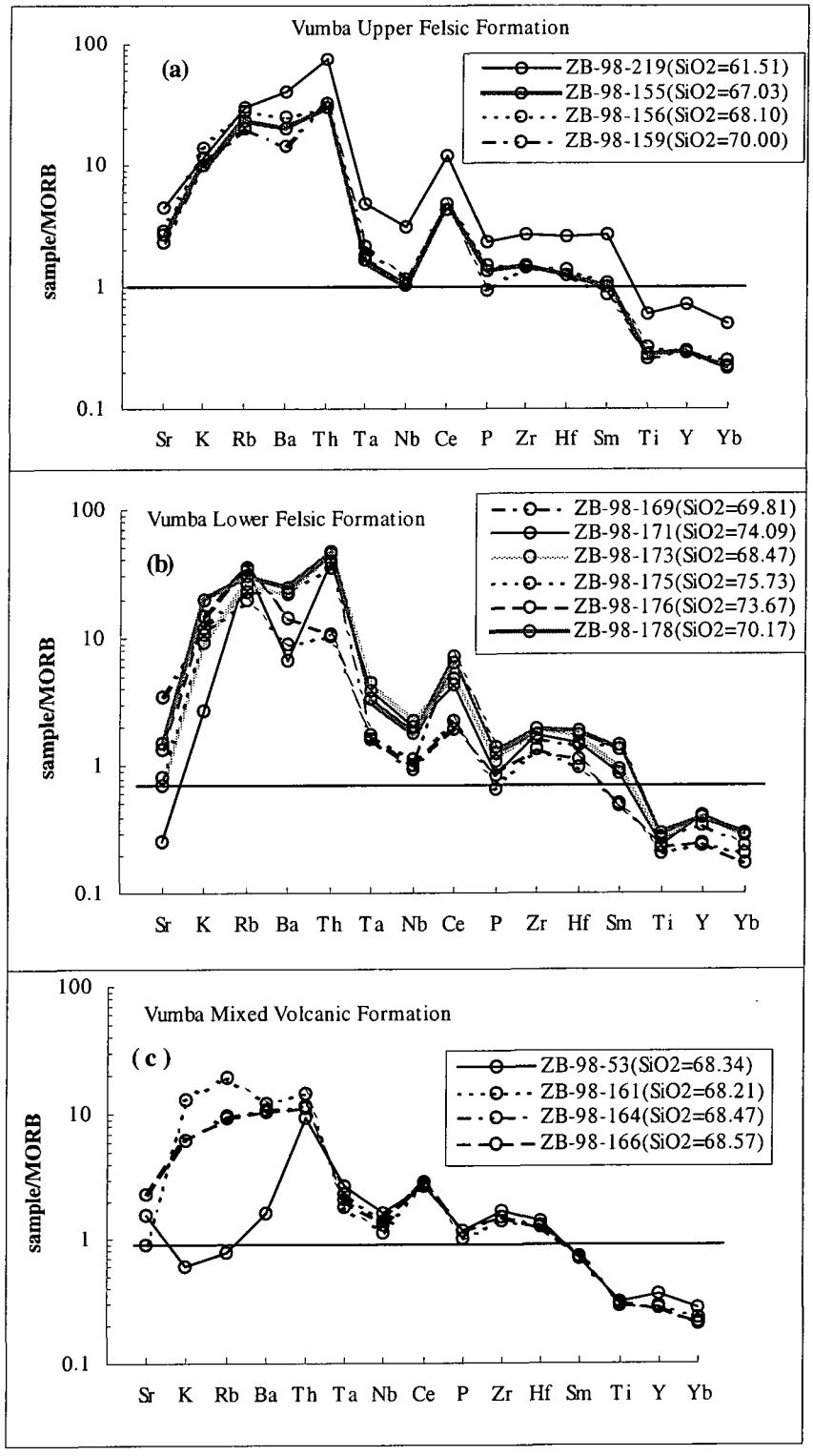

Figure 6.4: N-MORB normalised patterns for the felsic metavolcanics from the Vumba granite-greenstone terrain. N-MORB normalising values are taken from Pearce (1983).

6.2.2.3. Geotectonic setting

Pearce et al. (1984) have devised tectonic discrimination diagrams based on the incompatible trace elements for granitic/rhyolitic rocks. The analyses of the felsic metavolcanics from the Vumba granite-greenstone terrain plot in the 'Volcanic Arc Granitoids + Syn-Collision Granitoids' (VAG + Syn-COLG) field in Figure 6.5a and they are similar to VAG according to Figure 6.5b. The felsic metavolcanics resemble the granitoids from the Vumba granite-greenstone terrain in these diagrams (see chapter 3, section 3.2.3.2). It is important to realise that volcanic arc granitoids and post-collision granitoids cannot be distinguished from each other on the basis of the tectonic diagrams of Pearce et al. (1984). Therefore field edifice is required to distinguish between the two. This aspect is covered in the discussion chapter.

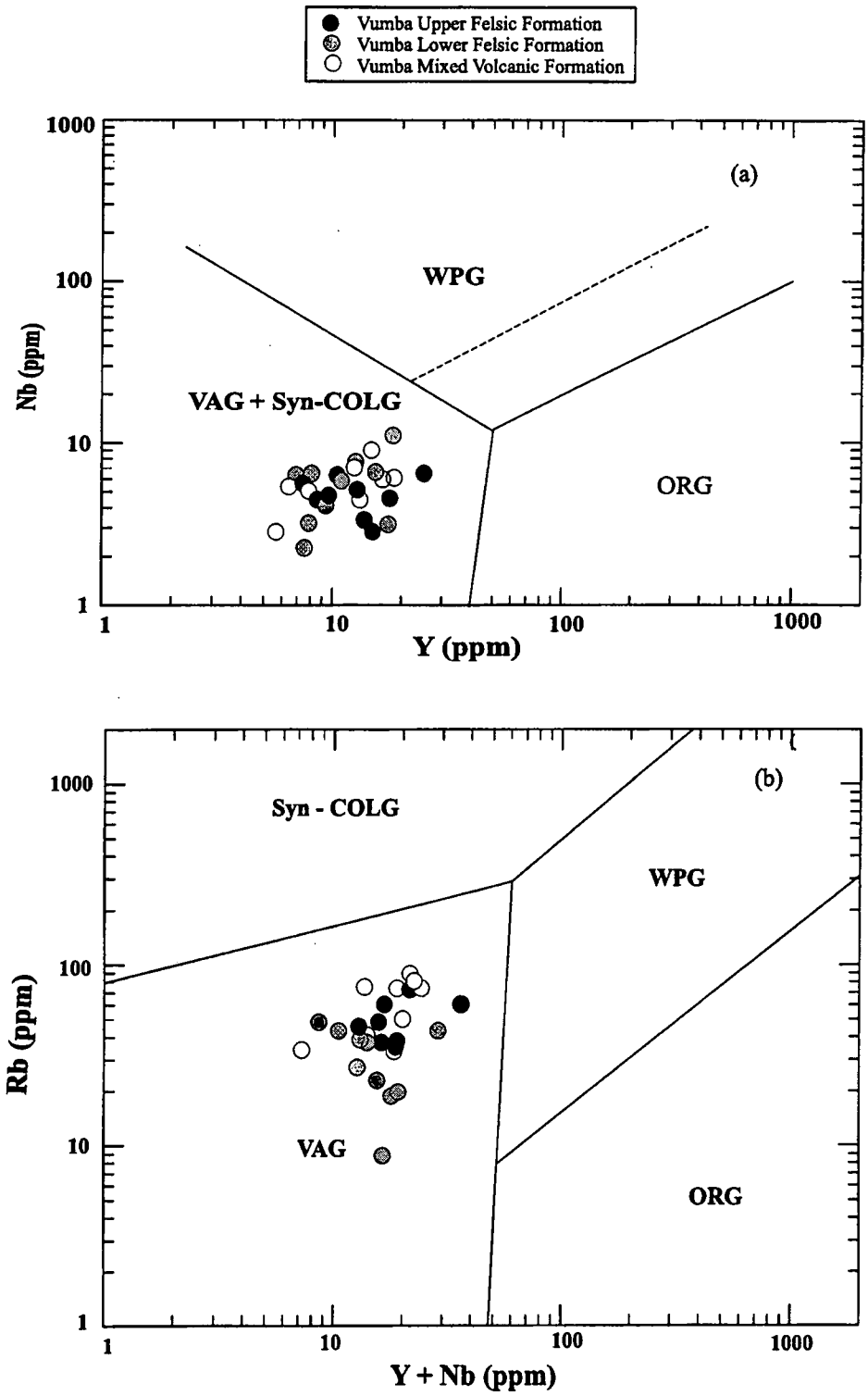

Figure 6.5: Plot of the felsic metavolcanics from the Vumba granite-greenstone terrain on tectonic discrimination diagrams of Pearce et al. (1984). Abbreviation: ORG-oceanic ridge granite; COLG-collision granite; VAG-volcanic arc granite and WPG-within plate granite.

6.3. Summary

Petrological and geochemical characteristics of the felsic metavolcanics from the Vumba granite-greenstone terrain have revealed that they are meta-dacites/rhyodacites not metarhyolites as concluded by previous investigations. The felsic metavolcanics are characterised by hornblende and biotite as the mafic phases. Muscovite and calcite are ubiquitous in the felsic metavolcanics.

Major element geochemical characteristics indicate that the felsic metavolcanics are essentially medium-K calc-alkaline and have I-type melt affinity. Trace element characteristics in conjunction with major element geochemistry suggest partial melting of subducting basalt could have been the source of the felsic metavolcanics from the Vumba granite-greenstone terrain. In addition, the tectonic discrimination diagrams suggest a volcanic arc setting for the felsic metavolcanics.

Chapter 7

PETROGENESIS OF THE AMPHIBOLITES AND FELSIC METAVOLCANICS

7.1. Introduction

This chapter employs Ti, Zr, Y and Nb elements in an attempt to describe the petrogenetic relationship between amphibolites and felsic metavolcanic rocks from the Vumba granite-greenstone terrain. These elements are high field strength, therefore they are not usually transported in aqueous fluids. This renders them suitable for studying ancient metamorphosed lavas such as the Archaean greenstone rocks.

7.2. Ti, Zr, Y and Nb modelling

Quantitative modelling of fractional crystallisation has been carried out to evaluate the variations in Ti, Zr, Y and Nb concentrations in both the amphibolites and the felsic metavolcanics with the aim of unravelling any petrogenetic link between the two. Initially, the HFSE were plotted versus SiO_2 as the index of differentiation to determine their variation trends during differentiation. It is apparent from Fig.7.1 that Ti, Y and Zr exhibit a negative correlation with SiO_2, which indicates that the elements are being depleted during differentiation. The SiO_2-Nb variation diagram displays an ambiguous trend, particularly in the felsic metavolcanics. Nevertheless, Nb yields an insignificant negative correlation with differentiation.

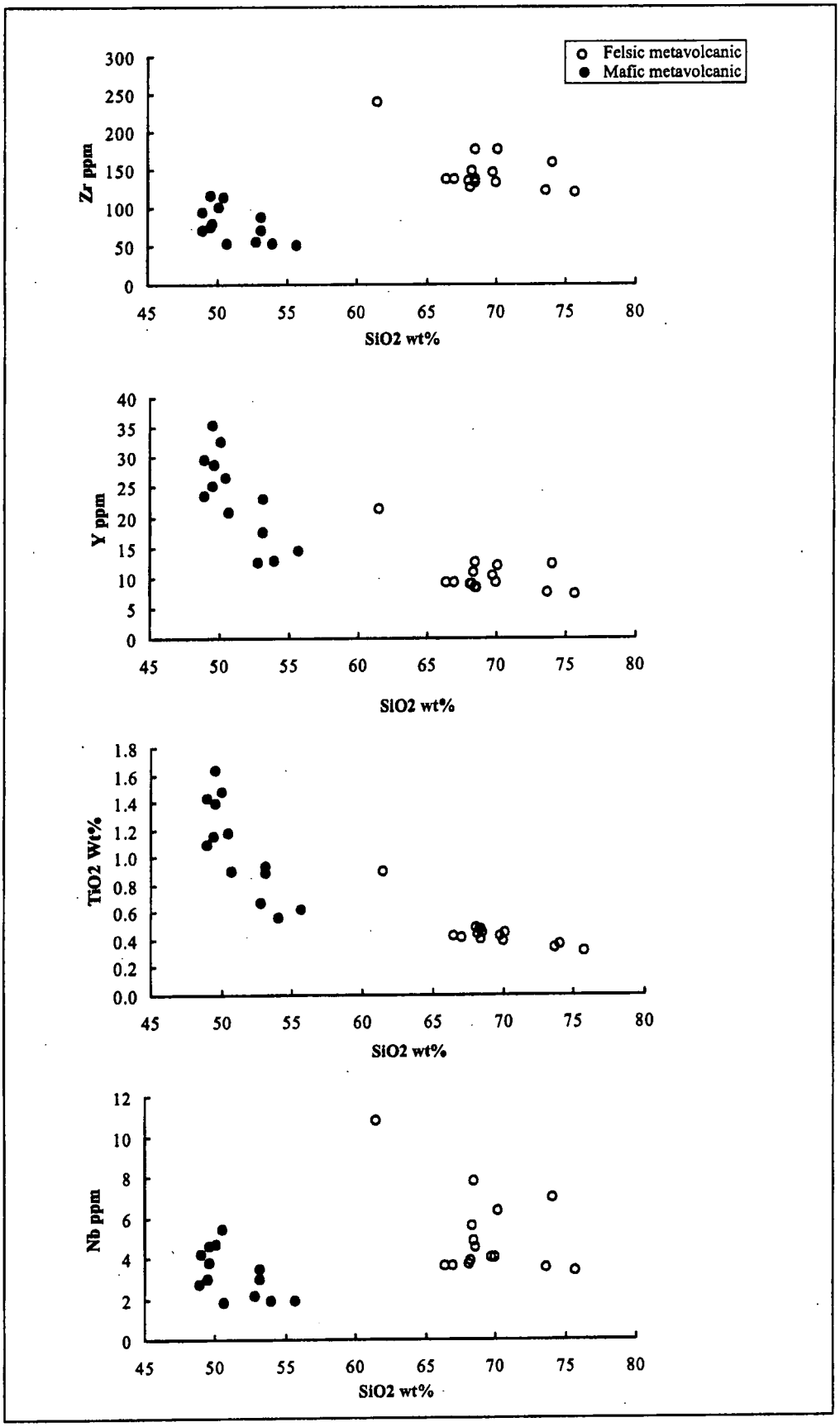

Figure 7.1: Y, Ti, Zr and Nb versus SiO_2 plots for the metavolcanics from the Vumba granite-greenstone terrain. All the HFSE (high field strength elements) are decreasing with the index of differentiation (SiO_2).

Y-Zr, Ti-Zr and Nb-Zr variation diagrams are presented in Figure 7.2. It is apparent from the Figure that the mafic and felsic data points exhibit separate distinct trends in all the variation diagrams. The variation in the Ti, Y, Zr and Nb contents of a magma as it evolves from basic to acidic composition by fractional crystallisation can be interpreted in terms of the nature and proportion of crystallising phases (Pearce and Norry, 1979). Theoretical fractionation trends for the crystallisation of single phases from the magma are drawn and compared with observed trends in the Vumba metavolcanics (Fig.7.2). The Rayleigh equation given below was applied to calculate the theoretical fractionation vectors. The length of each vector was calculated for 50% fractional crystallisation.

$$C_L/C_o = F^{(D-1)} \qquad (\text{Eq. } 1)$$

where

C_L: *weight concentration of a trace element in the liquid*

C_o: *the weight concentration of a trace element in the parental liquid*

F : *the fraction of melt remaining*

D : *bulk distribution coefficient of the fractionation assemblage during crystal fractionation.*

The mineral/melt partition coefficients (D) of Ti, Zr, Y and Nb used for modelling (e.g. olivine, clinopyroxene, plagioclase, hornblende, biotite, and orthopyroxene in basic and acid magmas) were obtained from Pearce and Norry (1979). See Table 7.1 for the partition coefficients of various minerals for different magma compositions. The notation "a" and "b" attached to the mineral abbreviations in theoretical vectors indicate that the D value for a particular mineral in acidic and basic magma respectively was used.

composition	element	ol	pl	cpx	opx	hbl	mt	bi + zr	ap
Basic	Ti	0.02	0.04	0.3	0.1	1.5	7.5		
	Zr	0.01	0.01	0.1	0.03	0.5	0.1		
	Y	0.01	0.03	0.5	0.2	1.0	0.2		
	Nb	0.01	0.01	0.1	0.15	0.8	0.4		
Intermediate	Ti	0.03	0.05	0.4	0.25	3.0	9.0	1.5	
	Zr	0.01	0.03	0.25	0.08	1.4	0.2	1.2	
	Y	0.01	0.06	1.5	0.45	2.5	0.5	1.2	20
	Nb	0.01	0.025	0.3	0.35	1.3	1.0	1.8	
Acid	Ti	0.04	0.05	0.7	0.4	7.0	12.5	2.5	0.1
	Zr	0.01	0.1	0.6	0.2	4.0	0.8	2.0	0.1
	Y	0.01	0.1	4.0	1.0	6.0	2.0	2.0	40
	Nb	0.01	0.06	0.8	0.8	4.0	2.5	3.0	0.1

Table 7.1 Mineral-melt distribution coefficients for Ti, Zr, Y and Nb from Pearce and Norry (1979). Abbreviation: ap=apatite; bi=biotite; cpx=clinopyroxene; hbl = hornblende; mt = magnetite; ol = olivine; opx = orthopyroxene; pl = plagioclase; zr = zircon.

The felsic metavolcanics follow the trend designated "*a*" while the mafic metavolcanics follow *trend b* in all the three variation diagrams. Additionally, the two trends are sub-parallel. On the Y-Zr diagram (Fig.7.2a) the mineral vectors drawn using the Rayleigh equation (Eq. 1) predict that, for a basic magma, most crystallising phases will leave a residual liquid enriched in both Y and Zr. They also predict that crystallisation of amphibole, biotite and zircon will deplete the residual magma in Y and Zr at acidic compositions. Both amphibolites and felsic metavolcanics studied from the Vumba granite-greenstone terrain exhibit fractionation trends corresponding to depletion of Y and Zr. The observed trends *a* and *b* are equivalent to the modelled vector of $hbl_{0.7}$ + $bi_{0.3}$ (Fig.7.2). This is in line with the petrography of the amphibolites and felsic metavolcanics (chapters 4 and 6) to some extent

The theoretical mineral vectors on the Ti-Zr diagram (Fig.7.2b) reveal that biotite, amphibole and magnetite can cause Ti to decrease during fractional crystallisation. The observed trends both show decreasing Ti and Zr in the felsic and mafic metavolcanics consistent with a crystallising assemblage of $hbl_{0.7}$ + $bi_{0.3}$.

In the Nb-Zr diagram, most mineral vectors have slopes close to unity except biotite and magnetite. For all phases except amphibole and biotite, these elements increase during fractionation. However, the concentrations of Nb and Zr decrease during fractionation in the case of the amphibolites and felsic metavolcanics of Vumba granite-greenstone terrain. This is consistent with the modelled trends *b* and *a* from $hbl_{0.7}$ + $bi_{0.3}$ and $bi_{0.9}$ + $mt_{0.1}$ respectively. Thus it is evident from the modelled vectors that amphibole and to a lesser extent biotite played a major role in the fractional crystallisation process in amphibolites and felsic metavolcanics of the Vumba granite-greenstone terrain. This observation suggests a second possible origin for the felsic metavolcanics, that is they are end products of magmatic evolution by fractional crystallisation. However, the modelling of the HFSE negates a petrogenetic link between the mafic and the felsic metavolcanics by fractional crystallisation alone. The implication is that the two rock types originated from independent parental magmas.

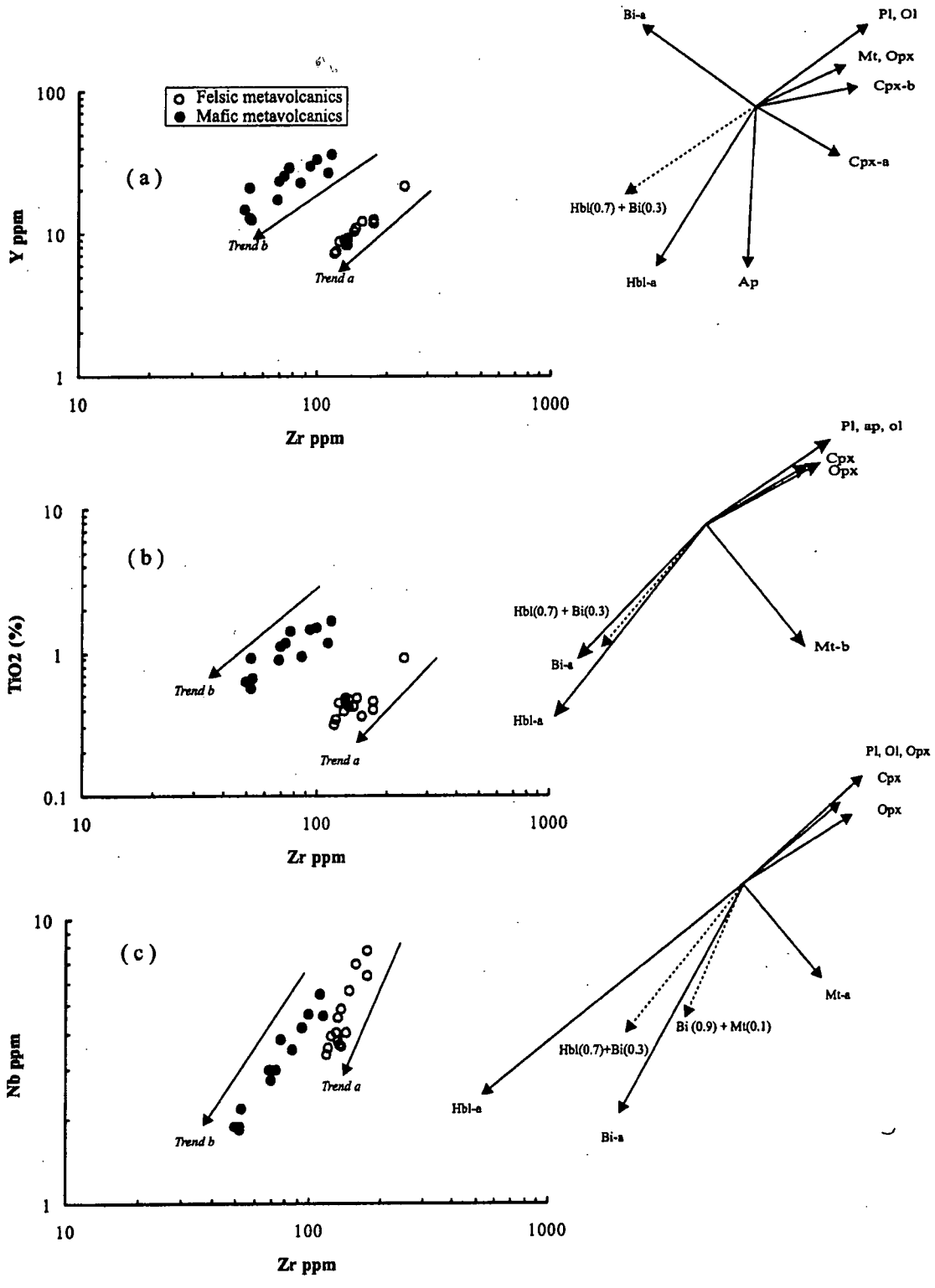

Figure 7.2a-c: Observed (dotted lines) and modelled (solid lines) fractionation trends on Y-Zr (a), TiO_2-Zr (b) and Nb-Zr (c) diagrams for the metavolcanics from the Vumba granite-greenstone terrain. Abbreviations: Ap-apatite; Bi-biotite; Cpx-clinopyroxene; Hbl-hornblende; Mt-magnetite; Ol-olivine; Opx-orthopyroxene; Pl-plagioclase; a-acidic; b-basic.

Chapter 8

DISCUSSION AND CONCLUSIONS

8.1. Introduction

The chief objectives of the study are, (1) to geochemically characterise the geology of the Vumba granite-greenstone terrain, (2) to constrain the age of the terrain, (3) discuss the evolution of the Vumba granite-greenstone terrain and (4) eventually propose a geotectonic model for the Vumba granite-greenstone terrain within the framework of the Zimbabwe craton. As a result, the discussion is focused on the geochemical characteristics and their tectonic implications as well as the regional geochronology.

8.2. Geochemistry

The SiO_2 contents in the metavolcanic rocks of the Vumba Volcanic Group show a bimodal distribution (mafic-felsic) with remarkable lack of intermediate compositions. Modelling of their high field strength elements (HFSE) negates any petrogenetic relationship between these mafic and felsic metavolcanics by fractional crystallisation alone. This is suggestive of two independent parental magmas for the mafic and felsic metavolcanics of the Vumba Volcanic Group.

The mafic metavolcanics of all the three formations have a basaltic composition, and they are characterised by flat REE profiles. Their geochemical patterns show slight systematic variation in terms of Nb anomalies from the VMVF to the VUMF. The Nb negative anomaly tends to diminish up the stratigraphy.

Felsic metavolcanics from the VMVF, VLFF and VUFF are rhyodacitic/dacitic in composition with similar REE and multi-element profiles. The REE profiles show

enrichment of LREEs relative to HREEs with negligible to no Eu anomalies. N-MORB normalised multi-element profiles of the felsic metavolcanics reveal that they are enriched in large ion lithophile elements (LILE), depleted of high field strength elements (HFSE) and have a negative Nb anomaly. The chemistry of the felsic metavolcanics suggests partial melting of amphibolitic rock as the source while modelling of the HFSE favours magmatic evolution by fractional crystallisation.

The granitoids associated with the metavolcanics described above have a broad range of silica contents (59 – 76 wt.%). However, most plutons are characterised by relatively restricted ranges in SiO_2 (66 – 76 wt.%) comparable to the felsic metavolcanics. Compositionally, they vary from quartz monzonitic through monzogranitic to granodioritic-tonalitic. All the granitoids of the Vumba granite-greenstone terrain rarely exhibit systematic trace element trends against SiO_2. They are all calc-alkalic except the Kalakamati Monzonite Pluton, which has an alkali-calcic character. They are also I-type granitoids.

The multi-element profiles for the granitoids of the Vumba granite-greenstone terrain do not resemble those of the upper and lower continental crust, except part of the Domboshaba Granite, which matches the upper continental crust profile. This observation does not favour crustal melting as the primary source of the granitoids. Most of these granitoids possess chemical characteristics of rocks formed by partial melting of subducted oceanic crust (Baker, 1979; Drummond and Defant, 1990; Wolde et al., 1996). These include: $\geq$ 15% Al_2O_3 at c.70% SiO_2, < 2.5% K_2O, < 4.5% CaO, 4 -5.5% Na_2O, low Y (< 15 ppm), high Sr (>300 ppm), enriched LREEs, depleted HREEs, high Sr/Y ratio (> 20), and no Eu anomaly or only a slight positive or negative one. The felsic metavolcanics exhibit similar geochemical characteristics, which suggest that they may be petrogenetically related. Thus the granodioritic-tonalitic granitoids are regarded as plutonic equivalents of the felsic metavolcanics.

The Kalakamati Monzonite Pluton, which is quartz monzonitic, is geochemically distinctive relative to the other G1 plutons. Its noteworthy characteristics include distinctly metaluminous character, fractionated but overall high REE abundances with negligible negative Eu anomaly, high Mg#, Zr, Ni and Cr. These observations have similarities to rocks identified as members of a mantle-derived suite in the Superior province (e.g. Beakhouse and McNutt, 1991 and references therein). The ultramafic source for these rocks is inferred from high Mg#, Ni and Cr whereas the REE fractionation is inherited from the source requiring that it be metasomatically enriched in LREEs prior to melting. This kind of origin is proposed in this study for the Kalakamati Monzonite Pluton.

Geochemistry of the Domboshaba Granite vividly indicates that its origin involved a heterogeneous source with an upper continental crust component.

The serpentinites have whole-rock compositions of 33 to 40 wt.% MgO, and 41 to 45 wt.% SiO_2 which is a characteristic of a dunitic composition. The whole-rock composition for the metapyroxenite contains 13 to 15 wt.% MgO, and 52 to 54 wt.% SiO_2. Both the rock types have similar flat REE and multi-element patterns, which differ in terms of element absolute abundances. This suggests a common source that experienced different degrees of partial melting. It is likely that they are residues of partial melting.

8.2. Geochronology

The U-Pb ages obtained from this study show that granitoid crystallisation ages in the Vumba granite-greenstone terrain range from 2696 ± 3.5 Ma to 2647 ± 4 Ma. This time span is similar to the range of published U-Pb zircon ages of 2710 ± 19 to 2646 ± 2.5 Ma for the contiguous Matsitama granite-greenstone terrain in NE

Botswana (see chapter 2). These U-Pb ages provide constraints on the timing of magmatic activity and deformation history. On the basis of currently available geochronological data, there is no evidence for the presence of rocks older than 2750 Ma in the Vumba granite-greenstone terrain.

The main crustal growth episode in the Zimbabwe craton occurred between 2720 and 2600 Ma when about 80% of rocks currently exposed on the craton were formed (Wilson et al, 1995; Dirks and Jelsma, 1998). During this period, deposition of the Upper Bulawayan greenstones and Shamvaian sediments was accompanied by the emplacement of granitoids belonging to the Sesombi and Wedza suites. Stabilisation of the craton was achieved around 2600 Ma after the emplacement of large volumes of crustally derived granites of the Chilimanzi suite (Dirks and Jelsma, 1993; 1998).

A comparison of crystallisation ages has been made in this study between rocks in NE Botswana and felsic rocks in the Zimbabwe craton. The comparison suggests that the tonalitic-granodioritic gneisses previously so-called G1 and G2 from NE Botswana may be correlatives of the Sesombi granitoids in Zimbabwe. The G1 Mashawe Pluton and the G2 Maebe gneisses have yielded crystallisation ages of 2686 ± 6 and 2690 ± 4 Ma respectively. Statistically, these ages are indistinguishable. The c.2700 Ma tonalitic-granodioritic Sesombi suite embraced a number of massive to slightly gneissic plutons intrusive into the Upper Bulawayan greenstones (Wilson et al., 1995). Moreover, the Sesombi suite is regarded as a plutonic expression of the same major magmatism that produced the felsic volcanism. However, specifically, the age of the G1 and G2 is about 15 Ma older than the age of the Sesombi granitoids (2668-2673 Ma) in the Midlands granite-greenstone terrain in Zimbabwe.

The G4, which was previously assumed to be part of the post-kinematic granitoids, has yielded the oldest age, which is odd with regard to the chronology of Key et al (1976). On the basis of field relationships and the new age data, this granitoid

is here reinterpreted as a synvolcanic intrusion. This rock resembles synvolcanic porphyries in the Midlands and Harare-Shamva (Dougherty-Page, 1994) granite-greenstone terrains in Zimbabwe (see Fig.1.1 for location). Nevertheless, the age of the G4 (c.2696 Ma) is about 15 Ma older than the age of porphyries and felsic volcanics (c.2680 Ma) in the Midlands granite-greenstone terrain. These clear disparities between the ages from the different granite-greenstone terrains emphasise that crustal growth was a diachronous phenomenon in the Zimbabwe craton.

The Domboshaba Granite (G5), which yielded the youngest age, is correlated with the Chilimanzi suites in Zimbabwe. Nonetheless, the G5 is c.40 Ma older than the Chilimanzi suites. The G2 contains amphibolitic gneissic xenoliths, which are (c.2733 Ma) 50 Ma older than the emplacement age. These xenoliths are presumably the remnants of the basement or older magmatic arc that collided with an oceanic plate during accretion. The deformation history in the Vumba granite-greenstone terrain can be pinned at 2.68 Ga, which is the age yielded by the youngest deformed granitoid.

High precision U-Pb zircon isotopic dating of the granitoids in the Vumba granite-greenstone terrain constrains the magmatic history of this terrain between 2647 ± 4 and 2733 ± 5 Ma. Finally, it revealed that the chronological nomenclature (G1 to G5) established by Key et al. (1976) for the granitoids in NE Botswana is invalid at least in the Vumba granite-greenstone terrain.

8.3. Geotectonic settings

Discussions on the tectonic settings to stabilisation of the Zimbabwe craton are generally centred around a continental rift-related model. That is the greenstone terrains are interpreted as rift-related sequences deposited on continental crust. Arguments in support of this model include the greenstone sequences overlying older continental crust and the recognition of a regional stratigraphy in the Belingwe granite-

greenstone terrain that has been correlated across much of the Zimbabwe craton (Bickle et al., 1994; Wilson et al., 1995; Dirk and Jelsma, 1998). This model was, however, challenged by Kusky and Kidd (1995) who argued that some Zimbabwe greenstone terrains are more like oceanic plateaux than rifts, and may be allochthonous.

Kusky (1998) subdivided the Zimbabwe craton into two domains which he termed the Northern and Southern magmatic belts. These domains flank the Tokwe terrain which is considered the nucleus of the Zimbabwe craton. The Vumba granite-greenstone terrain lies in the Northern magmatic belt while the Tati and the Matsitama granite-greenstone terrains (NE Botswana) are part of the Southern magmatic belt. According to Kusky (1998) the Northern magmatic belt comprises a series of calc-alkaline lavas and intercalated sedimentary rocks intruded by syn-volcanic plutons while the Southern domain consists of tholeiitic mafic-ultramafic-dominated greenstone terrains which formed as thick oceanic crust in a back-arc basin (which he termed Umtali sea) and later obducted onto the rift and passive margin sequence as the sea of Umtali closed at ca.2.7 Ga.

However, geochemical signatures from the granitoids and associated metavolcanics from the Vumba granite-greenstone terrain point toward generation of the magmas in a subduction or collision zone. The granitoids in the area engulf the metavolcanic sequence, which implies that they are relatively younger. The metavolcanic sequence is viewed as contemporaneous with subduction.

The mafic metavolcanics from the Vumba Volcanic Group possess geochemical signatures of lavas erupted at an active continental margin or a back-arc basin (see chapter 4). The associated felsic metavolcanics and the granitoids show volcanic arc or post-collision affinities. Since the mafic and felsic metavolcanics are considered synchronous, a volcanic arc setting is favoured for the metavolcanics of the

Vumba Volcanic Group. The granitoids are regarded as syn-volcanic and as plutonic equivalents of the felsic volcanism, which implies they are volcanic arc granitoids not post-collision except the Domboshaba Granite which is much younger than the rest of the granitoids. The Domboshaba Granite is likely to be a post-collision granitoid, which was generated after the cessation of the accretion process.

The possibility of a back-arc setting seems unlikely here because this model fails to account for the associated felsic metavolcanics and the granitoids. Moreover, in a back-arc setting there is commonly vast amount of metasediments, which is not the case in the Vumba granite-greenstone terrain. Additionally, mafic metavolcanics in back-arc settings are commonly tholeiitic not calc-alkaline like the Vumba Volcanic Group.

The petrogenesis of ultramafic intrusives which dissect Archaean granite-greenstone terrains is still a matter of controversy (e.g. Allegre, 1982; Campbell et al., 1989; Bickle, 1993; Arndt, 1994; Dostal and Mueller, 1997; Polat et al., 1999). Controversy focuses on whether a subduction related source or upwelling of a mantle plume acted as providers of thermal and material input. The mantle plume has been mostly proposed in greenstone terrains that have an assemblage of tholeiitic basalts, komatiitic basalts and komatiites where the komatiites and the basalts are regarded as the tail and head of the mantle plume respectively. It is also believed that subduction of an oceanic plate could lead to hydration of the overlying mantle wedge, which in turn would lower the mantle solidus temperature (Gallagher and Hawkesworth, 1992). This could result in a high degree of partial melting and would lead to an ultramafic residue. The origin of the ultramafic intrusives in the Vumba granite-greenstone terrain, which are regarded as cumulates, is more plausible by the subduction-related model. Nb depletion, high Th/Nb ratios and the association with the subduction-related rocks are inline with this model.

In view of all geochemical signatures from the geology of the Vumba granite-greenstone terrain, a continental arc setting is here proposed for this terrain. One question which remains, however, is that of the basement on which the lavas were erupted. It is envisaged that simultaneous subduction and melting of oceanic crust probably occurred along a volcanic arc (Fig. 8.1), which represented the nucleus of continental crust that may have been relatively thin and characterised by high geothermal gradients. The 2733 ± 5 Ma amphibolitic gneiss xenoliths preserved in the 2690 ± 4 Ma granitoids probably came from the basement.

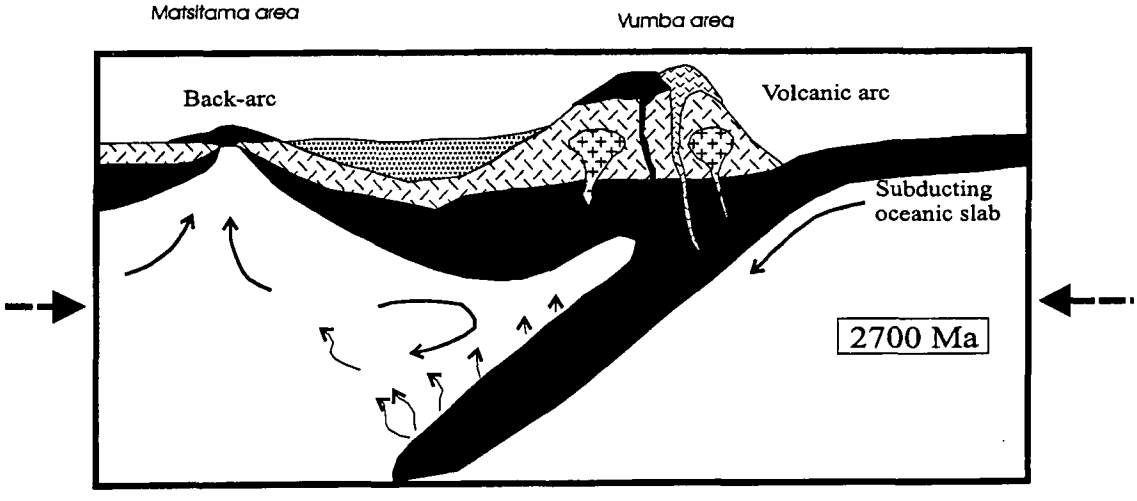

Figure 8.1. Cartoon to illustrate the geotectonic model proposed for the Vumba granite-greenstone terrain. An oceanic plate converging with a volcanic arc due to accretional processes at c 2700 Ma.

REFERENCES

Aldiss, D.T, 1991. The Motloutse Complex and the Zimbabwe craton/Limpopo belt transition in Botswana. *Precambrian Research*, v. 50, pp. 89-109.

Aldiss, D.T., 1989. The geology of the Shashe area. Geological Survey Botswana Bulletin No: 35, 132 pp.

Allegre, C.J., 1982. Genesis of Archaean komatiites in a wet ultramafic subducted plate, in Arndt, N.T. and Nisbet, E.G., (eds), *Komatiites*: London, George Allen and Unwin, pp. 495-500.

Arndt, N.T., 1994. Archaean komatiites, in Condie, K.C., (ed), *Archaean Crustal Evolution*: Amsterdam, Elsevier, pp. 11-44.

Arth, J.G., 1976. Behaviour of trace elements during magmatic processes and dacitic liquid and implications for the genesis of trondhjemitic-tonalitic magmas. *Geology*, v. 4, pp. 534-536.

Barton, J.M., Jr., Holzer, L., Kamber, B., Doig, R., Kramers, J.D. and Nyfeler, D., 1994. Discrete metamorphic events in the Limpopo belt, southern Africa: implications for the application of P-T paths in complex metamorphic terrains. *Geology*, v. 22, pp. 1035-1038.

Beakhouse, G.P. and McNutt, R.H., 1991. Contrasting types of late Archaean plutonic rocks in northwestern Ontario: implications for crustal evolution in the superior Province. Precambrian Research, v.49, pp. 141-165.

Ben-Avranham, J.W., 1991. The geology of the Harare greenstone belt and surrounding granitic terrain. Geological Survey of Zimbabwe, Bulletin No. 94, 213 pp.

Bennet, J.D., 1968. A provisional description of the geology of Mosetse-Matsitama area. Report of Geological Survey Botswana, No. JDB/19/68.

Bickle, M.J., Nisbet, E.G. and Martin, A., 1994. Archaean greenstone belts are not oceanic crust. *Journal of Geology*, v. 102, pp.121-138.

Bickle, M.J., Orpen, J.L., Nisbet, E.G. and Martin, A., 1993. Structure and metamorphism of the Belingwe greenstone belt and adjacent granite-gneiss terrain: the tectonic evolution of an Archaean craton. In: Bickle, M.J., Nisbet, E.G. (eds), *The geology of the Belingwe greenstone belt: a study of the evolution of Archaean continental crust.* Geological Society of Zimbabwe Special Publication No: 2, pp. 39-68.

Blenkinsop, T.G., Fedo, C.M., Bickle, M.J., Eriksson, K.A., Martin, A., Nisbet, E.G. and Wilson J.F., 1993. Ensialic origin for the Ngezi Group, Belingwe greenstone belt, Zimbabwe. *Geology*, v. 21, pp. 1135-1138.

Blenkinsop, T.G., Martin, A., Jelsma, H.A. and Vinyu, M.L., 1997. The Zimbabwe Craton. In: de Wit, M.J., Ashwal, L.D (eds), Greenstone belts. *Oxford University Press*, pp. 567-580.

Boynton, W.V., 1984. Geochemistry of the rare earth elements: meteorite studies. In: Henderson, P. (ed), *Rare Earth Element Geochemistry*. Elsevier, pp. 63-114.

Brake, C., 1996. Tholeiitic magmatism in the Belingwe greenstone belt, Zimbabwe. Unpublished Ph.D. Thesis, University of Edinburgh, U.K., 184 pp.

Campbell, I.H., Griffiths, R.W. and Hill, R.I., 1989. Melting in an Archaean mantle plume: heads it's basalts, tails it's komatiites. Nature, v. 339 (6227), pp. 697-699.

Cann, J.R., 1970. Rb, Sr, Y, Zr and Nb in some ocean floor basaltic rocks: *Earth and Planetary Science Letters*, v. 10, pp. 7-11.

Card, K.D., 1990. A review of the Superior Province of the Canadian Shield: A product of Archaean accretion. Precambrian Research, v. 48, pp. 99-156.

Carney, J.N., Aldiss, D.T. and Lock, N.P., 1994. *The geology of Botswana*. Botswana Geological Survey Bulletin No: 37, Government Printer, Gaborone 23-25 pp.

Chappell, B.W. and White, A.J.R., 1974. Two contrasting granite types. *Pacific Geology*, v.8, pp. 173-179.

Chauvel, G., Dupre, B. and Arndt, N.T., 1993. Pb and Nd isotopic correlation in Belingwe komatiites and basalts. In: Bickle, M.J., Nisbet, E.G., (eds), *The Geology of the Belingwe greenstone belt, Zimbabwe*. Geological Society of Zimbabwe Special Publication No: 2, pp. 167-174.

Collins, W.J., Beams, S.D., White, A.J.R. and Chappell, B.W., 1982. Nature and origin of A-type granites with particular reference to southeastern Australia. *Contributions to Mineralogy and Petrology*, v. 80, pp.189-200.

Compston, W., Williams, I. S, Kirschvink, J. L., Zhang, Z. and Ma, G., 1992. Zircon U-Pb ages for the Early Cambrian time-scale. *Journal of Geological Society, London*, v. 149, pp. 171-184.

Coward, M.P. and James, P.R., 1974. The deformation patterns of two Archaean greenstone belts in Rhodesia and Botswana. *Precambrian Research*, v. 1, pp. 235-258.

Cumming, G.L. and Richards, J.R., 1975. Ore lead isotope ratios in a continuously changing Earth. *Earth Planetary Science Letters*, v. 28, pp. 155-171.

Debon, F. and Le Fort, P., 1983. A chemical-mineralogical classification of common plutonic rocks and associations. Transactions of the Royal Society of Edinburgh Earth Sciences, v. 73, pp. 135-149.

Defant, M.J. and Drummond, M.S., 1990. Derivation of some modern arc magmas by melting of young subducted lithosphere. *Nature*, v. 347, pp. 662-665.

De Wit, M.J. and Ashwal, L.D., 1997, (eds). Tectonic evolution of greenstone belts: Oxford University on Geology and Geophysics no. 35, 809 p.

De Wit, J.M., Roering, C., Hart, R. J., Armstrong, R. A., De Ronde, C.E.J., Green, R.W.E., Tredoux, M., Peberdy, E. and Hart, R. A., 1992. Formation of an Archaean continent. *Nature*, v. 357, pp. 553-562.

De Wit, M.J., Hart, R.A. and Hart, R.J., 1987. The James-town ophiolite complex, Barberton Mountain belt: A section through 3.5 Ga oceanic crust: *Journal of African Earth Sciences*, v. 6, pp. 681-730.

Dirks, P.H.G.M. and Jelsma, H.A., 1998. Horizontal accretion and stabilisation of the Archaean Zimbabwe craton. *Geology*, v. 26, pp. 11-14.

Dirks, P.H.G.M. and Jelsma, H.A., 1998. Silicic layer-parallel shear zones in a Zimbabwean greenstone sequence: horizontal accretion preceding doming. *Gondwana Research*, v. 2, pp. 177-193.

Dodson, M.H., Compston, W., Williams, I.S. and Wilson, J.F., 1988. A search for ancient detrital zircons in Zimbabwe sediments. *Journal of Geological Society, London*, v. 145, pp. 977-983.

Dostal, J. and Mueller, W.U., 1997. Komatiite Flooding of a Rifted Archaean Rhyolitic Arc Complex: Geochemical Signature and Tectonic Significance of the Stoughton-Roquemaure Group, Abitibi Greenstone Belt, Canada. *Journal of Geology*, v. 105, pp. 545-563.

Dougherty-Page, J.S., 1994. The evolution of the Archaean continental crust of northern Zimbabwe, Unpublished Ph.D. Thesis, Open University, Milton Keynes, England, 244 pp.

Fedo, C.M., Eriksson, K.A. and Blenkinsop, T.G., 1995. Geologic history of the Archaean Buhwa greenstone belt and surrounding granite-gneiss terrane, Zimbabwe, with implications for the evolution of the Limpopo belt. *Canadian Journal of Earth Sciences*, v. 32, pp. 1977-1990.

Gallagher, K. and Hawkesworth, C., 1992. Dehydration melting and generation of continental flood basalts. *Nature*, v. 358, pp. 57-59.

Hoffman, P.F., 1991. On accretion of granite-greenstone terranes. In F. Robert, P.A. Shearan and S.B. Green (eds), Greenstone Gold and Crustal Evolution. Geological Association of Canada, Ontario, pp. 32-45.

Hofmann, A. W., 1988. Chemical differentiation of the earth: The relationship between mantle, continental crust and oceanic crust. Earth and Planetary Science Letters, v. 90, pp. 297-314.

Holzer, L., Frei, R., Barton, J.M., Jr. and Kramers, J.D., 1998. Unravelling the record of successive high grade events in the Central Zone of the Limpopo belt using Pb single phase dating of metamorphic minerals. *Precambrian Research*, v. 87, pp. 87-115.

Hunter, M.A., Bickle, M.J., Nisbet, A.M. and Chapman, H.J., 1998. Continental extensional setting for the Archaean Belingwe Greenstone Belt, Zimbabwe. *Geology*, v. 26, pp. 883-886.

Huppert, H. E. and Sparks, R.S.J., 1985. Cooling and contamination of mafic and ultramafic magmas during ascent through continental crust. Earth and Planetary Science Letters, v. 74, pp. 371-386.

Irvine, T.N. and Barager, W.R.A., 1971. A guide to the chemical classification of the common volcanic rocks. *Canadian Journal of Earth Science*, v. 8, pp. 523-448.

Jaeckel, P., Kroner, A., Kamo, S.L., Brandl, G. and Wendt, J.I., 1997. Late Archaean to early Proterozoic granitoid magmatism and high-grade metamorphism in the central Limpopo belt, South Africa. *Journal of Geological Society, London*, v. 154, pp. 24-44.

Janardhan, A.S., Newtown, R.C. and Hensen, E.C., 1982. The transformation of amphibolite facies gneiss to charnokite in Southern Karnataka and Northern Tamil Nadu, India: *Contributions to Mineralogy and Petrology*, v. 79, pp. 130-149.

Jelsma, H.A. and Dirks, P.H.G.M., 2000. Tectonic evolution of a greenstone sequence in northern Zimbabwe: sequential early stacking and pluton diapirism. Tectonics, v. 19, pp. 135-152.

Jelsma. H.A., Vinyu, M.L., Valbracht, P.J., Davies, G.R., Wijbrans, J.R. and Verdurmen, E.A.T., 1996. Constraints on Archaean crustal evolution of the Zimbabwe craton: a U-Pb zircon, Sm-Nd and Pb-Pb whole-rock isotope study. *Contribution to Mineralogy and Petrology*, v. 124, pp. 55-70.

Jochum, K.P., Arndt, N.T. and Hofmann, A.W., 1990. Nb-Th-La in komatiites and basalts: Constraints on komatiites petrogenesis and mantle evolution. Earth and Science Planetary Letters, v. 107, pp. 272-289.

Kamber, B.S., Kramers, J.D., Napier, R., Cliff, R.A. and Rollinson, H.R., 1995. The Triangle shear zone, Zimbabwe, revisited: new data document an important event at 2.0 Ga in the Limpopo Belt. *Precambrian Research*, v. 70, pp. 191-213.

Key, R.M., 1976. *The geology of the area around Francistown and Phikwe, northeast and central districts, Botswana.* District Memoir No: 3, Geological Survey Botswana, 121pp.

Key, R.M., Litherland, M. and Hepworth, J.V., 1976. The evolution of the Archaean crust of northeast Botswana. *Precambrian Research*, v. 3, pp. 375-413.

Kroner, A., Jaeckel, P., Brandle, G., Nemchin, A.A. and Pidgeon, R.T., 1999, Single zircon ages for granitoid gneisses in the Central Zone of the Limpopo belt, southern Africa and geodynamic significance. *Precambrian Research*, v. 93, pp. 299-337.

Kusky, T.M., 1998. Tectonic setting and terrane accretion of the Archaean Zimbabwe craton. Geology, v. 26, pp. 163-166.

Kusky, T.M. and Kidd, W.S.F., 1992. Remnants of an Archaean oceanic plateau, Belingwe greenstone belt, Zimbabwe. *Geology*, v. 20, pp. 43-46.

Kusky, T.M. and Winsky, P.A. 1995. Structural relationships along a greenstone/shallow water shelf contact, Belingwe greenstone belt, Zimbabwe. *Tectonics*, v. 14, pp. 448-471.

Le Maitre, R.W. (ed) with Bateman, P., Dubek, A., Keller, J., Lameyre, J., Le Bas, M.J., Sabine, P.A., Schmid, R., Sorensen, H., Streckeisen, A., Wooley, A.R. and Zanettin, B., 1989. *A classification of Igneous Rocks and Glossary of Terms: Recommendations of the International Union of Geological Sciences Subcommision on the Systematics of igneous rocks.* Blackwell, Oxford, 193 pp.

Lintern, B.C., 1982. The stratigraphy and structure of the Matsitama Schist Belt, northeast Botswana. Unpublished Ph.D. Thesis, Leeds University, U.K., 234 pp.

Litherland, M., 1973. Uniformitarian approach to Archaean 'Schist Relics'. *Nature*, v. 242, pp. 125-127.

Litherland, M., 1975. *The geology of the area around Maitengwe, Sebina and Tshesebe, Northeast and Central Districts, Botswana.* District Memoir No: 2, Geological Survey Botswana, 133 pp.

Luas, B. and Hawkesworth, C.J., 1994. The Generation of Continental Crust: An Integrated Study of Crust-Forming Processes in the Archaean of Zimbabwe. *Journal of Petrology*, v.35, pp. 43-93.

Ludtke, G., Mosigi, B. and Zeil, P., 1989. Mineral Exploration in the Vumba Schist Belt of Northeast Botswana. Final report. BGR, Hannover, Archive No: 105549, 93 pp.

Ludwig, K.R., 1999. Isoplot/Ex (version 2.00) _ A geochronological toolkit for Microsoft Excel. Berkeley Geochronology Center Special Publication Nr 1a, 46 pp.

Luhr, J.F., 1992. Slab-derived fluids and partial melting in subduction zones: Insights from two contrasting Mexican volcanoes (Colima and Ceboruco). *Journal of Volcanology and Geothermal Research*, v. 54, pp. 1-18.

Mahood, G. and Hildreth, W., 1983. Large partition coefficients for trace elements in high-silica rhyolites. *Geochemica et Cosmochima Acta*, v. 47, pp. 11-30.

Majaule, T. and Davis, D.W., 1998. U-Pb zircon dating and geochemistry of granitoids in the Mosetse area, NE Botswana, and tectonic implications. Geological Survey of Botswana, 50th Anniversary International Conference Abstract volume, 46-48.

Majaule, T., Hall, P. and Hughes, D., 1997. Geochemistry of mafic and ultramafic igneous rocks of the Matsitama supracrustal belt, northeastern Botswana - provenance implications. *South African Journal of Geology*, v. 100, pp. 169-179.

Martin, H., 1986. Effect of steeper Archaean geothermal gradients on geochemistry of subduction-zone magmas. *Geology*, v. 14, pp. 753-756.

McCarthy, T.S. and Groves, D.I., 1979. The Blue Tier Batholith, Northeastern Tasmania. A cumulate-like product of fractional crystallisation. *Contribution to Mineralogy and Petrology*, v. 71, pp. 193-209.

McCarthy, T.S. and Hasty, R.A., 1976. Trace element distribution patterns and their relationship to the crystallisation of granitic melts. *Geochimica Cosmochim Acta*, v. 40, pp. 1351-1358.

McCourt, S. and Armstrong, R. A., 1998. SHRIMP U-Pb zircon geochronology of granites from the Central Zone, Limpopo belt, southern Africa: implications for the age of the Limpopo Orogeny. *South African Journal of Geology*, v. 101, pp. 329-338.

McCourt, S. and Wilson, J.F., 1992. Late Archaean and early Proterozoic tectonics, Limpopo and Zimbabwe. In: Glover, J.E., Ho, S.E., (eds.), The Archaean: Terrains, Processes and Metallogeny. Proceedings of the Third International Archaean symposium, Perth, University of Western Australia Publication No: 22, pp. 237-246.

Mkweli, S., Kamber, B. and Berger, M., 1995. Westward continuation of the Craton-Limpopo Belt tectonic break in Zimbabwe and new age constraints on the timing of the thrusting. *Journal Geological Society, London*, v. 152, pp. 77-83.

Nash, W.P. and Crecraft, H.R., 1985. Partition coefficients for trace elements for trace elements in silicic magmas. *Geochemica et Cosmochimica Acta*, v. 49, pp. 2309-2322.

Nisbet, E.G., Wilson, J.F. and Bickle, M.J., 1981. The evolution of the Rhodesian craton and adjacent Archaean terrain: tectonic models. In: Kroner, A. (ed), *Precambrian Plate Tectonics*. Elsevier, Amsterdam, pp. 161-183.

Paces, J.B. and Miller, J.D., 1989. Precise U-Pb ages of Duluth Complex and related mafic intrusions, Northeastern Minnesota: Geochronological insights to physical, petrogenic, paleomagnetic and tectonomagmatic processes associated with the 1.1 Ga Midcontinent rift system. *Journal of Geophysical Research*, v. 98B, pp. 13997-14013.

Peacock, M.A., 1931. Classification of igneous rock series. *Journal of Geology*, v. 39, pp. 54-67.

Pearce, J.A. and Cann, J.R., 1973. Tectonic setting of basic volcanic rocks determined using trace element analyses. *Earth and Planetary Science Letters,* v. 19, pp. 290-300.

Pearce, J.A. and Norry, M.J., 1979. Petrogenetic implications of Ti, Zr, Y and Nb variations in volcanic rocks. *Contribution to Mineralogy and Petrology*, v. 69, pp.33-47.

Pearce, J.A. and Peate, D.W., 1995. Tectonic implications of the composition of volcanic arc magmas. *Annual Review of Earth and Planetary Sciences*, v. 23, pp. 251-285.

Pearce, J.A., 1982. Trace element characteristics of lavas from destructive plate boundaries. In: Thorpe, R.S. (ed), Andesites: *Orogenic Andesites and Related Rocks*. John Wiley, New York, pp. 525-548.

Pearce, J.A., 1983. Role of the sub-continental lithosphere in magma genesis at active continental margins. In: C.J. Hawkesworth and M.J. Norry (eds), *Continental Basalts and Mantle Xenoliths*, Shiva, U.K, pp. 230-249.

Pearce, J.A., 1996. A User's Guide to Basalt Discrimination Diagrams, in Wyman, D.A., ed., Trace Element Geochemistry of Volcanic Rocks: Applications for Massive Sulphide Exploration: *Geological Association of Canada*, Short Course notes, v. 12, p. 79-113.

Pearce, J.A., Harris, N.B.W. and Tindle, A.G., 1984. Trace element discrimination diagrams for the tectonic interpretation of granitic rocks. *Journal of Petrology*, v.25, pp. 956-983.

Peccerillo, A. and Taylor, S.R., 1976. Geochemistry of Eocene calc-alkaline volcanic rocks from the Kastamonu area, Northern Turkey. *Contributions to Mineralogy and Petrology*, v. 58, pp. 63-91.

Polat, A., Kerrich, R. and Wyman, D.A., 1999. Geochemical diversity in oceanic komatiites and basalts from the late Archaean Wawa greenstone belts, Superior Province, Canada: trace element and Nd isotope evidence for a heterogeneous mantle. *Precambrian Research*, v. 94, pp. 139-173.

Ridley, J.R. and Kramers, J.D., 1990. The evolution and tectonic consequences of a tonalitic magma layer within Archaean continents. *Canadian Journal of Earth Sciences*, v. 27, pp. 219-228.

Ridley, J.R., Vearncombe, J.R. and Jelsma, H.A., 1997. Relations between greenstone belts and associated granitoids. In: de Wit, M.J., Ashwal, L.D., (eds), *Greenstone belts*. Oxford University Press, pp. 376-397.

Rollinson, H., 1993. *Using Geochemical Data*: evaluation, presentation, interpretation. John Willey and Sons, New York.

Rollinson, H. and Blenkinsop, T., 1995. The magmatic, metamorphic and tectonic evolution of the Northern Marginal Zone of the Limpopo belt in Zimbabwe. *Journal of Geological Society, London*, v. 152, pp. 65-75.

Shand, S.J., 1951. Eruptive Rocks. John Wiley New York, 444 pp.

Scholey, S.P., 1992. The geology and geochemistry of the Ngezi group volcanics, Belingwe greenstone belt, Zimbabwe Unpublished Ph.D Thesis, University of Southampton, U.K., 184 pp.

Shervais, J.W., 1982. Ti-V plots and the petrogenesis of modern ophiolitic lavas. *Earth and Planetary Science Letters*, v. 59, pp. 101-118.

Streckeisen, A., 1976. To each plutonic rock its proper name. *Earth-Science Reviews*, v. 12, pp. 1-33.

Sun, S.S. and McDonough, W.F., 1989. Chemical and isotopic systematics of oceanic basalts: implications for mantle composition and processes: In: Saunders, A.D. and Norry, M.J. (eds), *Magmatism in the Ocean Basins*. Geological Society Special Publications No:42, pp. 313-345.

Taylor, P.N., Kramers, J.D., Moorbath, S., Wilson, J.F., Orpen, J.L. and Martin, A., 1991. Pb/Pb, Sm-Nd and Rb-Sr geochronology in the Archaean Craton of Zimbabwe. *Chemical Geology*, v. 87, pp. 175-196.

Taylor, S.R. and McLennan, S.M., 1981. The composition and evolution of the continental crust: rare earth element evidence from sedimentary rocks. *Philosophical Transactions of the Royal Society, London*, v. 301, pp. 381-399.

Thompson, R.N., 1982. British Tertiary volcanic province. *Scottish Journal of Geology*, v. 18, pp. 49-107.

Tindle, A.G. and Pearce, J.A., 1981. Petrogenetic modelling of insitu fractional crystallisation in the zoned Loch Doon pluton, Scotland. *Contributions to mineralogy and Petrology*, v. 78, pp. 196-207.

Tomschi, H.P., 1987. Goldvorkommenim Archaischen Harare-Bindura greenstone belt, Zimbabwe: Zusammenhange zwischen lagerstattenbildung und greenstone belt entwicklung. Unpublished Ph.D. Thesis, University of Koln, Germany, 279 pp.

Treloar, P.J. and Blenkinsop, T.G., 1995. Archaean deformation patterns in Zimbabwe: true indicators of Tibetan-style crustal extrusion or not? *Geological Society Special Publication*, v. 95, pp. 87-108.

Treloar, P.J., Coward, M.P. and Harris, N.B.W., 1992. Himalayan-Tibetan analogies for the evolution of the Zimbabwe Craton and Limpopo Belt. *Precambrian Research*, v. 55, pp. 571-587.

Van Breemen, O., 1970. Geochronology of the Limpopo orogenic belt, southern Africa. *Journal of African Earth Sciences*, v. 8, pp. 57-62.

Van Breemen, O. and Dodson, M.H., 1972. Metamorphic chronology of the Limpopo belt, southern Africa. *Geological Society of America*, Bulletin No: 83, pp. 2005-2018.

van de Wel, L., Barton, J. M., Jr. and Kinny, P.D. 1998. 1.02 Ga granite magmatism in the Tati Granite-Greenstone Terrane of Botswana: implications for mineralisation and terrane evolution. *South African Journal of Geology*, v. 101, pp. 67-72.

Vinyu, M.L., Frei, R. and Jelsma, H.A., 1996. Timing between granitoid emplacement and associated gold mineralisation: examples from the ca. 2.7 Ga Harare-Shamva greenstone belt, northern Zimbabwe. *Canadian Journal of Earth Sciences*, v. 33, pp. 981-992.

Weaver, B. and Tarney, J., 1884. Empirical approach to estimating the composition of the continental crust. *Nature*, v. 310, pp. 570-575.

White, A.J.R. and Chappell, B.W., 1977. Ultrametamorphism and granitoid genesis. *Tectonophysics*, v. 43, pp. 7-22.

Williams, I.S. and Claesson, S., 1987. Isotopic evidence for the Precambrian provenance and Caledonian metamorphism of high grade paragneisses from the Seve Nappes, Scandinavian Caledonides. II. Ion microprobe zircon U-Th-Pb. *Contribution to Mineralogy and Petrology*, v. 97, pp. 205-217.

Wilson, J.F., 1979. A preliminary reappraisal of the Rhodesian Basement Complex. In: Anhaeusser, C.R., Foster, R.P., Stretton, T., (eds), *A symposium on mineral deposits and transportation and deposition of metals.* Geological Society of South Africa Special Publication No: 5, pp. 1-23.

Wilson, J.F., 1981. The granite-gneiss greenstone shield, Zimbabwe. In: Hunter, D.H. (ed), *Precambrian of the Southern Hemisphere.* Elsevier, Amsterdam, pp. 454-488.

Wilson, J.F., Baglow, N., Orpen, J.L. and Tsomondo, J.M., 1990. A reassessment of some regional correlations of greenstone-belt rocks in Zimbabwe and their significance in the development of the Archaean craton. Extended Abstract: Third International Archaean Symposium, Perth 1990. Geoconferences, Perth, pp. 43-44.

Wilson, J.F., Nesbitt, R.W. and Fanning, C.M., 1995. Zircon geochronology of Archaean felsic sequences in the Zimbabwe craton: a revision of greenstone stratigraphy and a model for crustal growth. In: Coward, M.P., Ries A.C., (eds), *Early Precambrian Processes*. Geological Society of London Special Publication, v. 95, pp. 109-126.

Winchester, J.A. and Floyd, P.A., 1976. Geochemical magma type discrimination; application to altered and metamorphosed basic igneous rocks. *Earth and Planetary Science Letters*, v. 28, pp. 459-469.

Winchester, J.A. and Floyd, P.A., 1977. Geochemical discrimination of different magma series and their differentiation products using immobile elements. *Chemical Geology*, v. 20, pp. 325-343.

Wood, D.A., 1980. The application of a Th-Hf-Ta diagram to problems of tectomagmatic classification and to establishing the nature of crustal contamination of basaltic lavas of the British Tertiary volcanic province. *Earth and Planetary Science Letters*, v. 50, pp. 11-30.

APENDICES

APPENDIX A – *ANALYTICAL TECHNIQUES*

I. U-Pb ZIRCON ANALYSIS

The samples were crushed and the zircons separated using standard density and magnetic separation techniques. The final concentrate was handpicked under a binocular microscope and the zircon grains were mounted in epoxy together with the zircon standard AS3 (Duluth complex gabbroic anorthosite; Paces and Miller, 1989) and the standard SL13 of the Research School of Earth Sciences, Australian National University. The grains were then sectioned approximately in half, polished and photographed. Scanning Electron Microscope cathodoluminescence imaging was carried out to detect cores, rims and other complexities, which might be present, and to ensure no areas of mixed age were analysed.

The SHRIMP data have been reduced in a manner similar to that described by Compston et al. (1992) and Williams and Claesson (1987). U/Pb in the unknowns were normalised to a $^{206}*Pb/^{238}U$ value of 0.1859 (equivalent to an age of 1099.1 Ma) for AS3. The U and Th concentrations were determined relative to those measured in the SL13 standard and the common Pb correction was determined from the measured ^{204}Pb and using the appropriate common Pb isotopic compositions assuming the Cumming and Richards (1975) model. All ages calculations and statistical assessments of the data have been done utilising the geochronological software package Isoplot/Ex (version 2.00) of Ludwig (1999). Uncertainties in the isotopic ratios and ages in the data tables (and in the error bars in the plotted data) are reported at the 1σ level, but where ages are calculated from combined data or from regression analysis the errors quoted are 95% confidence limits.

II. MODAL ANALYSIS

The modal proportions of minerals in 27 granitoid samples are presented in Appendix B (II). The data were collected using a Swift Model F automatic point counter fitted with an automated stage. Samples were normal thin sections prepared for microscopic analysis. A total of 1200 points were counted on each specimen in such a way that the whole surface of thin section was covered.

Both major phases and minor phases are presented in the tables. Where "tr" appears in the tables it implies that the mineral was observed, but not point counted.

III. XRF ANALYSIS

III.1. Sample preparation

First and foremost fresh samples which were collected from the field were cut into small cubic slices using a diamond-saw. A jaw crusher was then utilised to crush the cubic slices into pieces less than 5 mm. The jaw crusher was thoroughly cleaned with a wire brush and alcohol after each sample to avoid contamination. Additionally, as a precaution to keep contamination minimal, samples were divided into groups (e.g. granitoids, mafic volcanics, ultramafics and felsic volcanics) which were treated at different periods of time. Approximately 100 grams of each crushed sample was pulverised into less than 200 mesh utilising an agate-ball grinding machine. After each sample thorough cleaning of the agate bowels and balls with water and alcohol was assured. At this stage, the samples are ready for the preparation of the pressed powder pellets and fusion discs for X-ray fluorescence spectrometry (XRF).

III.1.1. Preparation of the pressed powder pellets

Few drops of movoil (binding agent) were added to approximately 10 grams of each pulverised sample and thoroughly homogenised. After that they were pressed in stainless steel mould between a pair of steel discs using a hydraulic pellet press. Pellets were then labelled and placed into an oven for dryness about 100 °C prior to analysis. After that, these pellets were analysed for trace elements using X-ray fluorescence spectrometry (XRF).

III.1.2. Determination of loss on ignition (L.O.I)

About 4 grams of each sample powder was placed into a glass vial and labelled. These powder samples were then oven-dried at 110 °C for over an hour to remove surface water. They were then stored in a desiccator to avoid sample loss through spillage and surface water, which might be gained from the atmosphere.

About 3 grams from each sample was weighted and put into the porcelain crucibles. Ignitions were performed at about 900 °C for two and half-hours. After allowing samples to cool in a desiccator they were reweighed and eventually their loss on ignition was calculated from the difference in the weight.

III.1.3. Preparation of fused glass discs

Before making fusion discs, the flux (lithium tetraborate) was dried in the furnace overnight at 600 °C to remove any absorbed water or any other volatiles taken up from the atmosphere. Dried flux was stored in a desiccator during fused disc preparation.

Previously ignited samples were dried at 110 °C for about 24 hours. They were taken out from furnace and placed in desiccator for cooling. After that 0.45 grams of sample and 2.25 grams of flux was mixed using an agate-ball grinding mill. Then the mixture was transferred into platinum crucibles. After that they were placed into furnace at 1050 °C for 20 minutes.

After taking them out, molten samples were poured into the graphic moulds to give them a shape. After cooling on a cooling block, they were labelled and stored in a desiccator until they were taken to the X-ray fluorescence spectrometry (XRF) for analysis.

III.2. Analytical work

Major and trace elements were analysed by X-ray fluorescence spectrometry (XRF) using an automated Philips PW 1400 spectrometer with a Rh anode tube and automatic loader at the University of Durham. X-ray fluorescence analyses were conducted on about 120 samples from the Vumba granite-greenstone terrain. Major elements (SiO_2, TiO_2, Al_2O_3, Fe_2O_3, MnO, CaO, Na_2O, K_2O and P_2O_5) were analysed on fused glass discs and trace elements (Sc, V, Cr, Co, Ni, Cu, Zn, Ga, Rb, Sr, Y, Zr, Nb, Ba, La, Ce, Nd, Pb, Th and U) on pressed powder pellets. The XRF spectrometer was calibrated using a suite of analysed standards selected from approximately 15 international standards to cover the compositional range from ultramafic to felsic. Some of these standards and samples were run repeatedly to monitor machine drift. Analytical accuracy and precision were then calculated using international standards.

IV. ICP-MS ANALYSIS

To ensure dissolution, fused discs were used rather than powdered samples. Fused discs were prepared as mentioned in section III.1.3. After that, these fused disc samples were powdered using a hand agate grinder.

Small amount of powdered samples was placed into the labelled glass vials in an oven at 105 °C overnight to dry. Previously dishwasher-cleaned teflon containers were filled with 2 ml of Analar Nitric acid and left on a hot plate at 130-150 °C for at least 24 hours. After that teflon containers were washed with de-ionised water and placed them in the oven at 105 °C until they were dry. Previously overnight-dried powder samples were then weighed about 0.1 ± 0.001 gram using anti-static gun and transferred into labelled teflon containers. In addition to the samples, at least 6 international standards and two blanks were prepared.

After that, 2 ml of Aristar HNO_3 and 10-15 ml of de-ionised water were added into the teflon containing the 0.1 ± 0.001 gram of powder sample. Then the solution was agitated for a couple of minutes before they were placed on the hot plate for about 24 hours to ensure complete dissolution. The solutions were allowed to cool and spiked with 1.25 ml of internal standard. The internal standard was made of 2 ppm Re and Rh. After this stage, they were transferred into the 50 ml volumetric flasks and made up accurately to 50 ml with de-ionised water. Eventually a subset of trace (Sc, Cr, V, Ni, Co, Zn, Ga, Rb, Sr, Y, Zr, Nb, Cs and Ba) and rare earth elements (La, Ce, Pr, Nd, Sm, Eu, Gd, Tb, Dy, Ho, Er, Tm, Yb, Lu) were analysed by Inductively Coupled Plasma Mass Spectrometry (ICP-MS) at the University of Durham. The instrument used was a PE SCIEX ELAN 6000 ICP-MS.

APPENDIX B – *ANALYTICAL DATA*

APPENDIX B (I)

U-Pb Zircon analyses

Table 1.

Summary of SHRIMP U-Pb zircon results.

Grain spot	U (ppm)	Th (ppm)	Th/U	Pb* (ppm)	$^{204}Pb/^{206}Pb$	f_{206} %	Radiogenic Ratios δ $^{206}Pb/^{238}U$	±	$^{207}Pb/^{235}U$	±	$^{207}Pb/^{206}Pb$	±	Ages (in Ma) δ $^{206}Pb/^{238}U$	±	$^{207}Pb/^{235}U$	±	$^{207}Pb/^{206}Pb$	±	Conc. %
ZB98-92: G1 MashaweTonalitic orthogneiss																			
1.1	145	58	0.40	77	0.00086	1.172	0.4645	0.0088	11.806	0.254	0.1844	0.0015	2459	39	2589	20	2692	14	91
2.1	221	69	0.31	125	0.00049	0.663	0.5151	0.0088	13.075	0.241	0.1841	0.0009	2678	38	2685	18	2690	8	100
2.2	875	457	0.52	256	0.00097	1.327	0.2667	0.0042	4.803	0.084	0.1306	0.0008	1524	21	1785	15	2106	10	72
3.1	89	31	0.35	48	0.00057	0.773	0.4953	0.0104	12.537	0.318	0.1836	0.0022	2593	45	2646	24	2686	20	97
4.1	242	96	0.40	97	0.00506	6.905	0.3465	0.0074	8.780	0.262	0.1838	0.0034	1918	36	2315	28	2687	31	71
5.1	191	108	0.56	115	0.00010	0.14	0.5206	0.0093	13.217	0.260	0.1841	0.0012	2702	40	2695	19	2691	10	100
6.1	516	195	0.38	133	0.00379	5.164	0.2435	0.0039	5.158	0.140	0.1537	0.0030	1405	20	1846	23	2387	34	59
7.1	241	68	0.28	133	0.00007	0.094	0.5080	0.0096	12.763	0.253	0.1822	0.0007	2648	41	2662	19	2673	6	99
8.1	210	86	0.41	110	0.00061	0.826	0.4717	0.0082	12.023	0.237	0.1849	0.0014	2491	36	2606	19	2697	12	92
9.1	262	78	0.30	156	0.00140	1.909	0.5396	0.0094	13.627	0.298	0.1832	0.0021	2782	39	2724	21	2682	19	104
10.1	195	85	0.44	111	0.00101	1.381	0.4974	0.0097	12.590	0.284	0.1836	0.0017	2603	42	2650	21	2686	15	97
11.1	101	34	0.33	59	0.00015	0.208	0.5299	0.0106	13.414	0.303	0.1836	0.0015	2741	45	2709	22	2686	14	102
12.1	159	48	0.30	92	0.00012	0.159	0.5336	0.0122	13.534	0.328	0.1839	0.0011	2757	51	2718	23	2689	10	103
13.1	234	58	0.25	101	0.00203	2.765	0.3922	0.0068	9.502	0.217	0.1757	0.0023	2133	32	2388	21	2613	22	82
14.1	231	96	0.42	122	0.00044	0.597	0.4782	0.0083	11.884	0.224	0.1803	0.0010	2519	36	2595	18	2655	9	95
15.1	311	139	0.45	167	0.00037	0.503	0.4721	0.0084	11.998	0.229	0.1843	0.0009	2493	37	2604	18	2692	8	93
ZB98-67: Xenolith in G2 Sebina gneiss																			
1.1	159	91	0.57	93	0.000122	0.17	0.5085	0.0080	13.218	0.225	0.1885	0.0009	2650	34	2695	16	2730	8	97
2.1	121	42	0.35	72	0.000031	0.04	0.5381	0.0074	13.958	0.209	0.1881	0.0009	2775	31	2747	14	2726	8	102
2.2	226	61	0.27	127	0.001072	1.46	0.4958	0.0068	12.962	0.219	0.1896	0.0016	2596	29	2677	16	2739	14	95
3.1	76	32	0.42	46	0.000081	0.11	0.5315	0.0096	13.894	0.293	0.1896	0.0017	2748	41	2743	20	2739	15	100
4.1	62	37	0.60	41	0.000207	0.28	0.5646	0.0085	14.717	0.245	0.1891	0.0011	2885	35	2797	16	2734	9	106
5.1	72	43	0.60	46	0.000010	0.01	0.5447	0.0103	14.253	0.292	0.1898	0.0012	2803	43	2767	20	2740	10	102
6.1	60	28	0.46	38	0.000191	0.26	0.5556	0.0101	14.465	0.309	0.1888	0.0017	2849	42	2781	20	2732	15	104
7.1	144	98	0.68	91	0.000062	0.09	0.5337	0.0074	13.901	0.207	0.1889	0.0008	2757	31	2743	14	2733	7	101
8.1	145	64	0.44	71	0.000603	0.82	0.4397	0.0069	11.552	0.201	0.1905	0.0011	2349	31	2569	16	2747	10	86
9.1	143	68	0.47	87	0.000023	0.03	0.5359	0.0070	13.961	0.195	0.1889	0.0007	2766	30	2747	13	2733	6	101
10.1	88	23	0.26	51	0.000078	0.11	0.5327	0.0071	13.892	0.201	0.1892	0.0008	2753	30	2742	14	2735	7	101
11.1	106	42	0.39	65	0.000033	0.05	0.5498	0.0098	14.262	0.269	0.1881	0.0008	2825	41	2767	18	2726	7	104
12.1	79	29	0.37	46	0.000092	0.13	0.5226	0.0082	13.725	0.245	0.1905	0.0013	2710	35	2731	17	2746	11	99
13.1	78	27	0.35	46	0.000068	0.09	0.5298	0.0078	13.808	0.226	0.1890	0.0010	2741	33	2737	16	2734	9	100
14.1	229	50	0.22	88	0.000614	0.84	0.3523	0.0043	8.182	0.117	0.1684	0.0011	1946	20	2251	13	2542	11	77
15.1	49	23	0.46	29	0.000127	0.17	0.5270	0.0093	13.731	0.269	0.1890	0.0013	2729	39	2731	19	2733	11	100
ZB98-149: G2 Granitic gneiss																			
1.1	484	133	0.28	257	0.000014	0.019	0.4901	0.0055	12.440	0.148	0.1841	0.0005	2571	24	2638	11	2690	4	96
1.2	538	228	0.42	278	0.000015	0.02	0.4639	0.0054	11.623	0.146	0.1817	0.0006	2457	24	2575	12	2669	6	92
2.1	550	205	0.37	240	0.000027	0.037	0.3945	0.0124	9.552	0.315	0.1756	0.0013	2143	57	2393	31	2612	12	82
3.1	399	168	0.42	143	0.000254	0.346	0.3151	0.0037	6.987	0.093	0.1608	0.0008	1766	18	2110	12	2464	9	72
4.1	485	705	1.45	193	0.001469	2.01	0.2799	0.0279	6.257	0.667	0.1621	0.0044	1591	142	2012	98	2478	46	64
5.1	608	248	0.41	314	0.000642	0.876	0.3119	0.0034	7.018	0.089	0.1632	0.0009	1750	17	2114	11	2489	9	70
6.1	662	175	0.26	204	0.000052	0.071	0.2895	0.0033	5.892	0.072	0.1476	0.0005	1639	16	1960	11	2318	6	71
7.1	430	146	0.34	146	0.000232	0.316	0.3062	0.0035	6.795	0.088	0.1610	0.0008	1722	17	2085	12	2466	8	70
8.1	465	162	0.35	195	0.000013	0.018	0.3855	0.0044	9.093	0.109	0.1711	0.0004	2102	21	2347	11	2568	4	82
9.1	478	157	0.33	192	0.000039	0.053	0.3700	0.0045	8.424	0.107	0.1651	0.0004	2030	21	2278	12	2509	4	81
10.1	598	223	0.37	197	0.000035	0.047	0.3059	0.0142	6.169	0.331	0.1463	0.0032	1720	70	2000	48	2303	38	75
11.1	2624	2238	0.85	627	0.000224	0.306	0.1974	0.0020	2.887	0.031	0.1061	0.0003	1162	11	1379	8	1733	4	67
12.1	758	379	0.50	269	0.000095	0.13	0.3150	0.0036	6.489	0.078	0.1494	0.0004	1765	18	2044	11	2339	4	76
13.1	394	152	0.39	170	0.000129	0.176	0.3859	0.0043	9.210	0.110	0.1731	0.0005	2104	20	2359	11	2588	5	81
14.1	579	125	0.22	204	0.000060	0.082	0.3333	0.0038	7.388	0.090	0.1608	0.0005	1854	18	2160	11	2464	5	75
15.1	669	177	0.26	210	0.000081	0.11	0.2941	0.0032	5.941	0.069	0.1465	0.0004	1662	16	1967	10	2305	4	72

Table1.

(continued)

Grain spot	U (ppm)	Th (ppm)	Th/U	Pb* (ppm)	$^{204}Pb/^{206}Pb$	f_{206} %	Radiogenic Ratios δ						Ages (in Ma) δ						Conc. %
							$^{206}Pb/^{238}U$	±	$^{207}Pb/^{235}U$	±	$^{207}Pb/^{206}Pb$	±	$^{206}Pb/^{238}U$	±	$^{207}Pb/^{235}U$	±	$^{207}Pb/^{206}Pb$	±	
ZB98-44: G4 Tonalitic granitoid																			
1.1	254	125	0.49	152	0.00008	0.10	0.5282	0.0087	13.394	0.232	0.1839	0.0007	2734	37	2708	16	2689	6	102
2.1	434	240	0.55	193	0.00006	0.08	0.3931	0.0061	9.471	0.158	0.1748	0.0007	2137	28	2385	15	2604	7	82
3.1	325	178	0.55	191	0.00006	0.08	0.5093	0.0082	12.972	0.216	0.1847	0.0006	2654	35	2678	16	2696	5	98
4.1	291	133	0.46	167	0.00006	0.08	0.5113	0.0082	13.039	0.217	0.1850	0.0006	2662	35	2683	16	2698	5	99
5.1	327	135	0.41	190	0.00004	0.05	0.5195	0.0082	13.215	0.224	0.1845	0.0008	2697	35	2695	16	2694	7	100
6.1	214	97	0.46	127	0.00008	0.11	0.5272	0.0086	13.398	0.231	0.1843	0.0008	2729	36	2708	16	2692	7	101
7.1	306	132	0.43	178	0.00004	0.06	0.5173	0.0085	13.212	0.229	0.1852	0.0007	2688	36	2695	16	2700	6	100
8.1	144	76	0.53	85	0.00005	0.07	0.5143	0.0092	13.166	0.248	0.1857	0.0008	2675	39	2692	18	2704	7	99
9.1	275	126	0.46	155	0.00010	0.14	0.5017	0.0101	12.732	0.265	0.1841	0.0007	2621	43	2660	20	2690	6	97
10.1	256	119	0.47	144	0.00008	0.11	0.4965	0.0080	12.709	0.214	0.1857	0.0006	2599	35	2658	16	2704	6	96
12.1	189	80	0.42	108	0.00006	0.09	0.5115	0.0094	13.016	0.257	0.1846	0.0010	2663	40	2681	19	2694	9	99
13.1	362	149	0.41	209	0.00007	0.09	0.5172	0.0087	13.188	0.235	0.1850	0.0008	2687	37	2693	17	2698	7	100
14.1	217	95	0.44	124	0.00015	0.21	0.5077	0.0083	12.907	0.225	0.1844	0.0008	2647	36	2673	17	2693	7	98
15.1	162	79	0.49	92	0.00015	0.20	0.4998	0.0088	12.748	0.246	0.1850	0.0012	2613	38	2661	18	2698	10	97
ZB98-71: G5 Domboshaba Granite																			
1.1	304.3	111.9	0.37	167	0.000023	0.032	0.4979	0.0091	12.338	0.238	0.1797	0.0008	2605	39	2630	18	2650	7	98
2.1	174.1	150.7	0.87	104	0.000027	0.036	0.4880	0.0097	12.078	0.250	0.1795	0.0008	2562	42	2611	20	2648	7	97
3.1	365.6	495.1	1.35	244	0.000185	0.254	0.4934	0.0092	12.178	0.238	0.1790	0.0007	2585	40	2618	18	2644	7	98
4.1	292.5	448.5	1.53	189	0.000035	0.048	0.4690	0.0094	11.588	0.246	0.1792	0.0009	2479	41	2572	20	2645	8	94
5.1	281.3	435.5	1.55	179	0.000519	0.713	0.4509	0.0084	11.146	0.224	0.1793	0.0010	2399	37	2535	19	2646	9	91
6.1	532.9	1016	1.91	397	0.000016	0.022	0.5092	0.0085	12.630	0.218	0.1799	0.0005	2653	36	2652	16	2652	4	100
7.1	318.4	303	0.95	196	0.000025	0.034	0.4961	0.0093	12.283	0.239	0.1796	0.0006	2597	40	2626	18	2649	6	98
8.1	532.8	96.66	0.18	190	0.001171	1.609	0.3334	0.0058	7.350	0.152	0.1599	0.0015	1855	28	2155	19	2455	16	76
9.1	289	416.8	1.44	193	0.000094	0.129	0.4860	0.0087	11.997	0.222	0.1790	0.0006	2553	38	2604	18	2644	5	97
10.1	407	104	0.25	213	0.000035	0.048	0.4889	0.0084	12.047	0.216	0.1787	0.0006	2566	36	2608	17	2641	6	97
11.1	340	145	0.43	172	0.000252	0.349	0.4495	0.0079	10.942	0.203	0.1766	0.0008	2393	35	2518	17	2621	7	91
12.1	2815	703	0.25	1095	0.000029	0.04	0.3648	0.0071	8.886	0.186	0.1767	0.0010	2005	34	2326	19	2622	9	77

δ All ratios and ages are reported with 1σ errors; f_{206}% denotes the percentage of ^{206}Pb that is common Pb; for Conc.%, 100% denotes a concordant analysis.

APPENDIX B(II)

Modal analyses for the granitoids

APPENDIX B(II)

Modal analyses (based on 1200 points per sample arranged in order of increasing silica content). Values are in percent.

Unit	G5	G5	G5	G5	G5	G5	G5	G5	G1	G1	G1	G1	G1	G1
Pluton	Domboshaba	Domboshaba	Domboshaba	Domboshaba	Domboshaba	Vumba stock	Sechele	Sechele	Monzonite	Monzonite	Monzonite	Monzonite	Mashawe	Mashawe
Sample no	**ZB-98-70**	**ZB-98-69**	**ZB-98-74**	**ZB-98-76**	**ZB-98-77**	**ZB-98-78**	**ZB-98-79**	**ZB-98-81**	**ZB-98-83**	**ZB-98-84**	**ZB-98-85**	**ZB-98-87**	**ZB-98-95**	**ZB-98-90**
SiO_2 wt.%	69.36	70.78	72.69	73.12	74.14	66.45	71.19	71.23	59.78	59.82	64.21	66.33	74.06	75.03
Quartz	25	29	28	30	27	23	27	26	9	12	14	18	32	36
Alkali feldspar	34	34	26	29	26	17	16	19	27	28	28	35	19	13
Plagioclase	36	33	39	36	40	49	51	49	39	36	41	45	46	46
Amphibole	1	1	tr	2	0	7	2	tr	15	15	11	10	0	0
Biotite	4	4	5	3	5	2	4	5	6	5	4	3	3	3
Apatite	0	tr	1	tr	1	1	0	tr	1	1	tr	1	1	0
Zircon	tr	tr	0	tr	tr	tr	tr	0	1	tr	1	tr	1	0
Opaques	1	1	1	0	1	1	0	1	2	2	1	1	0	0

Unit	G1	G1	G1	G1	G1	G1	G2	G2	G2	G2	G2	G2	G2
Pluton	Mashawe	Mashawe	Shashe Drift	Shashe Drift	Kalakamati	Kalakamati	Maebe	Maebe	Maebe	Maebe	Maebe	Maebe	Maebe
Sample no	**ZB-98-89**	**ZB-98-92**	**ZB-98-10**	**ZB-98-93**	**ZB-98-20**	**ZB-98-96**	**ZB-98-132**	**ZB-98-145**	**ZB-98-144**	**ZB-98-147**	**ZB-98-139**	**ZB-98-146**	**ZB-98-143**
SiO_2 wt.%	75.67	76.09	67.92	68.31	69.13	69.91	67.05	67.61	68.61	68.91	69.76	70.10	72.95
Quartz	38	39	28	24	24	25	29	24	25	25	28	29	34
Alkali feldspar	16	11	8	10	22	24	7	11	7	9	8	9	8
Plagioclase	44	48	53	56	48	44	52	53	56	55	57	53	51
Amphibole	0	0	2	2	6	5	10	3	2	2	1	2	1
Biotite	4	3	8	7	tr	tr	2	9	8	8	5	6	5
Apatite	tr	0	0	tr	tr	1	tr	tr	tr	0	tr	0	1
Zircon	0	tr	tr	tr	0	0	tr	0	tr	0	tr	0	0
Opaques	tr	0	1	1	1	0	1	1	1	1	1	1	0

ABBREVIATIONS

ab: albite
an: anorthite
ap: apatite
C: corundum
cm: chromite
di: diopside
hy: hypersthene
il: ilmenite
or: orthoclase
ol: olivine
Q: quartz
zr: zircon

VLFF: Vumba Lower Felsic Formation
VLMF: Vumba Lower Mafic Formation
VMVF: Vumba Mixed Volcanic Formation
VUFF: Vumba Upper Felsic Formation
VUMF: Vumba Upper Mafic Formation

serpent: serpentine
metapyrox: metapyroxenite

APPENDIX B(III-a)

XRF whole-rock major and trace element data set for the granitoids

APPENDIX B(III-a)

XRF analyses for the granitoids from the Vumba granite-greenstone terrain.

Unit	G5	G5	G5	G5	G5	G5	G5
Pluton	Domboshaba	Domboshaba	Domboshaba	Domboshaba	Domboshaba	Domboshaba	Domboshaba
Sample no	**ZB-98-71**	**ZB-98-73**	**ZB-98-70**	**ZB-98-69**	**ZB-98-74**	**ZB-98-76**	**ZB-98-75**
wt %							
SiO_2	63.09	63.60	69.36	70.78	72.69	73.12	73.54
TiO_2	0.52	0.50	0.48	0.47	0.23	0.16	0.19
Al_2O_3	18.60	18.68	15.14	14.66	14.55	14.28	15.09
FeO_{total}	2.50	2.28	2.65	2.11	1.57	1.28	1.50
MnO	0.04	0.03	0.04	0.04	0.03	0.02	0.02
MgO	0.51	0.43	0.52	0.38	0.30	0.23	0.27
CaO	1.66	1.56	1.37	1.18	1.45	1.41	1.58
Na_2O	4.48	4.38	3.75	3.44	3.76	3.62	3.92
K_2O	7.50	7.56	5.57	6.18	4.44	4.54	4.28
P_2O_5	0.07	0.06	0.07	0.05	0.04	0.05	0.05
L.O.I.	1.13	0.54	0.66	0.53	0.56	0.50	0.67
TOTAL (on L.O.I. Free)	98.97	99.09	98.94	99.28	99.06	98.71	100.45
(ppm)							
Sc	4.6	1.0	4.5	2.6	0.2	4.2	3.0
V	17	5	12	9	14	14	12
Cr	3.1	4.9	8.0	2.3	7.8	11.1	3.5
Co	3.3	1.3	2.1	1.8	1.6	2.8	2.7
Ni	9.0	7.0	5.7	1.5	3.4	1.7	3.2
Cu	11.8	2.7	13.8	7.8	7.0	1.3	5.8
Zn	49.3	35.6	58.0	47.8	45.2	27.3	35.8
Ga	20.7	19.5	22.6	20.6	23.9	21.9	21.8
Rb	167.1	151.6	137.2	151.5	134.9	150.2	121.8
Sr	304.7	306.4	212.0	185.9	211.7	216.0	209.8
Y	17.7	24.5	18.9	26.3	3.6	1.4	6.1
Zr	457.2	274.4	381.4	381.8	132.6	105.5	157.8
Nb	10.8	10.4	5.1	6.4	6.0	3.5	4.7
Ba	1865	1883	1222	1284	1043	1287	1053
La	172.9	96.3	148.6	117.0	43.8	13.8	51.7
Ce	262.4	187.8	262.3	229.5	70.7	38.6	100.5
Nd	70.2	65.2	86.4	81.7	25.4	11.7	32.7
Pb	49.0	34.3	43.0	43.1	29.3	34.3	44.4
Th	77.3	55.3	116.5	125.6	30.8	22.8	50.5
U	2.5	3.9	8.5	10.9	5.1	2.6	10.3
CIPW (%)							
Q	3	4	21	23	29	30	30
or	44	45	33	37	26	27	25
ab	38	37	32	29	32	31	33
an	8	8	7	6	7	7	8
C					1	1	1
di							
hy	5	4	5	4	3	2	3
il	1	1	1	1			
ap							

APPENDIX B(III-a)

XRF analyses for the granitoids from the Vumba granite-greenstone terrain.

Unit	G5	G5	G5	G5	G5	G5	G1
Pluton	Domboshaba	Domboshaba	Vumba stock	Sechele	Sechele	Sechele	Monzonite
Sample no	**ZB-98-72**	**ZB-98-77**	**ZB-98-78**	**ZB-98-79**	**ZB-98-81**	**ZB-98-80**	**ZB-98-83**
wt %							
SiO_2	73.78	74.14	66.45	71.19	71.23	71.45	59.78
TiO_2	0.32	0.18	0.51	0.25	0.31	0.25	0.88
Al_2O_3	13.66	14.36	16.15	15.47	14.62	15.67	16.10
FeO_{total}	1.67	1.45	3.69	1.91	2.33	1.93	6.23
MnO	0.02	0.02	0.05	0.03	0.05	0.03	0.09
MgO	0.22	0.30	1.48	0.54	0.82	0.57	3.34
CaO	1.19	1.52	3.74	2.72	2.49	2.71	4.93
Na_2O	3.11	3.83	3.98	4.50	4.02	4.54	3.38
K_2O	5.49	4.45	2.82	2.62	3.41	2.76	4.11
P_2O_5	0.03	0.05	0.20	0.09	0.10	0.09	0.33
L.O.I.	0.75	0.63	1.20	0.68	0.84	0.71	0.70
TOTAL (on L.O.I. Free)	99.49	100.29	99.07	99.33	99.37	100.00	99.16
(ppm)							
Sc	1.8	2.8	6.2	1.5	1.0	0.9	9.6
V	16	7	52	16	29	16	111
Cr	5.1	5.1	16.8	20.4	13.2	6.1	63.7
Co	1.9	2.4	8.0	1.9	2.7	1.9	22.5
Ni	8.6	4.4	22.1	6.4	10.9	7.2	32.1
Cu	11.8	1.9	4.3	1.9	1.9	2.7	64.3
Zn	44.8	28.7	65.7	60.7	49.1	46.6	92.0
Ga	20.2	21.3	21.5	21.6	20.2	17.6	17.7
Rb	174.1	126.5	69.4	70.5	124.9	73.3	177.1
Sr	190.5	194.4	671.5	463.6	398.7	462.7	524.9
Y	16.6	4.1	8.4	9.5	8.6	9.5	26.5
Zr	419.8	153.6	140.3	132.8	123.8	136.0	248.4
Nb	8.4	2.5	5.0	8.6	9.3	8.0	13.1
Ba	1368	1097	1199	1106	611	1216	918
La	163.5	42.3	61.7	28.8	15.7	24.9	102.7
Ce	271.4	71.7	120.4	62.6	40.8	62.3	171.0
Nd	83.8	19.8	46.3	27.8	15.6	24.7	69.3
Pb	51.5	42.3	26.1	25.3	37.6	28.5	34.2
Th	81.1	52.3	21.2	18.3	27.0	18.9	40.1
U	2.9	7.3	2.5	2.8	11.0	1.9	5.8
CIPW %							
Q	31	30	20	27	27	27	7
or	33	26	17	16	20	16	24
ab	26	32	34	38	34	38	27
an	6	8	18	13	12	13	17
C							
di							5
hy	3	3	9	4	5	4	15
il	1		1		1	1	2
ap			1				1

APPENDIX B(III-a)

XRF analyses for the granitoids from the Vumba granite-greenstone terrain.

Unit	G1	G1	G1	G1	G1	G1	G1
Pluton	Monzonite	Monzonite	Monzonite	Monzonite	Monzonite	Monzonite	Mashawe
Sample no	**ZB-98-84**	**ZB-98-82**	**ZB-98-85**	**ZB-98-88**	**ZB-98-86**	**ZB-98-87**	**ZB-98-95**
wt %							
SiO_2	59.82	60.39	64.21	64.51	64.52	66.33	74.06
TiO_2	0.84	0.88	0.71	0.76	0.65	0.69	0.13
Al_2O_3	16.04	16.09	15.40	15.36	15.37	15.36	14.70
FeO_{total}	6.17	6.18	4.74	4.54	4.49	4.41	1.15
MnO	0.08	0.09	0.06	0.06	0.05	0.05	0.03
MgO	3.33	3.30	2.22	2.23	2.02	2.06	0.19
CaO	4.93	4.92	3.74	3.35	3.46	3.45	1.71
Na_2O	3.45	3.44	3.47	3.29	3.42	3.42	4.45
K_2O	3.97	4.10	4.58	4.71	4.83	4.81	3.43
P_2O_5	0.35	0.35	0.26	0.26	0.23	0.23	0.03
L.O.I.	0.63	0.70	0.58	0.81	0.71	0.61	0.64
TOTAL (on L.O.I. Free)	98.98	99.74	99.38	99.06	99.04	100.81	99.87
(ppm)							
Sc	11.5	12.2	9.2	6.9	6.0	8.1	0.7
V	108	115	82	77	75	73	4
Cr	65.4	66.1	54.1	53.1	50.6	50.6	3.1
Co	21.5	17.2	13.9	13.7	10.5	12.0	1.0
Ni	32.4	30.8	33.1	31.2	23.6	27.3	3.8
Cu	53.4	162.8	51.9	45.3	45.0	40.3	2.9
Zn	82.4	185.5	74.0	60.2	63.3	64.9	31.0
Ga	28.5	28.0	26.9	18.6	19.6	14.5	19.6
Rb	171.8	177.0	243.6	193.9	218.0	216.8	126.8
Sr	514.1	531.2	413.0	445.9	388.5	398.2	226.5
Y	22.8	24.8	21.6	19.0	21.8	26.2	4.1
Zr	269.4	278.6	346.9	335.1	303.7	317.6	79.5
Nb	11.2	12.9	10.2	9.1	10.9	13.2	8.1
Ba	891	933	826	1051	984	978	884
La	76.6	86.5	80.5	94.8	81.9	92.3	11.7
Ce	146.4	155.6	153.1	160.1	147.9	175.0	20.7
Nd	54.3	58.7	56.4	49.2	47.1	60.4	9.5
Pb	45.7	43.5	41.8	35.9	41.1	46.7	41.3
Th	38.3	35.1	73.5	86.4	91.2	94.5	25.4
U	6.7	7.2	10.3	2.9	6.1	12.0	8.4
CIPW (%)							
Q	7	7	14	15	14	16	30
or	24	24	27	28	29	28	20
ab	29	29	29	28	29	29	38
an	17	16	13	13	12	12	9
C							1
di	5	5	4	2	3	3	
hy	15	15	11	11	10	10	2
il	2	2	1	1	1	1	
ap	1	1	1	1	1	1	

APPENDIX B(III-a)

XRF analyses for the granitoids from the Vumba granite-greenstone terrain.

Unit	G1	G1	G1	G1	G1	G1	G1
Pluton	Mashawe	Mashawe	Mashawe	Mashawe	Shashe Drift	Shashe Drift	Shashe Drift
Sample no	**ZB-98-91**	**ZB-98-90**	**ZB-98-89**	**ZB-98-92**	**ZB-98-09**	**ZB-98-94**	**ZB-98-10**
wt %							
SiO_2	74.15	75.03	75.67	76.09	67.26	67.74	67.92
TiO_2	0.14	0.14	0.15	0.12	0.54	0.52	0.47
Al_2O_3	14.25	13.73	14.02	13.28	15.91	15.94	15.83
FeO_{total}	1.66	1.64	1.59	1.57	4.02	3.72	3.49
MnO	0.03	0.03	0.04	0.02	0.05	0.05	0.04
MgO	0.18	0.21	0.23	0.13	1.38	1.30	1.17
CaO	1.94	1.98	1.92	1.96	3.74	3.23	3.60
Na_2O	4.26	4.24	4.19	4.32	4.22	4.39	4.41
K_2O	2.51	2.17	2.63	1.80	1.86	1.90	1.89
P_2O_5	0.03	0.03	0.04	0.03	0.14	0.15	0.14
L.O.I.	0.64	0.63	0.53	0.46	1.28	1.11	0.86
TOTAL (on L.O.I. Free)	99.15	99.21	100.47	99.33	99.12	98.93	98.96
(ppm)							
Sc	1.5	0.5	0.8	4.5	2.4	1.0	2.3
V	3	5	7	2	58	61	56
Cr	5.0	1.6	1.7	13.7	18.4	22.5	13.6
Co	1.2	1.0	1.9	1.0	6.9	6.0	5.8
Ni	3.6	1.0	5.5	3.1	11.8	11.5	10.8
Cu	2.3	2.9	4.2	0.9	4.5	5.6	6.6
Zn	41.1	51.8	24.9	26.7	54.0	52.0	54.2
Ga	17.6	19.6	19.6	18.4	15.1	18.5	22.4
Rb	80.1	75.6	81.1	56.4	56.3	63.4	61.4
Sr	133.1	113.3	130.4	162.9	408.4	364.6	410.2
Y	13.2	11.9	8.0	7.1	7.6	8.1	6.5
Zr	78.2	90.4	91.4	77.5	142.5	138.2	125.7
Nb	5.4	7.1	3.0	4.2	2.2	4.5	5.7
Ba	587	423	639	542	490	463	406
La	11.2	10.2	14.1	11.9	34.8	39.8	30.6
Ce	27.5	28.4	31.9	35.0	67.1	65.6	54.3
Nd	10.5	10.9	10.9	10.9	23.5	19.5	18.0
Pb	31.2	23.2	25.0	25.0	11.4	22.9	15.7
Th	22.5	25.8	19.9	23.1	18.3	22.1	17.6
U	3.0	2.7	3.0	1.9	4.4	3.2	4.5
CIPW %							
Q	34	36	36	39	23	24	24
or	15	13	16	11	11	11	11
ab	36	36	35	37	36	37	37
an	10	10	9	10	18	15	17
C	1	1	1	1		1	
di							
hy	3	3	3	3	9	9	8
il					1	1	1
ap							

APPENDIX B(III-a)

XRF analyses for the granitoids from the Vumba granite-greenstone terrain.

Unit	G1	G1	G1	G1	G2	G2	G2
Pluton	Shashe Drift	Kalakamati	Kalakamati	Kalakamati	Maebe	Maebe	Maebe
Sample no	**ZB-98-93**	**ZB-98-20**	**ZB-98-96**	**ZB-98-97**	**ZB-98-135**	**ZB-98-138**	**ZB-98-136**
wt %							
SiO_2	68.31	69.13	69.91	69.60	65.19	65.36	65.89
TiO_2	0.49	0.39	0.34	0.36	0.58	0.62	0.51
Al_2O_3	15.60	15.72	15.53	15.37	16.58	16.36	16.81
FeO_{total}	3.55	2.74	2.46	2.53	4.54	4.59	4.51
MnO	0.04	0.03	0.02	0.03	0.06	0.06	0.05
MgO	1.23	0.76	0.68	0.70	1.47	1.50	1.30
CaO	3.62	2.44	2.35	2.27	4.64	4.53	4.31
Na_2O	4.35	4.12	3.77	4.02	4.56	4.43	4.65
K_2O	1.96	3.54	4.09	3.89	1.33	1.39	1.44
P_2O_5	0.14	0.10	0.10	0.10	0.17	0.16	0.16
L.O.I.	0.84	0.88	0.96	0.95	0.80	0.65	0.65
TOTAL (on L.O.I. Free)	99.29	98.97	99.26	98.86	99.12	99.00	99.63
(ppm)							
Sc	2.1	1.1	2.9	2.1	6.6	3.8	3.5
V	55	33	31	40	60	72	63
Cr	19.4	12.5	14.7	21.7	21.9	17.5	10.7
Co	8.6	2.5	2.8	4.4	6.2	7.5	9.0
Ni	8.9	11.2	8.3	10.3	12.2	12.2	11.4
Cu	7.9	2.1	1.6	1.1	7.3	8.1	17.6
Zn	62.0	55.4	48.7	61.4	52.0	64.4	64.1
Ga	21.1	19.6	21.5	19.4	20.8	21.6	19.5
Rb	61.1	110.5	99.1	112.5	65.8	41.5	45.5
Sr	403.0	300.7	322.9	275.2	390.8	387.5	387.6
Y	6.4	9.9	5.1	9.6	17.7	13.7	10.6
Zr	136.3	209.5	197.4	189.1	128.5	150.4	151.0
Nb	2.7	6.8	5.4	6.7	4.0	2.2	3.0
Ba	430	1142	1379	1184	387	392	427
La	33.4	70.4	64.7	76.6	14.5	11.7	8.2
Ce	59.0	128.7	111.6	132.2	43.3	29.0	23.6
Nd	18.9	39.8	30.6	42.6	16.4	14.5	9.6
Pb	18.5	29.4	27.8	31.6	19.5	9.9	11.3
Th	25.3	49.5	43.8	45.9	17.1	7.6	7.2
U	2.8	6.8	3.1	5.1	1.1	1.1	0.6
CIPW (%)							
Q	24	24	25	24	19	20	19
or	12	21	24	23	8	8	9
ab	37	35	32	34	39	37	39
an	17	12	12	11	21	21	21
C		1	1	1			
di					1	1	
hy	8	6	5	5	10	10	10
il	1	1	1	1	1	1	1
ap							

APPENDIX B(III-a)

XRF analyses for the granitoids from the Vumba granite-greenstone terrain.

Unit	G2	G2	G2	G2	G2	G2	G2
Pluton	Maebe	Maebe	Maebe	Maebe	Maebe	Maebe	Maebe
Sample no	**ZB-98-132**	**ZB-98-131**	**ZB-98-137**	**ZB-98-145**	**ZB-98-134**	**ZB-98-144**	**ZB-98-147**
wt %							
SiO_2	67.05	67.33	67.34	67.61	67.94	68.61	68.91
TiO_2	0.56	0.58	0.53	0.37	0.49	0.38	0.50
Al_2O_3	16.03	15.66	15.48	15.84	15.37	16.08	15.55
FeO_{total}	4.22	4.25	4.26	4.38	4.00	3.86	3.56
MnO	0.05	0.05	0.06	0.06	0.06	0.05	0.03
MgO	1.41	1.36	1.24	1.11	1.16	1.02	1.03
CaO	4.11	4.17	3.85	3.83	3.75	3.86	3.39
Na_2O	4.22	4.24	4.16	4.10	4.18	4.23	4.59
K_2O	1.59	1.39	2.08	1.93	2.06	1.70	1.59
P_2O_5	0.15	0.15	0.12	0.16	0.13	0.14	0.10
L.O.I.	1.15	1.26	0.70	0.71	0.74	0.76	0.64
TOTAL (on L.O.I. Free)	99.38	99.17	99.13	99.38	99.13	99.92	99.25
(ppm)							
Sc	4.4	8.5	4.1	5.9	0.9	6.0	3.4
V	67	72	65	42	75	44	58
Cr	16.4	18.3	17.0	21.5	15.3	13.7	15.8
Co	8.4	7.1	8.4	4.8	7.7	4.9	3.4
Ni	13.6	13.6	12	8.3	15	7.7	9.1
Cu	11.6	16.3	8.9	4.5	31.8	6.1	6.2
Zn	58.0	48.1	68.2	70.6	70.4	59.8	56.7
Ga	25.6	21.6	22.9	15.7	23.1	17.8	22.7
Rb	43.2	39.6	70.7	67.5	40.3	66.6	69.1
Sr	415.2	406.4	198.5	207.4	211.4	201.9	375.1
Y	6.8	7.3	16.7	12.7	12.6	11.7	10.7
Zr	140.3	147.3	134.9	230.7	145.8	223.7	153.1
Nb	4.4	3.2	7.2	6.5	1.6	6.3	4.0
Ba	446	398	285	588	322	490	466
La	20.0	20.3	14.9	46.5	8.7	62.0	3.5
Ce	46.8	50.6	34.6	92.2	28.0	105.7	10.7
Nd	18.1	16.6	16.9	29.5	13.0	29.7	6.4
Pb	12.3	15.0	16.1	19.1	14.9	16.8	12.3
Th	11.6	10.6	15.5	14.0	2.5	28.1	7.9
U	1.5	1.8	1.3	2.1	1.2	1.8	2.3
CIPW (%)							
Q	23	24	23	24	24	25	25
or	9	8	12	11	12	10	9
ab	36	36	35	35	35	36	39
an	20	20	17	18	17	18	16
C						1	
di			1		1		
hy	10	9	9	10	8	8	8
il	1	1	1	1	1	1	1
ap							

APPENDIX B(III-a)

XRF analyses for the granitoids from the Vumba granite-greenstone terrain.

Unit	G2	G2	G2	G2	G2	G2	G2
Pluton	Maebe	Maebe	Maebe	Maebe	Maebe	Maebe	Maebe
Sample no	**ZB-98-139**	**ZB-98-146**	**ZB-98-133**	**ZB-98-142**	**ZB-98-140**	**ZB-98-149**	**ZB-98-141**
wt %							
SiO_2	69.76	70.10	70.15	70.43	70.52	70.75	72.26
TiO_2	0.32	0.45	0.38	0.30	0.42	0.32	0.34
Al_2O_3	16.20	15.14	15.13	15.47	14.93	15.04	15.15
FeO_{total}	2.41	3.06	3.06	2.70	3.54	2.93	2.32
MnO	0.02	0.03	0.03	0.03	0.03	0.03	0.03
MgO	0.72	0.94	0.95	0.73	0.86	0.72	0.65
CaO	3.50	3.26	3.24	3.27	3.33	3.42	3.10
Na_2O	4.73	4.39	4.39	4.52	4.48	4.33	4.68
K_2O	1.64	1.51	1.85	1.67	1.36	1.43	1.39
P_2O_5	0.09	0.08	0.11	0.10	0.10	0.09	0.09
L.O.I.	0.59	0.57	0.43	0.81	0.97	0.61	0.79
TOTAL (on L.O.I. Free)	99.40	98.97	99.29	99.21	99.57	99.06	100.00
(ppm)							
Sc	0.7	2.8	6.1	3.1	2.9	1.3	1.7
V	36	46	51	28	53	28	40
Cr	7.5	21.0	16.2	15.1	13.9	10.6	13.5
Co	3.1	4.0	3.4	3.3	2.7	4.1	4.5
Ni	9.8	12.5	12.3	6.5	8	5.5	3.5
Cu	6.2	3.6	2.2	2.1	2.6	2.3	1.9
Zn	45.8	48.7	45.9	43.7	50.9	56.2	35.4
Ga	20.7	22.6	18.7	20.8	20.4	15.8	23.7
Rb	50.0	60.8	54.7	65.1	37.4	59.7	37.3
Sr	354.2	385.0	396.7	207.7	241.1	220.2	423.1
Y	6.3	6.1	7.3	6.6	9.4	3.3	3.5
Zr	124.7	129.1	115.5	122.1	121.3	176.4	117.6
Nb	4.3	7.3	3.5	5.3	2.6	7.3	3.1
Ba	451	409	489	373	481	363	425
La	31.4	12.8	10.8	25.6	31.3	35.6	6.3
Ce	64.6	44.2	31.7	40.2	56.8	54.4	16.1
Nd	17.1	16.2	12.3	12.3	16.0	17.5	7.6
Pb	15.8	14.1	22.3	19.6	19.4	21.7	14.8
Th	16.0	13.1	11.8	19.3	17.4	27.5	20.1
U	2.9	1.9	2.5	1.8	5.6	2.1	2.3
CIPW (%)							
Q	26	29	27	28	29	30	31
or	10	9	11	10	8	8	8
ab	40	37	37	38	38	37	40
an	17	16	16	16	16	17	15
C							
di							
hy	5	7	7	6	7	6	5
il	1	1	1	1	1	1	1
ap							

APPENDIX B(III-a)

XRF analyses for the granitoids from the Vumba granite-greenstone terrain.

Unit	G2	G2
Pluton	Maebe	Maebe
Sample no	**ZB-98-148**	**ZB-98-143**
wt %		
SiO_2	72.68	72.95
TiO_2	0.22	0.29
Al_2O_3	14.66	14.75
FeO_{total}	2.08	2.24
MnO	0.02	0.02
MgO	0.49	0.60
CaO	3.17	2.90
Na_2O	4.32	4.24
K_2O	1.23	1.47
P_2O_5	0.07	0.08
L.O.I	0.68	0.67
TOTAL (on L.O.I. Free)	98.95	99.54
(ppm)		
Sc	0.4	2.0
V	15	23
Cr	6.1	13.8
Co	2.9	3.5
Ni	7.6	3.4
Cu	4.1	2.7
Zn	36.7	33.8
Ga	23.1	18.7
Rb	48.8	51.4
Sr	177.7	184.0
Y	4.6	4.2
Zr	120.5	158.5
Nb	5.5	5.9
Ba	419	569
La	19.4	31.9
Ce	41.4	52.1
Nd	15.7	16.3
Pb	16.7	17.1
Th	20.9	30.4
U	4.5	2.9
CIPW (%)		
Q	34	34
or	7	9
ab	37	36
an	15	14
C	1	1
di		
hy	4	5
il		1
ap		

APPENDIX B(III-b)

ICP-MS whole-rock data set for the granitoids

APPENDIX B(III-b)

XRF and ICP-MS whole-rock results of the granitoid samples from the Vumba granite-greenstone terrain

Unit	G5	G5	G5	G5	G5	G5	G5
Pluton	Domboshaba	Domboshaba	Domboshaba	Domboshaba	Domboshaba	Domboshaba	Vumba stock
Sample no	**ZB-98-71**	**ZB-98-70**	**ZB-98-69**	**ZB-98-74**	**ZB-98-76**	**ZB-98-75**	**ZB-98-78**
wt %							
SiO_2	63.09	69.36	70.78	72.69	73.12	73.54	66.45
TiO_2	0.52	0.48	0.47	0.23	0.16	0.19	0.51
Al_2O_3	18.60	15.14	14.66	14.55	14.28	15.09	16.15
FeO_{total}	2.50	2.65	2.11	1.57	1.28	1.50	3.69
MnO	0.04	0.04	0.04	0.03	0.02	0.02	0.05
MgO	0.51	0.52	0.38	0.30	0.23	0.27	1.48
CaO	1.66	1.37	1.18	1.45	1.41	1.58	3.74
Na_2O	4.48	3.75	3.44	3.76	3.62	3.92	3.98
K_2O	7.50	5.57	6.18	4.44	4.54	4.28	2.82
P_2O_5	0.07	0.07	0.05	0.04	0.05	0.05	0.20
L.O.I.	1.13	0.66	0.53	0.56	0.50	0.67	1.20
TOTAL (on L.O.I. Free)	98.97	98.94	99.28	99.06	98.71	100.45	99.07
(ppm)							
Sc	31.7	34.8	30.8	35.4	34.2	34.6	32.0
V	8.9	10.7	6.6	9.2	8.9	6.9	45.1
Cr	9.2	19.9	23.6	14.1	14.3	28.8	31.1
Co	1.5	2.6	1.5	2.2	1.6	1.8	10.4
Cu	21.4	22.4	24.5	6.3	5.1	7.8	38.9
Zn	136.2	136.6	70.3	126.7	76.6	80.5	167.7
Ga	20.0	16.6	14.9	18.6	17.0	18.7	20.2
Rb	172.3	142.7	151.3	138.6	152.2	127.6	69.9
Sr	313	207	187	216	234	206	673
Y	17.3	18.5	27.8	4.5	4.5	4.5	11.2
Zr	555.4	466.5	403.8	134.6	104.5	161.7	196.0
Nb	11.6	10.2	6.8	5.3	4.4	4.4	6.4
Cs	1.1	1.6	1.3	1.2	1.5	1.2	1.3
Ba	1913	1214	1299	1029	1310	1080	1208
La	60.70	54.17	42.54	14.21	5.90	16.41	23.69
Ce	307.92	280.77	237.20	55.02	35.22	79.05	125.96
Pr	33.63	31.13	28.31	6.66	3.82	8.21	14.64
Nd	111.92	106.85	106.35	21.79	13.06	27.49	51.99
Sm	13.34	15.13	18.27	2.96	1.97	3.85	7.31
Eu	3.42	3.04	3.44	0.94	0.98	0.93	1.92
Gd	8.67	9.99	13.91	2.29	1.45	2.70	4.81
Tb	0.83	0.99	1.58	0.21	0.17	0.25	0.52
Dy	3.67	4.41	7.20	0.99	0.82	1.02	2.34
Ho	0.58	0.69	1.12	0.15	0.14	0.15	0.36
Er	1.62	1.73	2.68	0.39	0.35	0.39	0.94
Tm	0.25	0.23	0.31	0.05	0.05	0.05	0.13
Yb	1.81	1.70	2.05	0.35	0.36	0.37	0.84
Lu	0.31	0.30	0.32	0.06	0.07	0.06	0.12
Hf	13.01	10.82	9.70	3.88	3.52	4.87	4.87
Ta	0.95	0.65	0.86	0.23	0.28	0.09	0.53
Pb	44.91	44.75	46.45	39.69	36.73	45.55	29.43
Th	69.76	103.94	106.39	27.44	15.38	41.83	20.36
U	4.33	10.17	9.36	7.98	6.60	9.07	3.74

APPENDIX B(III-b)

XRF and ICP-MS whole-rock results of the granitoid samples from the Vumba granite-greenstone terrain

Unit	G5	G5	G1	G1	G1	G1	G1
Pluton	Sechele	Sechele	Monzonite	Monzonite	Monzonite	Monzonite	Mashawe
Sample no	**ZB-98-79**	**ZB-98-80**	**ZB-98-83**	**ZB-98-84**	**ZB-98-82**	**ZB-98-87**	**ZB-98-95**
wt %							
SiO_2	71.19	71.45	59.78	59.82	60.39	66.33	74.06
TiO_2	0.25	0.25	0.88	0.84	0.88	0.69	0.13
Al_2O_3	15.47	15.67	16.10	16.04	16.09	15.36	14.70
FeO_{total}	1.91	1.93	6.23	6.17	6.18	4.41	1.15
MnO	0.03	0.03	0.09	0.08	0.09	0.05	0.03
MgO	0.54	0.57	3.34	3.33	3.30	2.06	0.19
CaO	2.72	2.71	4.93	4.93	4.92	3.45	1.71
Na_2O	4.50	4.54	3.38	3.45	3.44	3.42	4.45
K_2O	2.62	2.76	4.11	3.97	4.10	4.81	3.43
P_2O_5	0.09	0.09	0.33	0.35	0.35	0.23	0.03
L.O.I	0.68	0.71	0.70	0.63	0.70	0.61	0.64
TOTAL (on L.O.I. Free)	99.33	100.00	99.16	98.98	99.74	100.81	99.87
(ppm)							
Sc	31.8	32.4	30.2	29.1	30.9	29.3	32.9
V	13.9	14.7	101.8	98.1	104.8	63.3	4.7
Cr	18.9	19.2	68.7	66.8	74.4	47.4	20.6
Co	3.1	3.3	20.0	19.2	20.9	11.7	1.4
Cu	14.2	21.7	95.9	86.7	210.0	67.0	51.5
Zn	123.2	207.8	401.1	425.3	459.5	212.3	532.1
Ga	18.6	18.5	19.2	19.6	20.4	18.1	20.5
Rb	72.5	74.5	179.8	174.2	191.4	205.5	127.4
Sr	460	459	535	523	548	383	229
Y	9.5	9.0	24.0	23.4	27.4	25.0	5.8
Zr	143.4	143.8	417.5	351.5	388.2	401.9	74.5
Nb	6.5	7.0	15.0	14.1	16.3	17.1	7.5
Cs	2.5	2.4	6.6	6.8	7.0	2.8	2.3
Ba	1133	1209	975	938	972	1000	893
La	10.05	9.82	31.48	23.54	26.67	29.22	4.30
Ce	59.47	58.22	152.27	138.65	150.31	171.37	24.92
Pr	7.08	6.83	19.65	16.68	18.83	20.37	2.73
Nd	26.48	25.85	74.57	64.40	72.93	74.66	9.49
Sm	4.45	4.26	12.01	11.33	12.93	12.31	1.76
Eu	1.25	1.26	2.40	2.26	2.59	1.91	0.64
Gd	3.42	3.30	9.29	8.37	9.51	8.85	1.39
Tb	0.41	0.37	1.06	1.01	1.14	1.08	0.17
Dy	1.80	1.74	5.02	4.69	5.26	5.01	1.01
Ho	0.29	0.30	0.83	0.80	0.91	0.85	0.18
Er	0.76	0.70	2.08	1.99	2.31	2.15	0.47
Tm	0.11	0.10	0.29	0.27	0.33	0.30	0.08
Yb	0.68	0.61	1.87	1.84	2.03	1.98	0.51
Lu	0.10	0.10	0.30	0.28	0.32	0.29	0.09
Hf	3.76	3.75	10.13	8.32	9.35	10.51	2.49
Ta	0.50	0.48	1.07	0.99	1.15	1.62	1.02
Pb	21.56	22.06	36.70	37.16	40.95	42.06	38.69
Th	11.68	11.53	32.91	32.50	33.05	79.76	15.03
U	1.58	1.53	7.71	10.48	13.62	9.94	4.79

APPENDIX B(III-b)

XRF and ICP-MS whole-rock results of the granitoid samples from the Vumba granite-greenstone terrain

Unit	G1	G1	G1	G1	G1	G1	G1
Pluton	Mashawe	Mashawe	Mashawe	Shashe Drift	Shashe Drift	Shashe Drift	Kalakamati
Sample no	**ZB-98-91**	**ZB-98-90**	**ZB-98-89**	**ZB-98-09**	**ZB-98-10**	**ZB-98-93**	**ZB-98-20**
wt %							
SiO_2	74.15	75.03	75.67	67.26	67.92	68.31	69.13
TiO_2	0.14	0.14	0.15	0.54	0.47	0.49	0.39
Al_2O_3	14.25	13.73	14.02	15.91	15.83	15.60	15.72
FeO_{total}	1.66	1.64	1.59	4.02	3.49	3.55	2.74
MnO	0.03	0.03	0.04	0.05	0.04	0.04	0.03
MgO	0.18	0.21	0.23	1.38	1.17	1.23	0.76
CaO	1.94	1.98	1.92	3.74	3.60	3.62	2.44
Na_2O	4.26	4.24	4.19	4.22	4.41	4.35	4.12
K_2O	2.51	2.17	2.63	1.86	1.89	1.96	3.54
P_2O_5	0.03	0.03	0.04	0.14	0.14	0.14	0.10
L.O.I.	0.64	0.63	0.53	1.28	0.86	0.84	0.88
TOTAL (on L.O.I. Free)	99.15	99.21	100.47	99.12	98.96	99.29	98.97
(ppm)							
Sc	33.0	33.0	33.5	30.6	29.8	32.4	31.3
V	4.1	4.5	5.3	52.7	45.2	51.7	25.8
Cr	14.3	19.9	21.4	27.8	16.7	35.3	13.2
Co	1.3	1.6	1.3	10.2	8.3	9.1	5.5
Cu	40.5	62.4	36.1	36.4	19.4	57.2	13.9
Zn	439.6	428.7	355.1	373.4	151.4	588.1	165.5
Ga	16.3	14.8	15.2	19.3	18.1	19.3	21.2
Rb	84.6	74.0	83.3	58.9	61.3	68.5	111.2
Sr	136	135	139	405	390	412	297
Y	11.0	11.3	8.0	7.8	7.0	7.6	9.6
Zr	90.6	94.6	99.0	164.6	163.2	162.9	224.0
Nb	7.3	6.8	6.5	4.0	3.6	4.0	9.2
Cs	1.7	1.9	2.4	0.8	1.4	1.6	1.0
Ba	592	412	635	473	404	420	1132
La	7.01	6.89	8.69	12.49	14.19	11.43	23.43
Ce	39.95	38.89	46.13	65.34	74.73	61.48	113.61
Pr	4.42	4.25	4.84	7.22	7.87	6.66	11.89
Nd	15.51	14.89	16.26	24.08	26.37	23.51	39.95
Sm	2.89	3.00	2.44	3.22	3.26	3.16	6.22
Eu	0.69	0.64	0.72	0.92	0.89	0.89	1.22
Gd	2.63	2.68	2.01	2.27	2.43	2.48	4.72
Tb	0.36	0.36	0.27	0.30	0.27	0.27	0.51
Dy	1.74	1.86	1.33	1.48	1.33	1.42	2.33
Ho	0.33	0.36	0.26	0.26	0.24	0.24	0.33
Er	0.95	0.99	0.67	0.76	0.67	0.71	0.82
Tm	0.16	0.16	0.11	0.11	0.11	0.10	0.10
Yb	1.02	1.04	0.80	0.71	0.71	0.69	0.64
Lu	0.18	0.18	0.13	0.13	0.12	0.12	0.09
Hf	2.97	3.05	2.96	4.11	4.22	4.11	5.64
Ta	1.12	1.08	0.90	0.37	0.36	0.39	0.93
Pb	24.77	22.25	21.43	13.08	13.10	17.66	27.74
Th	16.29	16.44	12.45	13.33	14.04	13.07	39.99
U	4.09	2.49	2.15	2.93	2.86	3.14	5.29

APPENDIX B(III-b)

XRF and ICP-MS whole-rock results of the granitoid samples from the Vumba granite-greenstone terrain

Unit	G1	G1	G2	G2	G2	G2	G2
Pluton	Kalakamati	Kalakamati	Maebe	Maebe	Maebe	Maebe	Maebe
Sample no	**ZB-98-97**	**ZB-98-96**	**ZB-98-136**	**ZB-98-131**	**ZB-98-144**	**ZB-98-147**	**ZB-98-139**
wt %							
SiO_2	69.60	69.91	65.89	67.33	68.61	68.91	69.76
TiO_2	0.36	0.34	0.51	0.58	0.38	0.50	0.32
Al_2O_3	15.37	15.53	16.81	15.66	16.08	15.55	16.20
FeO_{total}	2.53	2.46	4.51	4.25	3.86	3.56	2.41
MnO	0.03	0.02	0.05	0.05	0.05	0.03	0.02
MgO	0.70	0.68	1.30	1.36	1.02	1.03	0.72
CaO	2.27	2.35	4.31	4.17	3.86	3.39	3.50
Na_2O	4.02	3.77	4.65	4.24	4.23	4.59	4.73
K_2O	3.89	4.09	1.44	1.39	1.70	1.59	1.64
P_2O_5	0.10	0.10	0.16	0.15	0.14	0.10	0.09
L.O.I.	0.95	0.96	0.65	1.26	0.76	0.64	0.59
TOTAL (on L.O.I. Free)	98.86	99.26	99.63	99.17	99.92	99.25	99.40
(ppm)							
Sc	31.3	28.8	30.9	30.3	32.2	29.7	31.0
V	24.5	22.4	54.6	58.1	34.9	45.7	28.5
Cr	19.4	18.0	15.8	33.3	21.2	23.0	17.9
Co	4.7	4.3	9.1	9.4	7.3	7.8	4.7
Cu	38.4	49.7	57.2	86.1	39.6	45.3	43.3
Zn	437.4	395.3	403.9	471.4	355.3	182.8	360.4
Ga	19.7	16.8	19.5	17.7	18.6	17.8	18.1
Rb	114.7	95.5	44.1	37.8	69.4	68.8	49.8
Sr	274	302	387	367	195	349	349
Y	9.7	5.1	9.8	9.7	9.4	8.4	4.8
Zr	211.5	202.2	185.3	161.2	295.1	159.9	145.0
Nb	8.8	2.8	3.3	4.4	7.1	5.7	4.5
Cs	0.9	0.8	1.2	0.6	1.0	1.3	1.2
Ba	1229	1420	424	393	499	470	438
La	21.07	20.71	4.17	9.55	23.06	1.50	13.40
Ce	102.76	98.04	29.02	53.56	106.96	13.06	63.10
Pr	10.75	9.93	3.59	5.90	10.45	1.70	6.17
Nd	36.33	32.37	14.71	21.46	33.65	7.58	19.61
Sm	5.76	4.23	2.83	3.13	4.79	2.08	2.42
Eu	1.26	1.13	0.97	0.97	1.05	0.70	0.88
Gd	4.23	2.81	2.51	2.81	3.38	2.23	1.61
Tb	0.48	0.29	0.34	0.35	0.38	0.31	0.18
Dy	2.32	1.25	1.88	1.83	1.92	1.78	0.84
Ho	0.34	0.21	0.34	0.36	0.31	0.30	0.16
Er	0.84	0.49	0.87	0.93	0.83	0.79	0.43
Tm	0.11	0.07	0.13	0.14	0.12	0.11	0.06
Yb	0.66	0.46	0.89	0.91	0.82	0.68	0.44
Lu	0.11	0.08	0.13	0.14	0.13	0.11	0.07
Hf	5.47	5.63	4.46	4.11	7.09	4.33	3.56
Ta	0.92	0.38	0.24	0.40	0.50	0.41	0.32
Pb	30.09	29.24	11.26	12.38	13.54	10.59	14.95
Th	38.40	36.13	2.57	8.00	19.47	1.94	10.36
U	5.22	2.92	0.77	1.08	0.84	0.77	1.77

APPENDIX B(III-b)

XRF and ICP-MS whole-rock results of the granitoid samples from the Vumba granite-greenstone terrain

Unit	G2	G2
Pluton	Maebe	Maebe
Sample no	**ZB-98-133**	**ZB-98-141**
wt %		
SiO_2	70.15	72.26
TiO_2	0.38	0.34
Al_2O_3	15.13	15.15
FeO_{total}	3.06	2.32
MnO	0.03	0.03
MgO	0.95	0.65
CaO	3.24	3.10
Na_2O	4.39	4.68
K_2O	1.85	1.39
P_2O_5	0.11	0.09
L.O.I	0.43	0.79
TOTAL (on L.O.I. Free)	99.29	100.00
(ppm)		
Sc	31.7	29.3
V	43.8	30.3
Cr	27.2	22.8
Co	6.6	5.0
Cu	38.6	39.9
Zn	384.6	263.8
Ga	17.2	16.1
Rb	54.4	34.9
Sr	371	384
Y	8.2	4.2
Zr	122.8	118.9
Nb	3.8	3.1
Cs	1.7	0.6
Ba	458	427
La	5.26	4.09
Ce	31.26	26.33
Pr	3.54	2.90
Nd	12.69	10.02
Sm	2.10	1.56
Eu	0.79	0.94
Gd	1.85	1.23
Tb	0.27	0.14
Dy	1.45	0.70
Ho	0.26	0.14
Er	0.68	0.39
Tm	0.10	0.08
Yb	0.67	0.42
Lu	0.12	0.08
Hf	3.32	3.17
Ta	0.47	0.30
Pb	15.24	12.35
Th	7.43	5.07
U	2.63	1.49

APPENDIX B(IV-a)

XRF whole-rock major and trace element data set for the amphibolites

APPENDIX B(IV-a)

XRF analyses of the amphibolites from the Vumba granite-greenstone terrain.

Rock unit	VUMF	VUMF	VUMF	VUMF	VLMF	VLMF	VLMF
Sample no	ZB-98-182	ZB-98-180	ZB-98-181	ZB-98-179	ZB-98-188	ZB-98-183	ZB-98-187
wt %							
SiO_2	49.55	50.67	52.72	53.14	47.45	48.95	48.99
TiO_2	0.83	1.51	0.63	0.82	1.18	1.00	1.34
Al_2O_3	14.84	14.14	15.57	14.87	16.96	15.67	16.29
FeO_{total}	12.01	15.36	9.34	10.39	13.24	12.91	12.78
MnO	0.19	0.23	0.16	0.16	0.18	0.16	0.20
MgO	7.35	5.45	7.72	6.62	8.01	7.08	8.40
CaO	12.06	9.93	10.89	9.85	10.70	11.28	9.48
Na_2O	2.23	2.37	2.23	2.37	2.40	1.97	2.79
K_2O	0.68	0.55	0.82	0.78	0.10	0.18	0.15
P_2O_5	0.07	0.15	0.06	0.09	0.11	0.08	0.12
L.O.I.	0.75	0.48	0.89	0.90	0.77	2.11	0.63
TOTAL (L.O.I. Free)	99.81	100.36	100.14	99.08	100.32	99.28	100.54
(ppm)							
Sc	54.9	43.1	40.7	29.3	46.1	38.6	39.2
V	258.0	247.3	235.7	253.5	273.1	252.3	279.3
Cr	347.7	98.3	304.2	203.9	303.1	321.7	268.8
Co	50.0	39.2	37.8	36.6	56.3	54.2	49.1
Ni	165.8	63.7	80.5	64.4	146.4	144.9	146.5
Cu	61.0	38.8	37.4	72.5	57.7	71.2	130.9
Zn	84.7	150.6	69.4	77.7	93.2	92.4	106.1
Ga	14.2	17.0	16.0	15.4	14.2	14.5	14.9
Rb	36.6	25.0	38.2	34.2	4.6	6.2	8.5
Sr	142.1	130.8	128.1	132.6	110.6	136.8	148.2
Y	17.7	28.9	13.2	17.4	21.3	19.0	32.2
Zr	47.1	92.9	49.4	71.4	70.3	63.4	87.2
Nb	1.5	4.5	2.8	2.4	4.0	1.7	4.9
Ba	99.5	66.0	160.1	224.5	30.7	25.0	33.4
La	0.9	6.8	5.3	6.8	2.4	2.0	3.4
Ce	1.2	15.4	19.5	18.9	12.2	4.2	4.9
Nd	0.9	2.4	4.7	12.5	3.9	2.1	2.5
Pb	5.4	2.5	6.6	15.4	15.9	2.4	1.7
Th	1.0	2.3	3.1	3.8	1.1	0.7	1.8
U	0.6	1.1	1.4	0.8	0.7	0.1	0.2
cipw (wt.%)							
Q	0	0	0.34	2.74	0	0	0
or	4.03	3.28	4.84	4.61	0.56	1.05	0.89
ab	18.87	20.05	18.87	20.05	20.31	16.67	23.61
an	28.48	26.32	30.07	27.65	35.23	33.40	31.49
di	25.64	18.57	19.38	17.16	14.25	18.37	12.26
hy	7.08	27.11	24.39	24.12	6.63	20.64	11.74
ol	12.81	0.29	0	0	19.54	5.78	16.48
il	1.57	2.87	1.19	1.55	2.25	1.90	2.54
ap	0.17	0.36	0.15	0.21	0.25	0.19	0.27

APPENDIX B(IV-a)

XRF analyses of the amphibolites from the Vumba granite-greenstone terrain.

Rock unit	VLMF	VLMF	VLMF	VMVF	VMVF	VMVF	VMVF
Sample no	ZB-98-184	ZB-98-186	ZB-98-185	ZB-98-217	ZB-98-199	ZB-98-203	ZB-98-198
wt %							
SiO_2	49.20	49.33	49.51	49.62	49.91	49.98	50.06
TiO_2	1.02	1.01	1.02	1.47	0.28	1.04	0.28
Al_2O_3	16.04	16.05	15.85	13.38	19.03	15.70	19.29
FeO_{total}	12.77	12.63	12.88	16.29	5.43	12.54	5.42
MnO	0.18	0.18	0.18	0.23	0.10	0.21	0.10
MgO	6.53	6.71	7.30	6.31	8.19	6.02	8.30
CaO	12.36	12.50	11.22	10.36	14.01	12.02	13.85
Na_2O	1.99	1.75	2.09	2.02	1.50	2.37	1.55
K_2O	0.10	0.18	0.09	0.17	0.51	0.31	0.55
P_2O_5	0.08	0.07	0.07	0.11	0.02	0.11	0.02
L.O.I.	1.02	2.41	1.82	0.71	1.69	0.87	1.70
TOTAL (L.O.I. Free)	100.28	100.42	100.21	99.96	98.98	100.30	99.43
(ppm)							
Sc	46.2	38.7	37.1	53.0	35.8	41.3	38.6
V	253.9	270.8	252.6	303.7	175.7	240.9	175.1
Cr	323.6	317.5	314.2	50.4	301.2	52.9	306.0
Co	49.3	54.4	49.7	54.6	31.1	49.8	33.8
Ni	154.8	144.0	148.2	46.4	211.9	66.8	216.8
Cu	90.0	132.0	63.7	243.7	61.4	10.2	34.4
Zn	86.4	97.2	82.1	125.2	49.1	110.6	42.6
Ga	14.0	14.8	13.5	13.9	16.1	15.9	15.4
Rb	0.7	8.3	3.8	3.7	30.4	11.9	33.8
Sr	200.3	138.7	137.5	128.0	142.6	162.8	139.5
Y	20.6	18.8	19.9	30.3	5.2	23.6	7.9
Zr	62.8	60.3	54.1	71.3	24.0	92.1	23.8
Nb	3.9	3.1	0.7	3.2	1.9	3.4	1.0
Ba	22.5	28.2	20.9	31.1	79.7	122.9	55.3
La	2.4	1.5	6.5	4.0	0.7	9.7	2.3
Ce	4.5	4.5	10.5	7.2	1.8	17.9	10.4
Nd	2.4	1.5	2.9	3.0	0.7	9.1	2.3
Pb	4.6	8.0	6.0	10.2	8.8	7.9	4.1
Th	0.9	1.2	0.0	0.1	2.6	2.0	2.1
U	0.6	0.5	0.1	0.1	1.1	0.8	0.9
cipw (wt.%)							
Q	0	0	0	0	0	0	0
or	0.61	1.08	0.53	1.01	3.05	1.85	3.26
ab	16.84	14.81	17.68	17.09	12.69	20.05	13.11
an	34.54	35.41	33.61	26.95	43.68	31.29	44.06
di	21.92	21.78	17.95	20.01	20.78	23.15	19.80
hy	17.00	20.03	21.01	29.26	14.06	13.86	13.58
ol	5.99	3.97	6.03	1.01	3.64	6.66	4.51
il	1.94	1.92	1.94	2.80	0.53	1.97	0.53
ap	0.20	0.18	0.18	0.25	0.05	0.26	0.05

APPENDIX B(IV-a)

XRF analyses of the amphibolites from the Vumba granite-greenstone terrain.

Rock unit	VMVF	VMVF	VMVF	VMVF	VMVF	VMVF	VMVF
Sample no	ZB-98-204	ZB-98-197	ZB-98-210	ZB-98-209	ZB-98-212	ZB-98-211	ZB-98-202
wt %							
SiO_2	50.06	50.09	50.47	50.55	51.17	51.42	52.35
TiO_2	1.34	0.29	1.03	1.04	0.57	0.58	0.58
Al_2O_3	13.59	18.62	14.68	14.55	14.78	14.74	16.85
FeO_{total}	14.20	5.59	12.19	12.97	9.52	9.51	7.92
MnO	0.21	0.11	0.21	0.24	0.14	0.14	0.16
MgO	6.27	8.56	6.18	6.25	10.53	10.60	6.21
CaO	11.11	13.81	12.11	11.72	9.58	9.34	13.60
Na_2O	1.96	1.52	2.50	2.31	2.77	2.76	1.50
K_2O	0.26	0.55	0.28	0.33	0.10	0.09	0.13
P_2O_5	0.14	0.03	0.12	0.11	0.08	0.07	0.06
L.O.I.	0.86	1.77	0.84	0.63	0.59	0.64	0.63
TOTAL (L.O.I. Free)	99.14	99.16	99.77	100.06	99.23	99.24	99.36
(ppm)							
Sc	41.1	33.6	39.8	29.8	30.0	33.5	47.5
V	287.3	181.1	234.9	240.2	171.5	195.4	245.6
Cr	85.3	307.8	49.2	55.6	584.2	582.1	309.8
Co	44.6	33.7	48.0	52.1	53.3	52.2	36.8
Ni	54.9	226.8	62.1	58.2	204.5	201.2	75.4
Cu	40.7	49.6	4.3	27.6	50.6	73.3	6.2
Zn	93.7	45.6	91.6	111.9	46.8	63.4	62.4
Ga	15.0	16.8	15.6	15.4	13.3	13.9	16.9
Rb	9.0	33.1	8.1	12.4	1.5	2.4	6.0
Sr	73.4	137.3	172.7	147.9	169.7	177.3	120.5
Y	28.7	5.2	21.5	19.6	17.0	15.1	12.2
Zr	90.2	26.8	92.8	89.3	57.7	62.1	47.7
Nb	3.7	1.5	5.5	6.9	4.0	3.7	1.2
Ba	40.1	88.4	104.2	100.6	34.6	32.5	31.8
La	6.3	1.9	11.3	6.5	2.9	5.7	2.8
Ce	9.7	9.2	26.7	18.9	12.7	12.9	11.9
Nd	9.0	2.4	15.6	11.5	5.0	4.2	4.0
Pb	5.4	1.5	5.0	7.6	9.4	2.5	7.1
Th	0.8	0.2	1.4	1.3	1.6	2.7	3.1
U	0.1	0.6	1.0	1.2	0.9	0.2	1.2
cipw (wt.%)							
Q	0.80	0	0	0	0	0	5.31
or	1.53	3.24	1.67	1.96	0.61	0.52	0.78
ab	16.58	12.86	21.15	19.54	23.44	23.35	12.69
an	27.53	42.38	28.01	28.37	27.60	27.59	38.87
di	22.35	20.99	26.16	24.32	15.85	14.93	23.23
hy	26.06	14.35	14.16	18.94	18.89	21.43	16.46
ol	0	4.21	5.20	3.44	10.63	9.21	0
il	2.55	0.55	1.96	1.97	1.08	1.10	1.09
ap	0.33	0.06	0.28	0.26	0.18	0.17	0.14

APPENDIX B(IV-a)

XRF analyses of the amphibolites from the Vumba granite-greenstone terrain.

Rock unit	VMVF	VMVF	VMVF	VMVF	VMVF	VMVF	VMVF
Sample no	ZB-98-201	ZB-98-208	ZB-98-200	ZB-98-215	ZB-98-213	ZB-98-214	ZB-98-13
wt %							
SiO_2	52.63	52.76	52.79	53.05	53.12	53.18	53.98
TiO_2	0.56	0.58	0.61	0.71	0.81	0.67	0.52
Al_2O_3	16.85	16.90	16.91	9.58	12.07	9.11	16.29
FeO_{total}	7.50	7.73	7.62	10.98	11.14	11.18	7.15
MnO	0.16	0.15	0.16	0.22	0.22	0.21	0.17
MgO	6.06	6.28	6.20	9.90	7.95	10.74	6.54
CaO	14.01	13.18	13.14	13.20	11.66	12.40	14.37
Na_2O	1.49	1.75	1.70	1.56	2.09	1.50	1.41
K_2O	0.11	0.12	0.12	0.07	0.14	0.06	0.07
P_2O_5	0.05	0.06	0.06	0.06	0.07	0.05	0.05
L.O.I.	0.66	0.63	0.58	2.44	2.27	1.59	0.66
TOTAL (L.O.I. Free)	99.42	99.51	99.31	99.32	99.26	99.11	100.55
(ppm)							
Sc	49.0	48.9	41.4	56.1	37.2	48.5	46.6
V	229.5	227.8	252.2	270.4	256.6	230.7	245.4
Cr	304.5	290.4	287.4	916.7	439.3	1282.3	260.5
Co	31.7	35.3	35.8	51.8	47.4	50.9	39.5
Ni	74.9	74.0	87.2	105.5	74.4	107.2	90.5
Cu	1.9	1.8	2.8	98.6	90.3	94.8	25.4
Zn	63.0	26.5	50.8	63.8	78.8	75.1	63.3
Ga	18.2	13.7	16.4	13.6	14.4	10.8	17.7
Rb	2.3	1.9	4.8	1.2	3.2	3.1	3.1
Sr	123.8	126.0	123.3	149.1	117.1	127.4	124.9
Y	13.3	9.8	11.1	13.9	18.4	15.9	11.6
Zr	46.2	45.9	45.7	49.2	58.2	44.9	49.7
Nb	1.2	1.5	2.5	1.6	1.2	5.0	2.0
Ba	35.2	33.5	42.7	25.4	56.9	39.2	25.6
La	1.9	4.1	6.0	4.7	6.2	3.5	3.1
Ce	4.2	15.6	5.9	3.2	17.9	8.4	2.1
Nd	2.3	4.5	3.1	5.3	9.4	2.8	1.4
Pb	1.4	15.3	8.1	7.2	3.7	8.9	7.3
Th	1.2	1.7	1.9	0.8	1.1	1.2	1.8
U	0.8	0.9	1.2	0.6	0.8	1.2	1.2
cipw (wt.%)							
Q	5.80	5.01	5.54	2.92	3.23	3.09	7.12
or	0.63	0.72	0.72	0.40	0.81	0.36	0.39
ab	12.61	14.81	14.38	13.20	17.68	12.69	11.93
an	38.98	37.91	38.16	18.94	23.16	17.95	37.93
di	24.82	22.27	21.91	37.81	28.28	35.34	27.05
hy	14.65	16.79	16.56	23.44	23.29	27.11	14.32
ol	0	0	0	0	0	0	0
il	1.07	1.10	1.16	1.35	1.54	1.28	0.99
ap	0.12	0.14	0.14	0.14	0.15	0.12	0.12

APPENDIX B(IV-a)

XRF analyses of the amphibolites from the Vumba granite-greenstone terrain.

Rock unit	VMVF
Sample no	ZB-98-23
wt %	
SiO_2	55.65
TiO_2	0.57
Al_2O_3	16.04
FeO_{total}	7.01
MnO	0.16
MgO	6.07
CaO	12.90
Na_2O	1.62
K_2O	0.06
P_2O_5	0.05
L.O.I.	1.01
TOTAL (L.O.I. Free)	100.14
(ppm)	
Sc	46.4
V	261.1
Cr	253.9
Co	33.7
Ni	73.3
Cu	14.6
Zn	53.2
Ga	16.2
Rb	2.6
Sr	127.3
Y	14.6
Zr	49.7
Nb	2.0
Ba	33.6
La	5.8
Ce	6.5
Nd	3.6
Pb	5.5
Th	2.7
U	1.2
cipw (wt.%)	
Q	10.35
or	0.37
ab	13.71
an	36.32
di	22.42
hy	15.08
ol	0
il	1.08
ap	0.13

APPENDIX B(IV-b)

ICP-MS whole-rock data set for the amphibolites

APPENDIX B(IV-b)

XRF and ICP-MS whole-rock results of the amphibolites from the Vumba granite-greenstone terrain

Rock unit	VMVF	VMVF	VUMF	VUMF	VUMF	VLMF	VLMF	VLMF
Sample no	ZB-98-13	ZB-98-23	ZB-98-179	ZB-98-180	ZB-98-182	ZB-98-183	ZB-98-185	ZB-98-187
wt %								
SiO_2	53.98	55.65	53.14	50.67	49.55	48.95	49.51	48.99
TiO_2	0.52	0.57	0.82	1.51	0.83	1.00	1.02	1.34
Al_2O_3	16.29	16.04	14.87	14.14	14.84	15.67	15.85	16.29
FeO_{total}	7.15	7.01	10.39	15.36	12.01	12.91	12.88	12.78
MnO	0.17	0.16	0.16	0.23	0.19	0.16	0.18	0.20
MgO	6.54	6.07	6.62	5.45	7.35	7.08	7.30	8.40
CaO	14.37	12.90	9.85	9.93	12.06	11.28	11.22	9.48
Na_2O	1.41	1.62	2.37	2.37	2.23	1.97	2.09	2.79
K_2O	0.07	0.06	0.78	0.55	0.68	0.18	0.09	0.15
P_2O_5	0.05	0.05	0.09	0.15	0.07	0.08	0.07	0.12
L.O.I.	0.66	1.01	0.90	0.48	0.75	2.11	1.82	0.63
TOTAL (L.O.I. Free)	100.55	100.14	99.08	100.36	99.81	99.28	100.21	100.54
(ppm)								
Sc	37.9	38.7	40.8	34.5	36.7	34.5	39.3	35.1
Ti	0.6	0.6	0.9	0.9	1.6	1.1	1.2	1.4
V	212.4	231.7	270.4	266.0	318.0	286.1	303.2	308.9
Cr	260.8	248.3	214.0	321.9	100.5	304.5	332.3	243.7
Co	42.7	35.7	42.7	54.1	49.6	53.3	58.4	52.4
Ni	100.6	83.6	73.4	187.5	70.3	159.1	229.0	161.2
Cu	36.6	3.4	77.0	50.9	31.4	74.9	66.4	125.3
Zn	57.0	29.8	55.7	51.9	69.0	68.4	51.4	56.0
Ga	14.3	14.4	16.2	15.1	19.1	17.2	18.4	18.7
Rb	0.9	1.0	39.9	31.1	21.4	4.3	2.3	5.2
Sr	137.2	133.2	140.7	144.4	128.4	142.3	146.6	139.9
Y	12.7	14.5	22.8	20.6	35.4	23.3	25.2	29.5
Zr	52.3	50.2	86.1	52.3	115.9	70.4	73.8	94.5
Nb	1.9	1.9	3.5	1.8	4.5	2.7	3.0	4.1
Cs	0.1	0.1	0.9	1.3	0.8	0.4	0.3	0.3
Ba	21.8	21.5	228.1	103.4	82.4	13.6	16.4	41.6
Ce	9.69	11.08	16.95	6.72	18.36	8.81	9.34	12.84
Pr	1.29	1.49	2.40	1.20	2.89	1.50	1.69	2.16
Nd	5.60	6.67	10.07	5.95	13.62	7.60	8.72	10.96
Sm	1.53	1.74	2.80	1.94	3.98	2.41	2.78	3.38
Eu	0.58	0.63	0.90	0.75	1.32	0.91	0.96	1.15
Gd	1.85	2.17	3.39	2.77	4.99	3.51	3.64	4.42
Tb	0.31	0.38	0.58	0.49	0.89	0.60	0.67	0.78
Dy	2.09	2.42	3.62	3.14	5.66	3.83	4.11	4.86
Ho	0.45	0.53	0.78	0.72	1.23	0.84	0.91	1.07
Er	1.25	1.46	2.18	1.94	3.46	2.28	2.49	2.85
Tm	0.21	0.25	0.35	0.32	0.57	0.37	0.42	0.49
Yb	1.24	1.47	2.16	2.03	3.49	2.33	2.53	2.88
Lu	0.21	0.24	0.33	0.32	0.58	0.40	0.41	0.48
Hf	1.30	1.31	2.20	1.26	2.79	1.75	1.85	2.38
Ta	0.14	0.13	0.23	0.12	0.29	0.16	0.18	0.26
Pb	2.03	1.04	1.67	0.73	1.04	-0.39	-0.40	0.88
Th	1.82	1.83	2.56	0.37	1.57	0.60	0.52	0.71
U	0.45	0.48	0.65	0.11	0.48	0.09	0.09	0.15

APPENDIX B(IV-b)

XRF and ICP-MS whole-rock results of the amphibolites from the Vumba granite-greenstone terrain

Rock unit	VMVF	VMVF	VMVF	VMVF	VMVF	VMVF	VMVF
Sample no	ZB-98-197	ZB-98-199	ZB-98-200	ZB-98-204	ZB-98-210	ZB-98-213	ZB-98-217
wt %							
SiO_2	50.09	49.91	52.79	50.06	50.47	53.12	49.62
TiO_2	0.29	0.28	0.61	1.34	1.03	0.81	1.47
Al_2O_3	18.62	19.03	16.91	13.59	14.68	12.07	13.38
FeO_{total}	5.59	5.43	7.62	14.20	12.19	11.14	16.29
MnO	0.11	0.10	0.16	0.21	0.21	0.22	0.23
MgO	8.56	8.19	6.20	6.27	6.18	7.95	6.31
CaO	13.81	14.01	13.14	11.11	12.11	11.66	10.36
Na_2O	1.52	1.50	1.70	1.96	2.50	2.09	2.02
K_2O	0.55	0.51	0.12	0.26	0.28	0.14	0.17
P_2O_5	0.03	0.02	0.06	0.14	0.12	0.07	0.11
L.O.I.	1.77	1.69	0.58	0.86	0.84	2.27	0.71
TOTAL (L.O.I. Free)	99.16	98.98	99.31	99.14	99.77	99.26	99.96
(ppm)							
Sc	34.1	30.5	38.9	40.3	39.2	39.8	35.0
Ti	0.3	0.3	0.7	1.5	1.2	0.9	1.4
V	145.2	127.9	234.7	342.5	282.3	269.5	356.0
Cr	301.4	272.2	288.6	127.4	56.7	440.1	32.3
Co	32.5	29.8	41.4	48.7	59.3	52.3	50.7
Ni	263.7	235.9	94.6	59.7	68.1	97.9	35.9
Cu	46.6	54.7	-4.0	43.3	4.1	89.0	246.8
Zn	42.8	21.2	38.8	70.4	79.2	63.6	76.2
Ga	14.2	13.7	15.1	18.0	18.8	14.8	16.9
Rb	29.7	26.6	1.0	6.6	6.9	2.1	1.4
Sr	149.8	147.2	134.8	72.4	188.3	117.6	117.9
Y	7.5	6.3	12.5	32.5	26.4	17.3	28.6
Zr	25.8	20.7	53.4	100.5	112.3	69.2	77.4
Nb	0.7	0.6	2.2	4.6	5.4	3.0	3.8
Cs	1.6	1.4	0.2	0.6	0.5	0.3	0.1
Ba	82.7	66.6	26.7	40.8	106.6	45.4	39.2
Ce	3.62	3.34	10.69	20.12	23.90	12.93	11.21
Pr	0.57	0.51	1.41	2.97	3.41	1.89	1.91
Nd	2.61	2.43	6.15	13.75	14.76	8.72	9.67
Sm	0.88	0.77	1.61	3.94	3.75	2.43	3.15
Eu	0.40	0.36	0.61	1.13	1.20	0.80	1.05
Gd	1.21	1.08	1.88	4.88	4.44	2.92	4.29
Tb	0.19	0.17	0.32	0.86	0.71	0.51	0.79
Dy	1.24	1.12	2.07	5.62	4.42	3.06	5.03
Ho	0.27	0.26	0.47	1.19	0.92	0.63	1.12
Er	0.73	0.66	1.31	3.33	2.48	1.68	3.11
Tm	0.12	0.10	0.21	0.56	0.40	0.27	0.51
Yb	0.68	0.63	1.29	3.46	2.46	1.59	3.11
Lu	0.10	0.10	0.21	0.57	0.40	0.25	0.50
Hf	0.59	0.53	1.43	2.67	2.74	1.78	2.12
Ta	0.04	0.04	0.16	0.28	0.33	0.20	0.17
Pb	3.83	1.81	1.69	0.67	3.37	1.94	-0.37
Th	0.36	0.32	1.92	1.88	1.21	1.97	0.56
U	0.09	0.08	0.54	0.38	0.44	0.47	0.11

APPENDIX B(V-a)

XRF whole-rock major and trace element data set for the ultramafic intrusives (serpentinite & metapyroxenite)

APPENDIX B(V-a)

XRF analyses of the ultramafic intrusives from the Vumba granite-greenstone terrain

Unit: Serpentinite						
Sample no	ZB-98-8	ZB-98-5	ZB-98-2	ZB-98-192	ZB-98-191	ZB-98-6
wt %						
SiO_2	41.33	41.55	42.47	43.02	43.55	44.71
TiO_2	0.10	0.14	0.16	0.16	0.17	0.25
Al_2O_3	1.90	2.17	2.24	2.71	2.55	3.38
FeO_{total}	14.76	14.64	13.87	13.25	13.58	14.44
MnO	0.11	0.19	0.17	0.22	0.23	0.19
MgO	40.30	40.26	40.05	39.37	39.33	33.15
CaO	0.09	0.09	0.06	0.05	0.15	3.35
Na_2O	0.00	0.03	0.01	0.00	0.00	0.04
K_2O	0.01	0.02	0.01	0.00	0.00	0.03
P_2O_5	0.01	0.01	0.01	0.01	0.01	0.05
L.O.I.						
TOTAL (L.O.I. Free)	98.60	99.09	99.04	98.79	99.57	99.57
(ppm)						
Sc	7.7	7.9	10.1	10.1	8.1	8.9
V	44	48	53	62	71	92
Cr	4098	3905	4156	3868	4129	2308
Co	110.3	140.2	156.8	135.4	143.4	132.4
Ni	3050	2457	2720	2578	2477	1949
Cu	1.9	2.9	20.6	14.5	10.4	12.8
Zn	47.8	57.7	59.0	67.7	59.8	70.1
Ga	0.9	1.2	0.8	1.6	1.3	1.4
Rb	0.9	2.1	1.4	4.0	1.7	2.6
Sr	6.2	3.0	6.7	2.9	3.0	22.5
Y	2	2	2.4	2.9	2.7	8.8
Zr	8.7	9.5	11.5	13.8	10.4	32.9
Nb	1.2	1.1	0.8	0.8	1.3	0.9
Ba	39.1	2.9	3.4	1.2	0.9	1.9
La	0.6	0.0	0.1	0.9	0.2	0.4
Ce	0.3	0.3	0.2	0.5	0.3	0.8
Nd	0.4	0.0	0.2	0.3	0.2	1.2
Pb	3.9	9.2	6.3	6.8	10.4	5.1
Th	0.9	0.4	0.6	1.0	1.4	0.1
U	0.8	0.2	0.6	0.7	0.8	0.3
cipw (%)						
Q	0	0	0	0	0	0
C	1.75	1.97	2.14	2.63	2.29	0
or	0.03	0.09	0.07	0.02	0.02	0.15
ab	0	0.21	0.05	0.01	0	0.30
an	0.41	0.40	0.23	0.20	0.69	8.99
di	0	0	0	0	0	5.87
hy	19.29	19.70	25.16	29.85	30.69	28.18
ol	75.56	75.03	69.77	64.47	64.22	54.17
cm	0.92	0.84	0.91	0.93	0.89	0.50
il	0.18	0.27	0.29	0.31	0.32	0.47
ap	0.02	0.02	0.03	0.02	0.02	0.11

APPENDIX B(V-a)

XRF analyses of the ultramafic intrusives from the Vumba granite-greenstone terrain

Unit: Metapyroxenite						
Sample no	ZB-98-43	ZB-98-195	ZB-98-196	ZB-98-193	ZB-98-39	ZB-98-194
wt %						
SiO_2	52.00	52.05	52.06	52.92	52.99	53.38
TiO_2	0.35	0.36	0.44	0.51	0.49	0.52
Al_2O_3	8.05	7.18	6.30	7.73	7.56	7.47
FeO_{total}	9.33	9.53	9.61	9.80	9.81	9.59
MnO	0.18	0.20	0.19	0.19	0.18	0.19
MgO	14.38	14.72	14.38	13.11	13.72	12.91
CaO	13.99	13.96	15.20	13.58	13.49	13.57
Na_2O	0.63	0.93	0.74	1.40	1.25	1.40
K_2O	0.45	0.09	0.07	0.08	0.08	0.08
P_2O_5	0.03	0.02	0.04	0.04	0.03	0.04
L.O.I.						
TOTAL (L.O.I. Free)	99.39	99.04	99.03	99.35	99.60	99.15
(ppm)						
Sc	57.4	58.6	67.2	58.3	69.3	63.5
V	222	221	252	244	221	242
Cr	1863	2048	1937	1520	2218	1496
Co	55.0	57.8	56.4	55.6	49.4	53.5
Ni	212	230	223	181	218	189
Cu	10.8	36.9	76.6	61.9	61.8	50.6
Zn	50.0	64.9	62.3	58.5	48.9	50.5
Ga	11.2	11.9	11.8	12.6	10.5	11.2
Rb	26.1	4.3	3.2	2.3	1.1	3.2
Sr	50.3	61.4	63.9	47.8	61.7	42.1
Y	6.4	10.2	9.9	13.4	12.3	13.2
Zr	29.8	28.2	31.1	39.8	42.9	39.2
Nb	1.1	0.9	0.2	1.1	1.0	5.4
Ba	126.2	47.5	56.7	76.7	50.1	56.2
La	5.0	0.5	3.2	3.0	4.8	5.1
Ce	7.1	6.4	2.5	5.8	6.2	5.8
Nd	3.5	2.1	1.6	2.6	3.5	4.7
Pb	3.1	0.7	0.7	1.3	5.8	5.4
Th	0.2	0.8	1.1	2.0	2.1	0.2
U	0.5	0.8	0.5	1.1	0.9	0.8
cipw (%)						
Q	0	0	0	0.18	0.26	1.28
C	0	0	0	0	0	0
or	2.67	0.53	0.43	0.49	0.50	0.44
ab	5.33	7.87	6.26	11.85	10.58	11.85
an	17.81	15.16	13.66	14.57	14.77	13.88
di	41.49	43.50	49.64	42.53	41.97	43.04
hy	29.15	28.05	26.68	27.64	29.45	26.56
ol	1.20	2.15	0.44	0	0	0
cm	0.40	0.44	0.29	0.33	0.41	0.29
il	0.67	0.68	0.83	0.96	0.93	1.00
ap	0.06	0.06	0.09	0.09	0.08	0.09

APPENDIX B(V-b)

ICP-MS whole-rock data set for the ultramafic intrusives

APPENDIX B(V-b)

XRF and ICP-MS whole-rock results of the ultramafic intrusives from the Vumba granite-greenstone terrain

Unit:	serpentin	serpentin	serpentin	metapyrox	metapyrox	metapyrox
Sample no	ZB-98-8	ZB-98-2	ZB-98-192	ZB-98-196	ZB-98-39	ZB-98-194
wt %						
SiO_2	41.33	42.47	43.02	52.06	52.99	53.38
TiO_2	0.10	0.16	0.16	0.44	0.49	0.52
Al_2O_3	1.90	2.24	2.71	6.30	7.56	7.47
FeO_{total}	14.76	13.87	13.25	9.61	9.81	9.59
MnO	0.11	0.17	0.22	0.19	0.18	0.19
MgO	40.30	40.05	39.37	14.38	13.72	12.91
CaO	0.09	0.06	0.05	15.20	13.49	13.57
Na_2O	0.00	0.01	0.00	0.74	1.25	1.40
K_2O	0.01	0.01	0.00	0.07	0.08	0.08
P_2O_5	0.01	0.01	0.01	0.04	0.03	0.04
L.O.I.						
TOTAL (L.O.I. Free)	98.60	99.04	98.79	99.03	99.60	99.15
(ppm)						
Sc	25.9	24.9	27.1	43.1	41.4	41.3
V	60.5	71.6	81.2	244.1	212.8	219.0
Cr	4259.1	4225.6	4301.2	1382.2	1900.6	1333.4
Mn	0.1	0.2	0.2	0.2	0.2	0.2
Co	114.1	161.6	154.9	58.1	53.7	54.4
Ni	3961.1	3265.6	3535.6	253.7	249.1	222.1
Cu	15.5	7.7	3.6	83.9	74.2	70.2
Zn	18.2	38.0	45.5	172.1	281.9	242.2
Ga	2.6	3.6	3.7	10.4	8.4	7.8
Rb	0.4	0.6	0.5	1.2	1.2	1.0
Sr	1.7	0.6	3.8	88.9	58.5	41.8
Y	1.9	3.0	4.2	14.8	12.3	14.1
Zr	10.7	16.4	13.3	38.6	40.0	36.4
Nb	0.4	0.5	0.4	1.7	1.6	1.5
Cs	0.1	0.1	0.2	0.2	0.1	0.1
Ba	56.3	17.7	21.7	34.4	32.9	47.3
La	0.02	0.10	0.01	0.38	0.14	0.19
Ce	1.66	1.49	2.21	7.01	7.90	8.72
Pr	0.26	0.25	0.35	1.15	1.15	1.32
Nd	1.15	1.18	1.65	5.12	5.06	6.00
Sm	0.35	0.39	0.56	1.64	1.48	1.60
Eu	0.08	0.14	0.21	0.56	0.49	0.54
Gd	0.37	0.47	0.65	2.22	1.97	2.18
Tb	0.05	0.07	0.11	0.38	0.34	0.38
Dy	0.33	0.53	0.73	2.44	2.07	2.41
Ho	0.08	0.12	0.16	0.51	0.45	0.51
Er	0.19	0.32	0.41	1.45	1.25	1.36
Tm	0.04	0.05	0.08	0.25	0.19	0.24
Yb	0.19	0.31	0.41	1.35	1.15	1.31
Lu	0.04	0.06	0.08	0.23	0.20	0.22
Hf	0.24	0.38	0.31	1.07	1.07	1.03
Ta	0.02	0.03	0.04	0.11	0.11	0.12
Pb	0.36	0.06	0.83	2.68	2.59	2.41
Th	0.13	0.19	0.22	0.79	1.24	1.19
U	0.07	0.04	0.05	0.23	0.34	0.34

APPENDIX B(VI-a)

XRF whole-rock major and trace element data set for the felsic metavolcanics

APPENDIX B(VI-a)

XRFanalyses for the felsic metavolcanics from the Vumba granite-greenstone terrain.

Rock unit	VUFF	VUFF	VUFF	VMVF	VUFF	VLFF	VUFF
Sample no	**ZB-98-219**	**ZB-98-154**	**ZB-98-153**	**ZB-98-160**	**ZB-98-155**	**ZB-98-172**	**ZB-98-156**
wt %							
SiO_2	61.51	62.68	66.45	66.73	67.03	67.45	68.10
TiO_2	0.96	0.45	0.44	0.59	0.44	0.43	0.53
Al_2O_3	16.95	14.05	13.52	16.13	13.63	12.95	16.27
FeO_{total}	6.27	4.07	3.45	4.35	3.40	2.15	3.28
MnO	0.09	0.20	0.14	0.08	0.14	0.24	0.08
MgO	2.55	4.12	2.97	1.70	2.98	1.08	1.06
CaO	5.43	9.04	7.40	4.24	7.43	11.49	3.58
Na_2O	4.04	2.48	3.25	4.36	3.25	3.06	4.22
K_2O	1.73	2.92	1.51	1.75	1.51	1.49	2.08
P_2O_5	0.28	0.13	0.15	0.18	0.16	0.12	0.18
L.O.I.	1.41	1.86	1.89	0.74	2.03	4.58	1.20
Total (on L.O.I. Free)	99.81	100.14	99.28	100.09	99.97	100.46	99.36
(ppm)							
Sc	11.6	9.3	8.3	3.3	8.8	7.4	10.2
V	93	54	59	67	57	61	66
Cr	15	22	54	26	24	60	57
Co	14.0	6.1	5.3	10.3	8.6	11.5	10.0
Ni	16	13	15	16	18	17	25
Cu	8	4	5	16	8	7	18
Zn	85	46	29	100	63	68	44
Rb	60.3	64.7	50.6	43.4	51.6	66.7	59.4
Sr	545	187	460	316	305	73	340
Y	22.8	14.7	8.6	15.3	12.3	11.5	10.4
Zr	223.5	145.2	121.3	168.0	114.1	145.6	130.6
Nb	6.3	3.7	4	8.7	2.4	5.3	5.0
Ba	745	476	540	432	411	459	511
La	55.7	28.3	11.1	18.5	11.9	34.2	20.6
Ce	118.4	48.4	28.6	52.9	23.9	58.7	38.9
Nd	48.8	24.2	18	26.2	13.4	19.6	16.9
Pb	27	11.7	11.4	8.3	17.3	4.6	15.8
cipw (wt.%)							
Q	13.63	14.48	23.33	20.75	23.86	24.92	24.63
or	10.25	17.27	8.94	10.37	8.93	8.84	12.29
ab	34.18	20.98	27.50	36.89	27.50	25.89	35.70
an	20.32	18.60	17.87	19.30	18.17	17.20	16.80
C	0	0	0	0	0	0	0.94
di	4.26	20.84	14.82	0.58	14.59	11.99	0
hy	13.17	6.47	5.38	10.30	5.44	0	7.33
il	1.82	0.85	0.84	1.12	0.84	0.82	1.00
zr	0.04	0.03	0.02	0.03	0.02	0.03	0.03
ap	0.66	0.32	0.36	0.43	0.37	0.29	0.42

APPENDIX B(VI-a)

XRFanalyses for the felsic metavolcanics from the Vumba granite-greenstone terrain.

Rock unit	VMVF	VMVF	VLFF	VMVF	VMVF	VMVF	VMVF
Sample no	**ZB-98-161**	**ZB-98-53**	**ZB-98-173**	**ZB-98-164**	**ZB-98-168**	**ZB-98-166**	**ZB-98-162**
wt %							
SiO_2	68.21	68.34	68.47	68.47	68.53	68.57	68.78
TiO_2	0.46	0.49	0.43	0.48	0.47	0.47	0.45
Al_2O_3	16.28	15.42	13.14	16.01	15.73	16.10	15.74
FeO_{total}	3.72	4.16	1.97	3.73	3.77	3.81	3.63
MnO	0.04	0.05	0.22	0.05	0.05	0.05	0.05
MgO	1.61	1.64	1.05	1.40	1.99	1.49	1.80
CaO	5.53	3.20	10.72	4.09	3.49	4.14	6.32
Na_2O	1.65	6.30	3.17	5.23	4.87	5.15	1.02
K_2O	1.97	0.09	1.38	0.94	1.06	0.94	2.09
P_2O_5	0.12	0.14	0.13	0.14	0.14	0.14	0.12
L.O.I.	2.34	0.48	4.58	0.86	1.01	0.71	2.30
Total (on L.O.I. Free)	99.59	99.83	100.69	100.54	100.10	100.87	100.01
(ppm)							
Sc	8.2	3	6.3	7.6	4.7	2.8	4.9
V	67	53	54	56	59	58	63
Cr	15	25	56	25	28	25	22
Co	16.3	11.9	8.8	10.2	11.0	8.9	9.6
Ni	22	24	16	13	13	15	17
Cu	6	35	4	17	15	14	3
Zn	61	45	54	72	51	62	42
Rb	41.7	8.3	62.9	21.7	27.5	22.3	48.7
Sr	111	188	83	270	260	289	113
Y	8.9	14	13.0	11.5	9.5	13.0	8.3
Zr	114.6	149.3	149.1	133.8	127.8	124.1	110.5
Nb	4.4	2.5	6.8	5.7	3.4	4.8	2.6
Ba	264	36	454	232	297	240	232
La	12.5	10.6	19.1	17.3	17.6	8.5	9.9
Ce	35.8	19.8	37.8	26	32.2	28.7	23.8
Nd	16.8	8.9	16.7	15.3	14.8	13.9	12.8
Pb	5.3	7.9	6.1	11.1	6.3	11.8	3.6
cipw (wt.%)							
Q	34.58	19.89	26.68	21.88	23.52	22.08	36.42
or	11.66	0.54	8.19	5.56	6.26	5.55	12.40
ab	13.96	53.30	26.82	44.25	41.20	43.57	8.63
an	26.84	13.56	17.56	17.46	16.54	18.08	30.76
C	1.61	0	0	0	0.52	0	0.53
di	0	1.37	11.21	1.75	0	1.42	0
hy	9.49	9.56	0	8.08	10.49	8.61	9.84
il	0.87	0.94	0.82	0.91	0.9	0.90	0.85
zr	0.02	0.03	0.03	0.03	0.03	0.02	0.02
ap	0.29	0.32	0.31	0.33	0.32	0.34	0.29

APPENDIX B(VI-a)

XRFanalyses for the felsic metavolcanics from the Vumba granite-greenstone terrain.

Rock unit	VLFF	VUFF	VMVF	VUFF	VLFF	VUFF	VUFF
Sample no	**ZB-98-170**	**ZB-98-158**	**ZB-98-167**	**ZB-98-157**	**ZB-98-169**	**ZB-98-159**	**ZB-98-218**
wt %							
SiO_2	68.82	69.37	69.38	69.49	69.81	70.00	70.04
TiO_2	0.46	0.42	0.47	0.42	0.44	0.43	0.41
Al_2O_3	15.24	14.75	15.65	14.95	15.85	15.73	15.45
FeO_{total}	3.52	3.71	3.39	4.04	2.67	3.63	3.76
MnO	0.09	0.08	0.05	0.08	0.05	0.07	0.07
MgO	1.44	1.40	1.47	1.50	1.56	1.39	1.39
CaO	4.87	4.33	4.00	3.74	4.38	3.80	3.71
Na_2O	4.44	3.70	4.88	3.68	3.90	3.94	3.89
K_2O	1.31	1.39	1.00	1.59	1.75	1.50	1.54
P_2O_5	0.16	0.12	0.14	0.10	0.17	0.11	0.11
L.O.I.	1.68	1.79	1.24	1.56	1.20	1.52	1.54
Total (on L.O.I. Free)	100.35	99.26	100.44	99.59	100.56	100.60	100.37
(ppm)							
Sc	10	5.5	6.5	11	3.8	4.6	1.8
V	66	66	60	54	61	59	55
Cr	28	48	30	27	27	39	32
Co	8.4	10.8	10.7	7.7	8.6	10.3	7.7
Ni	16	11	9	14	19	13	18
Cu	15	8	16	19	12	10	15
Zn	37	54	55	51	63	51	43
Rb	37.9	39.4	23.5	43.4	50.6	43.6	42.4
Sr	333	258	258	271	414	280	293
Y	11.3	12	10.7	9.9	13.7	9.1	11.2
Zr	136.9	109.0	127.2	113.8	134.9	125.4	120.1
Nb	3.4	2.7	4.4	3.7	4.6	3.5	3.8
Ba	427	279	244	292	468	288	335
La	33.1	23	21.1	28	37.1	28.4	24.2
Ce	53.4	43.1	35.9	53.7	60.6	46.7	49.2
Nd	30.5	20	11	26.4	21.9	19.9	21.8
Pb	13.2	17.6	6.0	18.9	30.2	23.3	24.6
cipw (wt.%)							
Q	24.57	29.19	24.77	29.21	27.42	28.90	29.13
or	7.77	8.20	5.90	9.39	10.39	8.90	9.10
ab	37.57	31.31	41.29	31.14	33.00	33.34	32.91
an	17.80	19.57	17.89	17.99	20.60	18.23	17.96
C	0	0	0	0.59	0	0.95	0.82
di	4.59	1.04	1.01	0	0.17	0	0
hy	6.52	8.54	8.07	9.86	7.58	8.89	9.13
il	0.87	0.80	0.89	0.81	0.84	0.81	0.79
zr	0.03	0.02	0.03	0.02	0.03	0.03	0.02
ap	0.38	0.28	0.34	0.25	0.40	0.26	0.26

APPENDIX B(VI-a)

XRFanalyses for the felsic metavolcanics from the Vumba granite-greenstone terrain.

Rock unit	VMVF	VMVF	VLFF	VMVF	VLFF	VLFF	VLFF
Sample no	**ZB-98-178**	**ZB-98-165**	**ZB-98-177**	**ZB-98-163**	**ZB-98-176**	**ZB-98-171**	**ZB-98-175**
wt %							
SiO_2	70.17	70.20	70.53	70.54	73.67	74.09	75.73
TiO_2	0.47	0.37	0.42	0.40	0.35	0.38	0.33
Al_2O_3	16.15	16.17	16.81	15.76	14.54	11.05	13.11
FeO_{total}	2.10	2.89	2.10	3.61	1.58	2.00	2.48
MnO	0.04	0.03	0.06	0.03	0.07	0.13	0.06
MgO	1.59	1.67	1.25	2.12	1.48	2.30	0.89
CaO	4.26	3.83	4.04	4.21	5.46	5.92	3.83
Na_2O	2.57	2.69	3.39	1.19	0.77	4.23	1.77
K_2O	2.90	2.44	1.52	2.36	2.17	0.41	1.58
P_2O_5	0.15	0.11	0.10	0.11	0.10	0.10	0.08
L.O.I.	1.94	3.11	1.76	2.09	2.30	1.12	1.91
Total (on L.O.I. Free)	100.41	100.39	100.21	100.33	100.18	100.61	99.85
(ppm)							
Sc	7.8	3.1	9.9	4.9	3.9	7.2	5.5
V	62	51	45	51	35	55	51
Cr	30	25	15	28	11	75	13
Co	8.7	8.5	4.1	8.7	8.6	6.5	9.9
Ni	12	15	16	23	22	23	22
Cu	3	4	2	14	13	3	33
Zn	52	51	27	48	28	103	30
Rb	70.6	53.2	45	43.9	69.5	74.8	40.3
Sr	191	239	144	100	148	32	95
Y	14.4	7.4	9.0	8.3	8.2	14.5	6.4
Zr	176.6	127.8	146.3	114.0	123.1	150.3	118.1
Nb	4.8	1.8	3.8	4.1	3.9	4.8	2.4
Ba	497	450	258	220	285	148	176
La	23	14.9	6.2	9.9	4.5	21.7	14.1
Ce	62.5	25.5	12.8	29.4	10.2	39.1	27.8
Nd	30.7	10.8	7.1	10.9	3.2	19.6	9.3
Pb	12.0	17.6	1.2	13.8	11.8	10.4	12.8
cipw (wt.%)							
Q	31.69	32.79	33.35	40.18	46.17	34.74	48.33
or	17.19	14.45	9.01	13.97	12.85	2.48	9.34
ab	21.74	22.76	28.68	10.07	6.51	35.79	14.98
an	20.33	18.54	19.60	20.35	26.67	9.94	18.66
C	1.34	2.32	2.42	3.80	1.16	0	1.66
di	0	0	0	0	0	15.33	0
hy	6.71	8.38	5.99	10.65	5.85	1.23	5.89
il	0.90	0.70	0.80	0.76	0.67	0.72	0.63
zr	0.04	0.03	0.03	0.02	0.02	0.03	0.02
ap	0.37	0.25	0.23	0.25	0.23	0.24	0.18

APPENDIX B(VI-b)

ICP-MS whole-rock data set for the felsic metavolcanics

APPENDIX B(VI-b)

XRF and ICP-MS whole-rock results of the felsic metavolcanics from the Vumba granite-greenstone terrain

Rock unit	VUFF	VUFF	VUFF	VUFF	VMVF	VMVF	VLFF	VMVF
Sample no	**ZB-98-219**	**ZB-98-153**	**ZB-98-155**	**ZB-98-156**	**ZB-98-161**	**ZB-98-53**	**ZB-98-173**	**ZB-98-164**
wt %								
SiO_2	61.51	66.45	67.03	68.10	68.21	68.34	68.47	68.47
TiO_2	0.96	0.44	0.44	0.53	0.46	0.49	0.43	0.48
Al_2O_3	16.95	13.52	13.63	16.27	16.28	15.42	13.14	16.01
FeO_{total}	6.27	3.45	3.40	3.28	3.72	4.16	1.97	3.73
MnO	0.09	0.14	0.14	0.08	0.04	0.05	0.22	0.05
MgO	2.55	2.97	2.98	1.06	1.61	1.64	1.05	1.40
CaO	5.43	7.40	7.43	3.58	5.53	3.20	10.72	4.09
Na_2O	4.04	3.25	3.25	4.22	1.65	6.30	3.17	5.23
K_2O	1.73	1.51	1.51	2.08	1.97	0.09	1.38	0.94
P_2O_5	0.28	0.15	0.16	0.18	0.12	0.14	0.13	0.14
L.O.I.	1.41	1.89	2.03	1.20	2.34	0.48	3.960	0.86
Total (on L.O.I. Free)	99.81	99.28	99.97	99.36	99.59	99.83	100.69	100.54
ppm								
Sc	47.5	34.3	42.8	42.3	35.0	48.8	42.8	37.2
V	74.2	48.4	46.1	46.5	44.9	49.6	36.6	43.4
Cr	3.1	35.2	55.9	50.7	15.5	26.2	52.7	29.9
Mn	0.1	0.1	0.1	0.1	0.1	0.1	0.2	0.1
Co	15.0	7.2	7.5	9.0	9.9	11.1	7.0	8.8
Ni	1.9	17.7	102.9	36.7	8.8	34.4	10.3	1.2
Ga	21.2	16.2	16.9	20.1	17.7	15.1	12.8	17.2
Rb	59.8	46.2	46.5	55.2	38.9	1.6	51.6	19.0
Sr	531.2	323.3	326.6	346.9	107.5	183.2	83.6	273.3
Y	21.3	9.1	9.0	8.7	8.7	10.8	12.4	8.3
Zr	239.2	136.0	137.0	134.5	126.1	148.8	177.1	137.0
Nb	10.8	3.6	3.6	3.7	3.9	5.6	7.7	4.8
Cs	5.4	1.7	1.8	2.3	1.0	0.3	3.6	0.5
Ba	794.5	398.8	406.0	492.2	237.0	32.5	439.7	215.6
La	52.53	16.75	16.94	18.68	9.39	8.27	20.51	10.04
Ce	120.59	43.12	43.22	47.29	28.00	26.45	47.64	29.34
Pr	13.87	4.82	4.85	5.31	2.96	2.83	4.81	3.11
Nd	52.77	19.58	19.33	21.44	12.34	11.90	18.25	13.07
Sm	8.97	3.32	3.31	3.59	2.36	2.31	3.09	2.36
Eu	2.49	0.96	0.98	1.13	0.77	0.84	0.87	0.81
Gd	6.48	2.47	2.47	2.56	1.95	2.09	2.79	1.88
Tb	0.91	0.33	0.35	0.36	0.29	0.32	0.45	0.30
Dy	4.43	1.61	1.62	1.73	1.58	1.82	2.29	1.57
Ho	0.79	0.31	0.30	0.30	0.30	0.34	0.42	0.29
Er	1.98	0.77	0.77	0.79	0.76	0.96	1.16	0.74
Tm	0.30	0.12	0.12	0.13	0.13	0.15	0.18	0.11
Yb	1.72	0.74	0.72	0.77	0.78	0.95	0.99	0.70
Lu	0.26	0.11	0.11	0.12	0.13	0.15	0.16	0.12
Hf	6.26	3.10	3.04	3.32	3.00	3.32	4.23	3.12
Ta	0.85	0.31	0.30	0.33	0.33	0.49	0.80	0.41
Pb	19.34	10.56	11.14	13.87	4.00	4.62	7.29	4.13
Th	15.02	5.90	5.94	5.98	2.93	1.84	9.13	2.31
U	4.27	1.41	1.44	1.56	0.81	0.44	2.52	0.67

APPENDIX B(VI-b)

XRF and ICP-MS whole-rock results of the felsic metavolcanics from the Vumba granite-greenstone terrain

Rock unit	VMVF	VLFF	VMVF	VLFF	VLFF	VLFF	VLFF
Sample no	**ZB-98-166**	**ZB-98-169**	**ZB-98-159**	**ZB-98-178**	**ZB-98-176**	**ZB-98-171**	**ZB-98-175**
wt %							
SiO_2	68.57	69.81	70.00	70.17	73.67	74.09	75.73
TiO_2	0.47	0.44	0.43	0.47	0.35	0.38	0.33
Al_2O_3	16.10	15.85	15.73	16.15	14.54	11.05	13.11
FeO_{total}	3.81	2.67	3.63	2.10	1.58	2.00	2.48
MnO	0.05	0.05	0.07	0.04	0.07	0.13	0.06
MgO	1.49	1.56	1.39	1.59	1.48	2.30	0.89
CaO	4.14	4.38	3.80	4.26	5.46	5.92	3.83
Na_2O	5.15	3.90	3.94	2.57	0.77	4.23	1.77
K_2O	0.94	1.75	1.50	2.90	2.17	0.41	1.58
P_2O_5	0.14	0.17	0.11	0.15	0.10	0.10	0.08
L.O.I.	0.71	1.20	1.52	1.94	2.30	1.12	1.91
Total (on L.O.I. Free)	100.87	100.56	100.60	100.41	100.18	100.61	99.85
ppm							
Sc	35.0	36.8	38.7	45.1	44.2	43.0	50.0
V	41.4	39.2	40.1	41.0	21.2	35.9	34.5
Cr	20.7	19.4	29.3	21.3	9.5	73.2	15.3
Mn	0.1	0.1	0.1	0.0	0.1	0.1	0.1
Co	8.7	7.5	6.5	6.0	7.7	6.2	9.2
Ni	1.8	12.5	9.2	2.9	15.2	14.0	12.8
Ga	16.7	19.3	18.3	19.5	14.5	13.3	13.3
Rb	18.7	45.3	40.6	59.8	69.1	67.9	39.8
Sr	281.3	412.6	280.2	178.7	159.9	30.8	97.4
Y	8.4	10.3	9.0	11.8	7.5	12.1	7.2
Zr	133.4	145.4	132.0	176.2	122.3	158.0	119.8
Nb	4.5	4.0	4.0	6.3	3.5	6.9	3.3
Cs	0.5	2.4	1.9	3.5	1.8	7.3	1.8
Ba	210.0	453.0	283.8	486.7	282.6	131.4	179.9
La	9.85	29.01	20.98	28.43	6.37	17.40	7.55
Ce	29.00	70.39	48.05	64.82	19.16	43.31	22.22
Pr	3.11	7.96	4.82	6.99	1.93	4.41	2.18
Nd	12.87	30.73	17.62	26.23	8.57	16.80	9.35
Sm	2.40	4.87	2.85	4.45	1.60	2.89	1.69
Eu	0.88	1.28	0.95	1.20	0.68	0.81	0.64
Gd	1.94	3.15	2.23	3.29	1.61	2.50	1.61
Tb	0.30	0.39	0.33	0.43	0.25	0.42	0.24
Dy	1.49	1.92	1.69	2.25	1.33	2.17	1.36
Ho	0.29	0.35	0.33	0.40	0.26	0.42	0.26
Er	0.78	0.90	0.86	1.07	0.66	1.07	0.70
Tm	0.12	0.14	0.13	0.17	0.11	0.17	0.11
Yb	0.72	0.82	0.86	1.01	0.58	1.01	0.69
Lu	0.13	0.14	0.13	0.15	0.09	0.16	0.12
Hf	3.03	3.53	3.03	4.53	2.71	3.60	2.38
Ta	0.37	0.32	0.39	0.60	0.29	0.70	0.29
Pb	4.68	10.98	7.92	9.60	5.20	3.03	4.73
Th	2.26	6.99	6.54	9.52	2.15	7.89	2.03
U	0.68	2.12	1.70	2.19	0.67	2.14	0.66

APPENDIX C

ACCURACY AND PRECISION OF ANALYTICAL DATA

APPENDIX C (I)

Accuracy and precision of XRF major element data

		AGV-1	MRG-1	G-1	PCC-1	DTS-1	NIM-D	QLO-1
SiO_2	*recommended*	**59.87**	**39.62**	**72.70**	**43.86**	**40.42**	**38.96**	**65.79**
	1st run	59.66	39.69	72.73	43.86	40.67	38.89	65.60
	2nd run	59.87	39.57	72.77				
	3rd run	60.16	39.83	72.75				
	4th run	59.69	39.83					
	5th run	60.16						
	6th run	60.17						
	Average	**59.95**	**39.73**	**72.75**				
	standard dev	*0.24*	*0.13*	*0.02*				
TiO_2	*recommended*	**1.07**	**3.82**	**0.27**	**0.01**	**0.01**	**0.02**	**0.62**
	1st run	1.07	3.81	0.27	0.01	0.01	0.02	0.61
	2nd run	1.07	3.80	0.27				
	3rd run	1.07	3.81	0.27				
	4th run	1.07	3.86					
	5th run	1.08						
	6th run	1.07						
	Average	**1.07**	**3.82**	**0.27**				
	standard dev	*0.00*	*0.03*	*0.00*				
Al_2O_3	*recommended*	**17.46**	**8.58**	**14.47**	**0.71**	**0.19**	**0.30**	**16.24**
	1st run	17.47	8.56	14.27	0.70	0.28	0.26	16.44
	2nd run	17.38	8.46	14.45				
	3rd run	17.36	8.47	14.46				
	4th run	17.39	8.55					
	5th run	17.53						
	6th run	17.45						
	Average	**17.43**	**8.51**	**14.39**				
	standard dev	*0.06*	*0.05*	*0.11*				
Fe_2O_3	*recommended*	**6.88**	**18.18**	**1.95**	**8.68**	**8.69**	**16.96**	**4.37**
	1st run	6.86	18.24	1.85	8.63	8.64	16.96	4.36
	2nd run	6.88	17.94	1.82				
	3rd run	6.91	18.26	1.85				
	4th run	6.77	18.12					
	5th run	6.85						
	6th run	6.92						
	Average	**6.87**	**18.14**	**1.84**				
	standard dev	*0.05*	*0.15*	*0.02*				
MnO	*recommended*	**0.09**	**0.17**	**0.03**	**0.13**	**0.12**	**0.22**	**0.09**
	1st run	0.10	0.17	0.03	0.12	0.12	0.23	0.09
	2nd run	0.10	0.17	0.03				
	3rd run	0.10	0.17	0.03				
	4th run	0.09	0.18					
	5th run	0.09						
	6th run	0.10						
	Average	**0.10**	**0.17**	**0.03**				
	standard dev	*0.01*	*0.01*	*0.00*				

		AGV-1	MRG-1	G-1	PCC-1	DTS-1	NIM-D	QLO-1
MgO	*recommended*	**1.56**	**13.73**	**0.36**	**45.71**	**49.64**	**43.51**	**1.00**
	1st run	1.57	13.72	0.38	45.64	49.90	43.17	1.13
	2nd run	1.59	13.75	0.37				
	3rd run	1.55	13.61	0.37				
	4th run	1.65	13.74					
	5th run	1.56						
	6th run	1.61						
	Average	**1.59**	**13.71**	**0.37**				
	standard dev	*0.04*	*0.06*	*0.01*				
CaO	*recommended*	**5.03**	**14.91**	**1.37**	**0.55**	**0.17**	**0.28**	**3.18**
	1st run	4.97	14.91	1.37	0.54	0.14	0.29	3.23
	2nd run	4.99	14.90	1.37				
	3rd run	4.96	14.89	1.36				
	4th run	5.01	15.21					
	5th run	5.04						
	6th run	5.02						
	Average	**5.00**	**14.98**	**1.37**				
	standard dev	*0.03*	*0.16*	*0.01*				
Na_2O	*recommended*	**4.34**	**0.75**	**3.34**	**0.03**	**0.02**	**0.04**	**4.22**
	1st run	4.34	0.77	3.36	0.02	0.02	0.06	4.28
	2nd run	4.36	0.78	3.40				
	3rd run	4.30	0.77	3.28				
	4th run	4.49	0.78					
	5th run	4.53						
	6th run	4.37						
	Average	**4.40**	**0.78**	**3.35**				
	standard dev	*0.09*	*0.01*	*0.06*				
K_2O	*recommended*	**2.96**	**0.18**	**5.52**	**0.01**	**0.00**	**0.01**	**3.61**
	1st run	2.97	0.19	5.52	0.00	0.00	0.01	3.61
	2nd run	2.99	0.20	5.53				
	3rd run	2.99	0.20	5.54				
	4th run	2.96	0.18					
	5th run	2.98						
	6th run	2.97						
	Average	**2.98**	**0.19**	**5.53**				
	standard dev	*0.01*	*0.01*	*0.01*				
P_2O_5	*recommended*	**0.50**	**0.08**	**0.08**	**0.00**	**0.00**	**0.01**	**0.25**
	1st run	0.49	0.08	0.08	0.01	0.00	0.01	0.26
	2nd run	0.49	0.07	0.08				
	3rd run	0.49	0.07	0.08				
	4th run	0.50	0.08					
	5th run	0.52						
	6th run	0.51						
	Average	**0.50**	**0.08**	**0.08**				
	standard dev	*0.01*	*0.00*	*0.00*				

APPENDIX C (II)

Accuracy and precision of XRF trace element data

		G2	GS-N	DR-N	RGM-1	QLO-1	DNC-1	BIR-1	W-2
Sc	*recommended*	3.5	7.3	28	4.4	8.9	31	44	35
	1st run	2.8	7.5	26.7	4.5	7.5	32.4	46.7	34.5
	2nd run	3.8	7.6	26.3	4.6	8.1	32.6		
	3rd run	2.6	8.7	28.1	3.4				
	Average	3.07	7.93	27.03	4.17	7.80	32.50		
	standard dev	*0.64*	*0.67*	*0.95*	*0.67*	*0.42*	*0.14*		
V	*recommended*	36	65	220	13	54	148	313	262
	1st run	36.9	68.9	221.4	13.6	53.4	146.4	317.9	260.7
	2nd run	36.1	62.6	218.4	13.2	55.0	148.2		
	3rd run	39.9	67.4	215.9	16.8				
	Average	37.63	66.30	218.57	14.53	54.20	147.30		
	standard dev	*2.00*	*3.29*	*2.75*	*1.97*	*1.13*	*1.27*		
Cr	*recommended*	9	55	42	3.7	3.2	285	382	93
	1st run	6.7	54.9	40.9	3.7	1.7	281.2	383.9	94.3
	2nd run	8.6	56.1	41.9	3.6	3.4	287.0		
	3rd run	7.5	58.9	43.6	2.8				
	Average	7.6	56.6	42.1	3.4	2.6	284.1		
	standard dev	*0.95*	*2.05*	*1.37*	*0.49*	*1.20*	*4.10*		
Co	*recommended*	4.6	65	35	2.0	7.2	56.0	51.4	44
	1st run	3.9	65.1	42.6	1.9	8.7	64.0	49.3	41.0
	2nd run	4.5	63.0	39.9	2.0	7.5	61.2		
	3rd run	4.7	68.4	37.8	0.9				
	Average	4.4	65.5	40.1	1.6	8.1	62.6		
	standard dev	*0.42*	*2.72*	*2.41*	*0.61*	*0.85*	*1.98*		
Ni	*recommended*	5.0	34	15	4.4	5.8	247	166	70
	1st run	6.0	34.4	17.4	4.5	6.0	243.5	172.2	67.0
	2nd run	5.6	34.1	16.8	4.5	5.9	245.2		
	3rd run	2.8	36.9	13.0	5.6				
	Average	4.8	35.1	15.7	4.9	6.0	244.4		
	standard dev	*1.74*	*1.54*	*2.39*	*0.64*	*0.07*	*1.20*		
Cu	*recommended*	11	20	50	11.6	29	96	126	103
	1st run	12.1	22.7	49.8	14.1	28.4	96.1	129.1	105.9
	2nd run	11.7	21.4	50.0	13.3	28.6	95.8		
	3rd run	12.6	22.2	49.0	12.6				
	Average	12.1	22.1	49.6	13.3	28.5	96.0		
	standard dev	*0.45*	*0.66*	*0.53*	*0.75*	*0.14*	*0.21*		
Zn	*recommended*	85	48	145	32	61	66	71	77
	1st run	84.2	49.7	144.1	34.2	65.5	66.3	75.7	73.7
	2nd run	85.6	50.0	144.8	33.6	64.1	66.4		
	3rd run	89.2	45.6	146.4	31.1				
	Average	86.3	48.4	145.1	33.0	64.8	66.4		
	standard dev	*2.58*	*2.46*	*1.18*	*1.64*	*0.99*	*0.07*		

		G2	GS-N	DR-N	RGM-1	QLO-1	DNC-1	BIR-1	W-2
Ga	*recommended*	**22**	**22**	**22**	**15.0**	**17**	**15**	**16**	**20**
	1st run	24.6	20.2	22.1	17.0	19.8	14.4	15.2	17.8
	2nd run	24.1	21.7	22.3	16.8	19.1	14.7		
	3rd run			20.9					
	Average	**24.4**	**21.0**	**21.8**	**16.9**	**19.5**	**14.6**		
	standard dev	*0.35*	*1.06*	*0.76*	*0.14*	*0.49*	*0.21*		
Rb	*recommended*	**170**	**185**	**73**	**149**	**74**	**4.5**	**0.3**	**20**
	1st run	165.7	184.8	71.6	147.7	71.5	4.7	0.1	23.4
	2nd run	166.7	184.5	71.8	148.5	72.4	4.6		
	3rd run	167.4	189.9	73.1	151.8				
	Average	**166.6**	**186.4**	**72.2**	**149.3**	**72.0**	**4.7**		
	standard dev	*0.85*	*3.03*	*0.81*	*2.17*	*0.64*	*0.07*		
Sr	*recommended*	**487**	**570**	**400**	**108**	**336**	**145**	**108**	**194**
	1st run	476.4	570.0	398.5	106.7	327.8	143.7	108.7	191.5
	2nd run	480.2	570.1	399.2	107.0	330.7	144.0		
	3rd run	476.7	576.6	396.7	112.7				
	Average	**477.8**	**572.2**	**398.1**	**108.8**	**329.3**	**143.9**		
	standard dev	*2.11*	*3.78*	*1.29*	*3.38*	*2.05*	*0.21*		
Y	*recommended*	**11.4**	**19**	**28**	**25**	**24**	**18**	**16**	**24**
	1st run	12.1	21.2	29.7	23.1	23.2	16.3	18.2	21.7
	2nd run	11.6	20.7	29.2	23.8	23.5	17.0		
	3rd run	10.4	19.5	26.3	25.5				
	Average	**11.4**	**20.5**	**28.4**	**24.1**	**23.4**	**16.7**		
	standard dev	*0.87*	*0.87*	*1.84*	*1.23*	*0.21*	*0.49*		
Zr	*recommended*	**300**	**235**	**125**	**219**	**185**	**41**	**22**	**94**
	1st run	292.6	230.2	133.9	221.7	181.4	41.2	24.8	88.4
	2nd run	294.5	232.6	127.5	220.0	182.8	41.3		
	3rd run	295.6	230.6	125.8	220.0				
	Average	**294.2**	**231.1**	**129.1**	**220.6**	**182.1**	**41.3**		
	standard dev	*1.52*	*1.29*	*4.27*	*0.98*	*0.99*	*0.07*		
Nb	*recommended*	**13**	**21**	**8**	**8.9**	**10.3**	**3.0**	**2.0**	**7.9**
	1st run	12.6	23.1	7.1	10.6	10.1	1.7	1.8	6.6
	2nd run	12.8	20.8	7.8	10.7	10.3	3.0		
	3rd run	12.5	22.4	9.0	9.5				
	Average	**12.6**	**22.1**	**8.0**	**10.3**	**10.2**	**2.4**		
	standard dev	*0.15*	*1.18*	*0.96*	*0.67*	*0.14*	*0.92*		
Ba	*recommended*	**1880**	**1400**	**385**	**807**	**1370**	**114**	**7.7**	**182**
	1st run	1830.5	1400.1	383.5	815.9	1364.5	115.3	14.6	173.4
	2nd run	1847.9	1400.4	384.0	810.1	1367.8	114.2		
	3rd run	1885.5	1442.5	381.2	817.6				
	Average	**1854.6**	**1414.3**	**382.9**	**814.5**	**1366.2**	**114.8**		
	standard dev	*28.11*	*24.39*	*1.49*	*3.93*	*2.33*	*0.78*		

		G-2	G-1	DR-N	RGM-1	AGV-1	SY3(2)	BIR-1	W-2
La	*recommended*	86	104	21	24	38	670	0.9	14.0
	1st run	89.2	105.1	21.9	18.5	43.1	662.4	1.9	12.7
	2nd run	88.3	104.6	21.5	19.6	41.8	665.4		
	3rd run	92.8	80.9	21.5	27.3				
	Average	90.1	96.9	21.6	21.8	42.5	663.9		
	standard dev	*2.38*	*13.83*	*0.23*	*4.79*	*0.92*	*2.12*		
Ce	*recommended*	159	171	46	47	67	1115	2.5	22
	1st run	165.9	184.5	41.5	44.2	67.3	1107.7	4.7	18.4
	2nd run	163.7	179.8	42.6	45.1	67.1	1110.2		
	3rd run	155.4		50.2	43.6				
	Average	161.7	182.2	44.8	44.3	67.2	1109.0		
	standard dev	*5.54*	*3.32*	*4.74*	*0.75*	*0.14*	*1.77*		
Nd	*recommended*	53	57	23	19	34	335	2.5	11.4
	1st run	54.3	59.4	18.2	17.4	34.5	340.5	1.8	9.5
	2nd run	53.9	58.6	19.5	18.8	34.1	337.9		
	3rd run	53.3		22.8	22.4				
	Average	53.8	59.0	20.2	19.5	34.3	339.2		
	standard dev	*0.50*	*0.57*	*2.37*	*2.58*	*0.28*	*1.84*		

		G2	GS-N	DR-N	RGM-1	QLO-1	DNC-1	BIR-1	W-2
Pb	*recommended*	31	53	55	24	20.4	6.3	3.2	9.3
	1st run	31.5	48.7	60.9	22.4	20.1	5.4	5.0	14.3
	2nd run	30.9	49.4	58.6	22.9	20.3	5.9		
	3rd run	33.5		53.1	20.3				
	Average	32.0	49.1	57.5	21.9	20.2	5.7		
	standard dev	*1.36*	*0.49*	*4.01*	*1.38*	*0.14*	*0.35*		
Th	*recommended*	24.6	42	5	15.1	4.5	0.2	0.0	2.2
	1st run	28.7	38.6	5.8	18.4	4.3	0.4	0.2	2.4
	2nd run	27.1	40.0	5.5	17.3	4.4	0.3		
	3rd run			5.0					
	Average	27.9	39.3	5.4	17.9	4.4	0.4		
	standard dev	*1.13*	*0.99*	*0.40*	*0.78*	*0.07*	*0.07*		
U	*recommended*	2.0	8	1.5	5.8	1.9	0.1	0.0	0.5
	1st run	2.4	6.4	2.7	2.9	1.2	0.9	0.8	1.1
	2nd run	2.1	6.8	2.1	3.3	1.5	0.8		
	3rd run			2.0					
	Average	2.3	6.6	2.3	3.1	1.4	0.9		
	standard dev	*0.21*	*0.28*	*0.38*	*0.28*	*0.21*	*0.07*		

APPENDIX C (III)

Accuracy and precision of ICP-MS trace element data

		AGV-1	BHVO-1	W2	G2
Cs	*recommended*	**1.26**	**0.13**	**0.87**	**1.33**
	1st run	1.24	0.12	0.86	1.30
	2nd run	1.27	0.10	0.84	1.32
	3rd run	1.28	0.09	0.80	1.33
	4th run	1.25	0.08	0.87	1.31
	Average	**1.26**	**0.10**	**0.84**	**1.32**
	standard dev	0.02	0.02	0.03	0.01
La	*recommended*	**38**	**15.8**	**10.61**	**86**
	1st run	38.64	15.7	10.55	86.45
	2nd run	38.45	15.53	10.16	86.80
	3rd run	38.20	15.31	10.20	86.15
	4th run	38.70	16.10	9.87	86.56
	Average	**38.50**	**15.66**	**10.20**	**86.49**
	standard dev	0.23	0.33	0.28	0.27
Ce	*recommended*	**66**	**39**	**23.03**	**159**
	1st run	67.18	37.60	22.64	158.10
	2nd run	67.58	39.40	22.71	158.76
	3rd run	67.23	38.36	21.95	158.11
	4th run	68.40	37.71	21.24	157.93
	Average	**67.60**	**38.27**	**22.14**	**158.23**
	standard dev	0.56	0.83	0.69	0.37
Pr	*recommended*	**6.5**	**5.7**	**2.94**	**19**
	1st run	8.31	5.52	2.98	17.61
	2nd run	8.54	5.46	2.76	17.28
	3rd run	8.58	5.71	2.92	18.40
	4th run	8.75	5.66	3.05	17.96
	Average	**8.55**	**5.59**	**2.93**	**17.81**
	standard dev	0.18	0.12	0.12	0.48
Nd	*recommended*	**34**	**25.2**	**13.2**	**53**
	1st run	33.75	25.85	13.21	55.30
	2nd run	33.88	25.98	13.45	55.57
	3rd run	34.42	26.07	13.66	55.73
	4th run	34.28	26.01	12.92	55.64
	Average	**34.08**	**25.98**	**13.31**	**55.56**
	standard dev	0.32	0.09	0.32	0.19
Sm	*recommended*	**5.9**	**6.2**	**3.36**	**7.2**
	1st run	5.89	6.18	3.33	7.48
	2nd run	5.96	6.22	3.24	7.61
	3rd run	5.90	6.17	3.14	7.22
	4th run	5.93	6.26	3.47	7.35
	Average	**5.92**	**6.21**	**3.30**	**7.42**
	standard dev	0.03	0.04	0.14	0.17

		AGV-1	BHVO-1	W2	G2
Eu	*recommended*	**1.66**	**2.06**	**1.12**	**1.41**
	1st run	1.67	2.04	1.10	1.50
	2nd run	1.68	2.01	1.08	1.48
	3rd run	1.64	2.02	1.07	1.52
	4th run	1.66	2.00	1.09	1.55
	Average	**1.66**	**2.02**	**1.09**	**1.51**
	standard dev	0.02	0.02	0.01	0.03
Gd	*recommended*	**5.2**	**6.4**	**3.63**	**4.1**
	1st run	5.31	6.04	3.65	3.61
	2nd run	4.98	6.49	3.69	3.76
	3rd run	4.82	6.68	3.50	3.84
	4th run	4.87	6.50	3.46	3.72
	Average	**5.00**	**6.43**	**3.58**	**3.73**
	standard dev	0.22	0.27	0.11	0.10
Tb	*recommended*	**0.71**	**0.96**	**0.62**	**0.48**
	1st run	0.72	0.95	0.62	0.48
	2nd run	0.68	0.96	0.59	0.47
	3rd run	0.68	0.98	0.60	0.48
	4th run	0.71	0.97	0.63	0.48
	Average	**0.70**	**0.97**	**0.61**	**0.48**
	standard dev	0.02	0.01	0.02	0.00
Ho	*recommended*	**0.73**	**0.99**	**0.74**	**0.37**
	1st run	0.69	0.98	0.75	0.38
	2nd run	0.68	0.99	0.77	0.36
	3rd run	0.70	0.99	0.73	0.39
	4th run	0.68	0.97	0.78	0.37
	Average	**0.69**	**0.98**	**0.76**	**0.38**
	standard dev	0.01	0.01	0.02	0.01
Dy	*recommended*	**3.8**	**5.2**	**3.71**	**2.5**
	1st run	3.68	5.22	3.72	2.12
	2nd run	3.66	5.24	3.76	2.25
	3rd run	3.70	5.31	3.68	2.31
	4th run	3.75	5.20	3.64	2.36
	Average	**3.70**	**5.24**	**3.70**	**2.26**
	standard dev	0.04	0.05	0.05	0.10
Er	*recommended*	**1.61**	**2.4**	**2.23**	**1.2**
	1st run	1.68	2.42	2.20	0.88
	2nd run	1.70	2.38	2.12	0.92
	3rd run	1.74	2.49	2.16	0.98
	4th run	1.76	2.36	2.08	0.95
	Average	**1.72**	**2.41**	**2.14**	**0.93**
	standard dev	0.04	0.06	0.05	0.04

		AGV-1	BHVO-1	W2	G2
Tm	*recommended*	**0.32**	**0.33**	**0.34**	**0.17**
	1st run	0.30	0.36	0.33	0.15
	2nd run	0.29	0.36	0.34	0.14
	3rd run	0.29	0.37	0.34	0.14
	4th run	0.28	0.35	0.32	0.15
	Average	**0.29**	**0.36**	**0.33**	**0.15**
	standard dev	0.01	0.01	0.01	0.01
Yb	*recommended*	**1.67**	**2.02**	**2.03**	**0.78**
	1st run	1.67	2.01	2.05	0.78
	2nd run	1.68	2.02	2.02	0.75
	3rd run	1.63	2.00	2.01	0.76
	4th run	1.71	2.04	1.98	0.76
	Average	**1.67**	**2.02**	**2.02**	**0.76**
	standard dev	0.03	0.02	0.03	0.01
Lu	*recommended*	**0.28**	**0.291**	**0.33**	**0.113**
	1st run	0.26	0.29	0.31	0.12
	2nd run	0.26	0.30	0.33	0.12
	3rd run	0.26	0.29	0.32	0.11
	4th run	0.28	0.30	0.33	0.11
	Average	**0.27**	**0.30**	**0.32**	**0.12**
	standard dev	0.01	0.01	0.01	0.01
Hf	*recommended*	**5.1**	**4.38**	**2.49**	**7.9**
	1st run	5.08	4.36	2.50	7.80
	2nd run	5.05	4.33	2.42	7.82
	3rd run	5.10	4.28	2.36	7.84
	4th run	5.12	4.40	2.39	7.87
	Average	**5.09**	**4.34**	**2.42**	**7.83**
	standard dev	0.03	0.05	0.06	0.03
Ta	*recommended*	**0.92**	**1.23**	**0.54**	**0.88**
	1st run	0.94	1.20	0.48	0.78
	2nd run	0.90	1.26	0.48	0.74
	3rd run	0.86	1.15	0.49	0.70
	4th run	0.85	1.15	0.50	0.81
	Average	**0.89**	**1.19**	**0.49**	**0.76**
	standard dev	0.04	0.05	0.01	0.05
Pb	*recommended*	**36**	**2.6**	**7.81**	**31**
	1st run	36.12	2.30	7.78	29.50
	2nd run	36.35	2.36	7.77	29.64
	3rd run	36.10	2.10	7.52	29.82
	4th run	35.96	1.98	7.39	29.79
	Average	**36.13**	**2.19**	**7.62**	**29.69**
	standard dev	0.16	0.18	0.19	0.15

		AGV-1	BHVO-1	W2	G2
Th	*recommended*	**6.5**	**1.08**	**2.04**	**24.6**
	1st run	6.55	1.27	2.18	25.08
	2nd run	6.58	1.28	2.16	25.50
	3rd run	6.48	1.27	2.15	26.00
	4th run	6.59	1.26	2.17	25.64
	Average	**6.55**	**1.27**	**2.17**	**25.56**
	standard dev	0.05	0.01	0.01	0.38
U	*recommended*	**1.89**	**0.42**	**0.5**	**2.04**
	1st run	1.88	0.42	0.49	2.05
	2nd run	1.92	0.44	0.50	2.06
	3rd run	1.89	0.41	0.51	2.07
	4th run	1.90	0.40	0.48	2.06
	Average	**1.90**	**0.42**	**0.50**	**2.06**
	standard dev	0.02	0.02	0.01	0.01

APPENDIX D

PEARSON PRODUCT-MOMENT COEFFICIENT OF CORRELATION

AMPHIBOLITE

	Sc	Ti	V	Cr	Ni	Ga	Y	Zr	Nb	Cs	Ce	Pr	Nd	Sm	Eu	Gd	Tb	Dy	Ho	Er	Tm	Yb	Lu	Hf	Ta	Th	U
Sc	1.00																										
Ti	0.29	1.00																									
V	0.43	0.94	1.00																								
Cr	-0.06	-0.55	-0.46	1.00																							
Ni	-0.59	-0.50	-0.59	0.59	1.00																						
Ga	0.28	0.90	0.79	-0.54	-0.29	1.00																					
Y	0.31	0.99	0.93	-0.57	-0.49	0.91	1.00																				
Zr	0.51	0.91	0.83	-0.59	-0.62	0.90	0.92	1.00																			
Nb	0.51	0.89	0.84	-0.64	-0.66	0.88	0.90	0.98	1.00																		
Cs	-0.52	-0.37	-0.54	0.12	0.60	-0.30	-0.31	-0.39	-0.43	1.00																	
Ce	0.68	0.68	0.64	-0.61	-0.75	0.68	0.71	0.90	0.91	-0.36	1.00																
Pr	0.61	0.80	0.75	-0.63	-0.70	0.80	0.83	0.96	0.97	-0.36	0.98	1.00															
Nd	0.55	0.88	0.82	-0.62	-0.66	0.86	0.90	0.99	0.99	-0.39	0.94	0.99	1.00														
Sm	0.45	0.95	0.89	-0.61	-0.59	0.91	0.96	0.98	0.98	-0.37	0.85	0.94	0.98	1.00													
Eu	0.37	0.97	0.89	-0.58	-0.53	0.94	0.98	0.97	0.96	-0.37	0.79	0.90	0.95	0.99	1.00												
Gd	0.35	0.98	0.92	-0.59	-0.53	0.92	0.99	0.95	0.94	-0.35	0.77	0.88	0.94	0.99	0.99	1.00											
Tb	0.34	0.99	0.94	-0.57	-0.52	0.91	0.99	0.92	0.92	-0.36	0.72	0.84	0.91	0.97	0.98	0.99	1.00										
Dy	0.32	0.99	0.94	-0.59	-0.52	0.90	0.99	0.92	0.91	-0.35	0.72	0.83	0.91	0.97	0.97	0.99	1.00	1.00									
Ho	0.29	0.99	0.94	-0.59	-0.50	0.90	1.00	0.90	0.89	-0.35	0.68	0.80	0.88	0.96	0.96	0.99	1.00	1.00	1.00								
Er	0.30	0.99	0.94	-0.61	-0.52	0.89	0.99	0.90	0.88	-0.34	0.68	0.80	0.88	0.95	0.96	0.98	0.99	1.00	1.00	1.00							
Tm	0.29	0.99	0.94	-0.60	-0.50	0.89	0.99	0.89	0.87	-0.35	0.67	0.79	0.87	0.95	0.95	0.98	0.99	0.99	1.00	1.00	1.00						
Yb	0.29	0.99	0.94	-0.60	-0.51	0.89	0.99	0.88	0.87	-0.33	0.67	0.79	0.87	0.95	0.95	0.98	0.99	0.99	1.00	1.00	1.00	1.00					
Lu	0.27	0.99	0.93	-0.60	-0.50	0.89	0.99	0.88	0.86	-0.34	0.66	0.78	0.86	0.94	0.95	0.97	0.99	0.99	1.00	1.00	1.00	1.00	1.00				
Hf	0.54	0.92	0.87	-0.60	-0.67	0.88	0.93	0.99	0.99	-0.43	0.90	0.96	0.99	0.99	0.97	0.95	0.94	0.93	0.91	0.91	0.90	0.90	0.90	1.00			
Ta	0.61	0.82	0.76	-0.52	-0.65	0.83	0.83	0.98	0.97	-0.43	0.95	0.98	0.98	0.93	0.91	0.88	0.84	0.83	0.80	0.80	0.79	0.79	0.78	0.97	1.00		
Th	0.80	0.07	0.16	-0.06	-0.70	-0.04	0.09	0.33	0.30	-0.38	0.57	0.45	0.35	0.23	0.14	0.11	0.10	0.10	0.06	0.08	0.07	0.07	0.06	0.36	0.43	1.00	
U	0.75	0.04	0.10	-0.15	-0.71	-0.02	0.07	0.36	0.32	-0.32	0.62	0.49	0.38	0.23	0.15	0.10	0.07	0.07	0.03	0.05	0.07	0.04	0.03	0.37	0.47	0.96	1.00

METAPYROXENITE

	Sc	Ti	V	Cr	Ni	Ga	Y	Zr	Nb	Cs	Ce	Pr	Nd	Sm	Eu	Gd	Tb	Dy	Ho	Er	Tm	Yb	Lu	Hf	Ta	Th	U
Sc	1.00																										
Ti	0.95	1.00																									
V	0.98	1.00	1.00																								
Cr	-0.41	-0.67	-0.59	1.00																							
Ni	0.48	0.20	0.29	0.60	1.00																						
Ga	0.99	0.90	0.94	-0.28	0.60	1.00																					
Y	0.74	0.91	0.87	-0.92	-0.23	0.64	1.00																				
Zr	0.98	0.88	0.92	-0.24	0.64	1.00	0.60	1.00																			
Nb	0.92	0.76	0.82	-0.03	0.78	0.97	0.43	0.98	1.00																		
Cs	0.88	0.70	0.77	0.06	0.84	0.94	0.34	0.96	1.00	1.00																	
Ce	-0.87	-0.68	-0.75	-0.09	-0.86	-0.93	-0.31	-0.95	-0.99	-1.00	1.00																
Pr	-0.45	-0.17	-0.26	-0.62	-1.00	-0.58	0.26	-0.61	-0.76	-0.82	0.84	1.00															
Nd	0.05	0.35	0.26	-0.93	-0.85	-0.09	0.71	-0.14	-0.34	-0.42	0.45	0.86	1.00														
Sm	0.88	0.98	0.96	-0.80	0.01	0.80	0.97	0.77	0.63	0.55	-0.53	0.02	0.52	1.00													
Eu	0.76	0.92	0.88	-0.91	-0.20	0.66	1.00	0.62	0.45	0.36	-0.33	0.23	0.69	0.98	1.00												
Gd	0.70	0.88	0.83	-0.94	-0.29	0.58	1.00	0.55	0.36	0.27	-0.24	0.32	0.76	0.95	1.00	1.00											
Tb	0.74	0.90	0.86	-0.92	-0.24	0.63	1.00	0.60	0.42	0.33	-0.30	0.27	0.72	0.97	1.00	1.00	1.00										
Dy	0.62	0.83	0.77	-0.97	-0.39	0.50	0.99	0.46	0.27	0.18	-0.15	0.42	0.82	0.92	0.98	1.00	0.99	1.00									
Ho	0.75	0.92	0.87	-0.91	-0.21	0.65	1.00	0.62	0.44	0.35	-0.32	0.24	0.70	0.98	1.00	1.00	1.00	0.98	1.00								
Er	0.82	0.96	0.92	-0.86	-0.10	0.73	0.99	0.70	0.54	0.46	-0.43	0.13	0.61	0.99	0.99	0.98	0.99	0.96	0.99	1.00							
Tm	0.55	0.77	0.71	-0.99	-0.47	0.42	0.97	0.38	0.18	0.09	-0.06	0.50	0.87	0.88	0.96	0.98	0.97	1.00	0.96	0.93	1.00						
Yb	0.84	0.96	0.94	-0.84	-0.07	0.76	0.99	0.73	0.57	0.49	-0.46	0.10	0.58	1.00	0.99	0.97	0.98	0.95	0.99	1.00	0.91	1.00					
Lu	0.84	0.96	0.93	-0.84	-0.07	0.75	0.99	0.98	0.56	0.48	-0.45	0.11	0.59	1.00	0.99	0.98	0.99	0.95	0.99	1.00	0.92	1.00	1.00				
Hf	0.99	0.91	0.94	-0.29	0.59	1.00	0.65	0.72	0.97	0.94	-0.93	-0.57	-0.08	0.81	0.67	0.59	0.64	0.51	0.66	0.74	0.43	0.76	0.76	1.00			
Ta	0.87	0.98	0.95	-0.82	-0.02	0.78	0.98	1.00	0.99	0.53	-0.50	0.05	0.55	1.00	0.98	0.96	0.98	0.93	0.98	1.00	0.89	1.00	1.00	0.79	1.00		
Th	-0.99	-0.99	-1.00	0.56	-0.33	-0.95	-0.85	-0.94	-0.84	-0.79	0.77	0.30	-0.22	-0.95	-0.86	-0.81	-0.84	-0.75	-0.85	-0.91	-0.68	-0.92	-0.92	-0.95	-0.94	1.00	
U	-1.00	-0.97	-0.99	0.47	-0.43	-0.98	-0.78	-0.97	-0.90	-0.85	0.83	0.40	-0.12	-0.91	-0.80	-0.74	-0.78	-0.67	-0.79	-0.86	-0.60	-0.87	-0.87	-0.98	-0.89	0.99	1.00

SERPENTINITE

	Sc	Ti	V	Cr	Ni	Ga	Y	Zr	Nb	Cs	Ce	Pr	Nd	Sm	Eu	Gd	Tb	Dy	Ho	Er	Tm	Yb	Lu	Hf	Ta	Th	U
Sc	1.00																										
Ti	0.17	1.00																									
V	0.50	0.94	1.00																								
Cr	1.00	0.19	0.52	1.00																							
Ni	0.35	-0.87	-0.64	0.32	1.00																						
Ga	0.13	1.00	0.92	0.16	-0.88	1.00																					
Y	0.56	0.91	1.00	0.58	-0.58	0.90	1.00																				
Zr	-0.50	0.77	0.50	-0.48	-0.99	0.79	0.44	1.00																			
Nb	-0.89	0.30	-0.05	-0.88	-0.74	0.33	-0.12	0.84	1.00																		
Cs	0.59	0.90	0.99	0.61	-0.55	0.88	1.00	0.40	-0.16	1.00																	
Ce	0.97	0.42	0.71	0.97	0.09	0.39	0.76	-0.26	-0.74	0.78	1.00																
Pr	0.90	0.58	0.83	0.91	-0.09	0.55	0.86	-0.08	-0.61	0.88	0.98	1.00															
Nd	0.87	0.64	0.87	0.88	-0.17	0.61	0.90	0.00	-0.54	0.91	0.97	1.00	1.00														
Sm	0.78	0.75	0.93	0.80	-0.32	0.72	0.96	0.15	-0.41	0.97	0.92	0.97	0.99	1.00													
Eu	0.58	0.90	1.00	0.60	-0.56	0.88	1.00	0.41	-0.15	1.00	0.77	0.88	0.91	0.96	1.00												
Gd	0.68	0.84	0.97	0.70	-0.45	0.82	0.99	0.29	-0.27	0.99	0.85	0.93	0.96	0.99	0.99	1.00											
Tb	0.62	0.88	0.99	0.64	-0.52	0.86	1.00	0.37	-0.19	1.00	0.80	0.90	0.93	0.97	1.00	1.00	1.00										
Dy	0.55	0.92	1.00	0.57	-0.60	0.90	1.00	0.45	-0.10	1.00	0.75	0.85	0.89	0.95	1.00	0.99	1.00	1.00									
Ho	0.60	0.89	0.99	0.62	-0.54	0.87	1.00	0.39	-0.17	1.00	0.79	0.89	0.92	0.97	1.00	0.99	1.00	1.00	1.00								
Er	0.42	0.96	1.00	0.45	-0.70	0.95	0.99	0.57	0.04	0.98	0.65	0.77	0.82	0.90	0.98	0.95	0.97	0.99	0.98	1.00							
Tm	0.58	0.90	1.00	0.60	-0.56	0.88	1.00	0.41	-0.15	1.00	0.77	0.88	0.91	0.96	1.00	0.99	1.00	1.00	1.00	0.98	1.00						
Yb	0.48	0.95	1.00	0.50	-0.65	0.93	1.00	0.52	-0.03	0.99	0.69	0.81	0.86	0.92	0.99	0.97	0.99	1.00	0.99	1.00	0.99	1.00					
Lu	0.61	0.89	0.99	0.63	-0.54	0.87	1.00	0.39	-0.18	1.00	0.79	0.89	0.92	0.97	1.00	1.00	1.00	1.00	1.00	0.98	1.00	0.99	1.00				
Hf	-0.45	0.80	0.55	-0.43	-0.99	0.82	0.49	1.00	0.81	0.45	-0.20	-0.02	0.05	0.20	0.46	0.35	0.42	0.50	0.44	0.62	0.46	0.56	0.44	1.00			
Ta	0.50	0.94	1.00	0.52	-0.64	0.92	1.00	0.50	-0.05	0.99	0.71	0.83	0.87	0.93	1.00	0.98	0.99	1.00	0.99	1.00	1.00	1.00	0.99	0.54	1.00		
Th	0.29	0.99	0.97	0.31	-0.80	0.99	0.95	0.68	0.18	0.94	0.53	0.67	0.73	0.82	0.95	0.90	0.93	0.96	0.94	0.99	0.95	0.98	0.94	0.72	0.97	1.00	
U	0.31	-0.89	-0.67	0.28	1.00	-0.90	-0.61	-0.98	-0.71	-0.59	0.05	-0.13	-0.21	-0.35	-0.59	-0.49	-0.56	-0.63	-0.58	-0.73	-0.59	-0.69	-0.57	-0.99	-0.67	-0.82	1.00

Felsic metavolcanics

	Sc	Ti	V	Ga	Rb	Sr	Y	Zr	Nb	Cs	Ba	La	Ce	Pr	Nd	Sm	Eu	Gd	Tb	Dy	Ho	Er	Tm	Yb	Lu	Hf	Ta	Pb	Th	U
Sc	1.00																													
Ti	0.18	1.00																												
V	0.08	0.90	1.00																											
Ga	-0.21	0.63	0.60	1.00																										
Rb	0.16	0.04	-0.16	0.07	1.00																									
Sr	-0.17	0.69	0.67	0.78	-0.03	1.00																								
Y	0.35	0.85	0.73	0.36	0.29	0.40	1.00																							
Zr	0.36	0.81	0.68	0.35	0.30	0.37	0.98	1.00																						
Nb	0.38	0.72	0.57	0.14	0.23	0.16	0.94	0.96	1.00																					
Cs	0.32	0.27	0.16	-0.02	0.73	-0.07	0.66	0.64	0.67	1.00																				
Ba	0.06	0.68	0.55	0.65	0.54	0.68	0.65	0.68	0.48	0.39	1.00																			
La	0.17	0.78	0.68	0.63	0.42	0.64	0.88	0.87	0.72	0.60	0.86	1.00																		
Ce	0.16	0.81	0.71	0.65	0.39	0.66	0.88	0.87	0.72	0.58	0.85	1.00	1.00																	
Pr	0.15	0.83	0.73	0.67	0.37	0.70	0.87	0.86	0.70	0.55	0.86	0.99	1.00	1.00																
Nd	0.15	0.84	0.75	0.68	0.36	0.72	0.87	0.85	0.69	0.53	0.87	0.98	0.99	1.00	1.00															
Sm	0.17	0.88	0.78	0.67	0.34	0.71	0.89	0.87	0.72	0.52	0.85	0.97	0.99	0.99	1.00	1.00														
Eu	0.20	0.93	0.81	0.69	0.27	0.75	0.88	0.85	0.71	0.45	0.83	0.94	0.96	0.97	0.98	0.99	1.00													
Gd	0.25	0.89	0.77	0.57	0.36	0.62	0.95	0.93	0.81	0.58	0.83	0.96	0.97	0.98	0.98	0.99	0.98	1.00												
Tb	0.29	0.89	0.76	0.47	0.35	0.53	0.98	0.96	0.88	0.64	0.76	0.93	0.93	0.93	0.93	0.95	0.94	0.98	1.00											
Dy	0.34	0.88	0.74	0.43	0.32	0.46	0.99	0.97	0.92	0.64	0.71	0.90	0.91	0.90	0.90	0.92	0.92	0.97	0.99	1.00										
Ho	0.34	0.86	0.73	0.37	0.32	0.43	0.99	0.97	0.92	0.66	0.67	0.89	0.89	0.89	0.88	0.90	0.90	0.96	0.99	1.00	1.00									
Er	0.38	0.85	0.71	0.35	0.29	0.39	0.99	0.98	0.94	0.65	0.65	0.87	0.88	0.87	0.86	0.88	0.88	0.94	0.98	0.99	0.99	1.00								
Tm	0.39	0.85	0.71	0.37	0.30	0.37	0.99	0.98	0.94	0.65	0.65	0.87	0.87	0.87	0.86	0.88	0.88	0.94	0.97	0.99	0.99	1.00	1.00							
Yb	0.38	0.85	0.76	0.38	0.23	0.38	0.99	0.96	0.93	0.63	0.60	0.86	0.86	0.85	0.85	0.87	0.87	0.93	0.96	0.98	0.98	0.99	0.99	1.00						
Lu	0.36	0.83	0.74	0.34	0.13	0.35	0.96	0.93	0.93	0.59	0.53	0.82	0.83	0.82	0.81	0.83	0.84	0.89	0.93	0.96	0.96	0.97	0.97	0.98	1.00					
Hf	0.29	0.84	0.69	0.46	0.33	0.42	0.96	0.99	0.92	0.61	0.75	0.90	0.90	0.89	0.89	0.90	0.88	0.95	0.96	0.97	0.95	0.96	0.97	0.94	0.91	1.00				
Ta	0.38	0.53	0.40	-0.02	0.28	-0.05	0.84	0.88	0.96	0.72	0.37	0.62	0.60	0.57	0.55	0.57	0.54	0.67	0.76	0.81	0.82	0.85	0.85	0.83	0.83	0.84	1.00			
Pb	0.14	0.73	0.69	0.71	0.38	0.82	0.63	0.62	0.39	0.30	0.92	0.84	0.84	0.86	0.87	0.86	0.86	0.82	0.74	0.68	0.65	0.62	0.61	0.60	0.52	0.67	0.25	1.00		
Th	0.20	0.65	0.56	0.43	0.58	0.41	0.86	0.88	0.78	0.76	0.82	0.94	0.92	0.90	0.89	0.88	0.82	0.90	0.89	0.87	0.87	0.86	0.86	0.84	0.78	0.90	0.75	0.75	1.00	
U	0.20	0.68	0.56	0.42	0.56	0.44	0.89	0.89	0.80	0.77	0.82	0.95	0.94	0.92	0.91	0.90	0.84	0.92	0.92	0.90	0.90	0.89	0.88	0.86	0.81	0.90	0.75	0.74	0.99	1.00